

1975

Partial Wave Treatments Of Diatomic Molecules

Mohammad Keramat Ali

Follow this and additional works at: <https://ir.lib.uwo.ca/digitizedtheses>

Recommended Citation

Ali, Mohammad Keramat, "Partial Wave Treatments Of Diatomic Molecules" (1975). *Digitized Theses*. 971.
<https://ir.lib.uwo.ca/digitizedtheses/971>

This Dissertation is brought to you for free and open access by the Digitized Special Collections at Scholarship@Western. It has been accepted for inclusion in Digitized Theses by an authorized administrator of Scholarship@Western. For more information, please contact tadam@uwo.ca, wlsadmin@uwo.ca.

PARTIAL WAVE TREATMENTS OF
DIATOMIC MOLECULES

by
M. Keramat Ali
Department of Physics

Submitted in partial fulfillment
of the requirements for the degree of
Doctor of Philosophy

Faculty of Graduate Studies
The University of Western Ontario
London, Ontario
April, 1975

© M. Keramat Ali 1975.

LIST OF FIGURES

Figure.	Description	Page
II.1-1	The coordinate system used in this thesis.	22
III.2-1	Division of the interval $\rho_B \leq r \leq \infty$ into small intervals for the stepwise solution of the radial equations.	51
IV.2-1	Normalized proton centred wave functions for the ground state H_2^+ -molecule for $R = 2$.	88
IV.2-2	Normalized proton centred wave functions for the ground state H_2^+ -molecule for $R = 4$.	89
IV.2-3	Normalized proton centred wave functions for the ground state H_2^+ -molecule for $R = 6$.	90
IV.2-4	Normalized midpoint centred wave functions for the ground state H_2^+ -molecule for $R = 2$.	91
IV.2-5	Normalized midpoint centred wave functions for the ground state H_2^+ -molecule for $R = 4$.	92
IV.2-6	Normalized midpoint centred wave functions for the ground state H_2^+ -molecule for $R = 6$.	93
F.1	The modulus of the electrostatic potential \tilde{U} at points along the z-axis for $R = 2$ and $\rho_A = \rho_B = R/2$.	181

ABSTRACT

One centre partial wave techniques are used to solve the Schrödinger wave equation for H_2^+ -like molecules as a function of the position of the expansion centre, ρ_A , the number of partial wave components, N , included in the calculation and the internuclear separation, R , in order to help (1) assess the convergence problems associated with the one centre method as a function of R , (2) determine the usefulness of the (floating) one centre method with respect to the evaluation of adequate results for the numerically small interaction energy and the molecular wave function for all values of R and (3) study the unification of the centre of nuclear charge one centre methods useful for small R with the long range intermolecular force methods appropriate for large R . To accomplish these goals it is necessary to solve coupled one centre partial wave differential equations to high partial wave order as a function of R and ρ_A . To do this semi-analytic techniques are developed to carry out the solution in a relatively economic manner. These semi-analytic techniques have potential use in other research areas.

Explicit floating one centre partial wave calculations are performed for the ground $1\sigma_g$ state H_2^+ molecule which has an electron exchange dominated interaction energy and therefore is an appropriate model for the purposes given above. While the results obtained here are considerably better than

previous one centre calculations over a wide range of R values they still do not yield adequate values of the interaction energy for intermediate values of R for practical values of N . The exact partial wave floating one centre results are also used to investigate the reasons for the slow convergence of the conventional one centre variational and perturbation theory results for the interaction energy obtained by using Slater, Gaussian or Laguerre type basis functions and "1s" or "Molecular Puff" zeroth order problems.

The results for the $1s\sigma_g$ state of the H_2^+ molecule are used to investigate several other features of the theory of intermolecular forces. For example the high partial wave order proton centred calculations show that the total interaction energy can be obtained by employing a proton centred wave function which contains no explicit terms representing the exchange of the electron between the two protons. Hence the conventional definitions of coulomb and exchange interaction energies, commonly used in the theory of intermolecular forces, are not rigorous. The ability of the proton centred results to represent electron exchange effects is also investigated by examining the cusp and symmetry characteristics of the proton centred results as a function of R and N . It appears for small R at least, that the high order partial wave proton centred orbitals are the first demonstration of a complete set of orbitals in the area of intermolecular forces which do not contain electron exchange effects explicitly in their functional form.

Finally a general discussion is given of the feasibility of using (floating) one centre techniques, and their generalization to a two floating centre approach for general diatomic molecules, for evaluating adequate values of the interaction energy. It appears that while these techniques are not particularly favourable for the evaluation of molecular interaction energies which are electron exchange dominated they may well be very useful in treating molecules having interaction energies with a large coulomb contribution in an effective practical way for all values of R . This latter point is illustrated by applying the (floating) one centre techniques of this work to the $1s\sigma$, $2s\sigma$ and $2p\sigma$ states of HeH^{++} .

ACKNOWLEDGEMENTS

The author wishes to express his deep appreciation and sincere gratitude to his supervisor, Professor William J. Meath, for continued encouragement and patient guidance during the progress of this work.

The author also wishes to thank the members of his advisory committee, in particular Professor P.A. Fraser for his careful reading of the thesis and for his helpful comments.

He also wishes to express his thanks to his colleagues for stimulating discussions. In particular, thanks are due to Dr. Joseph E. Kouba, Dr. Seamus F. O'Shea, Dr. Geoff D. Zeiss and Mr. Joseph F. Bukta for advice in computational matters.

The author also wishes to acknowledge the cooperation afforded him by the Physics and Chemistry Departments of the University of Western Ontario during his graduate studies.

The financial support provided by the Canadian International Development Agency is gratefully acknowledged.

Thanks are also due to Mrs. C. Atkinson for patient typing.

Finally, the author wishes to express his appreciation for the understanding and patience of his wife, Shahida Parvin.

TABLE OF CONTENTS

	Page
CERTIFICATE OF EXAMINATION.....	ii
ABSTRACT.....	iii
ACKNOWLEDGEMENTS.....	vi
LIST OF FIGURES.....	xiii
LIST OF TABLES.....	xv
CHAPTER I - INTRODUCTION.....	1
CHAPTER II - ONE CENTRE METHODS FOR THE EXACT SOLUTION OF THE WAVE EQUATION FOR H_2^+ -LIKE MOLECULES.....	20
II.1 The Schrödinger Wave Equation for H_2^+ -Like Molecules.....	20
II.2 Representation of the Wave Function in Spherical Polar Coordinates.....	21
II.3 General Discussion of the Solution of the Radial Wave Equations.....	26
II.3A The Choice of the Coordinate Origin.....	27
II.3A-1 Homonuclear H_2^+ -Like Molecules ($Z_A = Z_B$)..	27
II.3A-2 Heteronuclear H_2^+ -Like Molecules ($Z_A \neq Z_B$)..	30
II.3B The Boundary Conditions.....	32
CHAPTER III - THE EXACT SOLUTION OF THE RADIAL EQUATIONS FOR H_2^+ -LIKE MOLECULES.....	35
III.1 Division of the Configuration Space ($0 \leq r \leq \infty$) into Region I ($0 \leq r \leq \rho_B$) and Region II ($\rho_B \leq r \leq \infty$).....	35
III.2 The Analytic Solution of the Radial Equations.....	37

III.2A	The Analytic Solution of the Radial Equations in Region I ($0 \leq r \leq \rho_B$).....	38
III.2A-1	The Coordinate Origin at the Nucleus A ($\rho_A = 0, \rho_B = R$).....	38
III.2A-2	The Coordinate Origin at the Midpoint ($\rho_A = \rho_B = R/2$).....	41
III.2B	The Analytic Solution of the Radial Equations in Region II ($\rho_B \leq r \leq \infty$).....	43
III.2B-1	The Derivation of the Reduced Differential Equation.....	44
III.2B-2	The Solution of the Reduced Differential Equation.....	47
III.2B-3	The Stepwise Analytic Solution of the Radial Equations in Region II ($\rho_B \leq r \leq \infty$).....	50
III.2B-4	The Asymptotic Solution of the Radial Equations in Region II ($\rho_B \leq r \leq \infty$).....	54
III.3	The Numerical Solution of the Radial Equations.....	57
III.3A	The Matching Method for Solving the Radial Equations.....	59
III.3B	The Determination of the Parameters in the Matching Method.....	63

III.4 • A Discussion of the Determination of the Parameters in the Analytic Solution of the Radial Equations...	71
III.4A The Matching of the Stepwise Solution with the Asymptotic Solution....	72
III.4B The Initial Estimates of the Parameters in the Analytic Solution of the Radial Equations.....	74
III.4C The Choice of the Point at which the Stepwise Solu- tion is Matched with the Asymptotic Solution ($r = r_c$).....	75

CHAPTER IV - RESULTS AND GENERAL DISCUSSION OF THE EXACT ONE CENTRE SOLUTION FOR THE

H_2^+ MOLECULE.....	77
IV.1 The Interaction Energy for the Ground State of the H_2^+ Molecule.....	77
IV.1A The Ground State H_2^+ Inter- action Energy Obtained with $\rho_A = 0$ and $\rho_B = R$	78
IV.1B The Ground State H_2^+ Inter- action Energy Obtained with $\rho_A = \rho_B = R/2$	80
IV.1C The Ground State H_2^+ Inter- action Energy Obtained with $\rho_A = \rho_{op}$	83
IV.2 Normalized Wave Functions for the Ground State of the H_2^+ Molecule.....	86
IV.2A The Proton Centred Wave Function.....	87
IV.2B The Midpoint Centred Wave Function.....	87

CHAPTER V - DISCUSSION OF THE CONVERGENCE OF ONE CENTRE
RESULTS FOR THE GROUND STATE OF THE H_2^+
MOLECULE.....

95

V.1 Brief Review of the Variational and
Perturbation Procedures for Solving
the Schrödinger Equation.....

95

V.1A The Variational Procedure.....

96

V.1B The Rayleigh Schrödinger
Perturbation Procedure.....

96

V.2 The Exchange and Coulomb Energies
for the H_2^+ Molecule.....

97

• V.2A Variational Coulomb and Exchange
Energies for the H_2^+ Molecule.....

99

V.2B Perturbation Theory Coulomb and
Exchange Energies for the H_2^+
Molecule.....

100

V.3 Discussion of the Convergence Properties
of the Exact one Centre Results for the
Ground State of the H_2^+ Molecule.....

104

V.3A The Proton Centred Results.....

104

V.3B The Midpoint Centred Results.....

109

V.3C The Floating Centred Results.....

110

V.4 A Discussion of the Convergence
Problems of Conventional One Centre
Methods.....

111

V.4A The Conventional One Centre
Variational Results for the
 H_2^+ Molecule.....

113

V.4B The Conventional One Centre
Perturbation Results for the
 H_2^+ Molecule.....

119

CHAPTER VI - CONCLUSIONS.....

122

APPENDIX A - EXAMPLES OF THE USE OF THE ANALYTICAL
METHOD FOR SOLVING THE RADIAL EQUATIONS....

136

A.1	Solution of Radial Equations in Region I ($0 \leq r \leq \rho_B$).....	136
A.2	Solution of Radial Equations in Region II ($\rho_B \leq r \leq \infty$).....	138
A.3	The Matching of the Solutions of Radial Equations in Region I and Region II at $r = \rho_B$	140
A.4	The Matching of the Solutions of Radial Equations Obtained by the Stepwise Method.....	140
A.5	The Asymptotic Solution of Reduced Differential Equations in Region II....	141
A.6	The Matching of the Asymptotic Solution with the Stepwise Solution in Region II.....	143
APPENDIX B - A DISCUSSION OF THE CONVERGENCE OF THE SERIES REPRESENTING THE FUNCTIONS $\chi_s(r)$ AND $f_s(r)$ AND OF THE ASYMPTOTIC NATURE OF THE SERIES FOR $f_s(\xi)$		
B.1	Illustrations of the Convergence Properties of the Series for $\chi_s(r)$	144
B.2	Illustrations of the Convergence Properties of the Series for $f_s(t)$	146
B.2-1	The Choice of the Initial Estimates for Δ and j_m	147
B.2-2	Numerical Examples for the Convergence of the Series for $f_s(t)$	147
B.3	The Asymptotic Nature of the Series for the $f_s(\xi)$	149
APPENDIX C - EXAMPLES OF THE USE OF THE NUMERICAL METHOD FOR SOLVING THE RADIAL EQUATIONS...		
C.1	The Finite Difference Equations Representing the Radial Equations.....	156
C.2	The Choice of the Matching Point r_c	157

C.3	The Determination of the Parameters Appearing in the Matching Method.....	159
APPENDIX D	- ILLUSTRATIVE NUMERICAL VALUES OF THE PARAMETERS AND RELATED QUANTITIES APPEARING IN THE NUMERICAL METHOD FOR SOLVING THE RADIAL EQUATIONS.....	164
D.1	Examples of Numerical Values of $h, r_c,$ $r_\infty, \gamma, \delta E, E, {}^f C_1, \dots, {}^f C_N, {}^b C_1, \dots, {}^b C_N$	165
D.2	Richardson's h^2 -Extrapolation.....	167
APPENDIX E	- NORMALIZATION OF THE WAVE FUNCTIONS FOR THE GROUND STATE OF THE H_2 -MOLECULE.....	172
APPENDIX F	- CONVERGENCE OF THE SERIES FOR THE ELECTRO- STATIC POTENTIAL USED IN THE ONE CENTRE PARTIAL WAVE METHOD.....	178
APPENDIX G	- A DISCUSSION OF THE EVALUATION OF THE INTEGRALS AND CONSTANTS OF INTEGRATION APPEARING IN REFERENCE [7].....	199
G.1	The Evaluation of the Integrals.....	200
G.2	Evaluation of the Constants of Integration.....	202
APPENDIX H	- FLOATING ONE CENTRE PERTURBATION CALCULATIONS FOR H_2^+ -LIKE MOLECULES; COPIES OF REFERENCES [6] and [7].....	206
APPENDIX I	- OPTIMAL HELIUM AND CENTRE OF NUCLEAR CHARGE CENTRED PARTIAL WAVE CALCULATIONS FOR THE $1s\sigma, 2s\sigma$ AND $2p\sigma$ STATES OF HeH^{++} ...	207
REFERENCES	238
VITA	250

LIST OF FIGURES

Figure.	Description	Page
II.1-1	The coordinate system used in this thesis.	22
III.2-1	Division of the interval $0_B \leq r \leq \infty$ into small intervals for the stepwise solution of the radial equations.	51
IV.2-1	Normalized proton centred wave functions for the ground state H_2^+ -molecule for $R = 2$.	88
IV.2-2	Normalized proton centred wave functions for the ground state H_2^+ -molecule for $R = 4$.	89
IV.2-3	Normalized proton centred wave functions for the ground state H_2^+ -molecule for $R = 6$.	90
IV.2-4	Normalized midpoint centred wave functions for the ground state H_2^+ -molecule for $R = 2$.	91
IV.2-5	Normalized midpoint centred wave functions for the ground state H_2^+ -molecule for $R = 4$.	92
IV.2-6	Normalized midpoint centred wave functions for the ground state H_2^+ -molecule for $R = 6$.	93
F.1	The modulus of the electrostatic potential \tilde{U} at points along the z-axis for $R = 2$ and $\rho_A = \rho_B = R/2$.	181

- F.2 The modulus of the electrostatic potential \tilde{U} at points along the z-axis for $R = 4$ and $\rho_A = \rho_B = R/2$. 182
- F.3 The modulus of the electrostatic potential \tilde{U} at points along the z-axis for $R = 6$ and $\rho_A = \rho_B = R/2$. 183
- F.4 The modulus of the electrostatic potential \tilde{U} at points along the z-axis for $R = 8$ and $\rho_A = \rho_B = R/2$. 184
- F.5 The modulus of the electrostatic potential \tilde{U} at points along the z-axis for $R = 20$ and $\rho_A = \rho_B = R/2$. 185
- F.6 The modulus of the electrostatic potential \tilde{U} at points along the z-axis for $R = 2$ and $\rho_A = 0$ ($\rho_B = R$). 189
- F.7 The modulus of the electrostatic potential \tilde{U} at points along the z-axis for $R = 4$ and $\rho_A = 0$ ($\rho_B = R$). 190
- F.8 The modulus of the electrostatic potential \tilde{U} at points along the z-axis for $R = 6$ and $\rho_A = 0$ ($\rho_B = R$). 191
- F.9 The modulus of the electrostatic potential \tilde{U} at points along the z-axis for $R = 8$ and $\rho_A = 0$ ($\rho_B = R$). 192
- F.10 The modulus of the electrostatic potential \tilde{U} at points along the z-axis for $R = 20$ and $\rho_A = 0$ ($\rho_B = R$). 193

LIST OF TABLES

Table	Description	Page
I.1-1	The proton centred interaction energies for the ground state H_2^+ molecule as a function of R and N .	79
IV.1-2	The midpoint-centred interaction energies for the ground state H_2^+ molecule as a function of R and N .	81
IV.1-3	The floating centred interaction energies for the ground state H_2^+ molecule as a function of R and N .	85
V.2-1	A comparison of the coulomb and total perturbation theory interaction energies and the exact total interaction energy for the ground state H_2^+ molecule.	103
V.4-1	Some values of the one centre interaction energies for the ground states of the H_2^+ and H_2 molecules at their equilibrium separations.	112
B.1	Some values of the constants $a_0^{(s)}$, $h_0^{(s)}$, γ and r_c as functions of s and N for $R = 6$ and $\rho_B = R/2$.	151
B.2	Some values of the constants $a_0^{(s)}$, $h_0^{(s)}$, γ and r_c as functions of s and N for $R = 6$ and $\rho_B = R$.	152

- B.3 A comparison of the 3rd, 60th and the minimum of the terms $Q_j^{(s)} = |h_j^{(s)} \xi_c^j|$ occurring in the series for the $f_s(\xi_c)$ as functions of s and N for $R = 6$ and $\rho_B = R/2$. 153
- B.4 A comparison of the 3rd, 75th and the minimum of the terms $Q_j^{(s)} = |h_j^{(s)} \xi_c^j|$ occurring in the series for the $f_s(\xi_c)$ as functions of s and N for $R = 6$ and $\rho_B = R$. 154
- E.1 Some numerical values of the normalized Ψ and ψ at points along the z -axis for the ground state H_2^+ molecule for $R = 2$ and 6 with $\rho_B = R/2$ and R . 177
- I.1 A comparison of the helium and centre of nuclear charge centred partial wave interaction energies with the exact values for the $1s\sigma$ state HeH^{++} molecule as a function of R and N . 211
- I.2 A comparison of the helium and centre of nuclear charge centred partial wave interaction energies with the exact values for the $2s\sigma$ state HeH^{++} molecule as a function of R and N . 212
- I.3A A comparison of the proton centred partial wave interaction energies for the $2p\sigma$ state of HeH^{++} molecule with the exact values as a function of R and N . 213

I.3B

A comparison of the centre of nuclear charge centred partial wave interaction energies with the exact values for the $2p\sigma$ state HeH^{++} molecule as a function of R and N .

214

I.4

A comparison, for the $1s\sigma$ state HeH^{++} molecule, of the partial wave interaction energies with the exact values and with the non-expanded long range R^{-1} perturbation theory results as a function of R .

218

I.5

A comparison, for the $2p\sigma$ state HeH^{++} molecule, of the partial wave interaction energies with the exact values and with the non-expanded perturbation theory and expanded long range R^{-1} theory results as a function of R .

219.

The author of this thesis has granted The University of Western Ontario a non-exclusive license to reproduce and distribute copies of this thesis to users of Western Libraries. Copyright remains with the author.

Electronic theses and dissertations available in The University of Western Ontario's institutional repository (Scholarship@Western) are solely for the purpose of private study and research. They may not be copied or reproduced, except as permitted by copyright laws, without written authority of the copyright owner. Any commercial use or publication is strictly prohibited.

The original copyright license attesting to these terms and signed by the author of this thesis may be found in the original print version of the thesis, held by Western Libraries.

The thesis approval page signed by the examining committee may also be found in the original print version of the thesis held in Western Libraries.

Please contact Western Libraries for further information:

E-mail: libadmin@uwo.ca

Telephone: (519) 661-2111 Ext. 84796

Web site: <http://www.lib.uwo.ca/>

CHAPTER I

INTRODUCTION

One centre methods have often been used in molecular energy calculations; general reviews of these methods can be found in the articles by Bishop^{1(a)} and Hayes and Parr^{1(b)}. In this work we will be considering mostly diatomic molecules where the expansion centre for the one centre method is usually, but not always as discussed below, taken to be fixed at the internuclear midpoint in the case of homonuclear molecules and at the centre of nuclear charge in the case of heteronuclear diatomic molecules. The advantage of performing molecular calculations using one centre methods rather than the more common multi-centre methods, which involve including multi-centre electron exchange effects in the molecular wave function, is that the integrals occurring in the former approach are relatively easy to evaluate. However this advantage of one centre methods is sometimes more than offset by the fact that one centre calculations usually converge much more slowly than the multi-centre exchange calculations to acceptable results for molecular interaction energies and wave functions. If the one centre approach can be carried out through the first few orders of approximation this will often not be a serious problem for small values of the internuclear separation $R \lesssim R_e$, where R_e is the equilibrium value of the internuclear distance in a diatomic molecule.

However it is a very serious problem with the one centre method for moderately small, intermediate and large values of $R > R_e$, see for example Refs. [2-5] and Refs. [6-8] and some of the references therein. One of the purposes of this work is to examine this difficulty with the fixed one centre method and to study procedures⁶⁻⁸, which connect the one centre method with the theory of intermolecular forces, for extending the usefulness of the method as a function of internuclear separation.

The reasons for the difficulty with the fixed one centre approach for all but relatively small values of $R < R_e$ can be understood by considering the connection⁶⁻⁸ between this approach and the usual theory of long range intermolecular forces⁹⁻¹¹ which neglects both charge overlap and electron exchange effects⁹⁻¹⁴ between the interacting atoms. For a general diatomic molecule it is necessary to use a two centre multipolar approach in order to describe the dissociation of the molecule properly and to obtain reasonable results for the molecular interaction energy at large values of the internuclear distance R . These results are given as an expansion⁹⁻¹¹ involving inverse powers of the internuclear distance and are given in terms of R^{-1} expanded induction and dispersion energies and, in the case of the interaction of molecules involving permanent multipole moments, they also involve expanded first order interaction energies which result from the interaction of the permanent moments of the interacting molecules. While these R^{-1}

expanded results for the interaction energy are very useful and are relatively easy to evaluate since they involve^{9-11,15} the properties of the isolated molecules or atoms, they are obtained by neglecting charge overlap effects and correspond to an asymptotic expansion^{14,16,17} of the interaction energy in inverse powers of R which is valid, when used with care, for only quite large values of the internuclear separation^{13,14} 17,18. It is possible to modify the usual long range theory of intermolecular forces (interaction energies) to include charge overlap effects between the interacting atoms by, in effect, using the two-centre bipolar^{15,19} expansion of the molecular Hamiltonian in place of the long range multipolar expansion^{9-11,15} in the theoretical development of the problem. This yields^{14(a),20} an apparently convergent two-centre partial wave expansion for the interaction energy which involves^{14,20,21} the sum of nonexpanded induction, dispersion and first order energies which, however, appear to represent only the coulomb part^{15,21-23} of the total interaction energy for the interaction since the wave function for the treatment neglects electron exchange between the two interacting species.

Summarizing the first two paragraphs there are two very different approaches which can yield useful accurate results for the properties of a diatomic molecule for quite small and reasonably large values of the internuclear separation and one of the problems to be considered in this thesis is how to unite these two approaches. In their

region of validity both of these methods are considerably easier to employ than the common variational multi-centre exchange techniques which appear to be the only techniques that can, in general, yield satisfactory results for the interaction energy over the entire range of internuclear distances. Part of the purpose of this thesis is to make a contribution to the understanding of the connection between the one centre approach useful for small values of R and the long range approach useful for large R and to investigate a method, see also Refs. [6-8], which in principle can unite these two approaches in a useful smooth way for all values of R . The question of extending the well known long range multipolar techniques to intermediate and small values of R is a fundamental problem in the theory of intermolecular forces that has received much attention through the development of a variety of exchange perturbation theories²⁴⁻²⁶ which involve the evaluation of electron exchange corrections to the nonexpanded coulomb interaction energies. While many of the exchange perturbation theories are very elegant, they do have calculational problems associated with them that, in some respects, are not unlike those associated with the more common variational multi-centre exchange methods. The unification of the one centre and the long range approaches provides considerable insight into this difficult problem of extending the long range theory to smaller values of R and may eventually provide an

alternative procedure for accomplishing this goal.

There is only one type of molecule which lends itself to a direct comparison or connection between the one centre method useful for small values of R and the long range treatment useful for large values of R , namely a diatomic molecule which yields, upon dissociation, a pure nuclear charge and a nucleus with associated electrons. This situation arises because it is only for this type of molecule that the long range treatment can be carried out using a one centre expansion rather than the more usual two centre expansion; in this case¹⁴ the two centre bipolar expansion^{15,19} for the molecular Hamiltonian reduces to that obtained from using the one centre Laplace expansion. It therefore is clear that the H_2^+ -like molecule makes an ideal model for this type of investigation and it is used as such in subsequent parts of this thesis. The connection between the one centre methods useful for small and large values of R for this system has already been discussed by using Rayleigh Schrödinger perturbation theory and two choices for the unperturbed or zeroth order problem, namely the screened "1s" hydrogen atom and the molecular puff problem; see Refs. [6,7] which are included in Appendix H. In these papers the interaction energy is determined through third order, for both perturbation problems, as a function of internuclear separation, the charges of the nuclei, the position of the expansion centre and in the case of the screened "1s" problem as a function of the screening constant. Numerical calculations were performed

y 6

for the 1s ground states of the H_2^+ and HeH^{++} molecules and to a lesser extent for the 2pσ state of HeH^{++} and the ground state results were used as models for discussing the usefulness of allowing the expansion centre in the one centre method to be a function of nuclear configuration for H_2^+ -like molecules. These papers^{6,7} illustrate the connection between the short and long range one centre approaches ~~for~~ evaluating interaction energies and show that allowing the expansion centre in the one centre method to float as a function of internuclear separation unifies these two treatments and removes the severe divergence problems associated with the internuclear midpoint centred small R approach as R becomes at all large. On the other hand these results also show very clearly that the generalized floating one centre perturbation treatment is not capable of yielding adequate interaction energies for the exchange energy dominated ground state H_2^+ molecule unless R is quite large or R is quite small, less than or approximately equal to R_e say. The work of Ref. [7] also shows that the rather tedious extension to higher orders of perturbation theory would not alleviate the situation. In the case of the coulomb dominated ground state of HeH^{++} both the screened "1s" helium centred results and the screened "1s" energy optimized floating one centre results⁶ give excellent agreement with the exact values of the interaction energy. The results in Refs. [6,7] also show that it is critical to test the validity of the methods by comparing the calculated interaction energy with the "exact" interaction

energy. For example the floating one centre method is capable of giving the electronic or the total energy of the ground state H_2^+ molecule to within an error of approximately eight percent for all R whereas as it yields very poor results for the important interaction energy for all but quite small or quite large R values. In this thesis the interaction energy is used to test the validity of the one centre methods.

The extension of the floating one centre approach to a general diatomic molecule has been discussed by Pan⁸. In general, as pointed out above, one requires two expansion centres to represent the dissociation of a diatomic molecule. In Ref. [8] a bipolar two-centre partial wave treatment of the molecular Hamiltonian is carried out with the expansion centres being located along the internuclear axis of the diatomic molecule and being considered as a function of nuclear configuration. For small values of R the two centres can coalesce to yield the small R one centre method while as R becomes large the two centres can float to the nuclei of the diatomic molecule to yield the long range two centre results for the interaction energy. Reasonably extensive variational calculations⁸ for the ground state of the H_2 molecule employing Slater orbitals with variable screening constants and "principle" quantum numbers indicate that this approach does not yield adequate results for the interaction energy for the important intermediate range of internuclear separations. It is interesting to note that the convergence of the two floating centre results for the interaction energy

of the ground state of H_2 is better than that for the floating one centre results⁸ for H_2^+ . This is a consequence of molecular symmetry. When the energy optimized expansion centre for the H_2^+ calculation floats away from the internuclear midpoint, as R becomes large a mixture of u and g symmetry is introduced into the calculation of the $1\sigma_g$ ground state of H_2^+ . When this happens the results for the interaction energy will begin to represent the average of the ground $1\sigma_g$ state and the first excited state $2p\sigma_u$ state interaction energies which is an "experimental" definition^{27,28} of the coulomb energy frequently used in the literature. On the other hand in the two floating centre calculation for the ground state of the H_2 molecule the proper g symmetry can be maintained as the single expansion centre for small R splits into two expansion centres as R increases.

Although floating the expansion centre(s) in the treatments of diatomic molecules discussed in the preceding paragraphs can increase the rate of convergence of the fixed one centre methods useable for small values of R by allowing the expansion centre(s) to be a function of nuclear configuration, in general^{6-8,29-34} the improvement achieved to date by using this type of approach is not sufficient to remove the convergence difficulties of the fixed one centre method for many important values of the internuclear separation. However, except in the case of a few fixed centred low order partial wave calculations^{2(b), 2(c), 3, 35-37} for H_2^+ -like molecules which are not adequate for the purposes

of this thesis, the approximate wave functions used in all these calculations were chosen to have some preassigned functional form and hence, in general, they do not constitute the optimal one centre (or possibly two centres⁸) wave function for the problem with respect to the partial wave order consistent with the angular basis set used in the calculation.

One of the objects of this thesis is to carry out exact one centre partial wave treatments of the ground state H_2^+ molecule as a function of the position of the expansion centre, the number of partial wave components included in the calculation and the internuclear separation and to use the results to help assess the convergence problems associated with the one centre method as a function of R and the usefulness of the floating one centre method with respect to the evaluation of adequate results for the interaction energy and the molecular wave function for all values of R . As discussed previously the H_2^+ -like molecule is a very appropriate model for investigating the ideas discussed in this Chapter concerning the unification of the one centre methods useful for small R values with the long range intermolecular force approach. This is fortunate since the partial wave analysis can in principle, see below, be carried out to arbitrary order as a function of the position of the expansion centre, the partial wave order and the internuclear separation and then compared with the exact solutions³⁸⁻⁴⁰ that are available for many H_2^+ -like systems as a function of

10

R. Since the interaction energy for the $1s\sigma_g$ ground state of H_2^+ is electron exchange dominated until R is quite large and because of the cusp and symmetry (definite g symmetry) characteristics associated with this state of H_2^+ , see above and Chapters IV and V, this system is the most appropriate model of all the H_2^+ -like molecules for examining the difficulties associated with using (floating) one centre techniques for evaluating useful values of the interaction energy for all values of R. Since the wave functions generated in these partial wave calculations will be the optimal one centre wave functions for any given partial wave order of approximation and position of the expansion centre, these results will hopefully provide a definitive test regarding the usefulness of the floating one centre method on uniting the short and long range theories for this molecule. The work of Refs. [2(a), 2(b), 3, 7, 29, 35, 36, 41-43] suggests that the methods used in this work will in general be more suitable for H_2^+ -like systems with coulomb dominated interaction energies. Such systems include many excited states of the H_2^+ molecule and many heteronuclear H_2^+ -like molecules in a variety of states; the $1s\sigma$, $2s\sigma$ and $2p\sigma$ states of HeH^{++} are considered explicitly in Appendix I. The extension of the floating one centre method to the more general diatomic molecule has been considered previously in this chapter, see also Ref. [8], and will be discussed again briefly in Chapter VI.

Since it is necessary to solve coupled one centre partial

wave differential equations to high order, for both the wave function and the energy, as a function of the variables of the problem in order to achieve the purposes of this thesis, another important objective of this work is to develop "analytic" or semi-analytic techniques both to carry out the solution in a relatively economic manner and to complement existing numerical techniques for solving the problem. In addition to serving as a useful model for the investigating of the effectiveness of one centre methods in the evaluation of molecular interaction energies, the high order partial wave results for the wave function and the interaction energy of the $1\sigma_g$ state of H_2^+ also contributes in an important way to the understanding of the concepts of exchange and coulomb interaction energies frequently used in the theory of molecular interactions or intermolecular forces and the nature of complete one centre basis sets, see Secs. V.2 and V.3. Some of the points raised in this and the preceeding paragraph will be expanded upon in the remaining part of this chapter with appropriate references to the following sections of this thesis.

The electronic Schrödinger wave equation for the H_2^+ molecule, in the Born-Oppenheimer approximation^{11,44,45}, is given by

$$H\Psi = E\Psi \quad (I.1),$$

where

$$H = -\frac{\nabla^2}{2} + U \quad (I.2),$$

$$U = -\frac{Z_A}{r_A} - \frac{Z_B}{r_B} \quad (I.3),$$

Z_A and Z_B are the charges of the nuclei A and B respectively and r_A and r_B are the distances of the electron from these nuclei. It is well known that Eq. (I.1) is separable in confocal elliptic coordinates and exact solutions for many states of the H_2^+ -like molecule are known³⁸⁻⁴⁰ as a function of R .

However Eq. (I.1) is not separable in the spherical polar coordinate system which is commonly used in conventional one centre variational and perturbation methods. A convenient way to solve this equation in spherical polar coordinates is to expand both the wave function Ψ and the potential U in an infinite series of spherical harmonic functions. This procedure yields an infinite set of coupled second order eigenvalue radial wave differential equations which on approximation by a finite set of coupled differential equations have, see Chapter II for details, the form

$$\begin{aligned} & \left[\frac{d^2}{dr^2} + \frac{2}{r} \frac{d}{dr} + 2E - \frac{s(s+1)}{r^2} \right] R_s^m(r) \\ &= \sum_{L=0}^N \sum_{\ell=|L-s|}^{L+s} D(L, \ell, s, m) U_\ell R_L^m(r) \end{aligned} \quad (I.4),$$

where

$$\psi = \sum_{L=0}^N \sum_{m=-L}^L R_L^m(r) Y_L^m(\theta, \phi)$$

and

$$U = \sum_{\ell=0}^{\infty} U_{\ell}(r) \cdot Y_{\ell}^0(\theta, \phi) \sqrt{\frac{4\pi}{2\ell+1}}$$

Here $Y_{\ell}^m(\theta, \phi)$ are spherical harmonic functions^{36,47}, the coefficients $D(L, \ell, s, m)$ are independent of r, θ, ϕ and the functions $U_{\ell}(r)$ change form as a function of r and the choice of the coordinate origin.

Previously exact analytical solutions of Eqs. (I.4) have been obtained only for the case where $N = 0$ and $m = 0$ with the expansion centre fixed at the centre of nuclear charge^{2(c),37}, at a nucleus^{2(c)} and at an arbitrary point⁷ on the internuclear axis which corresponds to a double layer molecular puff calculation, see Ref. [7] which is included in Appendix H. Here an "analytic" (semi-analytic) solution of Eqs. (I.4) is discussed, see Sec. III.2, for arbitrary values of N and m and with the coordinate origin fixed at one of the nuclei or at the internuclear midpoint. Numerical techniques, involving the use of the matching method^{35,48}, which can be used to solve Eqs. (I.4) for an arbitrary choice of expansion centre, are discussed in Sec. III.3. Numerical solutions of these equations have been obtained^{2(b),3,35,36} previously for several specific one electron molecules, for small R and for small values of $N \leq 6$ and with the coordinate origin fixed at the internuclear midpoint or the centre of

nuclear charge. The "analytical" and the numerical techniques discussed in Secs. III.2 and III.3 are appropriate for solving Eqs. (I.4) for any H_2^+ -like molecule and therefore will be useful for future investigations involving molecules other than those considered explicitly here. In this work these methods are used to solve Eqs. (I.4) to obtain both the energy and the wave function of the $1s\sigma_g$ state of H_2^+ and the energies of the $1s\sigma$, $2s\sigma$ and $2p\sigma$ states of HeH^{++} as a function of the position of the expansion centre, the internuclear separation and for fairly large values of $N \leq 24$, see Chapter IV and Appendix I respectively. The "analytic" method is particularly useful for obtaining reasonably accurate results for the wave function in an economic manner; the behaviour of the wave function of the $1s\sigma_g$ state of H_2^+ as a function of the parameters of the problem is an important part of this work and is discussed in detail in Secs. IV.2 and V.3. The results of the numerical method not only provide a check on those obtained by the analytical method but also furnish a nice example of usefulness of numerical methods in a rather complicated problem. In both the analytical and the numerical methods the energy eigenvalues are obtained by employing iterative procedures, see Secs. III.3 and III.4.

In order to study, see Chapter IV, Sec. V.3 and Appendix I, the convergence difficulties of the one centre method and the ability of the floating one centre method to give a unified useful approach for studying the "interatomic"

interaction for the $1s\sigma_g$ state of H_2^+ and the $1s\sigma$, $2s\sigma$ and $2p\sigma$ states of HeH^{++} as a function of expansion centre, partial wave order and internuclear separation, it is necessary to have the capability of solving Eqs. (I.4) to quite high partial wave order for both the energy and the wave function. A low order partial wave calculation as a function of expansion centre and internuclear distance would not suffice for the purposes of this thesis. For example while relatively low order internuclear midpoint centred partial wave calculations 2(b), 2(c), 35, 36 are sufficient for the ground state H_2^+ molecule for small R , these low order calculations yield interaction energies having the wrong sign as R becomes at all large, see for example Refs. [2(b), 2(c), 37] and Sec. IV.1. Also to demonstrate the convergence properties of the proton centred results requires treating Eqs. (I.4) to very high partial wave orders, see Chapter IV and Sec. V.3. The techniques discussed in Secs. III.2 and III.3 accomplish these goals. The analytic method for solving Eqs. (I.4) is of particular interest because of its potential use in other research areas. For example the stepwise analytic procedure used to solve the coupled radial equations associated with Eqs. (I.4), see Sec. (III.2B-3) is rather interesting since by using this technique severe convergence problems associated with the solution of these coupled equations can be eliminated. This method has recently been used⁴⁹ to obtain a solution for the time dependence of a two level system in a sinusoidal field and this work has been extended⁵⁰

to obtain an exact solution for the time dependence of two-level and multi-level systems in a sinusoidal field for arbitrary field strengths and times which is very useful for studying problems in multi-photon spectroscopy⁵¹.

The results for the energies and wave functions of the model system, the ground state H_2^+ molecule, are given in Chapter IV as a function of internuclear separation, position of the coordinate origin and the number of coupled radial differential equations used to approximate the Schrödinger equation for the system. The convergence properties of these exact one centre partial wave results are discussed in Sec. V.3 by using the cusp characteristics^{1(a),2(a),35,52} of the wave function and the notion of coulomb and exchange energies^{15,21-23} which are introduced in Chapter IV and Sec. V.2 respectively. Appendix F contains a discussion of the connection between using a truncated (approximate) partial wave effective Hamiltonian to represent the interaction between the electron and the protons and the more standard finite ordered partial wave analysis given in Sec. II.2. This material contains a discussion of the representation of the coulomb singularities in the exact Hamiltonian by the effective Hamiltonian for both the proton centred and mid-point centred cases and is meant to augment the discussion of the convergence properties of the exact partial wave calculations as a function of internuclear distance, expansion centre and partial wave order given in Chapter IV. and Sec. V.3. These discussions of the exact one centre

results are used to examine the validity of the conventional definitions of coulomb and exchange interaction energies in Sec. V.3 and to discuss, see Sec. V.4, the convergence problems associated with the conventional variational one centre methods that employ Slater or Gaussian basis sets and with one centre perturbation theory calculations.

While the optimal partial wave floating one centre methods of this thesis are capable of unifying the centre of nuclear charge one centre methods useful for small R with the long range intermolecular force methods appropriate for large R , in practice these methods are not too practical for intermediate values of R for the exchange dominated ground state of H_2^+ , see Sec. IV.1 and Chapter VI. In principle these methods can yield reasonable results for the interaction energy of this molecule for all values of R , but in practice the calculations would have to be carried out to unrealistically high partial wave order to obtain adequate results for the interaction energy for some important intermediate values of R . This is not the case for many other one electron molecules whose interaction energy contains a substantial coulomb component. The results of the optimal one centre partial wave treatments of the $1s\sigma$, $2s\sigma$ and $2p\sigma$ states of HeH^{++} show that these molecules can be treated very effectively for all values of R by using the (floating) one centre methods of this thesis, see Chapter VI and Appendix I.

Some of the $1s\sigma$, H_2^+ results, especially those obtained

by the high order proton centred partial wave analysis, are significant in the general area of intermolecular forces. The partial wave calculations of the $1s\sigma_g$ state of H_2^+ show that the total interaction energy for this electron exchange dominated system can be obtained by employing a proton centred wave function which contains no explicit terms representing the sharing or the exchange of the electron between the two protons, see Sec. V.3. Another way of stating this point is that the proton centred partial wave calculation, which according to the usual interpretation should yield the nonexpanded first order energy plus the sum of nonexpanded induction energies to higher order in the "interatomic" perturbation, actually is capable of giving accurate results for the total interaction energy and not just an approximation to the coulomb energy. The ability of the high order proton centred results to represent electron exchange or interchange effects between the two protons can also be seen through the behaviour of the proton centred wave function of the number of partial wave components included in the wave function. When the expansion centre is located at a proton the wave function appears to have mixed (u,g)-symmetry and contains no terms explicitly representing electron exchange effects. However, as discussed in Sec. V.3, as the order of the proton centred partial wave treatment of the $1s\sigma_g$ state is increased, the proton centred wave function can take on the proper g-symmetry of the ground state molecule. The sort of behaviour of the proton centred

results has apparently not been observed before and is related to the symmetry dilemma for the $1s\sigma_g$ state of H_2^+ discussed by Katriel³⁴. The ability of the proton centred results to represent electron exchange effects between the two protons in H_2^+ depends on the internuclear separation value as discussed in Sec. V.3. The improved convergence properties of the optimal partial wave proton centred orbitals relative to conventional one centre basis orbitals, and to a lesser extent the analogous property for the midpoint centred orbitals, give hope that an analysis of the semi-analytical expressions for the partial wave orbitals given in Sec. III.2 may provide a means for generating new useful basis functions for molecular calculations. These and other consequences of the one centre (floating) partial wave work of this thesis together with suggestions for possible uses and extensions, are summarized in Chapter VI.

Atomic units⁵³ are used throughout this work. In atomic units (abbreviated as a.u.) the unit of length a_0 is the first Bohr radius of the hydrogen atom and $m = e = \frac{h}{2\pi} = 1$, where m and e are, respectively, the mass and the magnitude of the charge of an electron and h is Planck's constant. Numerically .1 a.u. of energy is $\frac{e^2}{a_0} \approx 27.21$ eV and $a_0 \approx 0.529$ Å.

CHAPTER II

ONE CENTRE METHODS FOR THE EXACT SOLUTION OF THE WAVE EQUATIONS FOR H_2^+ -LIKE MOLECULES

This chapter contains a general discussion of the one centre partial wave representation of the Schrödinger equation for an H_2^+ -like molecule. In this representation the problem of solving the Schrödinger equation is basically that of solving a set of coupled eigenvalue radial differential equations, see Sec. II.2. Sec. II.3 contains a general discussion of the choice of the expansion centre for the partial wave method and the boundary conditions associated with the solution of the radial eigenvalue equations.

II.1 THE SCHRÖDINGER WAVE EQUATION FOR H_2^+ -LIKE MOLECULES

In this work the one centre solution of the Schrödinger equation for a H_2^+ -like molecule is given in the Born Oppenheimer approximation^{44,45}. The time independent Schrödinger equation describing the motion of the electron of the H_2^+ -like molecule in the Coulomb field of the two fixed nuclei is given by

$$H\psi = E\psi \quad (II.1-1),$$

where H and E are, respectively, the electronic Hamiltonian and electronic energy. The total energy, E_T , of the system is defined by

$$E_T = E + \frac{Z_A Z_B}{R} \quad (\text{II.1-2}),$$

where Z_A and Z_B are the charges of the nuclei A and B, and R is the internuclear distance, see Fig. II.1-1. The quantity which plays a vital role in many chemical and physical processes is the interaction energy^{9,15,54}, E_{int} , which is a small part of E_T which determines intermolecular forces; in the Born-Oppenheimer approximation the force is proportional to the derivative of E_{int} with respect to R for atom-atom interactions. For an H_2^+ -like molecule which dissociates to form a one electron atom or ion, with principle quantum number n and nucleus A, one has

$$E_{\text{int}} = E_T + \frac{Z_A^2}{2n^2} \quad (\text{II.1-3}).$$

The electronic Hamiltonian H is given in atomic units⁵³ by

$$H = -\frac{\nabla^2}{2} + U; \quad U = -\sum_{\alpha} \frac{Z_{\alpha}}{r_{\alpha}} \quad (\text{II.1-4})$$

where the Z_{α} are the charges of the nuclei A and B and r_{α} is the distance between the electron and the nucleus α , see Fig. II.1-1. In the following sections of this chapter the exact one centre solution of Eq. (II.1-1) is discussed in some detail.

II.2 REPRESENTATION OF THE WAVE FUNCTION IN SPHERICAL POLAR COORDINATES

Equation (II.1-1) is not separable in the spherical polar coordinate system which is used to treat the H_2^+ -like molecule in this work. For the solution of Eq. (II.1-1) in this coordinate system, it is convenient to expand both U and Ψ in terms of an infinite series of spherical harmonic

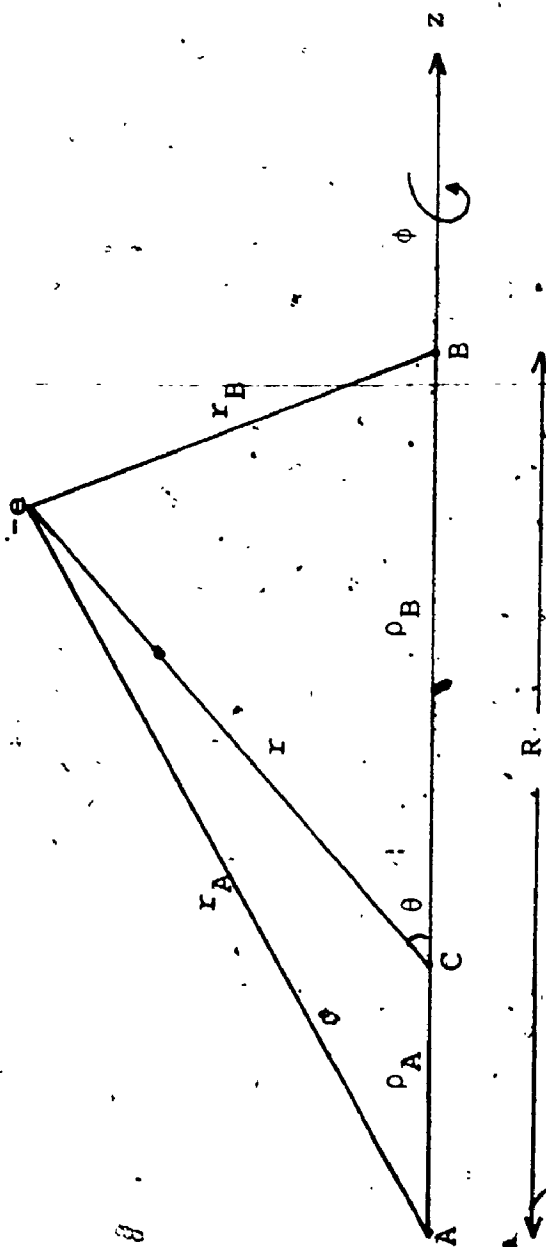


Figure II.1-1: The coordinate system used in this thesis, A and B are the positions of the two fixed nuclei with charges Z_A and Z_B and $-e$ is the instantaneous position of the electron. The origin of the right-handed coordinate system is at the point C on the line joining A and B. Here $\rho_A + \rho_B = R$ and for convenience we choose $\rho_A \leq \rho_B$.

functions^{2(b),35,55} Since the electrostatic potential, U , has azimuthal symmetry, it can be expanded⁵⁶ as†

$$U = - \sum_{\alpha=1}^2 \frac{Z_{\alpha}}{r_{\alpha}} = \sum_{\ell=0}^{\infty} U_{\ell} d_{\ell} Y_{\ell}^0(\theta, \phi) \quad (\text{II.2-1}),$$

where

$$d_{\ell} = \sqrt{\frac{4\pi}{2\ell+1}} \quad (\text{II.2-2}),$$

$$U_{\ell} = -[(-1)^{\ell} v_{\ell}(r, \rho_A) + v_{\ell}(r, \rho_B)] \quad (\text{II.2-3}),$$

$$v_{\ell}(r, \rho_{\alpha}) = \frac{r_{<}^{\ell}}{r_{>^{\ell+1}}} Z_{\alpha} \quad (\text{II.2-4})$$

and $Y_{\ell}^m(\theta, \phi)$ is a normalized spherical harmonic function^{46,47}. Here the electronic distance from the coordinate origin is denoted by r and the distance from the nucleus α ($\alpha = A, B$) to the coordinate origin is denoted by ρ_{α} , see Fig. II.1-1, where $\rho_A + \rho_B = R$. In Eq. (II.2-4) $r_{<}$ and $r_{>}$ are the lesser and greater, respectively, of r and ρ_{α} . The wave function, Ψ , is then expanded as

$$\Psi(r, \theta, \phi) = \sum_{\ell=0}^{\infty} R_{\ell}^m(r) Y_{\ell}^m(\theta, \phi) \quad (\text{II.2-5}),$$

where the coefficients of expansion, $R_{\ell}^m(r)$, are radial wave functions: In spherical polar coordinates ∇^2 is given by

$$\nabla^2 = \frac{1}{r^2} \frac{\partial}{\partial r} \left(r^2 \frac{\partial}{\partial r} \right) - \frac{L^2}{r^2} \quad (\text{II.2-6}),$$

where L is the orbital angular momentum operator for the

†Equation (II.2-1) is often expressed in terms of the Legendre polynomial $P_{\ell}(\cos \theta)$. The relation between $P_{\ell}(\cos \theta)$ and $Y_{\ell}^0(\theta, \phi)$ is given⁴⁶ by $P_{\ell}(\cos \theta) = d_{\ell} Y_{\ell}^0(\theta, \phi)$.

electron relative to the coordinate origin C, see Fig. II.1-1.

Having expanded U and ψ in terms of spherical harmonics, we can derive^{2(b), 35} the radial wave equations corresponding to the Schrödinger equation given in Eq. (II.1-1). Using Eqs. (II.1-4), (II.2-1), (II.2-5) and (II.2-6) in Eq. (II.1-1), we obtain

$$\sum_{L=0}^{\infty} \sum_{M=-L}^L \left\{ \frac{d^2}{dr^2} + \frac{2}{r} \frac{d}{dr} - \frac{L(L+1)}{r^2} + 2E - 2 \sum_{\ell=0}^{\infty} U_{\ell} d_{\ell} Y_{\ell}^0(\theta, \phi) \right\} R_L^M(r) Y_L^M(\theta, \phi) = 0 \quad (\text{II.2-7})$$

Multiplying Eq. (II.2-7) by $Y_S^{m*}(\theta, \phi)$ and integrating over all angular configuration space we obtain the radial wave equations

$$\left[\frac{d^2}{dr^2} + \frac{2}{r} \frac{d}{dr} + 2E - \frac{s(s+1)}{r^2} \right] R_s^m(r) = \sum_{L=0}^{\infty} \sum_{\ell=0}^{\infty} D(L, \ell, s, m) U_{\ell} R_L^m(r) \quad (\text{II.2-8}),$$

where

$$s = 0, 1, 2, \dots, \infty \quad (\text{II.2-9})$$

and

$$D(L, \ell, s, m) = -2 \sqrt{\frac{2L+1}{2s+1}} C(L \ell s; m 0) C(L \ell s; 0 0) \quad (\text{II.2-10}).$$

Here $C(\ell_1 \ell_2 \ell_3; m_1 m_2)$ is a Clebsh-Gordan coefficient⁴⁶. In obtaining Eq. (II.2-8) use was made of the relation⁴⁶

$$\begin{aligned} & \int_0^{\pi} \int_0^{2\pi} Y_{\ell_3}^{m_3}(\theta, \phi) Y_{\ell_2}^{m_2}(\theta, \phi) Y_{\ell_1}^{m_1}(\theta, \phi) \sin \theta \, d\theta \, d\phi \\ &= \left[\frac{(2\ell_1+1)(2\ell_2+1)}{4\pi(2\ell_3+1)} \right]^{\frac{1}{2}} C(\ell_1 \ell_2 \ell_3; m_1 m_2) C(\ell_1 \ell_2 \ell_3; 0 0) \end{aligned} \quad (\text{II.2-11})$$

Equation (II.2-8) is an infinite set of coupled differential equations for the radial wave functions $R_s^m(r)$. However it is clear from Eq. (II.2-8) that the differential equations are coupled only in the label s and not in m . Thus the energy eigenvalue, E , obtained by solving Eq. (II.2-8) can be characterized by a particular m value. Now we will verify the well known result^{22(b)} that the energy eigenvalue E depends only on the absolute value of the quantum number m . The Clebsh-Gordan coefficients satisfy the relation⁴⁶

$$C(\ell_1 \ell_2 \ell_3; m_1 m_2 m_3) = (-1)^{\ell_1 + \ell_2 - \ell_3} C(\ell_1 \ell_2 \ell_3; -m_1 -m_2 -m_3) \quad (\text{II.2-12})$$

Now the Clebsh-Gordon coefficient, $C(L\ell s; 00)$, in Eq. (II.2-10) vanishes unless

$$L + \ell + s \text{ is even} \quad (\text{II.2-13})$$

and

$$\ell = |L-s|, |L-s| + 1, \dots, L+s \quad (\text{II.2-14})$$

Using Eq. (II.2-13) and remembering that L , ℓ and s are integers, it can be seen that

$$(-1)^{L+\ell-s} = (-1)^{L+\ell+s-2s} = (-1)^{-2s} = 1.$$

Hence Eq. (II.2-12) gives

$$C(L\ell s; m0) = C(L\ell s; -m0) \quad (\text{II.2-15})$$

We then obtain from Eq. (II.2-10) the condition

$$D(L, \ell, s, m) = D(L, \ell, s, -m) \quad (\text{II.2-16})$$

Using Eq. (II.2-16) in Eq. (II.2-8) it follows that

$R_s^m(r)$ and $R_s^{-m}(r)$ satisfy the same differential equation.

Hence, the energy eigenvalues obtained with m and $-m$ are equal.

In principle the solution of the infinite set of differential equations, given by Eq. (II.2-8), will give the exact solution of Eq. (II.1-1). However, for practical applications we need to truncate the infinite series in Eq. (II.2-5). Let the infinite sum in Eq. (II.2-5) be approximated by a finite sum;

$$\psi(r, \theta, \phi) = \sum_{\ell=0}^N \sum_{m=-\ell}^{\ell} R_{\ell}^m(r) Y_{\ell}^m(\theta, \phi) \quad (\text{II.2-17}).$$

The derivation of the radial wave equations for the radial wave functions in this approximation, the $R_{\ell}^m(r)$, is analogous to the derivation of the wave equations for the exact radial wave functions $R_{\ell}^m(r)$. The result is given by

$$\begin{aligned} & \left[\frac{d^2}{dr^2} + \frac{2}{r} \frac{d}{dr} + 2E - \frac{s(s+1)}{r^2} \right] R_s^m(r) \\ &= \sum_{L=0}^N \sum_{\ell=|L-s|}^{L+s} D(L, \ell, s, m) U_{\ell} R_L^m(r) \quad (\text{II.2-18}), \end{aligned}$$

where

$$s = 0, 1, 2, \dots, N.$$

The limit on the sum over ℓ occurring on the right hand side of Eq. (II.2-18) is obtained by using Eq. (II.2-14).

II.3 DISCUSSION OF THE CHOICE OF THE COORDINATE ORIGIN AND THE BOUNDARY CONDITIONS FOR THE PARTIAL WAVE METHOD

In order to solve the radial wave equations given by Eq. (II.2-18), it is necessary to specify the choice of the coordinate origin since the term U_{ℓ} occurring in

Eq. (II.2-18) depends on this choice. Furthermore to be physically acceptable, the solution of Eq. (II.2-18) has to satisfy certain boundary conditions. In this section we study both of these points in some detail.

II.3A THE CHOICE OF THE COORDINATE ORIGIN

The choice of the coordinate origin becomes very important when we want to actually solve Eq. (II.2-18) and obtain the solution that best represents the exact solution of Eq. (II.1-1). In principle the solution of the infinite number of coupled differential equations given by Eq. (II.2-18) will yield the exact solution of Eq. (II.1-1) for an arbitrary choice of the coordinate origin. For any finite N , however, the solution of Eq. (II.2-18) may be a poor representation of the exact solution of Eq. (II.1-1) unless proper care is taken in choosing the coordinate origin^{6-8,33}

II.3A-1 HOMONUCLEAR H_2^+ -LIKE MOLECULES ($Z_A = Z_B$)

(a) The Coordinate Origin at the Midpoint

$$(\rho_A = \rho_B = R/2).$$

Here the coordinate origin is chosen at the internuclear midpoint (simply called the midpoint). This choice of the coordinate origin is logical from a molecular symmetry point of view. The work of Refs. 15-7,35,36,42] show that good results for the interaction energy, see Eq. (II.1-3), can be obtained with this choice of

the coordinate origin for equilibrium and small R but for large R the results, in general, misbehave.

With this choice of the coordinate origin Eq. (II.2-18) splits into two separate groups of coupled equations. The quantity U_ℓ in Eq. (II.2-18) is zero if ℓ is odd, see Eq. (II.2-3). Now ℓ can be even only when both of L and s are either odd or even, see Eq. (II.2-15). Thus the coupling term $D(L, \ell, s, m) U_\ell$ in Eq. (II.2-18) is non-zero if both L and s are either odd or even. In other words in the midpoint calculations for homonuclear H_2^+ -like molecules the odd and even s value equations couple separately. Writing Eq. (II.2-18) explicitly for odd values of s we obtain

$$\left[\frac{d^2}{dr^2} + \frac{2}{r} \frac{d}{dr} + 2E - \frac{s(s+1)}{r^2} \right] R_s^m(r) = \sum_{\substack{L=1 \\ L \text{ odd}}}^{2N-1} \sum_{\ell=|L-s|}^{L+s} D(L, \ell, s, m) U_\ell R_L^m(r) \quad (\text{II.3-1A}),$$

where

$$s = 2\mu + 1 \quad (\text{II.3-1B}),$$

$$\mu = 0, 1, 2, \dots, N-1 \quad (\text{II.3-1C}),$$

$$N = \frac{N+1}{2} \text{ for odd } N. \quad (\text{II.3-1D}),$$

$$N = \frac{N}{2} \text{ for even } N \quad (\text{II.3-1E}),$$

and

$$N \geq 1 \quad (\text{II.3-1F}).$$

It is clear that N is the total number of differential equations that couple with each other for odd values of s and that the values of L are also odd in this case. The corresponding equations for even values of s are given by

$$\left[\frac{d^2}{dr^2} + \frac{2}{r} \frac{d}{dr} + 2E - \frac{s(s+1)}{r^2} \right] R_s^m(r) = \sum_{\substack{L=0 \\ L \text{ even}}}^{2N-2} \sum_{l=|L-s|}^{L+s} D(L, l, s, m) U_{lL}^m(r) \quad (\text{II.3-2A}),$$

where

$$s = 2\mu \quad (\text{II.3-2B})$$

$$\mu = 0, 1, 2, \dots, N-1 \quad (\text{II.3-2C}),$$

$$N = \frac{N+1}{2} \text{ for odd } N \quad (\text{II.3-2D}),$$

$$N = \frac{N+2}{2} \text{ for even } N \quad (\text{II.3-2E})$$

and

$$N \geq 1 \quad (\text{II.3-2F})$$

It is clear that N , given by Eqs. (II.3-2D)-(II.3-2F), is the total number of differential equations that couple with each other for even values of s . In this case the values of L are also even. Equation (II.3-1A) is used for odd (u) states and Eq. (II.3-2A) is used for even (g) states of a homonuclear H_2^+ -like molecule in midpoint calculations.

(b) The Coordinate Origin at the Nucleus

$$A(\rho_A = 0, \rho_B = R).$$

In this treatment the coordinate origin is

chosen to be at one of the nuclei, A say. The work of Refs. [14,57-59] show that this choice of the coordinate origin gives accurate interaction energies for large values of R . It should be mentioned that for this choice of the coordinate origin we can not obtain separate groups of coupled differential equations for the g and u states of the molecule.

(c) The Coordinate Origin at a Floating Point

$$(\rho_A = \rho_{op}, \rho_B = R - \rho_{op})$$

Here $\rho_A = \rho_{op}$ and $\rho_B = R - \rho_{op}$ are obtained by minimizing the energy E with respect to the position of the coordinate origin and the calculations made by using ρ_{op} are called the floating centre calculations. From the variational principle it follows that for all R the floating centre results for the energy must be either lower than or the same as the results obtained by using choices (a) and (b) for the coordinate origin, see for example Refs. [29-33]. Unless $\rho_{op} = R/2$ we can not obtain, from Eq. (II.2-18), separate groups of coupled differential equations for the g and u states of the molecules.

II.3A-2 HETERONUCLEAR H_2^+ -LIKE MOLECULES ($Z_A \neq Z_B$)

(a') The Coordinate Origin at the Midpoint

$$(\rho_A = \rho_B = R/2).$$

Here the coordinate origin is chosen to be at the internuclear midpoint. The works of Refs. [6,5(b)]

show that for small R this choice of the coordinate origin gives reasonable interaction energies for H_2^+ -like molecules. A more suitable choice of the coordinate origin for small R will be, see Refs. [3,6,32], at the nuclear charge centre

$$\rho_A = \frac{Z_B R}{Z_A + Z_B} \quad \text{III.3-3).$$

(b') The Coordinate Origin at the Nucleus A.

$$(\rho_A = 0, \rho_B = R).$$

The dissociation of a heteronuclear H_2^+ -like molecule can produce

(1) a light atom or ion A + a heavy nucleus B
or

(2) a heavy ion A + a light nucleus B.

For intermediate and large R it is reasonable^{5,6} to choose the coordinate origin at the nucleus of the atom or ion A. For small R we can use either this choice or the choice given in (a') for the coordinate origin.

(c') The Coordinate Origin at the Floating Point

$$(\rho_A = \rho_{op}, \rho_B = R - \rho_{op}).$$

Here $\rho_A = \rho_{op}$ and $\rho_B = R - \rho_{op}$ are obtained by minimizing the energy with respect to the position of the coordinate origin. From the variational principle it follows that the energies obtained by using $\rho_A = \rho_{op}$ must be lower than or the same as the energies obtained by using (a') and (b') for

the choices of the coordinate origin, see for examples Refs. [6, 29(b), 29(c), 32].

II.3B THE BOUNDARY CONDITIONS

In the present work only bound states of H_2^+ -like molecules are considered. To be a physically admissible solution of Eq. (II.1-1), the wave function, ψ , and its gradient, $\nabla\psi$, have to be bounded and continuous[†] functions⁶⁰ of the coordinates of the electron. ψ also has to satisfy the condition^{60,61}

$$\langle \psi | \psi \rangle = \text{a finite number} \quad (\text{II.3-4}).$$

Because $Y_\ell^m(\theta, \phi)$ is a bounded and continuous function of θ and ϕ , the boundary conditions on ψ and $\nabla\psi$ impose, see Eq. (II.2-17), the following boundary conditions^{35,36} on the radial wave functions and their derivatives in the interval $0 \leq r \leq \infty$:

$$(1) \quad R_s^m(r) \text{ is bounded and continuous in } r$$

$$(2) \quad \frac{dR_s^m(r)}{dr} \text{ is bounded and continuous in } r$$

and

$$(3) \quad \int_0^\infty (R_s^m(r)r)^2 dr = \text{finite number}.$$

In order to solve Eq. (II.2-18), it is often convenient^{60,61} to eliminate the first derivative in the differential equation by substituting

$$rR_s^m(r) = F_s^m(r) \quad (\text{II.3-5}).$$

[†] ψ and $\nabla\psi$ are continuous except at the singularities of H .

The boundary conditions on $\tilde{R}_s^m(r)$ and $\frac{d\tilde{R}_s^m(r)}{dr}$ yield the following boundary conditions on $F_s^m(r)$ and $\frac{dF_s^m(r)}{dr}$:

(1') $F_s^m(r)$ is bounded and continuous in r

(2') $\frac{dF_s^m(r)}{dr}$ is bounded and continuous in r

and

(3') $\int_0^\infty (F_s^m(r))^2 dr = \text{finite number.}$

It is useful to consider in more detail the behaviour of $F_s^m(r)$ in the limits $r \rightarrow 0$ and $r \rightarrow \infty$. Since the wave function is bounded and satisfies the condition given by Eq. (II.3-4) the $F_s^m(r)$ satisfy the relation

$$\lim_{r \rightarrow 0} F_s^m(r) = \lim_{r \rightarrow \infty} F_s^m(r) = 0 \quad (\text{II.3-6}).$$

Substitution of Eq. (II.3-5) in Eq. (II.2-18) gives

$$\begin{aligned} & \left[\frac{d^2}{dr^2} + 2E - \frac{s(s+1)}{r^2} \right] F_s^m(r) \\ &= \sum_{\ell=0}^N \sum_{\ell=|L-s|}^{L+s} D(L, \ell, s, m) U_\ell F_{L_\ell}^m(r) \end{aligned} \quad (\text{II.3-7}).$$

In the limit $\rho_B < r \rightarrow \infty$, Eq. (II.3-7) can be written, neglecting all the $\frac{1}{r}$ terms, see Eq. (II.2-3), as⁶²

$$\frac{d^2 F_s^m(r)}{dr^2} + 2E F_s^m(r) \sim 0 \quad (\text{II.3-8}).$$

The general solution of Eq. (II.3-8) is given by

$$F_s^m(r) = A e^{-\sqrt{2E} r} + B e^{+\sqrt{2E} r} \quad (\text{II.3-9}).$$

For $E < 0$ (bound states), $F_S^m(r)$ can be bounded in $0 \leq r \leq \infty$ only when $B = 0$. Thus as $r \rightarrow \infty$, $F_S^m(r)$ behaves as

$$F_S^m(r) \sim e^{-\sqrt{-2E} r} \quad (\text{II.3-10})$$

CHAPTER III
THE EXACT SOLUTION OF THE RADIAL EQUATIONS
FOR H_2^+ -LIKE MOLECULES

In this chapter the radial equations, given by Eq. (II.3-7) are solved for the bound states of H_2^+ -like molecules. These equations are solved here by both analytical and numerical methods. The discussion of the analytical method is given in Sec. III.2 and that of the numerical method is given in Sec. III.3.

III.1 DIVISION OF THE CONFIGURATION SPACE ($0 \leq r \leq \infty$) INTO REGION I ($0 \leq r \leq \rho_B$) AND REGION II ($\rho_B \leq r \leq \infty$)

The main difficulty in solving the radial equations is due to the term U_ℓ in Eq. (II.3-7). With the coordinate origin located at an arbitrary point between $\rho_A = 0$ and $\rho_A = R/2$, see Fig. II.1-1, and Eq. (II.2-3), U_ℓ can assume different functional forms depending on the part of the radial configuration space ($0 \leq r \leq \infty$) under consideration;

Region 1 ($0 \leq r \leq \rho_A$; ρ_B ; $\rho_A, \rho_B \neq 0$)

$$U_\ell = -[(-1)^\ell \frac{Z_A}{\rho_A^{\ell+1}} + \frac{Z_B}{\rho_B^{\ell+1}}] r^\ell \quad (\text{III.1-1})$$

Region 2 ($0 \leq \rho_A \leq r \leq \rho_B$; $\rho_B \neq 0$)

$$U_\ell = -[(-1)^\ell \frac{Z_A \rho_A^\ell}{r^{\ell+1}} + \frac{Z_B r^\ell}{\rho_B^{\ell+1}}] \quad (\text{III.1-2})$$

and

Region 3 ($0 \leq \rho_A \leq \rho_B \leq r \leq \infty$)

$$U_\ell = -[(-1)^\ell Z_A \rho_A^\ell + Z_B \rho_B^\ell] \frac{1}{r^{\ell+1}} \quad (\text{III.1-3}).$$

Since U_ℓ changes form as a function of r , it is difficult to obtain a single functional form, valid in the entire region $0 \leq r \leq \infty$, for the radial functions $F_s^m(r)$. It is therefore convenient to solve Eq. (II.3-7) in the three regions, specified by Eqs. (III.1-1)-(III.1-3), separately. By matching these separate solutions and their first derivatives at the common boundaries, the $F_s^m(r)$ can be obtained for the total region $0 \leq r \leq \infty$.

Various choices of the coordinate origin have been discussed in Sec. II.3A. Two of these choices, namely, "The Coordinate Origin at the Midpoint ($\rho_A = \rho_B = R/2$)" and "The Coordinate Origin at the Nucleus A ($\rho_A = 0, \rho_B = R$)" are based on well developed physical or symmetry arguments. Both of these choices correspond to dividing the region $0 \leq r \leq \infty$ into two and not three regions;

Region I $0 \leq r \leq \rho_B$ (III.1-4)

and

Region II $\rho_B \leq r \leq \infty$ (III.1-5).

In Sec. III.2 the analytic solution of Eq. (II.3-7) is given for $\rho_A = 0$ and $\rho_A = R/2^\dagger$. It is important to realize

[†]In practical uses of the analytical method these two choices for ρ_A will cover all R values for which the one centre approach yields reasonable results, see Chapters IV and V and also Refs. [8,29(a)].

that in the most general case, the coordinate origin is located at a floating point (where $\rho_A = \rho_{op}$, $0 \leq \rho_A \leq \rho_B$), see cases (c) and (c') of Secs. II.3A-1 and II.3A-2.

Because of the mixed form of U_ℓ in Region 2, see Eq. (III.1-2), it is tedious to solve Eq. (II.3-7) analytically when $0 < \rho_A < \rho_B$. The numerical solution, given in Sec. III.3, is valid for all choices for ρ_A .

The solutions of Eq. (II.3-7), see Sec. III.2, are expressed in terms of the energy, E , and constants of integration. The energy and the constants of integration are determined in Sec. III.4 by demanding that the $F_s^m(r)$ satisfy the conditions (1'), (2') and (3') of Sec. II.3B.

III.2 THE ANALYTIC SOLUTION OF THE RADIAL EQUATIONS

The radial equations, given by Eq. (II.3-7), are solved analytically in this section. The solutions obtained here are valid for all bound states of a H_2^+ -like molecule.

For the approximate wave function, given by Eq. (II.2-17), there are $(N+1)$ coupled differential equations to solve for any given value of m . See Sec. II.3A. For the sake of clarity in notation the subscript m can be suppressed. Thus we write

$$D(L, \ell, s) = D(E, \ell, s, m) \quad (\text{III.2-1})$$

and

$$F_s(r) = F_s^m(r) \quad (\text{III.2-2})$$

Using this notation Eq. (II.3-7) assumes the form

$$\left[\frac{d^2}{dr^2} + 2E - \frac{s(s+1)}{r^2} \right] F_s(r) = \sum_{L=0}^N \sum_{\ell=|L-s|}^{L+s} D(L, \ell; s) U_\ell F_L(r) \quad (\text{III.2-3}).$$

In what follows Eq. (III.2-3), which is the same as Eq. (II.3-7), is solved in Region I and Region II, see Eqs. (III.1-4) and (III.1-5).

III.2A THE ANALYTIC SOLUTION OF THE RADIAL EQUATIONS IN REGION I ($0 \leq r \leq \rho_B$)

The solutions of Eq. (III.2-3) with the coordinate origin at one of the nuclei, $\rho_A = 0$, and at the inter-nuclear midpoint, $\rho_A = R/2$, are given below for $0 \leq r \leq \rho_B$.

III.2A-1 THE COORDINATE ORIGIN AT THE NUCLEUS A ($\rho_A = 0, \rho_B = R$)

In order to solve Eq. (III.2-3) in Region I, it is convenient to isolate the terms that give the correct behaviour of $F_s(r)$ in the limit $r \rightarrow 0$. In this region U_ℓ is given by, see Eq. (III.1-2),

$$U_\ell = -\left[\frac{Z_A}{r} \delta_{\ell 0} + \frac{Z_B r^\ell}{R^{\ell+1}} \right] \quad (\text{III.2-4}).$$

In the vicinity of the origin Eq. (III.2-3) can be written as

$$\left[\frac{d^2}{dr^2} - \frac{s(s+1)}{r^2} \right] F_s(r) \approx 0 \text{ for } s \neq 0 \quad (\text{III.2-5})$$

and

$$\left[\frac{d^2}{dr^2} + \frac{2Z_A}{r} \right] F_0(r) \approx 0 \text{ for } s = 0 \quad (\text{III.2-6}).$$

The term, $\frac{2Z_A}{r}$, in Eq. (III.2-6) is obtained from Eq. (III.2-3) by using the relation

$$D(L, 0, s) = 2\delta_{Ls} \quad (\text{III.2-7}).$$

Equation (III.2-7) is obtained from Eqs. (II.2-10), (III.2-1) and the relation⁴⁶

$$C(l_1 0 l_3; m_1 0 m_3) = \delta_{l_1 l_3} \delta_{m_1 m_3} \quad (\text{III.2-8}).$$

Equations (III.2-5) and (III.2-6) are similar to the limiting differential equations for the hydrogen atom as $r \rightarrow 0$, see for example Merzbacher⁶². The solutions of these equations, that satisfy the relations given by Eq. (II.3-6), behave as

$$\lim_{r \rightarrow 0} F_s(r) \sim r^{s+1} \text{ for } s \geq 0 \quad (\text{III.2-9}).$$

$F_s(r)$ is hence written as

$$F_s(r) = r^{s+1} \chi_s(r) \quad (\text{III.2-10}),$$

where the $\chi_s(r)$ are to be determined. Substitution of Eq. (III.2-10) in Eq. (III.2-3) gives

$$\begin{aligned} & \left[\frac{d^2}{dr^2} + \frac{2(s+1)}{r} \frac{d}{dr} + 2E \right] \chi_s(r) \\ &= \sum_{L=0}^N \sum_{l=|L-s|}^{L+s} D(L, l, s) U_l r^{L-s} \chi_L(r). \end{aligned} \quad (\text{III.2-11}).$$

We try a series expansion[†] for $\chi_s(r)$ in the form

[†]The system of $(N+1)$ second order differential equations represented by Eq. (III.2-11) can be transformed into a system of $2(N+1)$ first order differential equations

$$\chi_s(r) = \sum_{j=0}^{\infty} a_j^{(s)} r^j \quad (\text{III.2-12})$$

Substituting Eq. (III.2-12) into Eq. (III.2-11), using Eqs. (III.2-4) and (III.2-7) and comparing the coefficients of equal powers of r gives

$$a_0^{(s)} \neq 0, a_1^{(s)} = -\frac{Z_A a_0^{(s)}}{1+s} \quad (\text{III.2-13}),$$

$$a_{j+2}^{(s)} = -\frac{2[Z_A a_{j+1}^{(s)} + E a_j^{(s)} + T_j^{(s)}]}{(j+2)(j+3+2s)} \quad (\text{III.2-14}),$$

where

$$T_j^{(s)} = \frac{1}{2} \sum_{L=0}^N \sum_{\ell=|L-s|}^{L+s} D(L, \ell, s) Z_B a_{j-L-\ell+s}^{(L)} / R^{\ell+1} \quad (\text{III.2-15})$$

and

$$a_v^{(s)} = 0, v < 0; j - L - \ell + s \leq j \quad (\text{III.2-16}).$$

In Eq. (III.2-16), $j - L - \ell + s \leq j$ since the maximum value of $-L - \ell + s = 0$. This follows, see Eq. (II.2-14), since the minimum value of $\ell = |L-s|$.

for $\chi_s(r)$ and $\frac{d\chi_s(r)}{dr}$. A general discussion on systems of first order differential equations can be found in, for example Refs. [63,64]. It can be shown, using Ref. [63], that the system of first order differential equations for

$\chi_s(r)$ and $\frac{d\chi_s(r)}{dr}$ has a unique solution with the form of

$\chi_s(r)$ given by Eq. (III.2-12).

If the energy, E , and the constants of integration, $a_0^{(s)}$, are known then Eqs. (III.2-13) - (III.2-16) can be used to calculate the higher order coefficients, $a_{j+2}^{(s)}$, for the series for the $\chi_s(r)$, see Eq. (III.2-12). A discussion of the determination of E and $a_0^{(s)}$ is given in sec. III.4. Appendix B contains a discussion of the convergence of the series for the $\chi_s(r)$.

III.2A-2 THE COORDINATE ORIGIN AT THE MIDPOINT

$$(\rho_A = \rho_B = R/2)$$

Here the term U_ℓ is given by, see Eq. (III.1-1),

$$U_\ell = -[(-1)^\ell z_A + z_B] \frac{2^{\ell+1} r^\ell}{R^{\ell+1}} \quad (\text{III.2-17}).$$

In the limit $r \rightarrow 0$, Eq. (III.2-3) can be written as

$$\frac{d^2 F_s(r)}{dr^2} - \frac{s(s+1)}{r^2} F_s(r) \simeq 0 \text{ for } s \neq 0 \quad (\text{III.2-18})$$

and

$$\frac{d^2 F_0(r)}{dr^2} + b^2 F_0(r) \simeq 0 \text{ for } s = 0 \quad (\text{III.2-19}),$$

where

$$b^2 = 2[E + \frac{2Z}{R}], \quad Z = z_A + z_B \quad (\text{III.2-20}).$$

The form of the solution of Eq. (III.2-18) has already been discussed in Sec. III.2A-1. The general solution of Eq. (III.2-19) is given by

$$F_0(r) = A \sin(br) + B \cos(br) \quad (\text{III.2-21}).$$

Since $\lim_{r \rightarrow 0} F_0(r) = 0$, see Eq. (II.3-6), $B = 0$ in

Eq. (III.2-21). From the form of the solution of Eq. (III.2-18), see Eq. (III.2-9), and from the limiting behaviour of $\sin(br)$ as $r \rightarrow 0$, it can be seen that for midpoint calculations the form of $F_s(r)$ is given by Eq. (III.2-10).

The procedure for finding the recursion relations for the coefficients for $\chi_s(r)$ is almost identical with that used for the solution of the analogous problem with the coordinate origin at the nucleus A, see Sec. III.2A-1. The only difference is that Eq. (III.2-17) and not Eq. (III.2-4) has to be used in Eq. (III.2-11). The recursion relations for the coefficients are as follows:

$$a_0^{(s)} \neq 0; a_1^{(s)} = 0 \quad (\text{III.2-22})$$

$$a_{j+2}^{(s)} = - \frac{2[Ea_j^{(s)} + T_j^{(s)}]}{(j+2)(j+3+2s)} \quad (\text{III.2-23}),$$

where

$$T_j^{(s)} = \frac{1}{2} \sum_{L=0}^N \sum_{\ell=|L-s|}^{L+s} D(L, \ell, s) \{ (-1)^\ell Z_A + Z_B \}$$

$$\frac{2^{\ell+1}}{R^{\ell+1}} a_{j-L-\ell+s}^{(L)} \quad (\text{III.2-24A}),$$

and

$$a_v^{(s)} = 0, v < 0; j - L - \ell + s \leq j \quad (\text{III.2-24B}).$$

There is one important difference in the recursion relations for the expansion coefficients for the two choices for ρ_A , namely, $\rho_A = 0$ and

$\rho_A = R/2$. When the coordinate origin is at the internuclear midpoint, $\rho_A = R/2$, $a_{j+2}^{(s)} = 0$ if $(j+2)$ is odd. To show this we notice that $D(L, l, s) = 0$ unless $L+l+s$ is even, see Eq. (II.2-13). Hence the subscript of the coefficients $a^{(L)}$, see Eq. (III.2-24A), given by $j-L-l+s = j+2s-(L+l+s)$ is an odd number if j is odd. Therefore, from Eq. (III.2-23), it can be seen that the coefficients with odd and even subscripts couple separately. Since $a_1^{(s)} = 0$, $a_{j+2}^{(s)} = 0$ for odd values of j for any Z_A , Z_B and n .

III.2B THE ANALYTIC SOLUTION OF THE RADIAL EQUATION IN REGION II ($\rho_B \leq r \leq \infty$)

The solution of the radial equations in Region II is considerably more complicated than the corresponding solution in Region I. In Region II, it is convenient to write $F_S(r)$ as

$$F_S(r) = y(r)f_S(r) \quad (\text{III.2-25A}),$$

where

$$\lim_{r \rightarrow \infty} F_S(r) \sim y(r) \quad (\text{III.2-25B}).$$

The differential equation for $f_S(r)$, which is obtained from that for $F_S(r)$, see Eq. (III.2-3), is called the reduced differential equation. If $f_S(r)$ is expanded in a power series about $r = \infty$, the series represents the asymptotic solution of the reduced differential equation, see Sec. III.2B-4. If however $f_S(r)$ is expanded in a series about $r = d$, where d is finite, and if the coefficients of the expansion are properly determined, then the series for $f_S(r)$ provides a convergent series solution of the reduced

differential equation, see Sec. III.2B-2. There is one practical difficulty in this latter procedure, namely a one step series solution for $f_g(r)$, expanded about $r = d$, is a very slowly convergent series for arbitrary values of r for any particular choice of d in Region II. To alleviate this practical difficulty, a stepwise method is discussed in Sec. III.2B-3.

III.2B-1 THE DERIVATION OF THE REDUCED DIFFERENTIAL EQUATION

To derive the reduced differential equation, one must know the form of $y(r)$, see Eq. (III.2-25A), which gives the correct behaviour of $F_g(r)$ in the limit $r \rightarrow \infty$. In Chapter II, one possible form of $F_g(r)$, given by Eq. (II.3-10), is obtained by solving Eq. (II.3-8) which is obtained from the radial equation, see Eq. (II.3-7), by ignoring terms that behave as $(\frac{1}{r})$ and higher powers of $(\frac{1}{r})$ in the limit $r \rightarrow \infty$. We begin the derivation of the reduced differential equation by finding a better approximate form for $F_g(r)$, as $r \rightarrow \infty$.

Let the function $y(r)$, see Eq. (III.2-25A), be expressed⁶⁵ as

$$y = r^{C_1} e^{C_2 r} \quad (\text{III.2-26})$$

where the constants C_1 and C_2 have to be determined.

The inclusion of an exponential term in Eq.

(III.2-26) is suggested by the form of $F_g(r)$ given by Eq. (II.3-10). In Region II, the term U_2 is given by, see Eq. (III.1-3),

$$U_l = -\frac{Z}{r} \delta_{l0} + \frac{\alpha_l}{r^{l+1}} \Gamma_{l0} \quad (\text{III.2-27}),$$

where

$$Z = Z_A + Z_B; \Gamma_{l0} = 1 - \delta_{l0}; \alpha_l = -[(-1)^l Z_A \rho_A^l + Z_B \rho_B^l] \quad (\text{III.2-28}).$$

Using Eqs. (III.2-7) and (II.2-25A)-(III.2-28) in the radial equation for $F_s(r)$, see Eq. (III.2-3), yields

$$\begin{aligned} & \left[\frac{d^2 f_s}{dr^2} + 2 \left(\frac{C_1}{r} + C_2 \right) \frac{df_s}{dr} \right] r^{C_1} e^{C_2 r} \\ & + \left[C_2^2 + 2E + \frac{2C_1 C_2 + 2Z}{r} \right] F_s(r) \\ & + \left[\frac{C_1(C_1 - 1) - s(s+1)}{r^2} \right] F_s(r) \\ & = \sum_{L=0}^N \sum_{l=|L-s|}^{L+s} D(L, l, s) \frac{\alpha_l}{r^{l+1}} F_L(r) \Gamma_{l0}, \\ & s = 0, 1, 2, \dots, N \end{aligned} \quad (\text{III.2-29}).$$

The constants C_1 and C_2 are chosen so that the second term on the left hand side of Eq. (III.2-29) vanishes, that is

$$C_2 = -K = -\sqrt{-2E}; C_1 = \frac{Z}{K} \quad (\text{III.2-30}).$$

With these choices for C_1 and C_2 , $F_s(r)$ becomes, see Eq. (III.2-25A)

$$F_s(r) = r^{\frac{Z}{K}} e^{-Kr} f_s(r) \quad (\text{III.2-31}).$$

The exponential term in Eq. (III.2-31) is the same as the approximate form of $F_s(r)$ given by Eq. (II.3-10). To complete the derivation of the

improved form of $F_s(r)$ as $r \rightarrow \infty$, the behaviour of $f_s(r)$ as $r \rightarrow \infty$ must be investigated. To do this neglect all terms behaving as $(\frac{1}{r})^j$, $j = 2, 3, \dots$ in Eq. (III.2-29) and use Eq. (III.2-30) to give

$$\frac{d^2 f_s}{dr^2} + 2\left(\frac{Z}{Kr} - K\right) \frac{df_s}{dr} = 0 \quad (\text{III.2-32}).$$

The general solution of Eq. (III.2-32) is given by

$$f_s(r) = A + B \int^r e^{2Kx} x^{-\frac{2Z}{K}} dx \quad (\text{III.2-33}),$$

where A and B are constants of integration. Since $F_s(r)$ must be finite in $0 \leq r \leq \infty$, see Sec. II.3B, $B = 0$ in Eq. (III.2-33). Thus one finds that,

$$\lim_{r \rightarrow \infty} f_s(r) = \text{constant} \quad (\text{III.2-34})$$

and hence

$$\lim_{r \rightarrow \infty} F_s(r) \sim r^{\frac{Z}{K}} e^{-Kr} \quad (\text{III.2-35}).$$

In order to obtain the required reduced differential equation for $f_s(r)$ all the terms in Eq. (III.2-29) are divided by $r^{C_1} e^{C_2 r}$, where C_1 and C_2 are given by Eq. (III.2-30). This process yields

$$\begin{aligned} & \left[\frac{d^2}{dr^2} + 2\left(\frac{Z}{Kr} - K\right) \frac{d}{dr} + \frac{A_s}{r^2} \right] f_s(r) \\ &= \sum_{L=0}^N \sum_{\ell=|L-s|}^{L+s} D(L, \ell, s) \frac{a_\ell}{r^{\ell+1}} f_L(r) \Gamma_{\ell 0} \end{aligned} \quad (\text{III.2-36}),$$

where

$$s = 0, 1, 2, \dots, N$$

and

$$A_s = \frac{Z}{K} \left(\frac{Z}{K} - 1 \right) - s(s+1).$$

The reduced differential equation, given by Eq.

(III.2-36), is solved in the following sections.

III.2B-2. THE SOLUTION OF THE REDUCED DIFFERENTIAL EQUATION

To solve the reduced differential equation, given by Eq. (III.2-36), we start by defining a new independent variable, t ,

$$t = \frac{d}{r} - 1 \quad (\text{III.2-37}),$$

where

$$\rho_B \leq d \leq r < \infty \quad (\text{III.2-38}).$$

The solution given in this section is valid for an arbitrary value of d satisfying Eq. (III.2-38).

in terms of the new variable, t , Eq. (III.2-36)

becomes

$$\begin{aligned} & \left[\frac{d^2}{dt^2} + 2 \left(1 - \frac{Z}{K} \right) \frac{1}{1+t} + \frac{Kd}{(1+t)^2} \right] \frac{d}{dt} + \frac{A_s}{(1+t)^2} f_s(t) \\ &= \sum_{L=0}^N \sum_{\ell=|L-s|}^{L+s} B(L\ell s) (1+t)^{\ell-3} f_L(t) \Gamma_{\ell 0} \end{aligned} \quad (\text{III.2-39}),$$

where

$$B(L\ell s) = D(L, \ell, s) \alpha_{\ell} d^{1-\ell} \quad (\text{III.2-40}).$$

In Eq. (III.2-39), the coefficients of $f_s(t)$ and

$\frac{df_s(t)}{dt}$ are analytic at $t = 0$. Therefore $f_s(t)$

can be expanded in powers of t about $t = 0$ in the

form⁶³

$$f_s(t) = \sum_{j=0}^{\infty} g_j^{(s)} t^j \quad (\text{III.2-41}).$$

The Taylor series expansions⁶⁶ of $\frac{1}{1+t}$ and $\frac{1}{(1+t)^2}$ about $t = 0$ are given by

$$\frac{1}{1+t} = \sum_{\mu=0}^{\infty} (-t)^{\mu}; \quad \frac{1}{(1+t)^2} = \sum_{\mu=0}^{\infty} (\mu+1) (-t)^{\mu} \quad (\text{III.2-42}),$$

where $-1 < t \leq 0$, see Eq. (III.2-37). Thus Eq. (III.2-39) can be written as

$$\begin{aligned} & \left[\frac{d^2}{dt^2} + \left[\sum_{\mu=0}^{\infty} \Omega_{\mu} (-t)^{\mu} \right] \frac{d}{dt} + A_s \sum_{\mu=0}^{\infty} (\mu+1) (-t)^{\mu} \right] f_s(t) \\ &= \sum_{L=0}^N \sum_{\ell=|L-s|}^{L+s} B(L\ell s) (1+t)^{\ell-3} f_L(t) \Gamma_{\ell 0} \end{aligned} \quad (\text{III.2-43}),$$

where

$$\Omega_{\mu} = 2 \left[\left(1 - \frac{2}{K}\right) + Kd(\mu+1) \right] \quad (\text{III.2-44}).$$

Substituting Eqs. (III.2-41) and (III.2-42) in Eq. (III.2-43) and comparing the coefficients of equal powers of t yields

$$\begin{aligned} g_{j+2}^{(s)} &= - \frac{1}{(j+1)(j+2)} \left[\sum_{\mu=0}^j \{ (j-\mu+1) \Omega_{\mu} g_{j-\mu+1}^{(s)} \right. \\ &\quad \left. + A_s (\mu+1) g_{j-\mu}^{(s)} \} (-1)^{\mu} - T_j^{(s)} \right] \end{aligned} \quad (\text{III.2-45}),$$

where

$$\begin{aligned} T_j^{(s)} &= \sum_{L=0}^N \sum_{\ell=|L-s|}^{L+s} B(L\ell s) \sum_{\mu=0}^j (-1)^{\mu} g_{j-\mu}^{(L)} \\ &\quad [\delta_{\mu 0} \delta_{\ell 3} + \delta_{\ell 2} + (\mu+1) \delta_{\ell 1}]; \quad \ell = 1, 2, 3 \end{aligned} \quad (\text{III.2-46}),$$

$$T_j^{(s)} = \sum_{L=0}^N \sum_{\ell=|L-s|}^{L+s} B(L\ell s) \sum_{\mu=0}^{\ell-3} \frac{(\ell-3)!}{(\ell-3-\mu)! \mu!} g_{j-\ell+3+\mu}^{(L)}; \quad \ell > 3 \quad (\text{III.2-47})$$

and

$$g_v^{(s)} = 0, \quad v < 0 \quad (\text{III.2-48})$$

The upper limits on the sums over μ in Eqs. (III.2-45) and (III.2-46) are obtained by using Eq. (III.2-48).

With E as a parameter, all the higher order coefficients, $g_{j+2}^{(s)}$, can be expressed in terms of the independent coefficients $g_0^{(s)}$ and $g_1^{(s)}$ by using Eqs. (III.2-45)-(III.2-48). The coefficients $g_0^{(s)}$ and $g_1^{(s)}$ can be determined as a function of the energy eigenvalue and the independent expansion coefficients, the $a_0^{(s)}$, of the radial functions in Region I. This is done by smoothly matching the solutions of the radial equation in Region I and Region II at $r = \rho_B$, see Sec. III.2B-3 and Appendix A for a specific example.

The recursion relations for the coefficients of the series for $f_s(t)$ are valid for arbitrary α_ℓ , see Eqs. (III.2-28), (III.2-40) and (III.2-45)-(III.2-48). In order to obtain the solutions for the two special cases where (a) the coordinate origin is located at the nucleus A ($\rho_A = 0$, $\rho_B = R$) and (b) the coordinate origin is located at the inter-nuclear midpoint ($\rho_A = \rho_B = R/2$), two special values of α_ℓ are used for $B(L\ell s)$ in Eq. (III.2-40), namely

$$\alpha_\ell = -[Z_A \delta_{\ell 0} + Z_B R^\ell]; \quad \rho_A = 0, \quad \rho_B = R \quad (\text{III.2-49})$$

and

$$\alpha_\ell = -[(-1)^\ell z_A + z_B] \frac{R^\ell}{2^\ell}; \quad \rho_A = \rho_B = R/2 \quad (\text{III.2-50}).$$

Appendix B contains a discussion on the convergence of the series for $f_s(t)$ for these two special cases.

There is a practical difficulty in using the recurrence relations, given by Eqs. (III.2-45)-(III.2-48), to determine the expansion coefficients for the series for $f_s(t)$, see Eq. (III.2-41). The difficulty arises because of the sums over μ in Eq. (III.2-43). These sums originate from the infinite sums in Eq. (III.2-42) which do not converge if $t = -1$ and slowly converge unless $|t|$ is small compared to unity. On the other hand for small $|t|$ Eq. (III.2-43) can be adequately approximated by using sums with a small number of terms and this fact is used in the stepwise method for solving the radial equations that is discussed in the next section.

III.2B-3 THE STEPWISE ANALYTIC SOLUTION OF THE RADIAL EQUATIONS IN REGION II ($\rho_B \leq r \leq \infty$)

To proceed in a stepwise way to solve the radial equations, the interval $\rho_B \leq r \leq \infty$ is divided into small intervals as shown in Fig. III.2-1. Since $F_s(r)$ represents the radial function for all r , we distinguish the solutions of the radial equations in

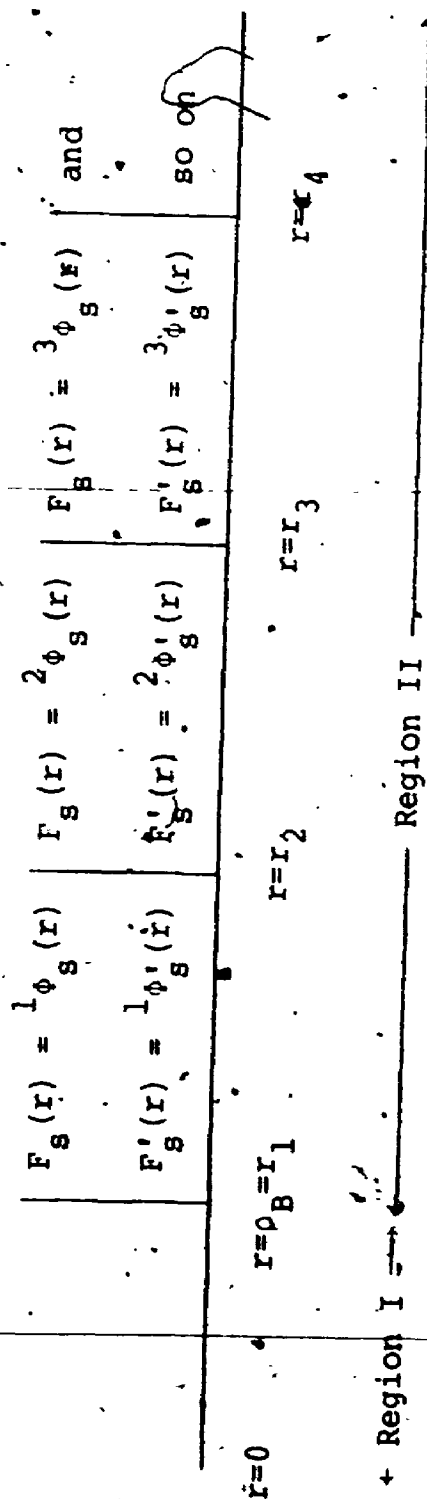


Figure III.2-1: Division of the interval $0 \leq r \leq \infty$ into small intervals for the stepwise solution of the radial equations given by Eq. (III.2-3).

the different intervals by the following definitions[†]

$$F_s(r) = {}^j\phi_s(r); \quad F'_s(r) = {}^j\phi'_s(r) \quad (\text{III.2-51A})$$

where

$$r_j \leq r \leq r_{j+1}; \quad j = 1, 2, \dots \quad (\text{III.2-51B})$$

For all j , ${}^j\phi_s(r)$ and ${}^j\phi'_s(r)$ are calculated by using Eqs. (III.2-31), (III.2-41) and (III.2-44) - (III.2-48). For different j , however, $g_0^{(s)}$ and $g_1^{(s)}$ have different values, see below.

To find the solutions of the radial equations the following steps are used:

(1) Find $F_s(r)$ and $F'_s(r)$ at $r = \rho_B$ from the solution of the radial equation in Region I. Find ${}^1\phi_s(r)$ and ${}^1\phi'_s(r)$ at $r = \rho_B = d = r_1$, that is at $t = 0$. The matching conditions

$$F_s(\rho_B) = {}^1\phi_s(\rho_B) \quad (\text{III.2-52A})$$

$$F'_s(\rho_B) = {}^1\phi'_s(\rho_B) \quad (\text{III.2-52B})$$

then give^{††} the values of $g_0^{(s)}$ and $g_1^{(s)}$ for the interval

[†]The prime denotes the first derivative of a quantity with respect to r .

^{††}The functions ${}^j\phi_s(r)$ and ${}^j\phi'_s(r)$ are obtained by using Eqs. (III.2-31), (III.2-41) and (III.2-51A). At $r = d$ that is at $t = 0$ these quantities are given by

$${}^j\phi_s(d) = d^{\frac{z}{K}} e^{-Kd} g_0^{(s)}$$

and

$${}^j\phi'_s(d) = {}^j\phi_s(d) \left[\frac{z}{Kd} - K \right] - \frac{d^{\frac{z}{K}} e^{-Kd} g_1^{(s)}}{d}$$

$r_1 \leq r \leq r_2$ in terms of the energy E and the constants of integration $a_0^{(s)}$, see Sec. III.2A. Calculate ${}^1\phi_s(r)$ and ${}^1\phi'_s(r)$ at $r = r_2$ using these values of $g_0^{(s)}$ and $g_1^{(s)}$ in the recursion relations for the coefficients of $f_s(t)$, see Eqs. (III.2-45)-(III.2-48).

(2) Find ${}^2\phi_s(r)$ and ${}^2\phi'_s(r)$ at $r = r_2 = d$ that is at $t = 0$ for the interval $r_2 \leq r \leq r_3$. Note the value of d here is different from that in point (1).

The matching conditions

$${}^1\phi_s(r_2) = {}^2\phi_s(r_2) \quad (\text{III.2-53})$$

and

$${}^1\phi'_s(r_2) = {}^2\phi'_s(r_2) \quad (\text{III.2-54})$$

give the values of $g_0^{(s)}$ and $g_1^{(s)}$ for the interval $r_2 \leq r \leq r_3$. Using these values of $g_0^{(s)}$ and $g_1^{(s)}$ for the interval $r_2 \leq r \leq r_3$, calculate ${}^2\phi_s(r)$ and ${}^2\phi'_s(r)$ at $r = r_3$.

(3) Repeat the procedure until r is sufficiently large that the radial functions $F_s(r)$ are zero for practical purposes. Appendix A contains a specific example of the stepwise method for solving the radial equations in Region II.

It is clear that the interval lengths (in terms of t for each interval), see Fig. III.2-1, are

$$\left| \frac{\rho_B}{r_2} - 1 \right|, \left| \frac{r_2}{r_3} - 1 \right|, \dots \quad \text{Now } r_2, r_3, \dots \text{ can be chosen such that } \Delta = \frac{\rho_B}{r_2} = \frac{r_2}{r_3} = \frac{r_3}{r_4} = \dots \quad \text{With these}$$

choices for r_2, r_3, \dots the interval length is constant

and it is given by $|\Delta - 1|$. It is important to note that although the interval length is constant in

terms of t , the interval length is not constant in terms of r . In any interval, $r_j \leq r \leq r_{j+1}$, t

satisfies the condition $0 \leq |t| \leq |\Delta - 1|$. By

choosing Δ large enough we can make $|t|$ sufficiently small for rapid convergence of the infinite series

in Eq. (III.2-43) (for example $\Delta = 0.7$ is sufficient for the ground state of the H_2^+ molecule for 7-coupled equations when $R = 4$ and $\rho_A = R/2$, see Appendix B).

As the stepwise process is carried forward from $r = \rho_B$ to large values of r the coefficients $g_{j+2}^{(s)}$ are expressed (through matching) in terms of the energy E and the constants of integration $a_0^{(s)}$ in every interval. Thus the only unknown quantities are E and the $a_0^{(s)}$. A discussion of the determination of E and $a_0^{(s)}$ is given in Sec. III.4.

III.2B-4 THE ASYMPTOTIC SOLUTION OF THE RADIAL EQUATIONS IN REGION II ($\rho_B \leq r \leq \infty$)

The stepwise method described in Sec. III.2B-3 becomes extremely laborious if the solutions are carried out too far from $r = \rho_B$. To reduce this practical difficulty an asymptotic solution of the radial equations is useful. When the asymptotic solution is matched with the solution obtained by the stepwise method, the $F_g(r)$ can be obtained for the entire region $0 \leq r \leq \infty$.

The coefficients of $\frac{df_s(r)}{dr}$ and $f_s(r)$ in Eq. (III.2-36) are analytic for all r in the interval $0 < \rho_B \leq r \leq \infty$. However the point $r = \infty$ is an irregular singular point, see for example Morse and Feshbach⁶⁷, in this equation. A series in power of $(\frac{1}{r})$ for $f_s(r)$ will provide an asymptotic solution of Eq. (III.2-36), see for example Tricomi⁶⁵ for the solution of an equation similar to the homogeneous part of the reduced differential equation given by Eq. (III.2-36). In order to find the asymptotic solution of the reduced differential equation we define a new independent variable, ξ , as

$$\xi = \frac{\rho_B}{r} \quad (\text{III.2-55}).$$

In terms of ξ Eq. (III.2-36) becomes

$$\begin{aligned} & \left[\frac{d^2}{d\xi^2} + 2 \left[\left(1 - \frac{Z}{K}\right) \frac{1}{\xi} + \frac{K\rho_B}{\xi^2} \right] \frac{d}{d\xi} + \frac{A_s}{\xi^2} \right] f_s(\xi) \\ &= \sum_{L=0}^N \sum_{\ell=|L-s|}^{L+s} B(L\ell s) \xi^{\ell-3} f_L(\xi) \Gamma_{\ell 0} \end{aligned} \quad (\text{III.2-56}),$$

where $B(L\ell s)$ is obtained by substituting $d = \rho_B$ in Eq. (III.2-40). It is obvious that the point $\xi = 0$ or $r = \infty$ is an irregular singular point in Eq. (III.2-56).

Let the function $f_s(\xi)$ be written as

$$f_s(\xi) = \sum_{j=0}^{\infty} h_j^{(s)} \xi^j \quad (\text{III.2-57}).$$

Substituting Eq. (III.2-57) in Eq. (III.2-56) and

comparing the coefficients of equal powers of ξ gives

$$h_{j+1}^{(s)} = \frac{1}{2K\rho_B(j+1)} \left[\sum_{L=0}^N \sum_{\ell=|L-s|}^{L+s} B(L\ell s) h_{j-\ell+1}^{(L)} \Gamma_{\ell 0} - \left\{ j(j+1 - \frac{2Z}{K}) + A_s \right\} h_j^{(s)} \right] \quad (\text{III.2-58}),$$

where $h_v^{(s)} = 0$, $v < 0$. With E as a parameter, the coefficients $h_{j+1}^{(s)}$ can be expressed in terms of the constants $h_0^{(s)}$ by using Eq. (III.2-58). The recursion relations, given by Eq. (III.2-58), provide the expansion coefficients for only one[†] solution of Eq. (III.2-56). As j increases the series representing the $f_s(\xi)$, see Eq. (III.2-57), appears to diverge asymptotically by demonstration, see Appendix B. The asymptotic divergence of this series for $f_s(\xi)$ is difficult to show analytically by using the many term recursion formula for $h_{j+1}^{(s)}$ given by

[†]The general form of the solution of the reduced differential equation in the limit that $r \rightarrow \infty$ or $\xi \rightarrow 0$, see Eq. (III.2-55), is given by Eq. (III.2-33). The solution provided by the recursion relations, given by Eq. (III.2-58), is regular at $\xi \rightarrow 0$ and corresponds to the part of Eq. (III.2-33) that behaves as the constant, A , in the limit $r \rightarrow \infty$. The second solution of Eq. (III.2-56) is irregular at $\xi \rightarrow 0$ and therefore not admissible as a physical solution. It corresponds to the term involving the constant B in Eq. (III.2-33).

Eq. (III.2-58). In order to obtain a physically acceptable solution of the reduced differential equation the divergent series is truncated, that is

$$f_s(\xi) = \sum_{j=0}^{M_s} h_j^{(s)} \xi^j \quad (\text{III.2-59}),$$

where M_s is chosen such that $|h_{M_s+1}^{(s)} \xi^{M_s+1}|$ is the smallest term in this series for any particular choice of ξ . The final form for $f_s(\xi)$ is obtained by adding a correction term to Eq. (III.2-59), see Morse and Feshbach⁶⁷, to give

$$f_s(\xi) = \sum_{j=0}^{M_s} h_j^{(s)} \xi^j + \frac{1}{2} h_{M_s+1}^{(s)} \xi^{M_s+1} \quad (\text{III.2-60}).$$

To obtain $f_s(\xi)$ for the two special cases where

- (a) the coordinate origin is located at the nucleus A ($\rho_A = 0$, $\rho_B = R$) and (b) the coordinate origin is located at the internuclear midpoint ($\rho_A = \rho_B = R/2$), the appropriate value of ρ_A has to be used in α_ℓ , see Eqs. (III.2-28) and (III.2-40).

III.3 THE NUMERICAL SOLUTION OF THE RADIAL EQUATIONS

In this section the radial equations given by Eq. (III.2-3), are solved by using numerical methods. These numerical methods are valid for all choices for ρ_A see Sec. II.3A, and for all eigenstates of an H_2^+ -like molecule. The results obtained by these methods can be used to cross-check those of the analytical method, see Chapter IV, and also furnish nice examples of usefulness of numerical methods in a rather complicated problem. A very useful

discussion of the numerical techniques used here is given by Fox^{35,48}.

Equation (III.2-3) is a system of (N+1) coupled differential equations belonging to a boundary value as well as an eigenvalue problem. The boundary conditions on $F_s(r)$ have been discussed in Sec. II-3B. The eigenvalue, E , has to be determined such that the solutions of the radial equations satisfy these boundary conditions. In order to solve the problem numerically, the differential equations are replaced by finite-difference equations. To obtain the finite-difference equations we approximate the second derivative of $F_s(r)$ ^{35,48,68} by

$$\frac{d^2 F_s}{dr^2} \approx \frac{1}{h^2} [F_s(r+h) - 2F_s(r) + F_s(r-h)] \quad (\text{III.3-1}),$$

where h is the grid size. Substitution of Eq. (III.3-1) into Eq. (III.2-3) yields[†] the finite-difference equations that represent the original coupled set of radial equations;

$$F_s(r+h) = \left[\frac{s(s+1)}{r^2} - 2E \right] h^2 + 2] F_s(r) - F_s(r-h) + h^2 \sum_{L=0}^N \sum_{\ell=|L-s|}^{L+s} D(L, \ell, s) U_{\ell} F_L(r) \quad (\text{III.3-2})$$

$s = 0, 1, 2, \dots, N$

[†]Although the first derivative is absent from Eq. (III.2-3), Numerov's method^{68,69} is not efficient for the coupled radial differential equations of this thesis.

In Eq. (III.3-2) the quantities $D(L, l, s)$ and U_l are given by their defining equations (III.1-1)-(III.1-3) and (III.2-1).

III.3A THE MATCHING METHOD FOR SOLVING THE RADIAL EQUATIONS

Equations (III.3-2) are used to obtain the numerical solution of the radial equations by the matching method. ^{35, 48, 68}

The basic ideas involved in this method are summarized by the following three points:

(1) The Forward Solution.

First consider the positive sign on the left hand side of Eq. (III.3-2). If E , $F_s(0)$ and $F_s(h)$ are given for all s then, by setting $r = h$, this equation can be solved algebraically for $F_s(2h)$. After obtaining $F_s(2h)$ and setting $r = 2h$ one can then find $F_s(3h)$ by using Eq. (III.3-2). This step by step method can be applied repeatedly until the $F_s(r)$ have been found at equidistant points in the entire region $0 \leq r \leq r_\infty$, where r_∞ is a sufficiently large value of r such that $F_s(r_\infty)$ is zero for practical purposes. The radial functions obtained by this procedure are called the forward solution of the radial equations (simply called the forward solution). The forward solution and related quantities, see later, are specified by the superscript, f , as for example in $F_s^f(r)$.

In order to carry out the forward integration by this step by step method it is necessary to know E , $F_s(0)$ and $F_s(h)$ for all values of s . Of these necessary quantities only $F_s(0)$ is provided by the boundary conditions on $F_s(r)$, namely $F_s(0) = 0$, see Eq. (II.3-6). In order to

obtain the forward solution under these circumstances, we introduce the following quantity

$$F_s(h) = f_{C_s} \quad (\text{III.3-3}),$$

where f_{C_s} is a constant yet to be determined. With initial estimates of E and all the f_{C_s} , the forward integration can be performed by using Eqs. (III.3-2) and (III.3-3).

It is important to note that one of the $(N+1)$ parameters $f_{C_0} \dots f_{C_N}$ can be assigned an arbitrary value which can later be fixed by normalization; we choose

$$f_{C_0} = 1 \quad (\text{III.3-4}).$$

This choice for f_{C_0} determines the size of $F_s(r)$ obtained by the forward integration. With f_{C_0} fixed by Eq. (III.3-4), one needs to estimate $(N+1)$ parameters, that is E , $f_{C_1} \dots f_{C_N}$. If the initial estimates of these $(N+1)$ parameters do not correspond to an eigenstate of the molecule, then the forward integration will not yield $f_{F_s}(r_\infty) = 0$. One can then adjust the parameters until the boundary condition on $F_s(r)$ is satisfied at $r = r_\infty$ (the boundary condition at $r = 0$ is automatically satisfied when the forward integration is started from the origin). In this way the numerical solution of the radial equations can, in principle, be found; see however point (3) below.

(2) The Backward Solution.

Now consider the negative sign on the left hand side of Eq. (III.3-2). If E , $F_s(r_\infty)$ and $F_s(r_\infty - h)$ are given for all s then, by setting $r = r_\infty - h$ in this equation, it can be solved for $F_s(r_\infty - 2h)$. After finding $F_s(r_\infty - 2h)$ and setting

$r = r_\infty - 2h$ in Eq. (III.3-2) one can obtain $F_s(r_\infty - 3h)$.

This step by step method can be continued until the $F_s(r)$ have been found at equidistant points in the entire region $0 \leq r \leq r_\infty$. The solution of the radial equations obtained by this procedure is called the backward solution. The backward solution and related quantities, see later, are specified by the superscript b as for example in ${}^bF_s(r)$. Of the quantities E , $F_s(r_\infty)$ and $F_s(r_\infty - h)$ necessary to perform the backward integration only $F_s(r_\infty)$ is provided by the boundary condition on $F_s(r)$, namely $F_s(r_\infty) = 0$; see

Sec. II.3B. Let us define

$$F_s(r_\infty - h) = {}^bC_s \quad (\text{III.3-5}),$$

where the constant bC_s has to be determined. With initial estimates for E and all the bC_s the backward integration can be carried out. One of the $(N+1)$ quantities ${}^bC_0 \dots {}^bC_N$ can be assigned an arbitrary value; choose for example

$${}^bC_0 = 1 \quad (\text{III.3-6}).$$

This choice for bC_0 determines the size of the backward solution. After choosing bC_0 , we are left with $(N+1)$ parameters, namely $E, {}^bC_1 \dots {}^bC_N$. If the initial estimates of these parameters are not those associated with an eigenstate of the molecule, the backward solution will not produce ${}^bF_s(0) = 0$. One can then adjust the parameters until ${}^bF_s(0) = 0$ for all s and thus, in principle, find the numerical solution of the radial equations; see point (3) below.

(3) The Solution Obtained by the Matching Method.

In principle the methods described in points (1) and (2) can be used to find the energy eigenvalue and the radial functions. However these methods have a practical difficulty associated with them. In practice the forward and backward integrations are not performed using exact values of the parameters E and C 's. If the integrations are carried out from one boundary to the other using even moderately accurate values of the parameters, significant round off errors build up in the solutions⁴⁸. As a result, parameters of very high accuracy are needed in these methods to obtain reasonably accurate radial functions. This problem can be avoided by following a different approach. In the new approach, after assigning initial estimates to E , f_{C_s} and b_{C_s} ($f_{C_0} = b_{C_0} = 1$), the radial equations are integrated both in the forward direction from $r = 0$ and in the backward direction from $r = r_\infty$ up to an inner point $r = r_C$. Since the radial functions, $F_s(r)$, must be continuous at $r = r_C$, the parameters are adjusted by an iterative method, see Sec. III.3B, until the $F_s(r_C)$ and $F'_s(r_C)$ obtained by the forward and backward integrations agree within a preset accuracy. A discussion of the choice of r_C is given by Fox⁴⁸; see also Appendix C.

III.3B THE DETERMINATION OF THE PARAMETERS IN THE MATCHING METHOD

In order to obtain the radial functions by the matching method^{35,48,68}, the values of the variable parameters must be adjusted until the forward and backward solutions match smoothly at $r = r_C$.

First consider an ideal situation where the exact value of E and, for $f_{C_0} = b_{C_0} = 1$, the exact values of $f_{C_1}, \dots, f_{C_N}, b_{C_1}, \dots, b_{C_N}$ are known. Under these circumstances both forward and backward integrations will give

accurate radial functions in the interval $0 \leq r \leq r_\infty$.

However the functions $f_{F_s}(r)$ and $b_{F_s}(r)$ will not match at any particular inner point r_C in this interval since the sizes of the forward and backward solutions are arbitrarily fixed by the choice $f_{C_0} = b_{C_0} = 1$. But since both $f_{F_s}(r)$ and $b_{F_s}(r)$ are solutions of the radial equations with the same eigenvalue, one is a constant, γ , times the other (it can easily be seen from the radial equations, see Eq. (III.2-3), that $F_s(r)$ and $\gamma F_s(r)$ are solutions associated with the same energy eigenvalue). Thus the forward and the backward solutions can be matched by requiring

$$G_s(E, f_{C_1}, \dots, f_{C_N}, b_{C_1}, \dots, b_{C_N}) = f_{F_s}(r_C) - \gamma b_{F_s}(r_C) = 0, \\ s = 0, 1, \dots, N \quad (\text{III.3-7})$$

and

$$G'_s(E, f_{C_1}, \dots, f_{C_N}, b_{C_1}, \dots, b_{C_N}) = f'_{F_s}(r_C) - \gamma b'_{F_s}(r_C) = 0, \\ s = 0, 1, \dots, N \quad (\text{III.3-8}).$$

Since the $F_s(r)$ are exact radial functions[†] γ can be obtained from either Eqs. (III.3-7) or (III.3-8) for any choice of s in this ideal case. The size of the overall solution is then determined by adjusting f_{C_0} so that the usual normalization condition on Ψ is satisfied; $\langle \Psi | \Psi \rangle = 1$.

We now consider a situation where exact values of E , f_{C_s} , b_{C_s} and γ ($f_{C_0} = b_{C_0} = 1$) are not known. In this case one has to solve Eqs. (III.3-7) and (III.3-8) for the values of these quantities that correspond to an eigenstate of the molecule. In order to solve these equations Newton's iterative method⁷⁰ can conveniently be used. The solution by this iterative method is started with initial estimates of the variable parameters which are denoted by $(E)_0$, $(f_{C_s})_0$ and $(b_{C_s})_0$. If the values of f_{F_s} , b_{F_s} and their derivatives are obtained by using the estimated instead of the exact values of the parameters, no single value of γ will satisfy the $(2N+2)$ simultaneous equations given by Eqs. (III.3-7) and (III.3-8). However to proceed with the iterative method γ can be fixed by one of these equations. We choose

[†]The fixing of γ by this procedure is entirely equivalent to adjusting b_{C_0} in order to obtain the continuity of $F_s(r)$ at $r = r_C$. It is important to note that both the determination of γ or the determination of b_{C_0} affects the other coefficients of the backward solution.

$$(G_0)_0 = 0$$

which yields

$$\gamma = \frac{(f_{F_0}(r_C))_0}{(b_{F_0}(r_C))_0} \quad (\text{III.3-9})$$

The use of this value of γ in the remaining $(2N+1)$ equations will result in non-vanishing values for $(G_K)_0$, $K = 1, 2, \dots, N$ and $(G'_s)_0$, $s = 0, 1, \dots, N$. The problem is then to adjust the values of the parameters such that $(G_s)_0$ and $(G'_s)_0$ vanish when $(G_0)_0$ is made to vanish. Let the initial estimates of the parameters be expressed in terms of their exact values by

$$E = (E)_0 + \delta E, \quad f_{C_K} = (f_{C_K})_0 + \delta f_{C_K}, \quad b_{C_K} = (b_{C_K})_0 + \delta b_{C_K}, \\ K = 1, 2, \dots, N \quad (\text{III.3-10})$$

where in general δX is the discrepancy between the estimated and exact values of a given variable X . By expanding the exact functions G_s and G'_s in Taylor Series about the initial estimates of the parameters we obtain

$$G_K = (G_K)_0 + \sum_{j=1}^N \left[\left(\frac{\partial G_K}{\partial f_{C_j}} \right)_0 \delta f_{C_j} + \left(\frac{\partial G_K}{\partial b_{C_j}} \right)_0 \delta b_{C_j} \right] + \left(\frac{\partial G_K}{\partial E} \right)_0 \delta E \\ + \text{Higher order terms} = 0, \quad K = 1, 2, \dots, N \quad (\text{III.3-11})$$

and

$$G'_s = (G'_s)_0 + \sum_{j=1}^N \left[\left(\frac{\partial G'_s}{\partial f_{C_j}} \right)_0 \delta f_{C_j} + \left(\frac{\partial G'_s}{\partial b_{C_j}} \right)_0 \delta b_{C_j} \right] + \left(\frac{\partial G'_s}{\partial E} \right)_0 \delta E \\ + \text{Higher order terms} = 0, \quad s = 0, 1, \dots, N, \quad (\text{III.3-12})$$

If $(G_K)_0$, $(G'_s)_0$ and the partial derivatives of G_s and G'_s with respect to the parameters are known, see below, then

by neglecting higher order terms Eqs. (III.3-11) and (III.3-12) can be solved to find approximate values of δE , $\delta^f C_s$ and $\delta^b C_s$. Using these approximate values of the δX 's in Eq. (III.3-10) improved values of the parameters can be obtained. By using the improved values as the initial values for the parameters the process can be iterated until a given accuracy is obtained for E , fC_1, \dots, fC_N , bC_1, \dots, bC_N . At this stage the matching parameter γ can be obtained from Eq. (III.3-7) (or equivalently from Eq. (III.3-8)) with any choice of s . The functions $fF_s(r)$ and $bF_s(r)$ constitute the solution of the radial equations, given by Eq. (III.2-3), in the intervals $0 \leq r \leq r_C$ and $r_C \leq r \leq r_\infty$ respectively. The overall size of the solution is fixed by the normalization condition $\langle \psi | \psi \rangle = 1$. In this way the values of the parameters and hence the eigensolution of the radial equations are obtained by the matching method.

In order to discuss the solutions of Eqs. (III.3-11) and (III.3-12), when higher order terms are neglected, it is convenient to express these equations in matrix form;

$$g = -D\delta \quad (\text{III.3-13A}).$$

In this result the column matrices g and δ and the square matrix D are defined as follows:

$$g = \begin{pmatrix} g_f \\ g_b \end{pmatrix}, \quad \delta = \begin{pmatrix} \delta_f \\ \delta_b \end{pmatrix}, \quad D = \begin{pmatrix} D_f & D_b \\ D'_f & D'_b \end{pmatrix} \quad (\text{III.3-13B}).$$

$$(g_0)_K = (G_K)_0 \quad (\text{III.3-13C}),$$

$$(g_0)_i = (G_{i-1}^*)_0 \quad (\text{III.3-13D}),$$

$$(d_f)_K = \delta^f C_K \quad (\text{III.3-13E}),$$

$$(d_b)_i = (1 - \delta_{i,N+1}) \delta^b C_i + \delta_{i,N+1} \delta E \quad (\text{III.3-13F}),$$

$$(D_f)_{Kj} = \left[\frac{\partial G_K}{\partial^f C_j} \right]_0 \quad (\text{III.3-13G}),$$

$$(D_b)_{K\mu} = (1 - \delta_{\mu,2N+1}) \left[\frac{\partial G_K}{\partial^b C_{\mu-N}} \right]_0 + \delta_{\mu,2N+1} \left[\frac{\partial G_K}{\partial E} \right]_0 \quad (\text{III.3-13H}),$$

$$(D_f^*)_ij = \left[\frac{\partial G_{i-1}^*}{\partial^f C_j} \right]_0 \quad (\text{III.3-13I}),$$

$$(D_b^*)_i\mu = (1 - \delta_{\mu,2N+1}) \left[\frac{\partial G_{i-1}^*}{\partial^b C_{\mu-N}} \right]_0 + \delta_{\mu,2N+1} \left[\frac{\partial G_{i-1}^*}{\partial E} \right]_0 \quad (\text{III.3-13J})$$

and

$$K = 1, 2, \dots, N; \quad i = 1, 2, \dots, N+1; \quad j = 1, 2, \dots, N;$$

$$\mu = N+1, N+2, \dots, 2N+1. \quad (\text{III.3-13K}).$$

The solution of Eq. (III.3-13A) is formally given by

$$\delta = -(D)^{-1} g \quad (\text{III.3-14}).$$

It is obvious that to find δ by using Eq. (III.3-14) one must know $(G_K)_0$, $(G_s^*)_0$ and the partial derivatives of G_K and G_s^* with respect to the variable parameters, see Eqs.

(III.3-13A)-(III.3-13K). For notational convenience define the following quantities:

$$f_{W_{Kj}}(r) = \frac{\partial^f F_K(r)}{\partial^f C_j}, \quad b_{W_{Kj}}(r) = \frac{\partial^b F_K(r)}{\partial^b C_j},$$

$$f_{M_K}(r) = \frac{\partial^f F_K(r)}{\partial E}, \quad b_{M_K}(r) = \frac{\partial^b F_K(r)}{\partial E},$$

$$j = 1, 2, \dots, N; K = 1, 2, \dots, N \quad (\text{III.3-15})$$

and

$$f_{W'_{sj}}(r) = \frac{\partial^f F'_s(r)}{\partial^f C_j}, \quad b_{W'_{sj}}(r) = \frac{\partial^b F'_s(r)}{\partial^b C_j},$$

$$f_{M'_s}(r) = \frac{\partial^f F'_s(r)}{\partial E}, \quad b_{M'_s}(r) = \frac{\partial^b F'_s(r)}{\partial E},$$

$$j = 1, 2, \dots, N; s = 0, 1, \dots, N \quad (\text{III.3-16}).$$

Using the definitions of the W's and M's given by Eq. (III.3-15) the partial derivatives of G_s , obtained from Eq. (III.3-7), can be expressed as

$$\frac{\partial G_K}{\partial^f C_j} = f_{W_{Kj}}(r_C) - b_{F_K}(r_C) \frac{\partial \gamma}{\partial^f C_j}; K, j = 1, 2, \dots, N \quad (\text{III.3-17}),$$

$$\frac{\partial G_K}{\partial^b C_j} = -[\gamma b_{W_{Kj}}(r_C) + b_{F_K}(r_C) \frac{\partial \gamma}{\partial^b C_j}]; K, j = 1, 2, \dots, N \quad (\text{III.3-18})$$

and

$$\frac{\partial G_K}{\partial E} = f_{M_K}(r_C) - \gamma b_{M_K}(r_C) + b_{F_K}(r_C) \frac{\partial \gamma}{\partial E}, \quad K = 1, 2, \dots, N \quad (\text{III.3-19}).$$

The partial derivatives of γ occurring in these equations can be evaluated from Eq. (III.3-9) and are given by

$$\frac{\partial \gamma}{\partial^f C_j} = \frac{f_{W_{0j}}(r_C)}{b_{F_0}(r_C)}, \quad \frac{\partial \gamma}{\partial^b C_j} = -\gamma \frac{b_{W_{0j}}(r_C)}{b_{F_0}(r_C)} \quad (\text{III.3-20})$$

and

$$\frac{\partial \gamma}{\partial E} = \frac{f_{M_0}(r_C) - \gamma b_{M_0}(r_C)}{b_{F_0}(r_C)} \quad (\text{III.3-21}),$$

where we have used the relations

$$\frac{\partial b_{F_s}}{\partial f_{C_j}} = \frac{\partial f_{F_s}}{\partial b_{C_j}} = 0 \quad (\text{III.3-22}).$$

Similar expressions can be found for the partial derivatives of G'_s by using Eqs. (III.3-8) and (III.3-16); these expressions read as

$$\frac{\partial G'_s}{\partial f_{C_j}} = f_{W'_{sj}}(r_C) - b_{F'_s}(r_C) \frac{\partial \gamma}{\partial b_{C_j}};$$

$$s = 0, 1, \dots, N; j = 1, 2, \dots, N \quad (\text{III.3-23}),$$

$$\frac{\partial G'_s}{\partial b_{C_j}} = -[\gamma b_{W'_{sj}}(r_C) + b_{F'_s}(r_C) \frac{\partial \gamma}{\partial b_{C_j}}];$$

$$s = 0, 1, \dots, N; j = 1, 2, \dots, N \quad (\text{III.3-24})$$

and

$$\frac{\partial G'_s}{\partial E} = f_{M'_s}(r_C) - \gamma b_{M'_s}(r_C) - b_{F'_s}(r_C) \frac{\partial \gamma}{\partial E};$$

$$s = 0, 1, 2, \dots, N \quad (\text{III.3-25}).$$

It is clear that in order to solve Eqs. (III.3-11) and (III.3-12) by the matrix method it is necessary to obtain the functions $W_{Kj}(r)$ and $M_K(r)$ where

$$W_{sj}(r) = f_{W_{sj}}(r) \text{ or } b_{W_{sj}}(r); M_s(r) = f_{M_s}(r) \text{ or } b_{M_s}(r)$$

$$(\text{III.3-26}).$$

The derivatives with respect to r of these functions can be obtained by using a finite difference formula, see

Appendix C. In order to find the functions themselves we differentiate the radial equations, given by Eq. (III.2-3), with respect to the parameters $E, f_{C_1}, \dots, f_{C_N}, b_{C_1}, \dots, b_{C_N}$. By changing the order of differentiation in the resulting equations it follows that

$$\begin{aligned} \left[\frac{d^2}{dr^2} + 2E - \frac{s(s+1)}{r^2} \right] M_s(r) + 2F_s(r) \\ = \sum_{L=0}^N \sum_{\ell=|L-s|}^{L+s} D(L, \ell, s) U_\ell(r) M_L(r) \\ s = 0, 1, \dots, N \end{aligned} \quad (\text{III.3-27})$$

and

$$\begin{aligned} \left[\frac{d^2}{dr^2} + 2E - \frac{s(s+1)}{r^2} \right] W_{sj}(r) \\ = \sum_{L=0}^N \sum_{\ell=|L-s|}^{L+s} D(L, \ell, s) U_\ell(r) W_{Lj}(r) \\ s = 0, 1, \dots, N; j = 1, 2, \dots, N \end{aligned} \quad (\text{III.3-28}).$$

Equations (III.3-27) and (III.3-28) are similar in form to the radial equations and the forward and backward integrations for the functions $W_{sj}(r)$ and $M_s(r)$ can be accomplished by employing the step by step method used for the solution of the radial equations themselves, see Sec. III.3A. The boundary conditions for $W_{Kj}(r)$ and $M_K(r)$ are obtained from those for the radial functions $F_s(r)$, see Eqs. (III.3-4), (III.3-3)-(III.3-6), (III.3-15) and (III.3-16). The boundary values of these functions are given by

$$\begin{aligned} f_{M_s}(0) = b_{M_s}(r_\infty) = f_{M_s}(h) = b_{M_s}(r_\infty - h) = 0 \\ s = 0, 1, \dots, N \end{aligned} \quad (\text{III.3-29})$$

and

$$f_{W_{sj}}(0) = b_{W_{sj}}(r_\infty) = 0, \quad f_{W_{sj}}(h) = b_{W_{sj}}(r_\infty - h) = \delta_{sj}$$

$$s = 0, 1, \dots, N; \quad j = 1, 2, \dots, N \quad (\text{III.3-30}).$$

Integrating Eqs. (III.2-3), (III.3-27) and (III.3-28) we obtain the functions $F_s(r)$, $M_s(r)$ and $W_{sj}(r)$. The derivatives with respect to r of these functions can be obtained by using a finite difference formula, see Appendix C. In this way all the quantities necessary to obtain δ from Eq. (III.3-14) are known. In order to ensure the continuity of the $F_s(r)$ at $r = r_C$, δ is made sufficiently small by this iterative process, see Appendix D.

III.4 A DISCUSSION OF THE DETERMINATION OF THE PARAMETERS IN THE ANALYTIC SOLUTION OF THE RADIAL EQUATIONS

The coefficients of the series solution for the radial equations in Region I, see Sec. III.2A, and through matching the coefficients of the stepwise solution of the radial equations in Region II, see Secs. III.2B-1 - III.2B-3, depend on the energy E and the constants of integration $a_0^{(s)}$ introduced in Region I. The coefficients of the asymptotic solution of the radial equations also depend on E and the constants $h_0^{(s)}$, see Sec. III.2B-4. In order to find the radial functions, $F_s(r)$, in the complete interval $0 \leq r \leq \infty$, the stepwise solution in Region II must be matched smoothly with the asymptotic solution. In the discussion of the matching procedure that follows the quantities E , $a_0^{(s)}$ and $h_0^{(s)}$ are collectively called "the parameters" of the analytic solution of the radial equations. The

conditions of smooth matching of the stepwise and the asymptotic solutions of the radial equations is the final step that determines these parameters for a given eigenstate of the molecule.

III.4A THE MATCHING OF THE STEPWISE SOLUTION WITH THE ASYMPTOTIC SOLUTION

The method of matching the stepwise solution with the asymptotic solution is analogous to the matching of the forward and backward solutions of the numerical method, see Sec. III-3B. The radial functions that are obtained by the stepwise solution of the radial equations in Region II are called the $^fF_s(r)$ (the symbol used here is the same as that used for the forward solution in the numerical method). In order to find the $^fF_s(r)$, one must know the $N+2$ parameters $E, a_0^{(0)}, \dots, a_0^{(N)}$. One of the constants of integration can be arbitrarily assigned a numerical value which can later be fixed by the normalization of the complete wave function ψ ; we choose

$$a_0^{(0)} = 1 \quad (\text{III.4-1}).$$

This choice of $a_0^{(0)}$ is analogous to the choice of fC_0 made in the numerical method, see Eq. (III.3-4). Let the asymptotic solution of the radial equations be called the $^bF_s(r)$ (the symbol used here is the same as that used for the backward solution in the numerical method). The $(N+2)$ parameters $E, h_0^{(0)}, \dots, h_0^{(N)}$ are required in order to determine the $^bF_s(r)$ and one of the $h_0^{(s)}$ can be assigned an arbitrary value; we choose

$$h_0^{(0)} = 1 \quad (\text{III.4-2})$$

This choice of $h_0^{(0)}$ is analogous to the choice of b_{C_0} in the numerical method, see Eq. (III.3-6). If the value of E and, for $a_0^{(0)} = h_0^{(0)} = 1$, the values of $a_0^{(1)}, \dots, a_0^{(N)}$, $h_0^{(1)}, \dots, h_0^{(N)}$ are known then the matching conditions for $f_{F_s}(r)$ and $b_{F_s}(r)$ are given by

$$G_s(E, a_0^{(1)}, \dots, a_0^{(N)}, h_0^{(1)}, \dots, h_0^{(N)}) = f_{F_s}(r_C) - \gamma b_{F_s}(r_C) = 0$$

$$s = 0, 1, \dots, N \quad (\text{III.4-3})$$

and

$$G'_s(E, a_0^{(1)}, \dots, a_0^{(N)}, h_0^{(1)}, \dots, h_0^{(N)}) = f'_{F_s}(r_C) - \gamma b'_{F_s}(r_C) = 0$$

$$s = 0, 1, \dots, N \quad (\text{III.4-4}),$$

where γ is fixed by any one of these equations and r_C is the matching point; the choice of r_C is discussed in Sec. III.4C.

In actual practice the exact values of the parameters $E, a_0^{(1)}, \dots, a_0^{(N)}, h_0^{(1)}, \dots, h_0^{(N)}$ are not known and the problem therefore is to solve Eqs. (III.4-3) and (III.4-4) for these parameters. Using initial estimates for these parameters an iterative process is used to solve Eqs. (III.4-3) and (III.4-4); the choice of the initial estimates is discussed in Sec. III.4B. This iterative^{70,71} method is completely analogous to that in the numerical method discussed in Sec. III.3B; in the numerical method the parameters $E, f_{C_1}, \dots, f_{C_N}, b_{C_1}, \dots, b_{C_N}$ are determined by solving Eqs. (III.3-7) and (III.3-8) whereas in this analytical method the parameters $E, a_0^{(1)}, \dots, a_0^{(N)}, h_0^{(1)}, \dots, h_0^{(N)}$ are determined by solving Eqs. (III.4-3) and (III.4-4). The

derivatives of G_s and G'_s with respect to E , $a_0^{(1)}, \dots, a_0^{(N)}$ and $h_0^{(1)}, \dots, h_0^{(N)}$ requires term by term differentiation of the series for the two solutions for $F_s(r)$ in Region II. The differentiation of the asymptotic solution with respect to E , and $h_0^{(1)}, \dots, h_0^{(N)}$ is straightforward. On the other hand the differentiation of the stepwise series with respect to E , $a_0^{(1)}, \dots, a_0^{(N)}$ is messy since the coefficients $g_0^{(s)}$ and $g_1^{(s)}$, and hence $g_j^{(s)}$ for $j > 1$, are complicated functions of E and $a_0^{(s)}$, see Eqs. (III.2-45)-(III.2-48), (A-21) and (A-22).

III.4B THE INITIAL ESTIMATES OF THE PARAMETERS IN THE ANALYTIC SOLUTION OF THE RADIAL EQUATIONS

The analytic method for solving the radial equations requires initial estimates of the parameters E , $a_0^{(1)}, \dots, a_0^{(N)}$, $h_0^{(1)}, \dots, h_0^{(N)}$ (the numerical method discussed in Sec. III.3B required initial estimates of E , f_{C_1}, \dots, f_{C_N} , b_{C_1}, \dots, b_{C_N}). The values of these parameters for a given value of N (that is $(N+1)$ coupled equations) can be estimated by examining the trend in the values of these parameters as a function of increasing small values of N . For example it is not difficult to obtain a satisfactory estimate of the parameters for $N = N_0$ if the values of these parameters are known for $N = N_0 - 1$ and $N = N_0 - 2$. The data for the ground state H_2^+ molecule show, see Tables B-1 and B-2, that for small $N \leq 2$, the $a_0^{(s)}$ and $h_0^{(s)}$ are of the order of unity. For large values of N the $a_0^{(s)}$ and $h_0^{(s)}$ approach zero as s increases since the higher order partial wave contributions to the energy is

usually small. This observation of course depends on R, ρ_B and on the molecular state under consideration. In general the iterative process is not very sensitive to the initial estimates of the parameters $a_0^{(s)}$ and $h_0^{(s)}$. Far more important is the estimate of the energy eigenvalue E since, in general, the iterative process converges to the exact eigenvalue E which is closest to the initial estimate of E . Useful estimates of E can be obtained by using several approaches. Very often approximate values of E for many eigenstates of one electron molecular systems can be obtained from existing theoretical and experimental studies. If these are not available the calculations can be started at small R by using the united atom limit for the energy of the molecule and/or at large R by using the separated atom energy limit of the molecule.

III.4C THE CHOICE OF THE POINT AT WHICH THE STEPWISE SOLUTION IS MATCHED WITH THE ASYMPTOTIC SOLUTION ($r = r_C$)

The asymptotic solution of the radial equations is given

by the expression $F_s(r) = r^{\frac{Z}{K}} e^{-Kr} f_s(\xi)$ where $\xi = \frac{\rho_B}{r}$; see Eqs. (III.2-31) and (III.2-55): It is clear from this result that the order of the error in $F_s(r)$ is given by that in $f_s(\xi)$. The order of the error in $f_s(\xi)$, see Eq. (III.2-60), is given by the smallest term $|h_{M_s+1}^{(s)} \xi^{M_s+1}|$ in the series for $f_s(\xi)$, see for example Refs. [72,73]:

For the calculations relevant to this work the order of the error in $f_s(\xi)$, for a fixed value of N , is

approximately the same or less than the error in the asymptotic radial function, $F_0(r)$, corresponding to the dominant partial wave component of ψ , see Appendix C.

In order to find the matching point ξ_C or $r_C = \frac{r_B}{\xi_C}$ the variable ξ is chosen so that the term $|h_{M_0+1}^{(0)} \xi^{M_0+1}| \sim \epsilon$,

where ϵ is the order of the acceptable numerical error in the radial functions. It should be pointed out that the

term $|h_{M_0+1}^{(0)} \xi_C^{M_0+1}|$, and hence the error in the radial

functions, can be made as small as one likes by choosing ξ_C small enough, that is r_C large enough.

CHAPTER IV

RESULTS AND GENERAL DISCUSSION OF THE EXACT ONE CENTRE SOLUTION FOR THE H_2^+ MOLECULE

The ground state H_2^+ energy and wave function, obtained by the one centre methods discussed in Chapter III, are discussed in this chapter. The purpose here is not to present an exhaustive list of data but to show the trend in the energy and the wave function as a function of R , ρ_A and the number of coupled differential equations, N , used in the exact partial wave solution of the Schrödinger equation for the problem, see Eqs. (II.2-8), (II.2-17) and (II.2-18). The numerical method, that was initially investigated, is used to calculate only the energy while the analytical method is used to calculate the energy and the wave function as a function of R , ρ_A and N . A more detailed discussion of the convergence properties of these results is given in Chapter V.

IV.1 THE INTERACTION ENERGY FOR THE GROUND STATE OF THE H_2^+ MOLECULE

The interaction energy E_{int} , see Eqs. (II.1-2) and (II.1-3), plays an important role in chemical and physical processes; the electronic and total energies, E and E_T , are not very sensitive to changes in R for intermediate and

large R . Here the ground state E_{int} for the H_2^+ molecule is evaluated as a function of R , ρ_A and N ; see Tables IV.1-1-IV.1-3. The results obtained by the numerical method are extrapolated results obtained by using the Richardson's h^2 -extrapolation technique^{74,75} discussed in Appendix D. For common values of R , ρ_A and N the results of the analytical and numerical methods agree with each other, at least to the number of significant figures given in Tables IV.1-1 and IV.1-2.

IV.1A THE GROUND STATE H_2^+ INTERACTION ENERGY OBTAINED WITH $\rho_A = 0$ and $\rho_B = R$

The ground state interaction energy, obtained with the coordinate origin fixed at one of the nuclei, see Sec. II.3A-1, is given in Table IV.1-1 as a function of $N = N+1$, where N is defined by Eq. (II.2-17), for $R = 2, 4, 6, 8, 15$ and 20 . The exact interaction energy³⁸⁻⁴⁰ E_{int} (exact), is also included in this table. The results in Table IV.1-1 show, for a given N , that as R increases the discrepancy between the approximate and exact interaction energies first increases and then decreases. For $R \leq 4$ one obtains at least 86% of the exact interaction energy by solving 14 coupled differential equations while for $R \geq 15$ employing only 2 coupled differential equations yields at least 91% of the exact interaction energy. The behaviour of the proton centred results for small and large R is not hard to understand. With this choice of the expansion centre one obtains the united atom limit^{5,6,76} as $R \rightarrow 0$

2

OF/DE

3

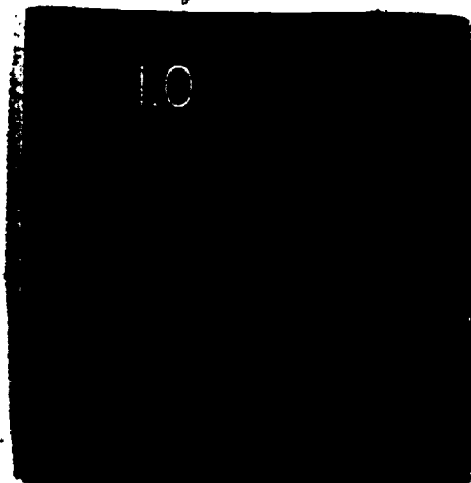


TABLE IV.1-1: The proton centred ($\rho_A = 0$, $\rho_B = R$) interaction energies for the ground state H_2^+ molecule as a function of R and N . The numbers with the symbol * are obtained only by the numerical method while the other results are obtained by both the numerical and the analytical methods. Here the E_{int} (exact) are the exact interaction energies³⁸⁻⁴⁰.

N	$-E_{int}$				
	R = 2	R = 4	R = 6	R = 8	R = 15 R = 20
1	-0.2177(-1)	-0.3812(-3)	-0.6861(-5)		-0.1914(-8)* -0.5000(-11)*
2	0.2755(-1)	0.8401(-2)	0.1815(-2)	0.5625(-3)*	0.4460(-4)*
3	0.5476(-1)	0.1266(-1)	0.2194(-2)	0.6146(-3)*	0.1422(-4)*
4	0.7156(-1)	9.1619(-1)	0.2390(-2)	0.6277(-3)*	0.1423(-4)*
5	0.8200(-1)	0.1958(-1)	0.2548(-2)		0.4550(-4)*
6	0.8854(-1)	0.2291(-1)	0.2704(-2)	0.6388(-3)*	0.4550(-4)*
7	0.9272(-1)	0.2609(-1)	0.2870(-2)		
8	0.9546(-1)	0.2902(-1)	0.3054(-2)		
9	0.9730(-1)	0.3161(-1)	0.3259(-2)		
10	0.9858(-1)	0.3385(-1)	0.3488(-2)	0.6565(-3)*	0.4550(-4)*
11	0.9948(-1)	0.3575(-1)*	0.3742(-2)*	0.6619(-3)*	
12	0.1001(0)*	0.3734(-1)*		0.6677(-3)*	
13	0.1006(0)*	0.3866(-1)*		0.6741(-3)*	
14	0.1010(0)*	0.3975(-1)*			
exact	0.1026(0)	0.4608(-1)	0.1197(-1)	0.2570(-2)	0.4894(-4) 0.1426(-4)

and the long range induction energy^{9,14,17,57} for large R .

It is important to realize that although the proton centred calculations yield reasonable values for E_{int} for large R with small N , very large values of N are required to remove the small discrepancy between the one centre and the exact results for large R . For example at $R = 15$ the results quoted for the E_{int} in Table IV.1-1 are the same for $N = 4$ and 10. For intermediate values of R it is clear that one will need to solve quite a large number of coupled differential equations to obtain reasonable results for the interaction energy. For example when $\rho_A = 0$ and $R = 8$ only 26% of the E_{int} (exact) is obtained by solving 13 coupled differential equations.

IV.1B THE GROUND STATE H_2^+ INTERACTION ENERGY OBTAINED WITH $\rho_A = \rho_B = R/2$

The midpoint centred results for the interaction energy, see Sec. II.3A-1, are given in Table IV.1-2 as a function of N , see Eqs. (II.3-2A) - (II.3-2G), for $R = 2, 4, 6$ and 8. Midpoint calculations for large R values have not been performed since it can be seen from the trend in the results of this table that it will require a large value of N for large R in order to obtain even the correct sign for the interaction energy, see also below. The midpoint results for $R = 2$ and $N = 1$ and 4 agree with the extrapolated results obtained by Temkin^{2(b)} and Cohen and Coulson³⁵.

TABLE IV.1-2: The midpoint centred ($\rho_A = \rho_B = R/2$) interaction energies for the ground state H_2^+ molecule as a function of R and N . The numbers with the symbol* are obtained only by the numerical method while the other results are obtained by both the numerical and the analytical methods. Here the E_{int} (exact) are the exact interaction energies³⁸⁻⁴⁰

N	$-E_{int}$			
	R = 2	R = 4	R = 6	R = 8
1	0.1850(-1)	-0.9200(-1)	-0.1786(0)	
2	0.8368(-1)	-0.8546(-2)	-0.9090(-1)	
3	0.9644(-1)	0.2254(-1)	-0.4270(-1)	
4	0.9997(-1)	0.3454(-1)	-0.1850(-1)	
5	0.1013(0)	0.3973(-1)	-0.6151(-2)	
6	0.1018(0)	0.4226(-1)	0.5151(-3)	
7	0.1021(0)	0.4362(-1)	0.4341(-2)	
8	0.1023(0)	0.4441(-1)	0.6663(-2)	
9	0.1024(0)	0.4490(-1)	0.8141(-2)	-0.6058(-2)*
10	0.1024(0)*		0.9124(-2)*	-0.3936(-2)*
11			0.9800(-2)*	
12			0.1028(-1)*	
13			0.1063(-1)*	
exact	0.1026(0)	0.4608(-1)	0.1197(-1)	0.2570(-2)

The values for E_{int} given in Table IV.1-2 show that for a given N the discrepancy between E_{int} and $E_{\text{int}}(\text{exact})$ increases as R increases when $\rho_A = \rho_B = R/2$. For example the values of E_{int} obtained with $N = 9$ are 99.8%, 97.4% and 68.0% of the $E_{\text{int}}(\text{exact})$ for $R = 2, 4$ and 6 respectively. For intermediate and large values of R the wrong sign for E_{int} is obtained in the midpoint calculations unless N is chosen to be sufficiently large. For example the solution of 3, 6 and more than 10 coupled differential equations are required to obtain the correct sign for the E_{int} for $R = 4, 6$ and 8 respectively. Since N will have to be very large to obtain reasonable E_{int} for large R , there is clearly a practical difficulty in using the one centre methods with the coordinate origin located at the midpoint for these values of R . For large R a more convenient choice of the coordinate origin is at one of the nuclei, see Sec. IV.1A. On the other hand for small $R \leq 2$ the midpoint calculations with even $N = 1$ yield the proper sign for E_{int} , see Table IV.1-2. Comparison of the results in Tables IV.1-1 and IV.1-2 show that for small R , although the proton centred results are quite reasonable, it is more convenient to choose the expansion centre at the midpoint rather than at a proton.

The practical difficulty associated with the midpoint centred calculations for large R does not imply that these calculations will not eventually converge to reasonable results for the interaction energy for large R . Indeed

comparing the results in Tables IV.1-1 and IV.1-2 indicates that if $N > N_0(R)$, where $N_0(R)$ is the minimum value of N required to obtain the proper sign for E_{int} for a given value of R with $\rho_A = R/2$, it is then computationally more convenient to choose the expansion centre at the midpoint rather than at a proton. For a given value of R as N increases beyond $N_0(R)$, the rate of convergence of the calculated E_{int} to $E_{\text{int}}(\text{exact})$ is faster for $\rho_A = R/2$ than for $\rho_A = 0$. The real advantage of the proton centred calculations over the midpoint centred calculations for large R is that the former yield reasonable values for E_{int} with small N while the latter requires a large value of $N > N_0(R)$. The difference in the rates of convergence of these two calculations, when $N > N_0(R)$, can be understood from the facts that (1) for $N > N_0(R)$ the optimum expansion centre tends to be located at the internuclear midpoint, see Sec. IV.1C below, and (2) for the ground state H_2^+ molecule, the partial wave components in ψ that contribute to the energy for $\rho_A = R/2$ are $0, 2, 4, \dots, 2N - 2$ while those for $\rho_A \neq R/2$ are $0, 1, 2, \dots, N-1$ for a given fixed value of N .

IV.1C THE GROUND STATE H_2^+ INTERACTION ENERGY OBTAINED WITH $\rho_A \neq \rho_{\text{op}}$

From the above discussion it is clear that for small R the expansion centre can be most conveniently chosen at the midpoint and for large R it is convenient to choose the centre at one of the nuclei. The purpose of this section is to see if the rate of convergence of the one centre

method for intermediate R can be increased by allowing the expansion centre to be a function of the molecular configuration.

Table IV.1-3 contains the results for the floating centre calculations, see Sec. II.3A-1, for $R = 4$ and 6 as a function of N and $\rho_A = \rho_{op}$. The results in this table are obtained by minimizing the energy, using a trial and error method, with respect to the position of the expansion centre; for minimum energy $\rho_A = \rho_{op}$. Although the data for the floating centre results are far from being complete, they are sufficient to show the kind of improvement one will obtain for other intermediate R values. For a given R and common values of N the midpoint results in Table IV.1-2 are lower than the optimized results in Table IV.1-3. This is not in violation of the variational principle since, in the midpoint calculations, the odd s value radial equations do not contribute to the ground state H_2^+ interaction energy, see Sec. II.3A-1.

Comparing the proton centred and the ρ_{op} results, see Tables IV.1-1 and IV.1-3; it can be seen that the value of E_{int} can be improved by floating the centre of expansion away from the proton and for every R and N there is an optimum value of ρ_A . However the labour involved in minimizing E_{int} with respect to ρ_A can be quite significant compared to the improvement in the calculated value of E_{int} . Hence it is usually more convenient to increase N keeping ρ_A fixed rather than varying ρ_A and keeping N fixed. For

TABLE IV.1-3: The floating centred ($\rho = \rho_{op}$) interaction energies for the ground state H_2^+ molecule as a function of R and N . The results of this table are obtained only by the numerical method. The E_{int} (exact) are the exact interaction energies³⁸⁻⁴⁰.

N	R = 4			R = 6		
	ρ_{op}	E_{int}	ρ_{op}	E_{int}	ρ_{op}	$-E_{int}$
3	0.2000(0)	0.1314(-1)				
4	0.3000(0)	0.1707(-1)				
5	0.6000(0)	0.2145(-1)	0.1000(0)			0.2565(-2)
6	0.1000(1)	0.2641(-1)	0.1500(0)			0.2718(-2)
7	0.1950(1)	0.3448(-1)	0.2000(0)			0.2892(-2)
8			0.2000(0)			0.3095(-2)
9			0.3000(0)			0.3330(-2)
10			0.4000(0)			0.3609(-2)
11			0.6000(0)			0.3943(-2)
12			0.8000(0)			0.4344(-2)
13			0.1000(1)			0.4830(-2)
14			0.1500(1)			0.5430(-2)
15			0.1700(1)			0.6148(-2)
exact		0.4608(-1)				0.1197(-1)

example when $R = 4$, the ρ_{op} result is $\sim 28.5\%$ of $E_{int}(\text{exact})$ for $N = 3$ while the proton centre result is $\sim 35.1\%$ of $E_{int}(\text{exact})$ for $N = 4$.

The floating centre results show that as N increases $\rho_{op} \rightarrow R/2$ for all R and that the value of N , for which the centre starts floating away from the proton, increases as R increases. For large R where the proton centred calculations give quite reasonable values for E_{int} with small N , the expansion centre will float away from the proton to an optimum value of ρ_A as N increases in order to recover the small discrepancy between E_{int} and $E_{int}(\text{exact})$. Comparing the results in Tables IV.1-1 - IV.1-3 it can be seen that if the value of N used in the one centre calculations is such that $N > N_0(R)$, see Sec. IV.1B, it is much more convenient to choose the expansion centre at the midpoint rather than at a proton or at a phantom floating expansion centre. On the other hand if $N < N_0(R)$ it is more convenient to choose the expansion centre at a proton since the labour involved in optimizing the position of the expansion centre can be quite significant compared to the improvement in E_{int} for such values of N .

IV.2 NORMALIZED WAVE FUNCTIONS FOR THE GROUND STATE OF THE H_2^+ MOLECULE

In this section, the normalized exact³⁸ and approximate wave functions, Ψ and $\tilde{\Psi}$, are discussed at points along the z -axis (that is, with the polar angle $\theta = 0$ or π , respectively; for the positive or negative values of the

z-coordinate) of the spherical polar coordinate system used in this work, see Figure II.1-1. A discussion of the normalization of both of these functions is given in Appendix E.

IV.2A THE PROTON CENTRED WAVE FUNCTIONS

The wave functions obtained with the expansion centre fixed at a proton ($\rho_A = 0$) are shown in Figs. IV.2-1 - IV.2-3 as a function of R and N . The exact wave functions³⁸, are also illustrated in these figures. These results show that the wave function, for small N , overestimates the cusp^{2(a),35,52} at the nucleus, A , at which the coordinate origin is located and underestimates the cusp at the other nucleus, B . As N increases Ψ tends to produce identical cusps at the two nuclei. As R increases the extent of the overestimation of the cusp at the nucleus A and the extent of the underestimation of the cusp at the nucleus B increases for a given N and the rate of convergence of Ψ to ψ as a function of N becomes slower as R increases.

IV.2B THE MIDPOINT CENTRED WAVE FUNCTIONS

The midpoint ($\rho_A = \rho_B = R/2$) centred wave functions are shown in Figs. IV.2-4 - IV.2-6 as a function of R and N . When $N = 1$ the approximate wave function Ψ does not have any cusp characteristic at the nuclear positions. As N increases the cusps at the two nuclei build up simultaneously. It can be seen that as N increases the main change in Ψ occurs in the neighbourhood of the nuclei; in general Ψ agrees with ψ , for reasonably large N , quite well at all

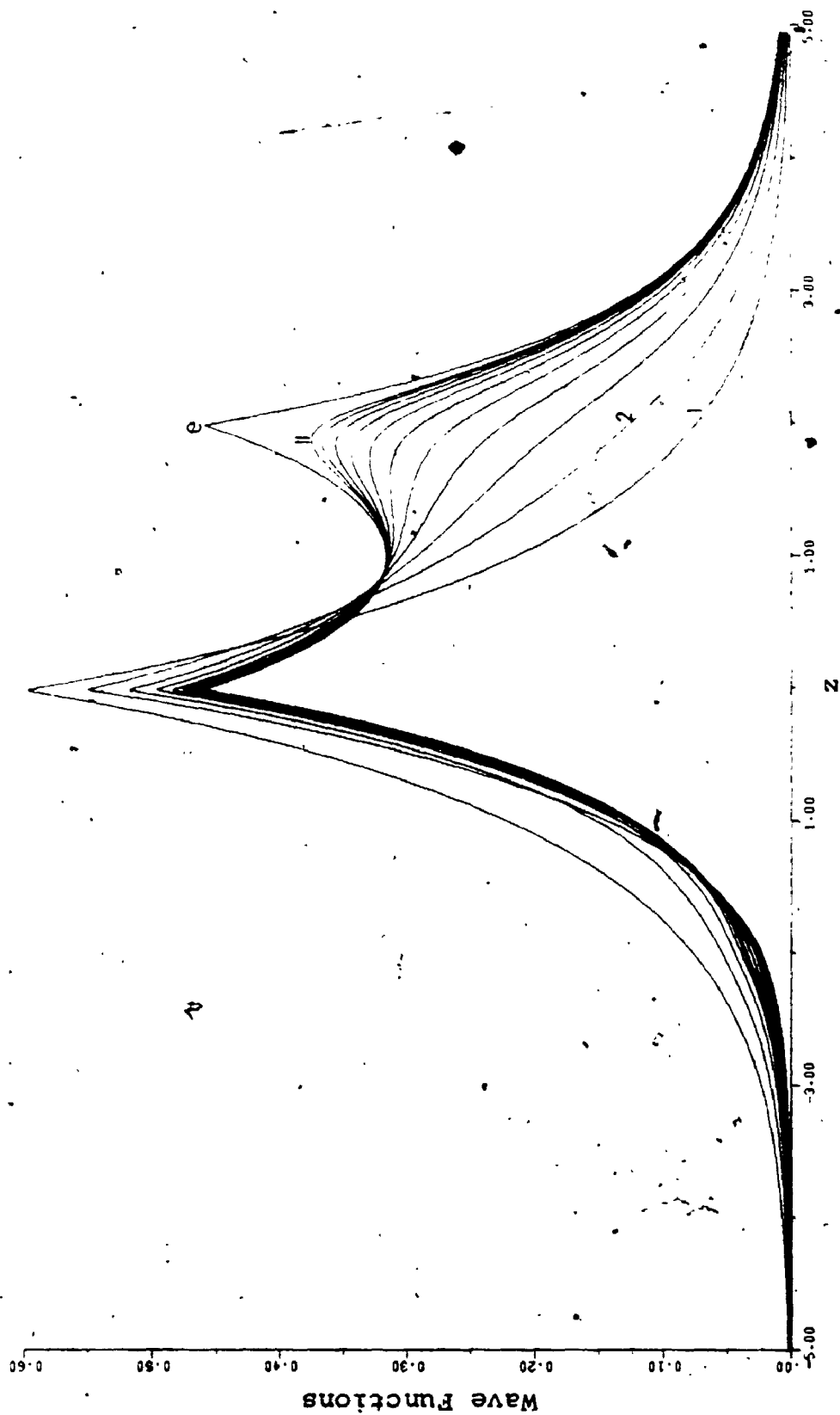


Figure IV.2-1: Normalized proton centred ($\rho_A = 0$, $\rho_B = R$) wave functions for the ground state H_2^+ molecule for $R = 2$ at points along the z -axis. The graphs 1,2,..., 11 are, respectively, obtained by solving $N = 1,2,\dots, 11$ coupled differential equations. The graph e shows the exact wave function.

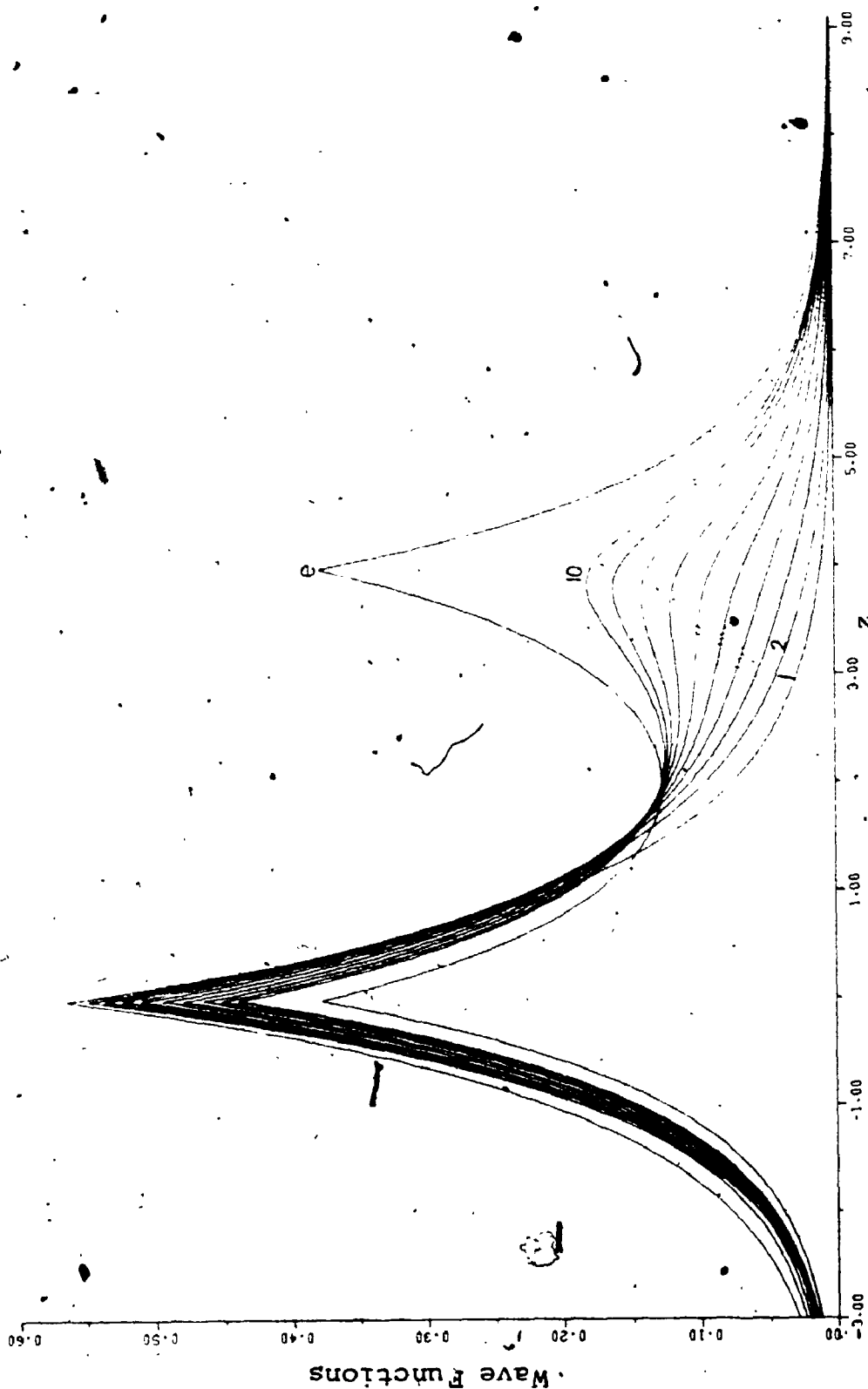


Figure IV.2-2: Normalized proton centred ($\rho_A = 0$, $\rho_B = R$) wave functions for the ground state H_2^+ molecule for $R = 4$ at points along the z-axis. The graphs 1, 2, ..., 10 are, respectively, obtained by solving $N = 1, 2, \dots, 10$ coupled differential equations. The graph e shows the exact wave function.

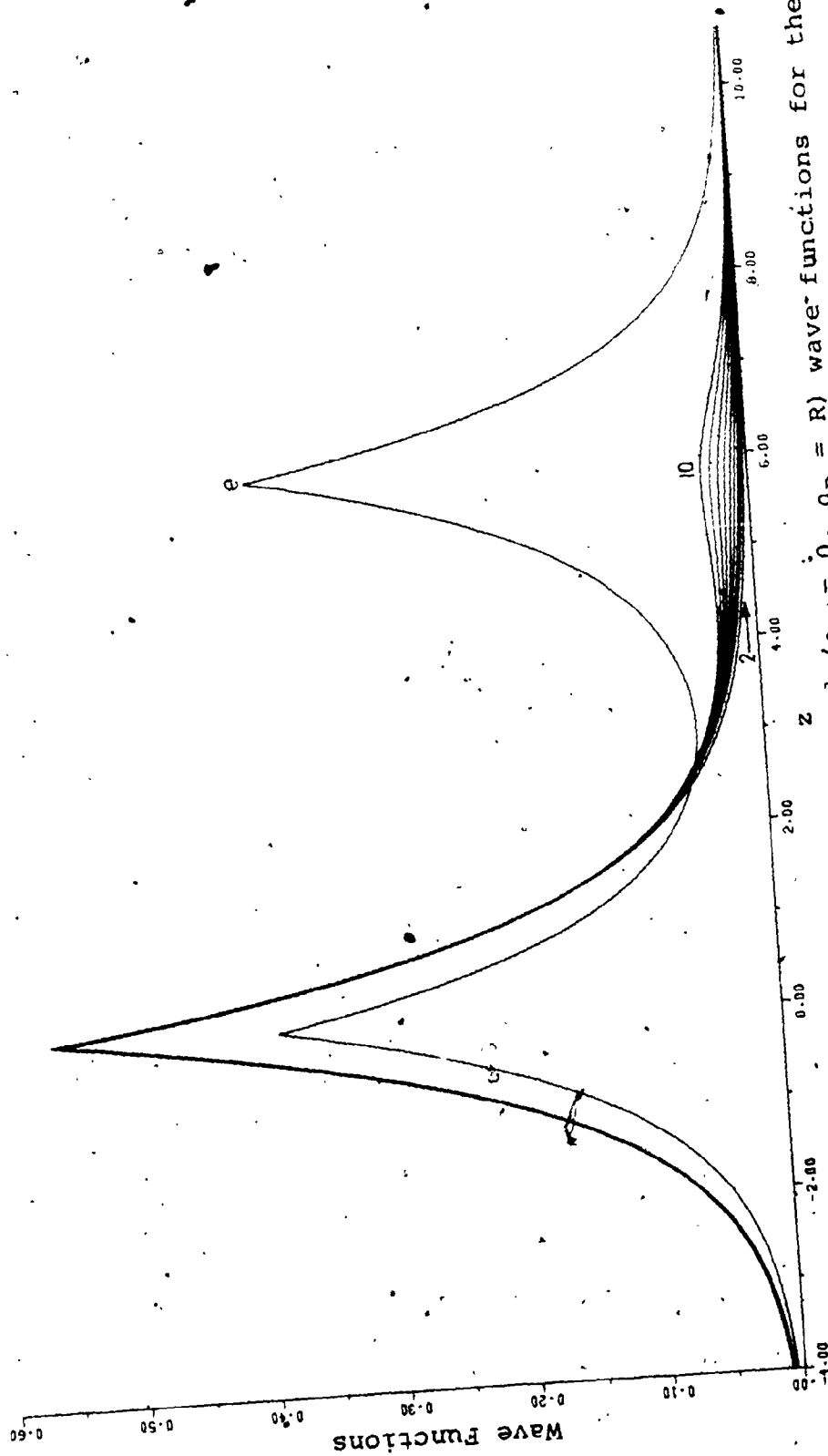


Figure IV.2-3: Normalized proton centred ($\rho_A = 0$, $\rho_B = R$) wave-functions for the ground state H_2^+ molecule for $R = 6$ at points along the z -axis. The graphs 2, ..., 10 are, respectively, obtained by solving $N = 2, \dots, 10$ coupled differential equations. The graph e shows the exact wave function.

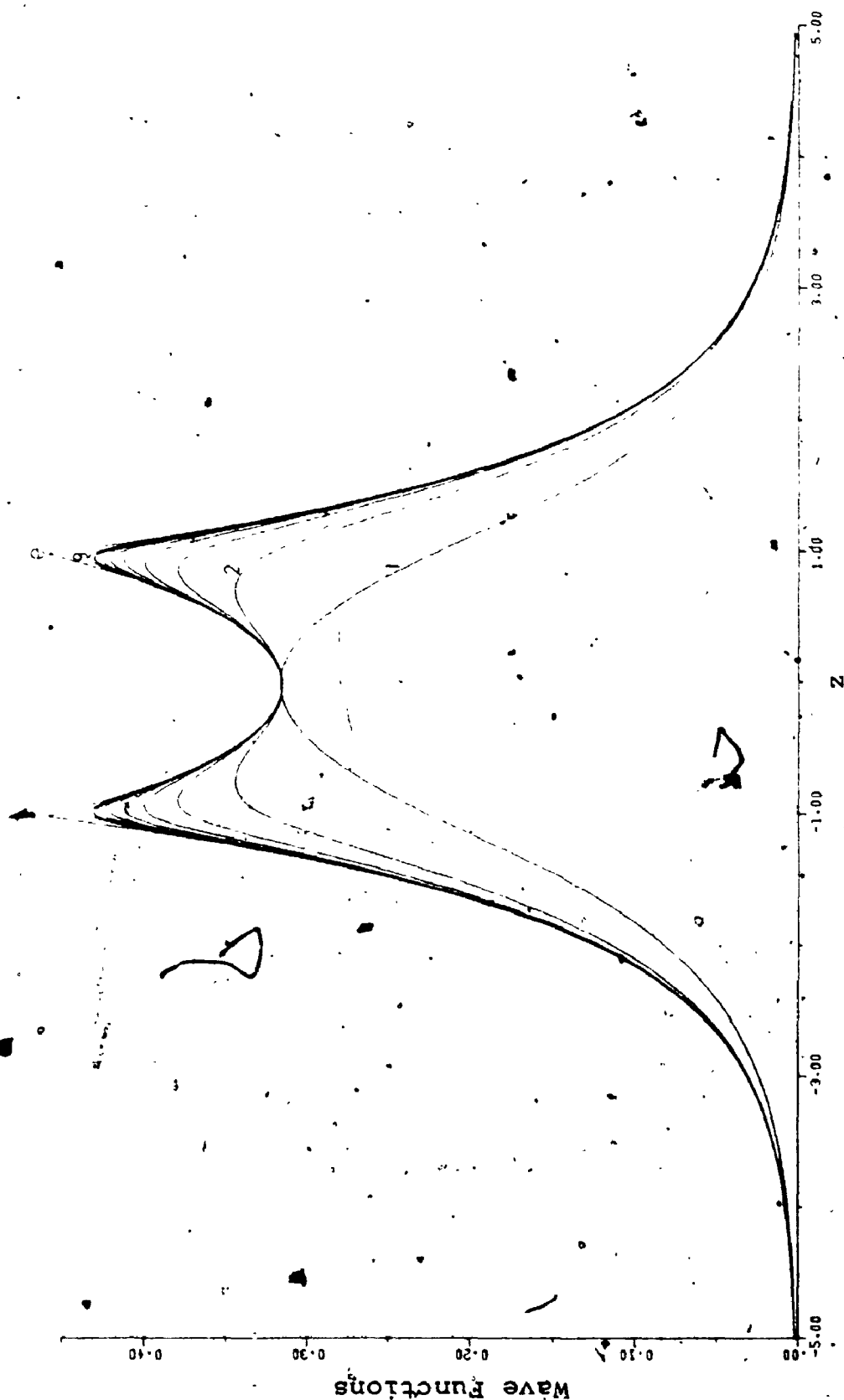


Figure IV.2-4: Normalized midpoint centred ($\rho_A = \rho_B = R/2$) wave functions for the ground state H_2^+ molecule for $R \approx 2$ at points along the z -axis.

The graphs 1, 2, ..., 9 are, respectively, obtained by solving $N = 1, 2, \dots, 9$ coupled differential equations. The graph e shows the exact wave function.

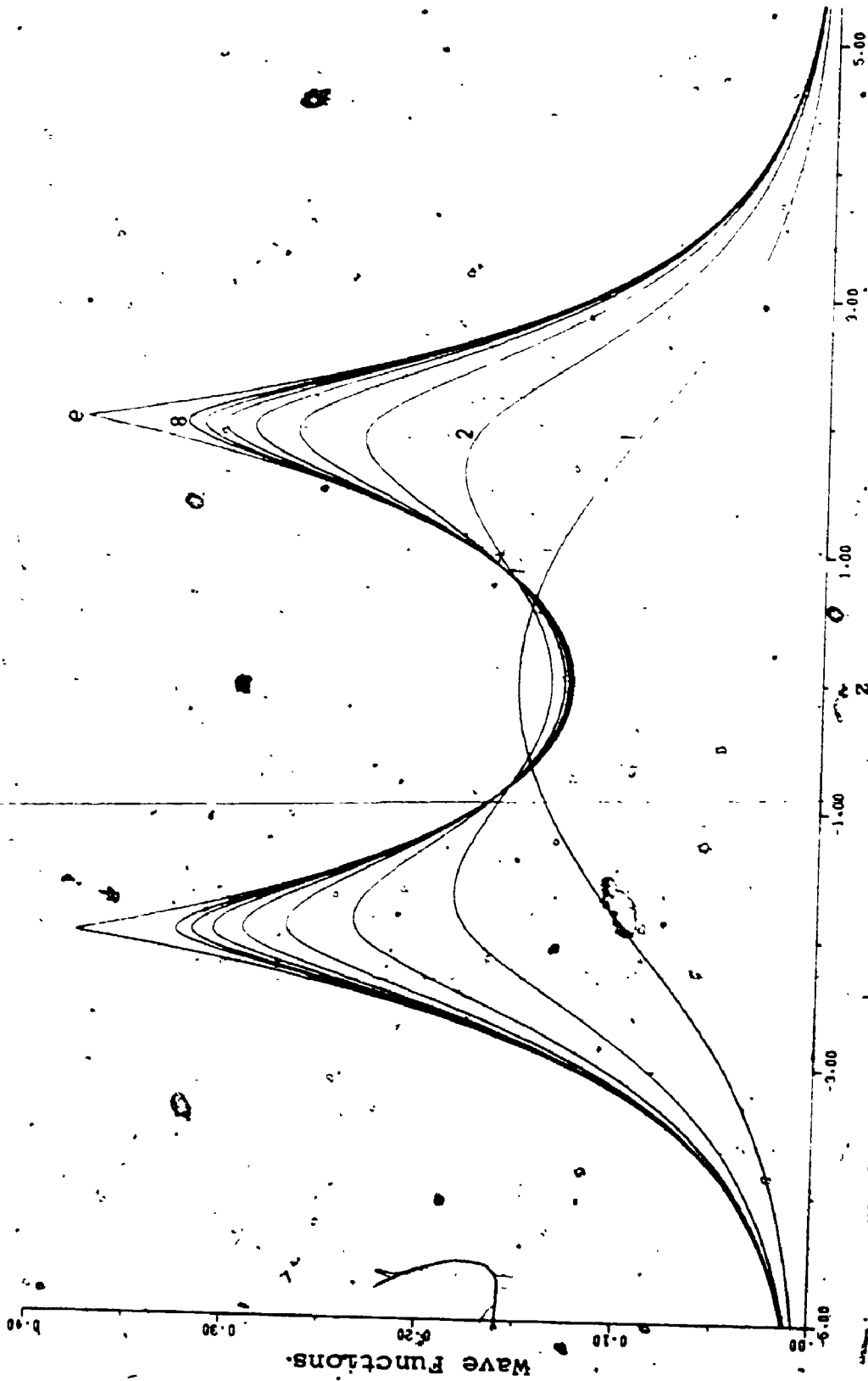


Figure IV.2-5. Normalized midpoint centred ($\rho_A = \rho_B = R/2$) wave functions for the ground state H_2^+ molecule for $R = 4$ at points along the z -axis. The graphs 1, 2, ..., 8 are, respectively, obtained by solving $N = 1, 2, 3, \dots, 8$ coupled differential equations. The graph e shows the exact wave function.

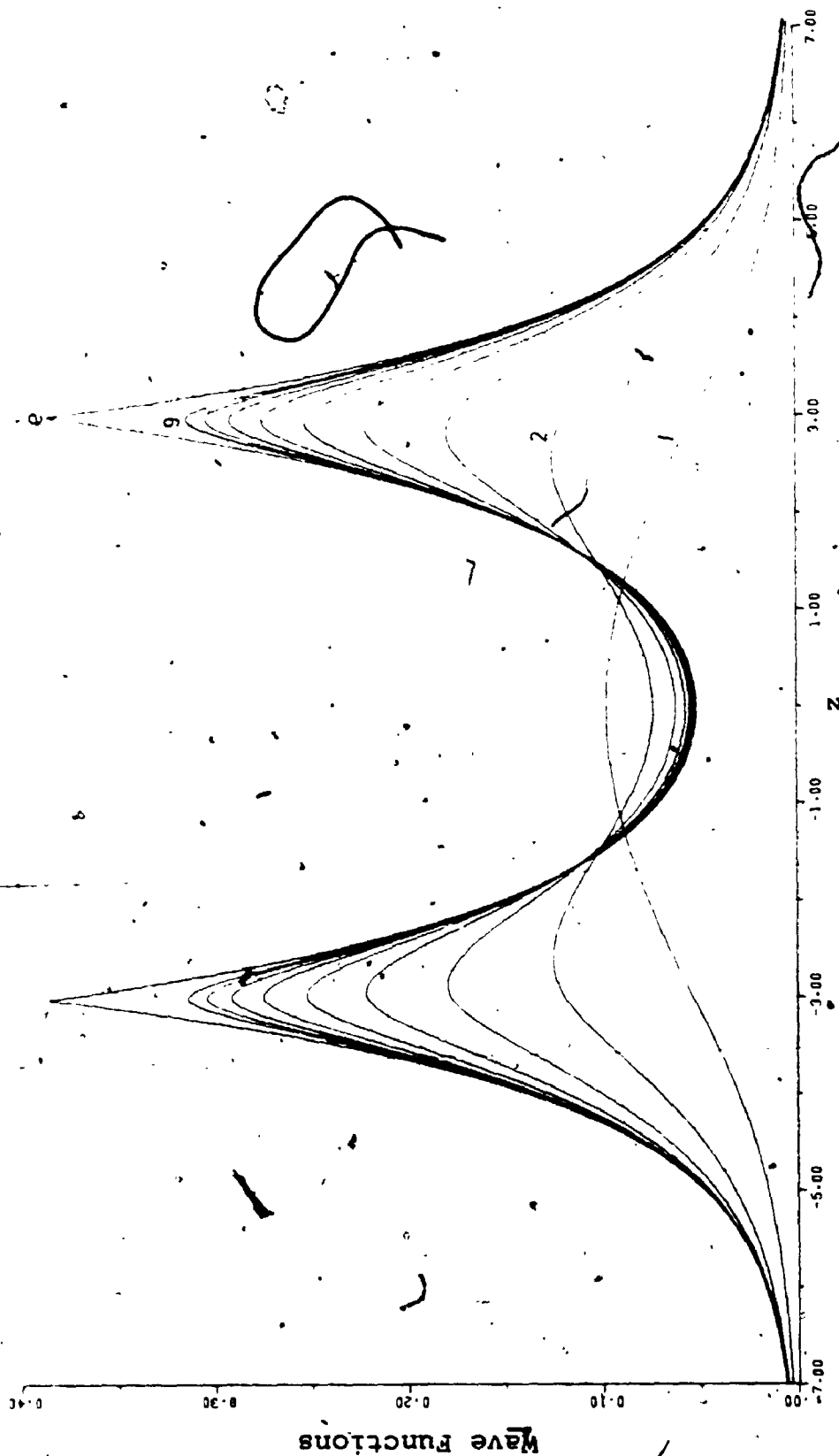


Figure IV.2-6: Normalized midpoint centred ($\rho_A = \rho_B = R/2$) wave functions for the ground state H_2^+ molecule for $R = 6$ at points along the z -axis. The graphs 1, 2, ..., 9 are, respectively, obtained by solving $N = 1, 2, \dots, 9$ coupled differential equations. The graph e shows the exact wave function.

points except in the neighbourhood of the nuclei. For a given N the rate of convergence of $\tilde{\Psi}$ to Ψ decreases as R increases.

A partial explanation of the trends in the energy and the wave function, as a function of R , ρ_A and N can be given on the basis of the convergence of the approximate electrostatic potential \tilde{U} as a function of R , ρ_A and N , see Appendix F; the exact electrostatic potential U of the molecule is replaced by \tilde{U} because of the approximation of the exact wave function Ψ by $\tilde{\Psi}$. For example it is shown in Appendix F that as $R \rightarrow \infty$, for finite N and $\rho_A = R/2$, $\tilde{U} \rightarrow 0$ and hence for such values of R , ρ_A and N the midpoint calculations will yield the free electron state solution of the Schrödinger equation and not the desired bound state solution. This then explains the poor convergence of the $\rho_A = R/2$ results discussed in Sec. IV.1B for large values of R .

CHAPTER V

DISCUSSION OF THE CONVERGENCE OF ONE CENTRE RESULTS FOR THE GROUND STATE OF THE H_2^+ MOLECULE

The exact one centre partial wave results for the energy and wave function of the ground state of the H_2^+ molecule are given in Chapter IV as a function of R , ρ_A and N . It was observed in Chapter IV that the rates of convergence of the calculated interaction energies to the corresponding exact values are in general slow as a function of N for the important intermediate values of R in the proton centred calculations and for all but small values of R in the midpoint centred calculations. These convergence problems are discussed in this chapter by using both the notion of coulomb and exchange energies^{15,22,23} and the cusp characteristics^{2(a),35,52} of the one centre wave functions. These discussions of the exact one centre results are then used in Sec. V.4 to discuss the convergence problems of the more conventional one centre variational and perturbation procedures.

V.1 BRIEF REVIEW OF THE VARIATIONAL AND PERTURBATION PROCEDURES FOR SOLVING THE SCHRÖDINGER EQUATION

A brief review of the variational⁷⁷ and Rayleigh
Schrödinger perturbation^{55,77-79} methods for solving the

Schrödinger equation for a physical system is given in this section. These variational and perturbation methods are used in Secs. V.2A and V.2B to define the coulomb and exchange energies which are later used in Sec. V.3 to discuss the convergence of the one centre results for the ground state of the H_2^+ molecule.

V.1A THE VARIATIONAL PROCEDURE

The variational procedure⁷⁷ gives an upper bound, E , to the ground state energy of a physical system, that is

$$E \leq \bar{E} = \frac{\langle \bar{\psi} | H | \bar{\psi} \rangle}{\langle \bar{\psi} | \bar{\psi} \rangle} \quad (V.1-1),$$

where E is the exact ground state energy, H is the Hamiltonian and $\bar{\psi}$ is a ground state trial wave function, respectively, for the system under consideration. The wave function $\bar{\psi}$ can be chosen in many different ways, see for example below. Indeed the partial wave methods discussed in Chapter III are variational in nature.

V.1B THE RAYLEIGH SCHRÖDINGER PERTURBATION PROCEDURE

The Rayleigh Schrödinger perturbation method^{55,77-79} depends on the decomposition of the Hamiltonian H . In general the Hamiltonian can be written in the form

$$H = H_0 + V \quad (V.1-2),$$

where H_0 and V , respectively, are the zeroth order Hamiltonian and the perturbation. The zeroth-order energy, $E^{(0)}$, and wave function, $\psi^{(0)}$, are solutions to the unperturbed Schrödinger equation

$$H_0 \psi^{(0)} = E^{(0)} \psi^{(0)} \quad (V.1-3).$$

The energy, through n^{th} order in V , is given^{55,78} by

$$E^{(n)} = E^{(0)} + E^{(1)} + E^{(2)} + \dots + E^{(n)} \quad (\text{V.1-4}),$$

where the perturbed energies through third order are given explicitly by

$$E^{(1)} = \langle \psi^{(0)} | V | \psi^{(0)} \rangle \quad (\text{V.1-5})$$

$$E^{(2)} = \langle \psi^{(0)} | V | \psi^{(1)} \rangle \quad (\text{V.1-6})$$

and

$$E^{(3)} = \langle \psi^{(1)} | V - E^{(1)} | \psi^{(1)} \rangle \quad (\text{V.1-7}).$$

The first order wave function, $\psi^{(1)}$, is obtained by solving the differential equation

$$[H_0 - E^{(0)}] \psi^{(1)} + (V - E^{(1)}) \psi^{(0)} = 0, \quad \psi^{(1)} \perp \psi^{(0)} \quad (\text{V.1-8}).$$

The difficulty in solving Eq. (V.1-8) depends not only on the nature of the physical problem but also on the choice of the unperturbed problem. The choice of the unperturbed problem is not unique but depends on physical intuition and mathematical convenience. In setting up the unperturbed problem two techniques are commonly used: (1) H_0 is chosen first and $\psi^{(0)}$ is obtained by solving Eq. (V.1-3) or (2) $\psi^{(0)}$ is chosen first and H_0 and V are constructed by using Sternheimer techniques^{55,78,80}.

V.2 THE EXCHANGE AND COULOMB ENERGIES FOR THE H_2^+ MOLECULE

The usual variational trial functions used in valence bond or molecular orbital theory calculations of the interaction energy for diatomic molecules are constructed from basis functions that are centred on the two nuclei of the

diatomic molecule. In these calculations it is conceptually convenient to decompose the total interaction energy into two parts, the coulomb energy and the exchange energy^{15,22,23}. The coulomb energy corresponds to the classical interaction between two individual charge distributions and does not allow for the quantum mechanical effect of electron exchange between the interacting species. The coulomb energy contains^{6,11} the R^{-1} long range interaction energy which dominates the energy of interaction at large values of the interatomic separation. The total interaction energy of a diatomic molecule also contains effects due to the exchange[†] of electrons between the two nuclei and the exchange interaction energy can be defined^{15,22,23} as the difference between the total interaction energy and the coulomb interaction energy. In this subsection the coulomb and exchange interaction energies for the ground state H_2^+ molecule will be discussed by using both the variational and perturbation theory approaches, see Sec. V.1. These results will then be used in Sec. V.3 to help discuss the convergence difficulties of the exact one centre results for the ground state H_2^+ molecule as a function of R .

[†]For the H_2^+ molecule, which is of special interest in this work, the effects due to the exchange or sharing of the electron between the interacting species are often called resonance effects^{15,22,81}.

V.2A VARIATIONAL COULOMB AND EXCHANGE ENERGIES FOR THE H_2^+ MOLECULE

In order to evaluate the coulomb energy a trial coulomb wave function ψ_c , which does not contain the electron exchange effects between the two protons explicitly, is used in Eq. (V.1-1). For the H_2^+ molecule ψ_c can be written as

$$\psi_c = \sum_{K=0}^{K_{\max}} C_K \phi_K(a) \quad (V.2-1),$$

where the basis function $\phi_K(a)$ are centred on proton A and, for any practical calculation K_{\max} is a finite number. The coulomb energy $\bar{E}(\text{coul})$ is obtained by minimizing the energy with respect to the expansion coefficients C_K and any nonlinear variational parameters contained in the $\phi_K(a)$. The coulomb interaction energy for the molecule is then given by

$$\bar{E}_{\text{int}}(\text{coul}) = \bar{E}(\text{coul}) + \frac{1}{2} \quad (V.2-2),$$

where the factor $-\frac{1}{2}$ represents the energy of the ground state H atom.

The total variational energy, \bar{E}_T , is obtained by using a trial wave function ψ_T , which includes electron exchange effects explicitly in Eq. (V.1-1). For the ground state of the H_2^+ molecule this trial function can be written in the form of a properly symmetrized version of the coulomb trial function, that is

$$\psi_T = \sum_{K=0}^{K_{\max}} d_K [\phi_K(a) + \sigma_K \phi_K(b)] \quad (V.2-3),$$

where $\phi_K(a)$ and $\phi_K(b)$ are basis functions centred on protons A and B respectively, $\sigma_K = \pm 1$ depending on the parity of $\phi_K(b)$ and for any practical calculation K_{\max} is a finite number. The total energy is obtained by minimizing the energy with respect to the variational parameters occurring in Ψ_T and the exchange and total interaction energies are then defined, respectively, by the relations

$$E_{\text{int}}(\text{exchange}) = E_T - E(\text{coul}) \quad (\text{V.2-4})$$

and

$$E_{\text{int}}(\text{total}) = E_T + \frac{1}{2} \quad (\text{V.2-5}).$$

V.2B. PERTURBATION THEORY COULOMB AND EXCHANGE ENERGIES FOR THE H_2^+ MOLECULE

In order to evaluate the coulomb energy in the perturbation method a coulomb zeroth order wave function $\psi_c^{(0)}$, which does not contain electron exchange effects between the protons explicitly is used for the unperturbed problem. For the ground state of the H_2^+ molecule $\psi_c^{(0)}$ can be chosen as

$$\psi_c^{(0)} = 1s_a \quad (\text{V.2-6}),$$

where $1s_a$ is a "1s" type hydrogenic wave function centred on proton A. The coulomb energy is then obtained by carrying out the energy calculations through a given order, n , in the perturbation and is given by, see Eq. (V.1-4),

$$E(\text{coul}) = E^{(0)}(\text{coul}) + E^{(1)}(\text{coul}) + \dots + E^{(n)}(\text{coul}) \quad (\text{V.2-7}).$$

The coulomb interaction energy $E_{\text{int}}(\text{coul})$, obtained through

n^{th} order in the perturbation, is given by a relation analogous to that given by Eq. (V.2-2).

In the perturbation method the total energy is obtained by using the zeroth order wave function $\psi_T^{(0)}$, which contains electron exchange effects explicitly the ground state of the H_2^+ molecule $\psi_T^{(0)}$ can be chosen as the properly symmetrized version of the coulomb zeroth order wave function given by Eq. (V.2-6),

$$\psi_T^{(0)} = C (1s_a + 1s_b) \quad (\text{V.2-8}),$$

where $1s_a$ and $1s_b$ are "1s" type hydrogenic functions centred on protons A and B respectively and C is a normalization constant. For this form of $\psi_T^{(0)}$ the H_0 and V can be constructed using Sternheimer techniques^{57,78,80} and the total energy is obtained by carrying out the calculations through higher orders in the perturbation. The exchange and total interaction energies in the perturbation method are then defined by relations analogous to those given by Eqs. (V.2-4) and (V.2-5).

Both the coulomb and the total energy perturbation theory calculations, defined by the zeroth order wave functions given by Eqs. (V.2-6) and (V.2-8) respectively, have been carried out through third order in the energy^{5(b),14(b),80}

These perturbation theory results[†] are compared in Table V.2-1 with the exact results³⁸⁻⁴⁰ for the interaction energy and the agreement between the total perturbation interaction energy and the exact results is very good. It appears that no accurate evaluation of the coulomb interaction energy by the variational procedure discussed in Sec. V.2A has been carried out. Many two centre variational calculations for the total interaction energy are available, see for example Refs. [82-86], and the "exact" calculations by Refs. [38-40] are essentially variational in nature. From the results given in Table V.2-1 it is clear that the coulomb interaction energy dominates the total interaction energy for sufficiently large values of R.

[†]The perturbation theory coulomb and total interaction energies given in Table V.2-1 were obtained using, respectively, the zeroth order wave functions $\psi_C^{(0)} = a e^{-sr_A}$ and $\psi_T^{(0)} = b(e^{-sr_A} + e^{-sr_B})$ where a and b are normalization constants and r_A and r_B are the distances from the electron to the nuclei A and B. The screening constant s, in each calculation, was chosen to optimize the energy through first order. The agreement between the perturbation theory and exact total interaction energy is very good. This can be improved by a more sophisticated choice for the two centre exchange zeroth order wave function, see Ref. [80].

TABLE V.2-1: A comparison of the coulomb and total perturbation theory interaction energies and the exact total interaction energy for the ground state H_2^+ molecule. These results are obtained from Refs. [5(b),14],[80] and [38-40] respectively. The energies $E_{\text{int}}(\text{coul}; 3)$ and $E_{\text{int}}(\text{total}; 3)$ correspond to the perturbation results carried through third order, see the text. The $E_{\text{int}}(\rho_A = 0)$ are the lowest proton centered results taken from Table IV.1-1 of this thesis. At $R = 20$ all the entries in this table agree with each other to three significant figures and give the value $E_{\text{int}} = -0.143(-4)$.

R	$-E_{\text{int}}(\text{coul}; 3)$	$-E_{\text{int}}(\text{total}; 3)$	$-E_{\text{int}}(\text{exact})$	$-E_{\text{int}}(\rho_A = 0)$
2	0.6250(-1)	0.1025(0)	0.1026(0)	0.1010(0)
3	0.3273(-1)	0.7735(-1)	0.7756(-1)	---
4	0.1290(-1)	0.4593(-1)	0.4608(-1)	0.3975(-1)
5	0.5089(-1)	0.2433(-1)	0.2442(-1)	---
6	0.2233(-2)	0.1194(-1)	0.1197(-1)	0.3742(-2)
8	0.6189(-3)	0.2560(-2)	0.2570(-2)	0.6741(-3)
10	0.2398(-3)	0.5767(-3)	0.5787(-3)	---
15	0.4547(-4)	0.4890(-4)	0.4893(-4)	0.4550(-4)

It is important to realize that in the conventional valence bond or molecular orbital theory, the approximate wave functions are constructed by using basis functions whose functional forms are predetermined. Hence these basis functions do not in general constitute the optimum basis set for these calculations. It will be seen in Sec. V.3 that if the basis functions are properly optimized the coulomb interaction energy, as defined in this section, can actually approximate the total interaction energy. The consequence of this with respect to the validity of the decomposition of the total interaction energy into definite coulomb and exchange components is discussed in the following section.

V.3 DISCUSSION OF THE CONVERGENCE PROPERTIES OF THE EXACT ONE CENTRE RESULTS FOR THE GROUND STATE OF THE H_2^+ MOLECULE

The purpose of this section is to discuss, in terms of the conventional ideas of electron exchange effects, the reasons for the relatively slow convergence of the exact one centre results for the interaction energy for the ground state of the H_2^+ molecule as a function of R , ρ_A and N .

V.3A THE PROTON CENTRED RESULTS

The proton centred results for the interaction energy converge, in general, slowly to the exact values. This is not hard to understand by using the cusp characteristic of the proton centred wave function as a function of R and N ,

see Sec. IV.2A, and the notion of exchange and coulomb energies presented in Sec. V.2.

A comparison of the proton centred interaction energies and the exact coulomb, exchange and total energies, see Table V.2-1, shows that the proton centred results are quite capable of reproducing the total interaction energy including electron exchange effects. For example when $R = 2, 4$ and 6 the proton centred interaction energies for $N = 14, 14$ and 11 , respectively, yield 98.4%, 86.3% and 31.3% of the total interaction energy. On the other hand the coulomb energies for these values of R give respectively 64.3%, 28.1% and 18.7% of the total interaction energy. However, as R becomes large, N must be taken very large in the proton centred calculations in order to represent accurately the small difference between the total and the coulomb energies for large values of R , see Sec. IV.1A. Thus as R becomes large and N is small the proton centred interaction energy appears to represent the coulomb energy and not the total energy. In principle for sufficiently large values of N the proton centred results approximate the total energy for all R .

The convergence properties of the proton centred results can be illustrated nicely by considering the behaviour of the wave function as a function of R and N . The exact stationary state wave function has identical cusps at the nuclear positions, see Figs: IV.2-1 - IV.2-3, which indicate that the electron is shared equally between the two identical

nuclei for any given value of R . On the other hand the wave function obtained by the proton centred calculations for small N , see Figs. IV.2-1 - IV.2-3, overestimates the cusp at the expansion centre A and underestimates the cusp at the nucleus B, that is the proton centred calculations poorly represent electron exchange effects between the protons for these values of N . Hence for small N the proton centred interaction energy tends to represent the coulomb interaction energy and not the total interaction energy which includes electron exchange effects. Further inspection of Figs. IV.2-1 - IV.2-3 shows that the overestimation of the cusp at A and the underestimation of the cusp at B is reduced as N increases. Thus in the limit of sufficiently large N , for a given value of R , the cusps at A and B become identical and agree with the exact cusps. Hence the proton centred calculations can yield the total interaction energy, which includes both exchange and coulomb interaction energies, for sufficiently large values of N .

Another way of explaining the convergence problem of the proton centred calculations is to consider the symmetry of the wave function. The trends in the proton centred wave functions shown in Figs. IV.2-1 - IV.2-3 show that for a given value of R the proton centred wave functions with small N do not have the g symmetry characteristic of the ground state of the H_2^+ molecule. However as N increases these wave functions tend to acquire the appropriate cusp characteristics and in the limit of sufficiently large

values of N the proton centred wave functions do have g symmetry.

The above discussion on the convergence of the proton centred calculations leads to the conclusion that these results for the energy and wave function will converge to the corresponding exact values in the limit of sufficiently large values of N for any given value of R . Thus electron exchange effects are included implicitly in these calculations even though the wave function is centred at one of the protons. Therefore in the proton centred calculations reported here there is no unique way of decomposing the total interaction energy into definite coulomb and exchange components as was discussed in Sec. V.2 for the more usual variational and perturbation calculations of the energy. It is important to realize that the proton centred results given in Table IV.1-1 are obtained with fully optimized basis functions for the H_2^+ molecule, see also Sec. V.4 below, that are obtained from an exact one centre treatment of the molecule.

There is no doubt that the decomposition of the total interaction energy into coulomb and exchange interaction energies is conceptually convenient in many variational and perturbation calculations. However, it is clear from our proton centred calculations that such decompositions are not rigorous and are clearly basis set dependent. This remark, which is based on our proton centred results, is not completely unexpected. That is in principle, by completeness arguments,

a variational proton centred calculation using a complete set of one centred wave functions will converge to the exact energy of the system. However most of the usual one centre trial functions, used for this type of calculation previously, are constructed from a finite number of Slater or Gaussian orbitals, see for example Refs. [2(a), 29, 34, 42, 87, 88] with linear and non-linear variational parameters. Although these functions constitute complete basis sets when a sufficiently large number of them are used in a given calculation, the basis sets constructed previously with limited numbers of these functions appear to be not even nearly complete.

It is clear from the previous discussions in this section that the ability of a proton centred calculation to represent electron exchange effects is intimately connected with the representation of the pure g symmetry in the corresponding trial wave function. It has been concluded previously, see Katriel³⁴, that once the expansion centre is shifted off the internuclear midpoint the wave function has a mixed u and g symmetry. The optimized proton centred calculations of this work show that about 98.4% of the total interaction energy and a reasonable representation of the g symmetry in the wave function is obtained with $N = 14$ for $R = 2$ and $\rho_A = 0$. On the other hand if Slater or Gaussian orbitals are used in a proton centred calculation an inconveniently large number of these functions would be required to obtain the electron exchange effects in the energy and the g

symmetry in the wave function.

V.3B THE MIDPOINT CENTRED RESULTS

The midpoint centred results for the energy converge to the exact values for any given R for sufficiently large values of N , see Sec. IV.1B. However, the rate of convergence of these results rapidly decreases with increasing values of R . This trend can be explained using the cusp characteristics of the midpoint centred wave functions.

It can be seen from Figs. IV.2-4 - IV.2-6 that in the midpoint centred calculations the electron is shared equally between the protons and the wave function has the proper g symmetry for all R and N . It is also clear from these figures that the slow convergence of these calculations, as R increases, arises from the difficulty in representing the correct height of the cusps at the nuclear positions for large R when the value of N is not sufficiently large. Hence the midpoint centred calculations are not suitable for describing the dissociation of the H_2^+ molecule, see the discussion in Sec. IV.1B and Appendix F. With finite values of N the midpoint centred calculations will yield a free electron and two bare protons and not the proper lower energy dissociation products, namely a hydrogen atom and a proton. In principle the correct dissociation products can be obtained by taking $N \rightarrow \infty$, see Appendix F, but this is clearly not feasible in practice.

V.3C THE FLOATING CENTRED RESULTS

The rate of convergence of the one centre results for a given R and N can be improved by optimizing the position of the expansion centre. However, as pointed out in Sec. IV.1C, for any practical calculation it is more convenient to fix the expansion centre either at a proton or at the internuclear midpoint depending on the values of R and N .

The reason why the expansion centre can float away from the proton or the midpoint for a given value of R can be explained on the basis of the above discussions for the proton and midpoint centred results. Unless N is sufficiently large the proton centred calculations overestimate the cusp at the expansion centre A and underestimate the cusp at the other nucleus B and hence yield wave functions with a mixed u and g symmetry. On the other hand for small N the midpoint centred calculations yield the proper g symmetry in the wave function but poorly represent the height of the cusps for all except very small R . Since both cusp and symmetry conditions (or equivalently exchange effects) in the wave function should be satisfied simultaneously in order to obtain the total exact interaction energy there is, for every R and N , an optimum position for the expansion centre so that these two conditions are accounted for optimally. For sufficiently large values of N this optimum position of the expansion centre is at the internuclear midpoint.

V.4 A DISCUSSION OF THE CONVERGENCE PROBLEMS OF CONVENTIONAL ONE CENTRE METHODS

One centre methods have often been used previously to calculate molecular energies, see for example the reviews [1]. The chief advantage of these one centre methods over the more common multicentre methods, which explicitly include electron exchange effects in the basis sets used in the calculations, is that the integrals occurring in the former approach are very easy to evaluate. However, the one centre methods suffer from the drawback that, in general, the results obtained by these methods converge slowly to the exact values.

Detailed model studies of the convergence properties associated with conventional one centre methods have been performed for the H_2^+ and H_2 molecules in or close to their equilibrium configuration with the expansion centre at the internuclear midpoint $\rho_A = R/2$; see for example Howell and Shull^{2(a)}, Hagstrom and Shull⁸⁹ and Joy and Handler^{88,90}.

Some of the one centre interaction energies for the ground states of these molecules corresponding to $\rho_A = R/2$ are given in Table IV.4-1. The slow rate of convergence of these results is clearly revealed by the fact that large basis sets or higher orders in the perturbation are required to obtain reasonable results for the interaction energy. For larger values of R the rate of convergence becomes much poorer for the midpoint centred calculations^{5-8,29,33,34}

In this section the exact one centre partial wave results, reported in Chapter IV for the ground state

TABLE V.4-1: Some values of the one centre interaction energies for the ground states of the H_2^+ and H_2 molecules at their equilibrium separations, $R = 2$ and $R = 1.4$ respectively. These results have been obtained with $\rho_A = R/2$ and by using either the perturbation method (Pert) or the variational method (Var).

$H_2^+, E_{int}^{38-40} = -0.1026(0)$			$H_2, E_{int}^{91} = -0.17447(0)$				
$-E_{int}$	Method	Number of basis func- tions or order of perturbation	Reference	$-E_{int}$	Method	Number of basis func- tions or order of perturbation	Reference
0.9563(-1)	Var	15	2(a)				
0.9893(-1)	Var	6	88	0.1588(0)	Var	7	92
0.1012(0)	Var	14	88	0.1604(0)	Var	7	93
0.1024(0)	Var	20	42	0.1614(0)	Var	44	89
0.7975(-1)	Pert	2	33	0.1675(0)	Var	20	94
0.8990(-1)	Pert	2	5(b)				
0.9053(-1)	Pert	2	6	0.1726(0)	Var	57	95
0.9608(-1)	Pert	3	7				
0.1027(0)	Pert	5	5(a)	0.1316(0)	Pert	3	5(a)
0.5956(0)	Pert	2	5(c)				

H_2^+ molecule, are compared with previous conventional one centre variational and perturbation results for this molecule. This comparison furnishes an assessment of (1) the quality of our optimal radial basis functions relative to the conventional Slater and/or Gaussian basis functions for one centre calculations and (2) the feasibility of conventional one centre calculations relative to our exact partial wave calculations.

V.4A THE CONVENTIONAL ONE CENTRE VARIATIONAL RESULTS FOR THE H_2^+ MOLECULE

In most previous ^{8,29,34,42,88,90} one centre variational calculations for the ground state H_2^+ molecule the trial wave functions,

$$\psi = \sum_{\ell=0}^N R_{\ell}(r) Y_{\ell}^0(\theta, \phi) \quad (V.4-1),$$

were chosen with the approximate form,

$$R_{\ell}(r) = \sum_{K=1}^{M_{\ell}} C_K^{(\ell)} \phi_K^{(\ell)}(r) \quad (V.4-2)$$

for the radial wave functions. In Eq. (V.4-2) the coefficients $C_K^{(\ell)}$ are linear variational parameters, M_{ℓ} is usually a relatively small number and the functions $\phi_K(r)$ may contain nonlinear variational screening parameters. It is clear from Eqs. (V.4-1) and (V.4-2) that for a fixed value of N the conventional one centre results have dual convergence problems, namely the convergence related to the series representation for both ψ and R_{ℓ} . On the other hand, for a fixed value of N , the convergence problem for the exact one.

centre partial wave calculations, discussed in Chapters III and IV, is associated only with the series for $\tilde{\Psi}$ and not for the \tilde{R}_ℓ . Therefore the conventional one centre variational results for E and $\tilde{\Psi}$ can at best converge to the corresponding values of the exact one centre results and it is obvious from the discussions of the exact one centre results, given in Chapter IV and Sec. V.3, that the conventional one centre variational methods can be feasible only for a limited range of R values.

The quality of the radial wave functions, $\tilde{R}_\ell(r)$, is quite important in determining the rate of convergence of one centre variational results. In what follows we briefly compare the exact one centre calculations of this thesis with some of the conventional one centre calculations for the ground state of H_2^+ that have been performed by using the following radial basis functions $\phi_K(r)$ to represent the radial wave function $\tilde{R}_\ell(r)$:

- (1) Slater orbitals, see for example Refs. [41,42,87,88]

$$\phi_K^{(\ell)}(r) = r^{n_K^{(\ell)}-1} e^{-\alpha_K^{(\ell)} r},$$

- (2) Modified Laguerre^{2(a)} functions[†]

$$\phi_K^{(\ell)}(r) = r^\ell \frac{L_{n_K+\ell+1}^{2\ell+2}(2\alpha_\ell r)}{n_K+\ell+1} e^{-\alpha_\ell r},$$

[†]These are orthogonalized Slater orbitals when the α_ℓ are either the same for all ℓ or the same for each given value of ℓ .

and

(3) Gaussian orbitals^{34,88,96-98}

$$\phi_K^{(\ell)}(r) = r^{n_K(\ell)} e^{-\alpha_K(\ell)r^2}$$

The rate of convergence of the one centre results obtained by using these various radial basis sets are different. For example Howell and Shull^{2(a)} obtained, using 15 modified Laguerre Functions (6 for $\ell = 0$, 5 for $\ell = 2$ and 4 for $\ell = 4$), the value $E_{\text{int}} = -0.9563(-1)$ for $R = 2$ and $\rho_A = R/2$. These authors used the same value for α_ℓ for a given ℓ . The exact value of the interaction energy for $R = 2$ is $E_{\text{int}}(\text{exact}) = -0.1026(0)$. The results of Table IV.1-2, show that 3 optimal basis functions (referred in this table as 3 coupled equations) with $\ell = 0, 2$ and 4 give $E_{\text{int}} = -0.9644(-1)$. Another example is given by the work of Joy and Handler⁸⁸ who obtained for $R = 2$ and $\rho_A = R/2$, using 14 Slater orbitals (4 for $\ell = 0$, 4 for $\ell = 2$, 2 for $\ell = 4$, 2 for $\ell = 6$ and 2 for $\ell = 8$), the result $\bar{E}_{\text{int}} = -0.101206(0)$ with integer principal quantum numbers, n_K , and $\bar{E}_{\text{int}} = -0.101211(0)$ with non-integer principle quantum numbers. It is clear from these results[†],

[†]See also the calculation of Joy and Handler⁸⁸ involving 6 Slater orbitals (2 for $\ell = 0$, 2 for $\ell = 2$ and 1 for each of $\ell = 4$ and 6) for $R = 2$ and $\rho_A = R/2$ which yields $\bar{E}_{\text{int}} = -0.9861(-1)$ and $-0.9893(-1)$, respectively, for integer and non-integer values of the principle quantum numbers.

see also Bishop,^{1(a)} that the improvement in the interaction energy with non-integer principle quantum numbers is not very significant. Performing equivalent calculations with Gaussian orbitals, Joy and Handler⁸⁸ found energies which were inferior to their results quoted above. An inspection of the results of Table IV.1-2 shows that 5 optimal basis functions with $\ell = 0, 2, 4, 6$ and 8 give $E_{\text{int}} = -0.1013(0)$. It appears that the most detailed one centre midpoint calculation for the ground state H_2^+ molecule has been performed by Hayes and Parr⁴². These authors obtained, using 20 Slater orbitals (4 for $\ell = 0$, 3 for $\ell = 2$, 2 for $\ell = 4$, 2 for $\ell = 6$, 2 for $\ell = 8$ and 1 for each of $\ell = 10, 12, 14, 16, 18, 20, 22$), the value $E_{\text{int}} = -0.1024(0)$ for $R = 2$ and $\rho_A = R/2$ with integer principle quantum numbers. It can be seen from Table IV.1-2 that 9 optimal basis functions with $\ell = 0, 2, 4, \dots, 16$ yield the value $E_{\text{int}} = -0.1024(0)$.

Very few conventional midpoint one centre variational calculations have been performed for intermediate and large values of R , see however Refs. [2(a), 8, 29, 34]. It is clear from the more extensive calculation of Ref. [8], see also the corresponding perturbation results of Refs. [5, 7, 37, 99] and our exact partial wave midpoint centred results given in Secs. IV.1B and V.3, that conventional midpoint centred variational calculations with limited numbers of basis functions, such as those given in points (1)-(3), will fail to reproduce (1) reasonable results for intermediate and large values of R and (2) the proper dissociation products

for this molecule. A natural way to attempt to overcome the difficulties associated with the fixed midpoint centred calculations is to allow the expansion centre to float in order to minimize the energy, see for example Refs. [6-8,29,33]. It is well known^{57-59,96,97} that the proton centred calculation can conveniently yield reasonable results for the interaction energy at large R . Thus since the energy optimized floating centre must shift to the proton for large, R , see Sec. V.3, Appendix F and Refs. [6-8,33], the difficulties associated with the fixed midpoint centred calculations for these values of R can be overcome by the floating centre method. However, it is evident from the work of Ref. [8], see also the discussion of the exact partial wave results given in Secs. IV.1 and V.3 and the corresponding one centre perturbation results of Refs. [5-7,14,59], that for intermediate values of R , all conventional one centre variational methods, employing a useable number of basis functions, will fail to yield reasonable results regardless of the position of the expansion centre. The conventional one centre variational calculations, see for example Refs. [8,29,34], indicate that for intermediate values of R the expansion centre is located at a proton[†] and not at the internuclear midpoint. However

[†]This observation is valid when basis functions with odd ℓ values are included in the calculation. If basis functions with only even ℓ values are used in the calculation, the expansion centre remains off the proton for fairly large

the exact one centre results of this thesis show, see Chapter IV and Sec. V.3, that when a sufficient number of properly optimized radial basis functions are used in the calculation the expansion centre floats away from the proton for intermediate values of R and in principle, with large enough basis sets, the floating centre will shift to the internuclear midpoint for all R .

All the available conventional one centre variational and perturbation results, see for example Refs. [5,8,14, 29,57,58] indicate that the proton centred results can, at most, account for the coulomb energy and not the total energy including electron exchange effects, see Sec. V.2. On the other hand, see Table IV.1-1, the exact optimized proton centred results are quite capable of accounting for the total energy including electron exchange effects. For example using $N = 14$ the proton centred exact partial wave interaction energies for $R = 2$ and 4 yield respectively 98.4% and 86.3% of the exact results, see Sec. V.3A. Equivalent results can not be obtained by conventional proton centred variational calculations without using a prohibitively large number of basis functions.

It is clear from these examples that the usefulness of the conventional one centre variational calculations, especially for the important intermediate values of R ,

values of R , see Refs. [8,34], in order to provide the characteristics of p functions in the calculations.

is reduced drastically with respect to the exact partial wave calculations as a result of the particular approximate forms of the radial basis functions used in these calculations.

V.4B THE CONVENTIONAL ONE CENTRE PERTURBATION RESULTS FOR THE H_2^+ MOLECULE

The Rayleigh Schrödinger perturbation method^{55,77-79} discussed in Sec. V.1, requires the decomposition of the exact Hamiltonian into an unperturbed Hamiltonian and a perturbation. Using one centre perturbation methods the Schrödinger equation for the H_2^+ molecule has been solved with two choices for the unperturbed Hamiltonian^{2(c),5-7,14,33,37,99},

$$H_0 = -\frac{\nabla^2}{2} - \frac{1}{r}, \quad V = \frac{1}{r} + U \quad (V.4-3)$$

and


$$H_0 = -\frac{\nabla^2}{2} + U_0, \quad V = U - U_0 \quad (V.4-4),$$

where r has been considered as a fixed constant as well as a variable parameter and U is defined by Eqs. (II.2-1) - (II.2-4). The unperturbed problems defined by Eqs. (V.4-3) and (V.4-4) are, respectively called the "Screened Hydrogen Atom" and "Molecular Puff" problems^{6,7,33,37}. The perturbation results obtained by using these zeroth order problems converge, in general, slowly to the exact values as a function of the order of perturbation^{2(c),5-7,14,33,37,99}. This convergence problem of the one centre perturbation

methods can be understood with the help of the exact partial wave results of this thesis.

It is clear from the radial wave equations given by Eqs. (II.2-18) that the single radial wave equation, specified by the value $s = 0$, constitutes the unperturbed problem for the scheme based on the Molecular Puff. On the other hand the perturbation scheme based on the Screened Hydrogen Atom is an approximation to that based on the Molecular Puff and in what follows only the Molecular Puff problem is considered.

It is clear from the results and discussions of the exact one-centre calculations, given in Chapter IV and Sec. V.3, that the Molecular Puff can become a reasonable approximation of the physical system only for small R when $\rho_A = R/2$ and for large R when $\rho_A = 0$. For intermediate values of R , irrespective of the choice for the expansion centre, the Molecular Puff poorly represents the actual physical problem and hence very high orders in the perturbation will be needed to obtain reasonable results. This explains the slow rate of convergence of the one-centre perturbation calculations for intermediate values of R , see for example Refs. [5,6,7,37]. For faster convergence of these results non-spherical components of U must be included in H_0 . For example with $\rho_A = R/2$ and $R = 4$ and 6 , respectively, one will probably find that many angular components of H , at least through $\ell = 4$ and $\ell = 10$, must be used in the unperturbed problem, H_0 , in order to yield



reasonable rates of convergence of the perturbation results for these values of R .

It is important to realize that the inclusion of non-spherical components in H_0 will make the perturbation theory calculations complicated and whether one centre perturbation calculations of this type are feasible or not remains to be seen. Thus the usefulness of one centre perturbation methods for our model system is limited to only small and large values of R .

CHAPTER VI

CONCLUSIONS

While the ground state H_2^+ molecule is not an all embracing model for determining the usefulness of fixed or floating one centre methods, it does provide a severe test of these techniques since the interaction energy for this molecule, in the language of valence bond theory or inter-molecular force theory, is electron exchange dominated. The convergence difficulties with the one centre approach as a function of expansion centre, partial wave order and inter-nuclear distance for most other one-electron molecules will not be as severe as for the $1s\sigma_g$ state of H_2^+ , see the relevant discussions in Chapter I and below. As pointed out in Chapter I the one centre method is not very applicable for the treatment of multi-electron diatomic molecules as R increases from the equilibrium separation; this point will also be discussed in more detail in what follows.

For small $R < 4$ the proton centred calculations can give reasonable values for the interaction energy and the wave function for the $1s\sigma_g$ state of H_2^+ while for large R these calculations can give reasonable values for the interaction energy but will fail to yield wave functions having the proper symmetry unless the calculation is carried out to prohibitively high partial wave order. The proton centred results for the interaction energy are good for sufficiently

large R because the contribution of electron exchange effects to the interaction energy becomes very small for these values of R and therefore the energy can be evaluated accurately by using a wave function of mixed (u,g)-symmetry. For intermediate values of R the rate of convergence of the proton centred partial wave results to the exact values is very slow and consequently, for these values of R , the proton centred calculations are not suitable for practical purposes. However, in principle it is clear that the proton centred results are quite capable of accounting for the total energy which includes electron exchange effects between the protons. The consequence of this observation is that the conventional definitions of coulomb and exchange energies, given in Sec. V.2, are basis set dependent and are not rigorous. The ability of a proton centred wave function to represent electron exchange effects is clearly significant in the area of intermolecular forces and is probably the underlying reason for the lack of uniqueness¹⁰⁰ in many of the exchange perturbation theories^{24-26,100} which involve the evaluation of electron exchange corrections to the coulomb interaction energy. It is clear, for relatively small R at least, that the sets of high order proton centred partial wave orbitals evaluated in this thesis are essentially complete and it appears that this is the first demonstration of a complete set of orbitals in the area of intermolecular forces which do not contain electron exchange effects explicitly in their functional form.

The exact midpoint centred partial wave calculations can provide reasonable results for the interaction energy and the wave function for the ground state H_2^+ molecule for $R \leq 6$ if the calculation is carried to reasonably high order and for these R values the midpoint centred results converge to the exact values much more rapidly than the proton centred results. On the other hand for large R the midpoint centred calculations are not feasible and to obtain reasonable results for the energy the expansion centre must be chosen at a proton. For intermediate values of $R > 6$ the midpoint centred results converge very slowly to the exact values and hence are not very useful for these R values. It is interesting to note that the midpoint centred wave functions have the proper g -symmetry of the ground state H_2^+ molecule for all partial wave orders and for all values of R while the proton centred wave functions, for any finite partial wave order, only approximate this symmetry. However even though the midpoint centred calculations have proper symmetry for all R the proton centred results for the interaction energy are much superior than the corresponding midpoint centre results for intermediate and large R values for any feasible partial wave order of approximation.

The floating one centre approach, which utilizes the energy optimized position of the expansion centre in the partial wave method, is very useful with respect to uniting the short and long range one centre approaches for evaluating the interaction energy for the $1s\sigma_g$ state of H_2^+ and in

understanding the misbehaviour of fixed expansion centre calculations as a function of R and N . However it is clear, see Sec. IV.1C, that this approach does not resolve the convergence problems associated with the one centre methods for intermediate values of R . For computational purposes a superposition of the proton and the internuclear midpoint centred methods is more feasible than the floating centre technique, see Secs. IV.1C and V.3C. While it is clear that the optimum results for the interaction energy obtained here, for common values of R , are substantially better than those obtained by our previous^{6,7} Rayleigh Schrödinger perturbation theory calculations based on the "1s" screened hydrogen atom or the molecular puff as zeroth order problems, it is equally clear that one would have to carry the exact partial wave proton and internuclear midpoint centred calculations of this thesis to unrealistically high order to obtain accurate results for the interaction energy for intermediate values of the internuclear separation, $7 \lesssim R \lesssim 12$ say.

The conventional one centre variational calculations using basis functions such as Slater, Gaussian or Laquerre functions, discussed in Sec. V.4A, suffer from a convergence problem which is much more severe than that for the exact partial wave calculations, that is, the optimal one centre basis set calculations for the molecule. This is because the conventional variational calculations are performed using approximations for the exact partial wave radial functions. Also, as discussed in Sec. V.4B, the one centre perturbation

calculations^{6,7} based on the screened "1s" or the "Molecular Puff" zeroth order problems are feasible only for small and large values of R . The practicability of one centre perturbation calculations with non-spherical components of the electrostatic potential in the unperturbed problem needs to be investigated, but it is clear that in this procedure the mathematical complexity of the perturbation treatment will increase enormously relative to the "1s" or "Molecular Puff" perturbation treatment and probably with respect to the exact partial wave calculations as well.

The analytic method, presented in Chapter III, for solving the radial differential equations not only provides a convenient alternative to the purely numerical methods for solving such equations but also provides the radial functions in "analytic" form. This analytic form can be used to study the behaviour of these radial functions as functions of Z_A , Z_B , N , R , ρ_A , and E . Since these partial wave orbitals appear to have much better convergence properties than the usual one centre basis functions, a detailed study of the radial part of the exact partial wave orbitals, as a function of expansion centre and internuclear distance, for the one electron molecular system may well be helpful in constructing new useful basis functions for molecular one (and two) centre calculations. It appears, see for example Ref. [101] no one centre analytic solution has been worked out in the χ_α calculation for the H_2^+ molecule for the region of this calculation which corresponds to Region II with $\rho_A = \rho_B = R/2$

of this thesis. The analytic solution presented in Chapter III for Region II with $\rho_A = \rho_B = R/2$ provides a solution for the corresponding region of the χ_α calculation and this solution should be useful in extending the work of Pettifor¹⁰¹ in illustrating the suggested¹⁰¹ importance of the nonspherical components of the potential in the χ_α calculation.

While the proton centred calculations with sufficiently large N can in principle yield accurate results for the ground state H_2^+ molecule for all R , this approach is not feasible for even moderately large R as discussed previously. An alternative procedure will be to perform variational (or perturbation) calculations using approximate wave functions constructed from a properly symmetrized linear combination of the optimal partial wave orbitals obtained with small N . The resulting functions will have appropriate cusp and symmetry properties. This alternative procedure will, however, involve more difficult integrals than the corresponding single centre calculation and would amount to constructing a wave function containing electron exchange effects explicitly.

In this work the ground state H_2^+ molecule has been investigated extensively since it is the most appropriate of all the H_2^+ -like molecules for examining the difficulties associated with using (floating) one centre methods for evaluating useful values of the interaction energy for all values of R and because, simultaneously, concepts relevant to the area of intermolecular forces, involving the notions of electron exchange effects and coulomb and exchange interaction energies, could be investigated by using this exchange

dominated homonuclear molecule as a model. The semi-analytical and the numerical techniques discussed in Secs. III.2 and III.3 are appropriate for solving the one centre partial wave problem for all states of the H_2^+ -molecule as a function of expansion centre, partial wave order and internuclear separation. Many of these molecules have interaction energies which have a large coulomb contribution and can therefore be treated much more effectively by (floating) one centre techniques than the ground state of H_2^+ . The results of the optimal one centre partial wave treatments of the $1s\sigma$, $2s\sigma$ and $2p\sigma$ states of the HeH^{++} molecule, given and discussed in Appendix I, indicate that many molecules of this type will be able to be treated in a unified effective way for all values of R by using (floating) partial wave one centre methods. Using the techniques discussed in this thesis very accurate results for the interaction energy, for all R , can be obtained for the $1s\sigma$ and $2s\sigma$ states of HeH^{++} by employing just 2 or 3 coupled equations in the one centre partial wave method while in the case of the more difficult $2p\sigma$ state over ninety-percent of the interaction energy can be obtained for all but some intermediate values of R , $3 \lesssim R \lesssim 7$ say, with $N \leq 7$. The corresponding accuracy can be obtained for $3 \lesssim R \lesssim 7$ by using extrapolation techniques to analyze the partial wave results corresponding to $N \leq 11$. Prototype calculations

for the H_2^+ molecule using the techniques discussed in Secs. III.2 indicate that many of the excited states of H_2^+ will be easier to treat than the $1\sigma_g$ state of H_2^+ and that higher energy states of a given symmetry are considerably easier to treat than the lowest energy state of that symmetry, see also for example [2(a), 2(b), 3, 35, 36, 41-43].

Although this thesis has been primarily concerned with one centre methods for H_2^+ -like molecules, one centre techniques have also been used to treat two electron diatomic molecules, see for example Table V.4-1 and Refs. [1]. Most of these attempts have used variational methods employing Slater, Gaussian or Laguerre type basis functions. However, Temkin and Bhatia^{4,102} have given one centre radial equations for the H_2 molecule with $\rho_A = \rho_B = R/2$. In principle the solution of these equations, and the above mentioned one centre variational and perturbation treatments, can yield accurate results for the molecule for all R . However as discussed in Chapter I, see also Ref. [8], it is not feasible to use one centre methods (midpoint or floating centred) to describe the behaviour of a general multi-electron diatomic molecule as R becomes at all large; this is particularly so when⁴ lower order partial wave calculations are under consideration. An alternative procedure, see Pan⁸, for treating a multi-electron diatomic molecule is to use the bipolar expansion^{14(a),15,19} to expand both the electrostatic potential V and the wave function Ψ in a two centre partial wave expansion. In the case of the two electron molecule H_2 , one obtains results of the form

$$V = \sum_{\ell_a} \sum_{\ell_b} \sum_m B_{\ell_a \ell_b}^m(r_1 r_2 R) Y_{\ell_a}^m(1) Y_{\ell_b}^{-m}(2)$$

and

$$\psi = \sum_{n_a} \sum_{n_b} \sum_{m_a} \sum_{m_b} R_{n_a n_b}^{m_a m_b}(r_1 r_2 R) Y_{n_a}^{m_a}(1) Y_{n_b}^{m_b}(2),$$

where r_1 is the distance between electron 1 and the centre a and r_2 is the distance between electron 2 and the centre b.

The expansion centres a and b can be located at any two points on the internuclear axis, see Ref. [8]. As discussed in Chapter I, the two expansion centres in this treatment can coalesce as R becomes small to yield the usual one centre approach useable for small values of the internuclear separation while as R becomes large the two expansion centres can float to the nuclei to give results corresponding to the long range treatment of molecular interaction energies. It is also important to note that this two centre partial wave approach involves, at most, the evaluation of two centre coulomb integrals, no electron exchange integrals occur in the treatment⁸. The bipolar expansion for V is the two centre analogue of the one centre Laplace expansion for the potential and wave function used previously in this thesis for the one electron problem. The radial equations for the $R_{n_a n_b}^{m_a m_b}(r_1 r_2 R)$ will probably be considerably more difficult to solve analytically than Eq. (II.2-18) for the one electron problem. In this event it may be easier to solve the Schrödinger equation for the molecule by using variational methods and employing an

approximate form for the radial wave function, see also Ref. [8], given for example by

$$R_{n_a n_b}^{m_a m_b}(r_1 r_2 R) \sim \tilde{R}_{n_a n_b}^{m_a m_b}(r_1 r_2 R) = \sum_{k_a, k_b} C(k_a, k_b) \phi_{k_a}(r_1) \phi_{k_b}(r_2),$$

where the basis functions ϕ_{k_a} and ϕ_{k_b} are centred on a and b respectively: Hopefully the functional form of the optimal radial functions for the H_2^+ molecule will provide valuable guidance either for solving the radial equations for the $R_{n_a n_b}^{m_a m_b}(r_1 r_2 R)$ or for finding the appropriate form for the functions ϕ_{k_a} and ϕ_{k_b} . Alternatively the Schrödinger equation for the H_2 molecule can be solved by perturbation procedures using the product of H_2^+ wave functions as the unperturbed wave function.

The convergence difficulties discussed for the exact floating one centre calculation of the $1s\sigma_g$ state of H_2^+ in this work suggests that the convergence of this two centre partial wave treatment for the ground state of H_2 will probably be slow for the interaction energy, as a function of intermediate values of R , even if the relevant two centre coupled differential equations can be solved exactly to a given partial wave order or accurately by using efficient basis sets and variational or perturbation techniques. This is because, like the $1s\sigma_g$ state of H_2^+ , the ground state of H_2 also has¹¹ an electron exchange dominated interaction energy. However because the two floating centre partial wave calculation can maintain the proper g -symmetry of the ground state of H_2 , for

all R , the convergence should be relatively better than that associated with the floating one centre calculation of the $1\sigma_g$ state of H_2^+ , see Chapter I and Ref. [8]. This two centre partial wave method should be more useful for many of the excited states of H_2 since many of these states have interaction energies which have a large coulomb component^{23(a),(c)} and are such that the average distances of the electrons from the nuclei are much greater than in the case of the ground state of H_2 for a given value of the internuclear separation. Therefore this approach may be quite useful in extending the usefulness of the one centre internuclear midpoint method^{4,102} useful for small values of R , to intermediate and large values of R for problems of this type.

While the practicality of the two centre partial wave method needs further investigation, it is clear that it can resolve the severe convergence problems associated with the evaluation of the interaction energy by using low order internuclear midpoint one centre partial wave methods for diatomic molecules that dissociate into two species containing electrons; H_2 is the simplest example of this type of molecule. For example, while the zeroth order partial wave internuclear midpoint centred calculation of the ground $1\Sigma_g^+$ state H_2 molecule by Bhatia and Temkin⁴ appears to give not unreasonable results for the total energy for values of R associated with the equilibrium internuclear separation, the more critical interaction energies obtained from Ref. [4] are positive for $R > 2$ and are not an adequate representation of the interaction

energy until R is very small approaching the united atom limit. Similar comments also apply to the evaluation of the interaction energy for the excited $1\sum_g^+$ states of H_2 by using the results of this⁴ zeroth order one centre partial wave calculation. Here the representation of the interaction energy obtained by the zeroth order one centre calculation can, in a sense, be worse than that for the ground state for a given value of R . This situation probably arises because, as pointed out by Bhatia and Temkin⁴, the zeroth order one centre approach cannot represent the degenerate configuration interaction states necessary¹⁰³ to obtain the double minimum¹⁰³ in the interaction energy for these states as a function of R . To improve these zeroth order calculations, as a function of R , it is probably necessary to go to higher partial wave orders of approximation and simultaneously allow the expansion centre to have the capability of splitting in two as discussed above. The two floating centre technique will be particularly helpful⁸ in improving the convergence of relatively low order calculations as a function of R . It would also be interesting to see if the double minima^{4,103} occurring in some of the excited $1\sum_g^+$ states of H_2 can be obtained by this type of extension of the work of Bhatia and Temkin⁴; they are absent in the zeroth order calculation as pointed out in Ref. [4].

In connection with the previous paragraph it is important to emphasize the point that the purpose of this thesis is to investigate the use of (floating) one (or two) centre partial wave methods in evaluating adequate results for the interaction

energy, which is the relatively small part of the total energy which determines the intermolecular forces, and hence the dynamics of an interaction, so critical for understanding and evaluating many physical and chemical processes involving the interaction of atoms and molecules as well as many properties of matter^{9,10,11,15}. In other areas of research it is not always so critical to achieve reasonable results for the interaction energy as a function of R . For example⁴ the results of low order one centre partial wave calculations can be useful in studying electron-atom or electron-molecule scattering problems and this was one of the purposes of the zeroth order one centre partial wave calculation of the $1\sum_g^+$ states of H_2 by Bhatia and Temkin⁴.

The evaluation of the interaction energy as a function of R for the ground states of the H_2^+ and H_2 molecules is difficult by either fixed or floating one (or two) centre methods since these interaction energies are electron exchange dominated. For this reason, as pointed out in Chapter I for the $1s\sigma_g$ state of H_2^+ , these molecules provide a severe test for the applicability of these methods. The work of Refs. [2(a), 2(b), 3, 35, 36, 41-43, 104], see also Appendix I and above, show that these techniques will be considerably more suitable for many excited state homonuclear and various heteronuclear one and two electron molecules. The methods discussed in the main portion of this thesis are directly applicable to the "coulomb dominated" one electron species and it is hoped that work discussed here, which augments the work by Y.H. Pan⁸ on the

two floating centre method, will also provide useful input into the treatment of general diatomic and polyatomic molecules by partial wave techniques.

APPENDIX A

EXAMPLES OF THE USE OF THE ANALYTICAL METHOD FOR SOLVING THE RADIAL EQUATIONS

This appendix contains examples of the use of the formal expressions given in Sec. III.2 for obtaining the analytical solution of the radial equations. In order to simplify the discussion 3-coupled equations with $s = 0, 1, 2$ and $m = 0$, see Eqs. (III.2-1) - (III.2-3), are considered. The examples in this appendix refer only to the case where the coordinate origin is located at one of the nuclei, see Secs. III.2A-1 and III.2B. The case where the coordinate origin is located at the internuclear midpoint is similar to that discussed here.

A.1 SOLUTION OF RADIAL EQUATIONS IN REGION I ($0 \leq r \leq \rho_B$)

The radial functions $F_s(r)$ are defined in terms of $\chi_s(r)$, see Eq. (III.2-10). The differential equations for $\chi_s(r)$, see Eq. (III.2-11), read as

$$H_0 \chi_0 = 2U_0 \chi_0 + \frac{2r}{\sqrt{3}} U_1 \chi_1 + \frac{2r^2}{\sqrt{5}} U_2 \chi_2 \quad (A.1),$$

$$H_1 \chi_1 = \frac{2}{\sqrt{3} r} U_1 \chi_0 + [2U_0 + \frac{4}{5} U_2] \chi_1 + [\frac{4}{\sqrt{15}} U_1 + \frac{6}{7} \sqrt{\frac{3}{5}} U_3] r \chi_2 \quad (A.2),$$

$$H_2 \chi_2 = \frac{2}{\sqrt{5} r^2} U_2 \chi_0 + [\frac{4}{\sqrt{15}} U_1 + \frac{6}{7} \sqrt{\frac{3}{5}} U_3] \frac{\chi_1}{r} + [2U_0 + \frac{4}{7} U_2 + \frac{4}{7} U_4] \chi_2 \quad (A.3),$$

where

$$H_s = \frac{d^2}{dr^2} + \frac{2(s+1)}{r} \frac{d}{dr} + 2E. \quad (A.4).$$

The functions, U_ℓ , in Eqs. (A.1) - (A.3) are defined by Eq. (III.2-4). The recursion relations for the expansion coefficients of $\chi_s(r)$, see Eqs. (III.2-13) - (III.2-16), yield for $j > 1$

$$a_2^{(s)} = - \frac{[Z_A a_1^{(s)} + E a_0^{(s)} + T_0^{(s)}]}{(3 + 2s)} \quad (A.5)$$

$$a_3^{(s)} = - \frac{2[Z_A a_2^{(s)} + E a_1^{(s)} + T_1^{(s)}]}{3(4 + 2s)} \quad (A.6),$$

where the $a_0^{(s)}$ are arbitrary and for $s = 0, 1, 2$ the $T_j^{(s)}$ are given by

$$T_j^{(0)} = Z_B \left[\frac{a_j^{(0)}}{R} + \frac{a_{j-2}^{(1)}}{\sqrt{3} R^2} + \frac{a_{j-4}^{(2)}}{\sqrt{5} R^3} \right] \quad (A.7)$$

$$T_j^{(1)} = Z_B \left[\frac{a_j^{(0)}}{\sqrt{3} R^2} + \frac{a_j^{(1)}}{R} + \frac{2a_{j-2}^{(1)}}{5R^3} + \frac{2a_{j-2}^{(2)}}{\sqrt{15} R^2} + \frac{3}{7} \sqrt{\frac{3}{5}} \frac{a_{j-4}^{(2)}}{R^4} \right] \quad (A.8)$$

and

$$T_j^{(2)} = Z_B \left[\frac{a_j^{(0)}}{\sqrt{5} R} + \frac{2}{\sqrt{15}} \frac{a_j^{(1)}}{R^2} + \frac{3}{7} \sqrt{\frac{3}{5}} \frac{a_{j-2}^{(1)}}{R^4} + \frac{a_j^{(2)}}{R} + \frac{2}{7} \frac{a_{j-2}^{(2)}}{R^3} + \frac{2}{7} \frac{a_{j-4}^{(2)}}{R^5} \right]. \quad (A.9)$$

It is clear from Eqs. (III.2-13) - (III.2-16) and (A.5) - (A.9) that if E and the $a_0^{(s)}$ are known all the higher order expansion coefficients can be found and hence the functions $\chi_s(r)$ determined. A discussion on the convergence of the series for $\chi_s(r)$, see Eq. (III.2-12), is given in Appendix B.

A.2 SOLUTION OF RADIAL EQUATIONS IN REGION II ($\rho_B \leq r \leq \infty$)

In Region II the functions $F_s(r)$ are defined in terms of $f_s(r)$, see Eq. (III.2-31). The problem is to find $f_s(r)$ for any given energy E , see Eq. (III.2-30). For $s = 0, 1, 2$ the reduced differential equations, given by Eq. (III.2-39) for the $f_s(t)$, where $t = \frac{d}{r} - 1$, yield

$$H_0 f_0 = \frac{2\alpha_1 f_1}{\sqrt{3} (1+t)^2} + \frac{2\alpha_2 f_2}{\sqrt{5} (1+t)d} \quad (\text{A.10})$$

$$H_1 f_1 = \frac{2\alpha_1 f_0}{\sqrt{3} (1+t)^2} + \frac{4\alpha_2 f_1}{5(1+t)d} + \left[\frac{4\alpha_1}{\sqrt{15} (1+t)^2} + \frac{6\sqrt{3}}{7} \frac{\alpha_3}{5d} \right] f_2 \quad (\text{A.11})$$

and

$$\begin{aligned} H_2 f_2 = & \frac{2\alpha_2 f_0}{\sqrt{5} (1+t)d} + \left[\frac{4\alpha_1}{\sqrt{15} (1+t)^2} + \frac{6\sqrt{3}}{7} \frac{\alpha_3}{5d^2} \right] f_1 \\ & + \left[\frac{4\alpha_2}{7(1+t)d} + \frac{4\alpha_4(1+t)}{7d^3} \right] f_2 \end{aligned} \quad (\text{A.12})$$

where

$$H_s = \frac{d^2}{dt^2} + 2 \left[\left(1 - \frac{Z}{K}\right) \frac{1}{1+t} + \frac{Kd}{(1+t)^2} \right] \frac{d}{dt} + \frac{A_s}{(1+t)^2} \quad (\text{A.13})$$

The quantities α_s , A_s and d are defined by Eqs. (III.2-28), (III.2-36), (III.2-37) and (III.2-38). The recursion relations, see Eqs. (III.2-45) - (III.2-48), for the expansion coefficients of $f_s(t)$ yield

$$g_2^{(s)} = -\frac{1}{2} [\Omega_0 g_1^{(s)} + A_s g_0^{(s)} - T_0^{(s)}] \quad (\text{A.14}),$$

$$g_3^{(s)} = -\frac{1}{6} [2\Omega_0 g_2^{(s)} - \Omega_1 g_1^{(s)} + A_s g_1^{(s)} + 2A_s g_0^{(s)} - T_1^{(s)}] \quad (\text{A.15}),$$

where the $g_0^{(s)}$ and $g_1^{(s)}$ are arbitrary and for $s = 0, 1, 2$ the $T_j^{(s)}$ are given by

$$T_j^{(0)} = \sum_{\nu=0}^j (-1)^\nu \left[\frac{2\alpha_1(\nu+1)}{\sqrt{3}} g_{j-\nu}^{(1)} + \frac{2\alpha_2}{d\sqrt{5}} g_{j-\nu}^{(2)} \right] \quad (\text{A.16}),$$

$$T_j^{(1)} = \sum_{\nu=0}^j (-1)^\nu \left[\frac{2\alpha_1(\nu+1)}{\sqrt{3}} g_{j-\nu}^{(0)} + \frac{4\alpha_2}{5d} g_{j-\nu}^{(1)} + \frac{4\alpha_1(\nu+1)}{\sqrt{15}} g_{j-\nu}^{(2)} \right] \\ + \frac{6\sqrt{3}}{7\sqrt{5}} \frac{\alpha_3}{d^2} g_j^{(2)} \quad (\text{A.17})$$

and

$$T_j^{(2)} = \sum_{\nu=0}^j (-1)^\nu \left[\frac{2\alpha_2}{\sqrt{5}d} g_{j-\nu}^{(0)} + \frac{4\alpha_1(\nu+1)}{\sqrt{15}} g_{j-\nu}^{(1)} \right. \\ \left. + \frac{4\alpha_2}{7d} g_{j-\nu}^{(2)} \right] + \frac{6\sqrt{3}}{7\sqrt{5}} \frac{\alpha_3}{d^2} g_j^{(1)} \\ + \frac{4\alpha_4}{7d^3} [g_{j-1}^{(2)} + g_j^{(2)}] \quad (\text{A.18})$$

It is evident from Eqs. (A.14) - (A.18) that if the $g_0^{(s)}$ and $g_1^{(s)}$ are known the higher order coefficients, $g_{j+2}^{(s)}$ for $j = 1, 2, \dots$, can be calculated and hence the functions $f_s(t)$ can be determined. A discussion on the convergence of the series for $f_s(t)$ is given in Appendix B.

In order to solve the radial equations by the stepwise method, see Sec. III.2B-3, the solutions in adjacent intervals need to be matched at common boundaries. An elaboration of the matching procedure is given in Sec. A.4. The stepwise solution when combined with the asymptotic solution, discussed in Sec. III.2B-4, provides radial functions in $\rho_B \leq r \leq \infty$. Sec. A.6 contains a discussion of the matching of the stepwise solution with the asymptotic solution in Région II. When radial functions in Region I are matched with those in Region II one obtains these functions in the complete radial interval $0 \leq r \leq \infty$.

A.3 THE MATCHING OF THE SOLUTIONS OF RADIAL EQUATIONS IN REGION I AND REGION II AT $r = \rho_B$

The variable t used in the solution of the reduced differential equations, given by Eq. (III.2-39), is equal to zero at $r = d = \rho_B$, see Eq. (III.2-37). The matching conditions of radial functions at $r = \rho_B$ are given by

$$F_S(\rho_B) \text{ in Region I} = F_S(\rho_B) \text{ in Region II} \quad (\text{A.19})$$

and

$$F'_S(\rho_B) \text{ in Region I} = F'_S(\rho_B) \text{ in Region II} \quad (\text{A.20}).$$

Using Eqs. (A.19) and (A.20) and the definitions of the $F_S(r)$ in Region I and Region II, see Eqs. (III.2-10), (III.2-31) and (III.2-41), it follows that

$$\rho_B^{s+1} \chi_S(\rho_B) = \rho_B^{\frac{Z}{K}} e^{-K\rho_B} g_0^{(s)} \quad (\text{A.21})$$

and

$$\begin{aligned} & \rho_B^S [(s+1) \chi_S(\rho_B) + \rho_B \chi'_S(\rho_B)] \\ &= \rho_B^{\frac{Z}{K}} e^{-K\rho_B} g_0^{(s)} \left[\frac{Z}{K\rho_B} - K \right] - \frac{\rho_B^{\frac{Z}{K}} e^{-K\rho_B} g_1^{(s)}}{\rho_B} \quad (\text{A.22}). \end{aligned}$$

These equations can be solved for the $g_0^{(s)}$ and $g_1^{(s)}$. Since $\chi_S(\rho_B)$ depends on E and $a_0^{(s)}$ it is clear that the $g_0^{(s)}$ and $g_1^{(s)}$ depend in a complicated way on these quantities.

Sec. III.4 contains a discussion on the determination of E and the $a_0^{(s)}$.

A.4 THE MATCHING OF THE SOLUTIONS OF RADIAL EQUATIONS OBTAINED BY THE STEPWISE METHOD

The matching conditions discussed in Sec. A.3 provides

the matching of the first interval at $r_1 = \rho_B$, see Sec. III.2B-3 and Fig. III.2-1. The $g_0^{(s)}$ and $g_1^{(s)}$ thus obtained can be used to find all the $g_{j+2}^{(s)}$ in the first interval by using the recursion relations given by Eqs. (III.2-45) - (III.2-48). These coefficients can then be used to find $f_s(t)$ and $f'_s(t)$ at the second boundary, that is when $t = \frac{\rho_B}{r_2} - 1$ or $d = \rho_B$ and $r = r_2$. Using these values of $f_s(t)$ and $f'_s(t)$ and the definition of $F_s(r)$ given by Eq. (III.2-31), we can then determine $F_s(r)$ and $F'_s(r)$ at $r = r_2$. The matching at the second boundary is then given by, see Eqs. (III.2-53) and (III.2-54),

$$F_s(r_2) = r_2^{\frac{Z}{K}} e^{-Kr_2} g_0^{(s)} \quad (A.23)$$

and

$$F'_s(r_2) = r_2^{\frac{Z}{K}} e^{-Kr_2} g_0^{(s)} \left[\frac{Z}{Kr_2} - K \right] - \frac{r_2^{\frac{Z}{K}} e^{-Kr_2} g_1^{(s)}}{r_2} \quad (A.24).$$

Since $F_s(r_2)$ and $F'_s(r_2)$ are known from the calculations in the first interval, Eqs. (A.23) and (A.24) can be used to find the $g_0^{(s)}$ and $g_1^{(s)}$ for the second interval. The process is then repeated as discussed in Sec. III.2B-3.

A.5 THE ASYMPTOTIC SOLUTION OF REDUCED DIFFERENTIAL EQUATIONS IN REGION II

The asymptotic solutions of the reduced differential equations are represented by the functions $f_s(\xi)$ where

$\xi = \frac{\rho_B}{r} - 1$. The $f_s(\xi)$ satisfy Eq. (III.2-56) which reads for $s = 0, 1, 2$, as

$$H_0 f_0 = \frac{2\alpha_1 f_1}{\sqrt{3} \xi^2} + \frac{2\alpha_2 f_2}{\sqrt{5} \xi \rho_B} \quad (\text{A.25})$$

$$H_1 f_1 = \frac{2\alpha_1 f_0}{\sqrt{3} \xi^2} + \frac{4\alpha_2 f_1}{5\xi \rho_B} + \left[\frac{4\alpha_1}{\sqrt{15} \xi^2} + \frac{6}{7\sqrt{5}} \frac{\alpha_3}{\rho_B} \right] f_2 \quad (\text{A.26})$$

$$H_2 f_2 = \frac{2\alpha_2 f_0}{\sqrt{5} \xi \rho_B} + \left[\frac{4\alpha_1}{\sqrt{15} \xi^2} + \frac{6}{7\sqrt{5}} \frac{\alpha_3}{\rho_B} \right] f_1 + \left[\frac{4\alpha_2}{7\xi \rho_B} + \frac{4\alpha_4 \xi}{7\rho_B^3} \right] f_2 \quad (\text{A.27}),$$

where

$$H = \frac{d^2}{d\xi^2} + 2 \left[\left(1 - \frac{Z}{K}\right) \frac{1}{\xi} + \frac{K\rho_B}{\xi^2} \right] \frac{d}{d\xi} + \frac{A_S}{\xi^2}.$$

The recursion relations, see Eq. (III.2-58), for the expansion coefficients of $f_s(\xi)$ give

$$h_1^{(0)} = \frac{1}{2K\rho_B} \left[\frac{2\alpha_1 h_0^{(0)}}{\sqrt{3}} - A_0 h_0^{(0)} \right] \quad (\text{A.28}),$$

$$h_1^{(1)} = \frac{1}{2K\rho_B} \left[\frac{2\alpha_1 h_0^{(0)}}{\sqrt{3}} + \frac{4\alpha_1}{\sqrt{15}} h_0^{(2)} - A_1 h_0^{(1)} \right] \quad (\text{A.29}),$$

$$h_1^{(2)} = \frac{1}{2K\rho_B} \left[\frac{4\alpha_1}{\sqrt{15}} h_0^{(1)} - A_2 h_0^{(2)} \right] \quad (\text{A.30}),$$

$$h_2^{(0)} = \frac{1}{4K\rho_B} \left[\frac{2\alpha_1 h_1^{(1)}}{\sqrt{3}} + \frac{2\alpha_2 h_0^{(2)}}{\sqrt{5}\rho_B} - \left(2 - \frac{2Z}{K} + A_0\right) h_1^{(0)} \right] \quad (\text{A.31}),$$

$$h_2^{(1)} = \frac{1}{4K\rho_B} \left[\frac{2\alpha_1}{\sqrt{3}} h_1^{(0)} + \frac{4}{5\rho_B} h_0^{(1)} + \frac{4\alpha_1}{\sqrt{15}} h_1^{(2)} - \left(2 - \frac{2Z}{K} + A_1\right) h_1^{(1)} \right] \quad (\text{A.32}),$$

$$h_2^{(2)} = \frac{1}{4K\rho_B} \left\{ \frac{2\alpha_2}{\sqrt{5}\rho_B} h_0^{(0)} + \frac{4\alpha_1}{\sqrt{15}} h_1^{(1)} + \frac{4\alpha_2}{7\rho_B} h_0^{(2)} - \left(2 - \frac{2Z}{K} + A_2\right) h_1^{(2)} \right\} \quad (\text{A.33}).$$

It is clear from Eqs. (A.28) - (A.33) that the $h_{j+1}^{(s)}$ can be found if K or E , see Eq. (III.2-30), and the $h_0^{(s)}$ are known, see Sec. III.4.

A.6 THE MATCHING OF THE ASYMPTOTIC SOLUTION WITH THE STEPWISE SOLUTION IN REGION II

The procedure for matching the stepwise solution with the asymptotic solution, in Region II, is analogous to that discussed in Sec. A.4 for matching solutions in adjacent intervals at the common boundaries in the stepwise method. The choice of the point $r = r_c$, where the asymptotic solution is matched with the stepwise solution, is discussed in Appendix B, see also Sec. III.4.

APPENDIX B

A DISCUSSION OF THE CONVERGENCE OF THE SERIES REPRESENTING THE FUNCTIONS $\chi_s(r)$ and $f_s(r)$ AND OF THE ASYMPTOTIC NATURE OF THE SERIES FOR $f_s(\xi)$

The differential equations satisfied by $\chi_s(r)$ and $f_s(t)$, see Eqs. (III.2-11) and (III.2-39), belong to the eigenstates of an H_2^+ -like molecule and hence physically acceptable solutions of these equations exist only for special values of the parameters E and $a_0^{(s)}$. A formal discussion of the convergence of infinite series solutions of differential equations of the type satisfied by $\chi_s(r)$ and $f_s(t)$ can be found in, for example, Zalman⁶³, Ince⁶⁴. Illustrations of the convergence of the series for $\chi_s(r)$ and $f_s(t)$ are given in Secs. B.1 and B.2 respectively and examples of the asymptotic nature of the series for $f_s(\xi)$ are given in Sec. B.3.

B.1 ILLUSTRATIONS OF THE CONVERGENCE PROPERTIES OF THE SERIES FOR $\chi_s(r)$

The functions, $\chi_s(r) = \sum_j a_j^{(s)} r^j$, are defined in the interval $0 \leq r \leq \rho_B$, see Eqs. (III.1-4) and (III.2-12), and hence if the series for $\chi_s(r)$ converges at $r = \rho_B$ it

will converge at any other point in this interval. The examples given here refer to the convergence of the series for $\chi_s(r)$ at $r = \rho_B$. In practice these series converge quite rapidly, for example:

(a) Set $R \leq 6$, $\rho_B = R/2$ and $N = 16^+$. The sum of 50 terms in the series for $\chi_s(r)$ yields results, for all the $\chi_s(r)$, that are accurate to at least 12 significant figures. For smaller values of N fewer terms are needed to obtain a given accuracy in the $\chi_s(r)$. For example when $N = 2(4)$, the sum of 25(34) terms yields the $\chi_s(r)$ accurate to at least 14 significant figures. In general, the number of terms needed to obtain a given accuracy in $\chi_s(r)$ increases as R increases. For example when $N = 4$, the sum of 28(34) terms yields the $\chi_s(r)$ accurate to at least 15 significant figures for $R = 2(6)$.

(b) Set $R \leq 6$, $\rho_B = R$ and $N = 8^{++}$. The sum of 80 terms in the series for $\chi_s(r)$ yields results, for all the $\chi_s(r)$, that are accurate to at least 10 significant figures. For smaller values of N fewer terms are needed to obtain a

⁺When $Z_A = Z_B$ and $\rho_B = R/2$, the odd and even s value radial equations couple separately, see Sec. III.3A-1. The ground state of a homonuclear H_2^+ -like molecule is then described by even s value radial equations and hence $N = 16$ implies 9-coupled differential equations.

⁺⁺When $\rho_B \neq R/2$ both even and odd s value radial equations couple together and hence $N = 8$ implies 9-coupled differential equations.

given accuracy in the $\chi_s(r)$. For example, where $N = 1(2)$, the sum of 43(50) terms yields the $\chi_s(1)$ accurate to at least 14 significant figures. In general, the number of terms needed to obtain a given accuracy in the $\chi_s(r)$ increases as R increases; when $N = 2$ the sum of 37(50) terms yields the $\chi_s(r)$ accurate to at least 14 significant figures for $R = 2(6)$.

B.2 ILLUSTRATIONS OF THE CONVERGENCE PROPERTIES OF THE SERIES FOR $f_s(t)$

The functions $f_s(t) = \sum_{v=0}^{\infty} g_v^{(s)} t^v$, are defined in a particular interval where the j^{th} interval is $r_j \leq r \leq r_{j+1}$, $j = 1, 2, \dots$, see Eq. (III.2-51B) and Fig. III.2-1. In terms of the variable $t = \frac{d}{r} - 1$, see Eq. (III.2-37), the length of the j^{th} interval is given by $\left| \frac{r_j}{r_{j+1}} - 1 \right|$. For fixed values of N , R and ρ_B this interval length is conveniently chosen to be a constant $|\Delta - 1| < 1$ for all j , see Sec. III.2B-3. In any given interval, the modulus of t is bounded between 0 and $|\Delta - 1|$; hence the series for $f_s(t)$ must converge at all points in the interval if it converges at the interval boundary r_{j+1} , where $|t| = |\Delta - 1|$. The examples given here refer to the convergence of the series for $f_s(t)$ at $|t| = |\Delta - 1|$.

In practice the function $f_s(t)$ is represented by a truncated power series of the form

$$f_s(t) \approx \sum_{j=0}^{j_m} g_j^{(s)} t^j.$$

It is clear that the value of j_m required to obtain a given accuracy in $f_s(t)$ depends on the choice made for Δ . There are, in principle, infinite numbers of (j_m, Δ) pairs that will yield $f_s(t)$ accurately. In practice Δ is chosen so that, for a given accuracy in $f_s(t)$, j_m is a convenient number for computational purposes. Suitable values of Δ and j_m are found by trial and error starting with the initial estimates Δ^0 and j_m^0 .

B.2-1 THE CHOICE OF THE INITIAL ESTIMATES FOR Δ AND j_m

The rate of convergence of the series for $f_s(t)$ is related to that of the series for the functions $\frac{1}{1+t}$ and $\frac{1}{(1+t)^2}$, see Eqs. (III.2-41) - (III.2-48). Therefore the estimate j_m^0 , for a given trial Δ^0 , is chosen to be the number of terms required to obtain a given accuracy in these functions. The series for these functions converge faster for larger values of $\Delta \leq 1$, that is for smaller values of $|t|$. For example when $t = \Delta^0 - 1 = -0.15 (-0.25) (-0.28) (-0.32) (-0.97)$, $\frac{1}{1+t}$ and $\frac{1}{(1+t)^2}$ are obtained accurate to 14 significant figures with $j_m^0 = 18 (24) (26) (29) (1018)$ respectively. Here the value of Δ^0 corresponding to $j_m^0 = 1018$ is considered to be inconvenient for computational purposes. The other (j_m^0, Δ^0) pairs for this example can be used as convenient estimates for (j_m, Δ) .

B.2-2 NUMERICAL EXAMPLES FOR THE CONVERGENCE OF THE SERIES FOR $f_s(t)$

Initially the summation of the series for $f_s(t)$ is

carried out, for all s , by using a suitable estimate of Δ and j_m , obtained by using the method of Sec. B.2-1. In some cases the estimated values of Δ and j_m yield the required accuracy in $f_s(t)$ while in other cases adjustments are needed in these values. It should be pointed out that the accuracy in $f_s(t)$ can be increased by decreasing $|\Delta-1|$ and/or increasing j_m ; the choice is a matter of computational convenience. Numerical examples for the convergence of $f_s(t)$ are given below:

(i) Set $R = 2$, $\rho_B = R$, $N = 8$ and $t = \Delta - 1 = -0.3200(0)$.

Since $\Delta = \frac{r_j}{r_{j+1}}$ and $r_1 = \rho_B$, see Fig. III.2-1 and Sec. III.2B-3, the interval boundaries in terms of the variable r are given by

$$r_{j+1} = \frac{\rho_B}{\Delta^j}, \quad j = 1, 2, 3, \dots$$

Here $\Delta = 1+t = 0.6800(0)$; hence $r_2 = 0.2941(1)$, $r_3 = 0.4325(1)$ and $r_4 = 0.6361(1)$. For this example the stepwise solution is matched with the asymptotic solution at $r = r_c = r_4$, see Sec. III.2B-4. The sum of 31 terms ($j_m = 30$, while $j_m^0 = 29$) in the series for $f_s(t)$, for all s , yields results that are accurate to at least 7 significant figures at r_2, r_3 and r_4 .

(ii) Set $R = 4$, $\rho_B = R$, $N = 8$ and $t = -0.2500(0)$.

Here $r_c = r_4$ and the sum of 41 terms ($j_m = 40$, but $j_m^0 = 24$) yields $f_s(t)$, for all s , accurate to at least 11 significant figures at r_2, r_3 and r_4 .

(iii) Set $R = 6$, $\rho_B = R$, $N = 8$, $t = -0.2500(0)$.

Here $r_c = r_3$ and the sum of 41 terms ($j_m^0 = 24$) yields $f_s(t)$;

for all s , accurate to at least 14 significant figures at r_2 and r_3 .

(iv) Set $R = 2$, $\rho_B = R/2$, $N = 16$ and $t = -0.2500(0)$. Here $r_C = r_6$ and the sum of 41 terms ($j_m^0 = 24$) yields $f_s(t)$, for all s , accurate to at least 6 significant figures at r_2, r_3, r_4, r_5 and r_6 .

(v) Set $R = 4$, $\rho_B = R/2$, $N = 16$ and $t = -0.2800(0)$. Here $r_C = r_4$ and the sum of 41 terms ($j_m^0 = 26$) yields $f_s(t)$, for all s , accurate to at least 4 significant figures at r_2, r_3 and r_4 .

(vi) Set $R = 6$, $\rho_B = R/2$, $N = 16$ and $t = -0.2500(0)$. Here $r_C = r_4$ and the sum of 41 terms ($j_m^0 = 24$) yields $f_s(t)$, for all s , accurate to at least 3 significant figures at r_2, r_3 and r_4 .

In general for a given Δ and j_m the accuracy in the $f_s(t)$ increases as N decreases for both $\rho_B = R$ and $\rho_B = R/2$. For example (a) for case (i) when $N = 2$ the $f_s(t)$, for all s , are obtained accurate to at least 11 significant figures at r_2, r_3 and r_4 and (b) when $N = 2$ case (v) yields $f_s(t)$, for all s , accurate to at least 15 significant figures at r_2, r_3 and r_4 .

B.3 THE ASYMPTOTIC NATURE OF THE SERIES FOR THE $f_s(\xi)$

The functions $f_s(\xi)$ satisfy the system of differential equations given by Eqs. (III.2-56) and the variable

$\xi = \frac{\rho_B}{r}$, see Eq. (III.2-55). The infinite series solution,

$f_s(\xi) = \sum_{j=0}^{\infty} h_j^{(s)} \xi^j$, for these equations diverge asymptotically

as a function of $\xi < 1$ for all R , ρ_B , E and s as j increases without restriction, see Sec. III.2B-4. The asymptotic nature of the series for the $f_s(\xi)$ is difficult to study analytically since the determination of the expansion coefficients, $h_j^{(s)}$, involves the multi-term recursion formulae given by Eqs. (III.2-58). In this Appendix we discuss the asymptotic nature of the series for the $f_s(\xi)$ by using numerical values of the terms $h_j^{(s)} \xi^j$. For illustrative purposes we consider the ground state of the H_2^+ molecule for the values $R = 6$, $\rho_B = R/2$ and $\rho_B = R$.

For given values of R , ρ_B and the number of coupled differential equations, N , see Sec. II.3A-1 and Chapter IV, the eigensolutions of the radial equations given by Eqs. (III.2-3) are obtained in the region $0 \leq r \leq \infty$ by matching the functions $r^{2/K} e^{-Kr} f_s(\xi)$ with the stepwise solution at the point $\xi = \xi_c$, that is at $r = r_c$; see Sec. III.4. This matching procedure involves the determination, see Sec. III.4, of the parameters E , $a_0^{(s)}$, $h_0^{(s)}$, γ and r_c which were introduced in Sec. III.2. The values of $a_0^{(s)}$, $h_0^{(s)}$, γ and r_c , for our specific examples, are given in Tables B-1 and B-2 as functions of N and s while the corresponding values of E are given in Tables IV.1-1 and IV.1-2. For given values of ρ_B and N , there is only one value for each of γ and r_c , see Sec. III.4.

In order to show the asymptotic nature of the series

TABLE B.1: Some values of the constants $a_0^{(s)}$, $h_0^{(s)}$, γ and r_c , introduced in sec/III.2, as functions of s and the number of coupled differential equations N , for $R = 6$ and $\rho_B = R/2$.

N	s	$a_0^{(s)}$	γ	$h_0^{(s)}$	r_c
1	0	0.1000(1)	0.5256(1)	0.1000(1)	0.9541(1)
	0	0.1000(1)	0.1190(2)	0.1000(1)	0.9541(1)
	2	0.2339(0)		0.1078(1)	
3	0	0.1000(1)	0.1694(2)	0.1000(1)	0.9541(1)
	2	0.2929(0)		0.3331(0)	
	4	0.2806(-1)		0.1801(0)	
4	0	0.1000(1)	0.2055(2)	0.1000(0)	0.9541(1)
	2	0.3207(0)		0.1380(0)	
	4	0.3294(-1)		0.2707(0)	
5	6	0.2916(-2)		0.2254(-1)	
	0	0.1000(1)	0.2233(2)	0.1000(1)	0.9541(1)
	2	0.3346(0)		0.1383(1)	
6	4	0.3532(-1)		0.2594(0)	
	6	0.3228(-2)		0.1757(-1)	
	8	0.2903(-3)		0.2540(-3)	
7	0	0.1000(1)	0.2336(2)	0.1000(1)	0.9132(1)
	2	0.3420(0)		0.1433(1)	
	4	0.3659(-2)		0.2933(0)	
8	6	0.3384(-2)		0.2520(-1)	
	8	0.3102(-3)		0.1196(-2)	
	10	0.2865(-4)		0.3565(-4)	

TABLE B.2: Some values of the constants $a_0^{(s)}$, $h_0^{(s)}$, γ and r_c , introduced in Sec. III.2, as functions of s and the number of coupled differential equations, N , for $R = 6$ and $\rho_B = R$.

N	s	$a_0^{(s)}$	γ	$h_0^{(s)}$	r_c
1	0	0.1000(1)	0.1367(3)	0.1000(1)	0.1908(2)
	0	0.1000(1)	0.1163(1)	0.1000(1)	0.1067(2)
	1	0.2831(-1)	0.1163(1)	0.1309(1)	
3	0	0.1000(1)	0.1487(1)	0.1000(1)	0.1067(2)
	1	0.2890(-1)		0.1632(1)	
	2	0.2949(-2)		0.1244(1)	
4	0	0.1000(1)	0.1809(1)	0.1000(1)	0.1067(2)
	1	0.2914(-1)		0.1839(1)	
	2	0.3029(-2)		0.1764(1)	
	3	0.3755(-3)		0.1003(1)	
5	0	0.1000(1)	0.1883(1)	0.1000(1)	0.1067(2)
	1	0.2932(-1)		0.1526(1)	
	2	0.3078(-2)		0.1094(1)	
	3	0.3887(-3)		0.2312(0)	
	4	0.5236(-4)		0.1691(1)	
6	0	0.1000(1)	0.2310(1)	0.1000(1)	0.1067(2)
	1	0.2949(-1)		0.1836(1)	
	2	0.3123(-2)		0.1733(1)	
	3	0.3989(-3)		0.1139(1)	
	4	0.5473(-4)		0.9800(0)	
	5	0.7719(-5)		0.1846(0)	

TABLE B.3: A comparison of the 3rd, 60th and the minimum of the terms $Q_j^{(s)} = |h_j^{(s)} \xi_C^j|$ occurring in the series for the $f_s(\xi_C)$, $\xi_C = \frac{\rho_B}{r_C}$, as functions of s and N for $R = 6$ and $\rho_B = R/2$, see the text.

N	s	j for minimum of the $Q_i^{(s)}$	$Q_3^{(s)}$	$Q_j^{(s)}$	$Q_{60}^{(s)}$
1	0	24	0.7244(-4)	0.2333(-16)	0.1170(-6)
2	0	26	0.2010(-1)	0.1361(-10)	0.4990(-2)
	2	26	0.8598(-1)	0.1281(-10)	0.3680(-2)
3	0	26	0.6154(-2)	0.2282(-11)	0.2302(-3)
	2	26	0.9112(-1)	0.1149(-10)	0.1023(-2)
	4	27	0.5497(-1)	0.1842(-11)	0.8939(-4)
4	0	27	0.2423(-1)	0.1429(-11)	0.8613(-4)
	2	35	0.8556(-1)	0.1053(-14)	0.1286(-5)
	4	27	0.3969(-1)	0.3093(-11)	0.1133(-3)
	6	29	0.2978(-1)	0.2858(-12)	0.3970(-5)
5	0	27	0.2405(-1)	0.1882(-11)	0.8361(-4)
	2	27	0.8443(-1)	0.3379(-11)	0.1250(-3)
	4	28	0.3440(-1)	0.5785(-12)	0.1264(-4)
	6	28	0.2083(-1)	0.5157(-12)	0.9080(-5)
	8	30	0.6912(-3)	0.5324(-13)	0.3237(-6)
6	0	26	0.2705(-1)	0.5533(-11)	0.9187(-3)
	2	26	0.9229(-1)	0.1085(-10)	0.1480(-2)
	4	27	0.4794(-1)	0.4262(-11)	0.3813(-3)
	6	28	0.3555(-1)	0.6029(-12)	0.2512(-4)
	8	28	0.5817(-2)	0.2354(-12)	0.7867(-5)
	10	30	0.4323(-3)	0.2100(-13)	0.1784(-6)

TABLE B.4: A comparison of the 3rd, 75th and the minimum of the terms $Q_j^{(s)} = |h_j^{(s)} \xi_C^i|$ in the series for the $f_g(\xi)$ at the point $\xi_C = \frac{\rho_B}{r_C}$ as functions of s and N for $R = 6$ and $\rho_B = R$, see the text.

N	s	j for minimum of the $Q_j^{(s)}$	$Q_3^{(s)}$	$Q_j^{(s)}$	$Q_{75}^{(s)}$
1	0	49	0.6404(-4)	0.4081(-26)	0.2756(-23)
2	0	30	0.3522(-1)	0.3645(-13)	0.3702(-1)
	1	30	0.2749(-1)	0.7379(-13)	0.7153(-1)
3	0	30	0.1978(-1)	0.1577(-12)	0.1715(0)
	1	30	0.1456(-1)	0.2520(-12)	0.2759(0)
	2	30	0.1117(0)	0.3239(-12)	0.3989(0)
4	0	30	0.1310(-1)	0.3289(-11)	0.3043(1)
	1	30	0.4010(-1)	0.7767(-11)	0.6731(1)
	2	30	0.1306(0)	0.7362(-11)	0.5450(1)
	3	32	0.1388(0)	0.1856(-11)	0.4053(-1)
5	0	30	0.2182(-1)	0.1831(-11)	0.1667(1)
	1	30	0.1578(-1)	0.4103(-11)	0.3272(1)
	2	30	0.1207(0)	0.4399(-11)	0.2617(1)
	3	31	0.3612(0)	0.5448(-11)	0.2845(1)
	4	31	0.4434(0)	0.1044(-10)	0.6672(1)
6	0	30	0.1345(-1)	0.4208(-11)	0.3793(1)
	1	30	0.4136(-1)	0.9936(-11)	0.8199(1)
	2	30	0.1579(0)	0.1038(-10)	0.6990(1)
	3	31	0.2235(0)	0.8003(-11)	0.3929(1)
	4	31	0.3784(-1)	0.7405(-11)	0.3033(1)
	5	31	0.4434(1)	0.1044(-10)	0.6672(1)

for the $f_s(\xi)$ for our specific examples, namely the ground state H_2^+ molecule with $R = 6$, $\rho_B = R/2$ and R , the numerical values of the terms, $h_j^{(s)} \xi^j$, have to be examined as a function of j . Since $0 \leq \xi \leq \xi_c$, where $\xi_c = \frac{\rho_B}{r_c}$, the series for the $f_s(\xi)$ has the most severe convergence problem at $\xi = \xi_c$ and hence the study of the asymptotic nature of this series will be numerically studied explicitly at $\xi = \xi_c$ only. This study shows, see for example below, that the absolute values of the terms in the expansion of the $f_s(\xi_c)$, namely the $Q_j^{(s)} = |h_j^{(s)} \xi_c^j|$, reduce to a minimum as a function of j for each s and then increase monotonically as j increases. For example the minimum and two other values of the $Q_j^{(s)}$ are compared in Tables B-3 and B-4 as functions of R , ρ_B , N and s . Further, as mentioned in Sec. III.4C, these minimum values of the $Q_j^{(s)}$ can be made as small as required by taking ξ_c small enough, that is, r_c large enough. The behaviour of the terms $h_j^{(s)} \xi^j$ for the specific examples considered here, demonstrates the asymptotic nature of the series for the $f_s(\xi)$, see also Jeffreys and Jeffreys^{72,73}.

APPENDIX C

EXAMPLES OF THE USE OF THE NUMERICAL METHOD FOR SOLVING THE RADIAL EQUATIONS

This Appendix contains examples of the use of the numerical method discussed in Sec. III-3 for solving the radial equations. In order to simplify the discussion only 2-coupled equations with $m = 0$ and $s = 0$ and 1 are considered here. The examples given here refer to the case where the coordinate origin is located at one of the nuclei, that is, $\rho_B = R(\rho_A = 0)$. The calculations, when the coordinate origin is located at an arbitrary point on the line joining the nuclei ($0 \leq \rho_A \leq \rho_B$), are similar to those discussed here.

C.1 THE FINITE DIFFERENCE EQUATIONS REPRESENTING THE RADIAL EQUATIONS

The general finite difference equation representing the radial equations is given by Eq. (III.3-2). For $m = 0$ and $s = 0$ and 1 this equation reads as

$$F_0(r+h) = [2h^2(U_0(r) - E) + 2]F_0(r) - F_0(r-h) + \frac{2h^2}{\sqrt{3}}U_1(r)F_1(r) \quad (C.1)$$

and

$$F_1(r \pm h) \doteq \frac{2h^2}{\sqrt{3}} U_1(r) F_0(r) + [2h^2 (U_0(r) + \frac{2}{5} U_2(r) + \frac{1}{r^2} - E) + 2] F_1(r) - F_1(r \mp h) \quad (C.2),$$

where the functions $U_\ell(r)$; $\ell = 0, 1, 2$ are defined by Eqs. (III.2-4) and (III.2-27). The step by step procedure discussed in Sec. III.3A is used to obtain, from Eqs. (C.1) and (C.2), the functions $^f F_S(r)$ and $^b F_S(r)$ at the matching point $r = r_c$; Sec. C.2 contains a discussion on the choice of r_c . In order to find the first derivatives $^f F'_S(r_c)$ and $^b F'_S(r_c)$, the forward and the backward integrations of the radial equations are carried "beyond" r_c to $r = r_c + 2h$ and $r = r_c - 2h$ respectively. The required derivatives can then be obtained by using a five point finite difference relation, see for example Milne¹⁰⁵, for the first derivative of a function $y_S(r)$ at $r = r_c$:

$$y'_S(r_c) \simeq \frac{1}{12h} [y_S(r_c - 2h) - 8y_S(r_c - h) + 8y_S(r_c + h) - y_S(r_c + 2h)] \quad (C.3).$$

C.2 THE CHOICE OF THE MATCHING POINT r_c

The choice of the matching point r_c is unimportant when "exact" values of the parameters E , $^f C_1$ and $^b C_1$ are used and when round off and truncation errors are avoided in the numerical method. In practice however, estimated values of the parameters are used in approximate finite difference equations to carry out the integration of radial equations. In such a situation the choice of r_c

becomes important; a poor choice of r_c may result in a divergent result for the "solution" of the radial equations or in a solution that does not correspond to the state of interest⁴⁸.

The matching point r_c can be different for different radial functions, however for computational convenience it is chosen to be the same for all radial functions associated with given values of R , E and ρ_B . For a given state of an H_2^+ -like molecule a suitable value of r_c can be found by numerical experimentation. Fox⁴⁸ has given a valuable discussion of the choice of r_c . In order to determine r_c , according to Fox, find the dominant[†] radial function, $F_s(r)$, for the state of interest. The matching point, r_c is that value of r for which the coefficient of $F_s(r)$

[†]For a given state of the molecule the dominant radial function is the one that makes the largest contribution to the energy. Previous one centre variational and perturbation calculations for the molecule provide useful information for determining the dominant radial function. For most values of R , ρ_A and the number of coupled differential equations, the dominant radial function correspond to $s' = 0$ for the ground state of the H_2^+ molecule. If the value of r_c determined from $s' = 0$ is not adequate for the purpose of matching the forward and backward solutions then other values of s' are investigated by trial and error method.

vanishes in the radial equation specified by $s = s'$; the coefficient of $F_{s'}(r)$ in this equation is given by, see eq. (III.2-3),

$$2E - \frac{s'(s'+1)}{r^2} - \sum_{\ell=0}^{2s'} D(s', \ell, s') U_{\ell}(r).$$

For the state of interest here, the ground state of H_2^+ , $F_{s'}(r) = F_0(r)$. Thus the zero of the function $2(E - U_0(r))$ provides r_c for this state of H_2^+ . In practice the correct value of E is not known before the problem is solved. In this work the value of r_c is chosen approximately equal to the zero of the function $E - U_0(r)$ for the initial estimate of E , see for example Appendix D.

C.3 THE DETERMINATION OF THE PARAMETERS APPEARING IN THE MATCHING METHOD

A formal discussion of the determination of the parameters in the matching method is given in Sec. III.3B. For our present example we need to determine the parameters E , f_{C_1} and b_{C_1} ; the conditions, $f_{C_0} = b_{C_0} = 1$, arbitrarily fix the sizes of the forward and backward solutions respectively, see Sec. III.3A. These parameters are obtained by solving Eqs. (III.3-7) and (III.3-8) which, for $s = 0, 1$, read as

$$G_0(E, f_{C_1}, b_{C_1}) = f_{F_0}(r_c) - \gamma b_{F_0}(r_c) = 0 \quad (C.4),$$

$$G_1(E, f_{C_1}, b_{C_1}) = f_{F_1}(r_c) - \gamma b_{F_1}(r_c) = 0 \quad (C.5),$$

$$G'_0(E, f_{C_1}, b_{C_1}) = f'_{F_0}(r_c) - \gamma b'_{F_0}(r_c) = 0 \quad (C.6)$$

and

$$G'_1(E, f_{C_1}, b_{C_1}) = f'_{F_1}(r_c) - \gamma b'_{F_1}(r_c) = 0 \quad (C.7).$$

Equations (C.4) - (C.7) are solved for $\gamma, E, {}^fC_1$ and bC_1 by Newton's iterative process⁷⁰ which is started with initial estimates of the parameters $E, {}^fC_1$ and bC_1 .

For any estimate of $E, {}^fC_1$ and bC_1 we find the values of the $F_S(r_C)$ and $F'_S(r_C)$ by procedures described in Sec. C.1. In order to use the iterative process the value of γ is fixed, in each iteration, by assuming that Eq. (C.4) is satisfied exactly by estimated values of $E, {}^fC_1$ and bC_1 , see Eq. (III.3-9). The Taylor series expansion of terms in Eqs. (C.5) - (C.7) is obtained by using $N = 1$ in Eqs. (III.3-11) and (III.3-12);

$$G_1 = 0 \approx (G_1)_0 + \left(\frac{\partial G_1}{\partial {}^fC_1} \right)_0 \delta {}^fC_1 + \left(\frac{\partial G_1}{\partial {}^bC_1} \right)_0 \delta {}^bC_1 + \left(\frac{\partial G_1}{\partial E} \right)_0 \delta E \quad (C.8),$$

$$G'_0 = 0 \approx (G'_0)_0 + \left(\frac{\partial G'_0}{\partial {}^fC_1} \right)_0 \delta {}^fC_1 + \left(\frac{\partial G'_0}{\partial {}^bC_1} \right)_0 \delta {}^bC_1 + \left(\frac{\partial G'_0}{\partial E} \right)_0 \delta E \quad (C.9)$$

and

$$G'_1 = 0 \approx (G'_1)_0 + \left(\frac{\partial G'_1}{\partial {}^fC_1} \right)_0 \delta {}^fC_1 + \left(\frac{\partial G'_1}{\partial {}^bC_1} \right)_0 \delta {}^bC_1 + \left(\frac{\partial G'_1}{\partial E} \right)_0 \delta E \quad (C.10).$$

where $(X)_0$ is the value of X corresponding to the initial values of the parameters $E, {}^fC_1$ and bC_1 . When $N = 1$ (hence $k = 1, i = 1, 2, j = 1$ and $\mu = 2, 3$) Eqs. (III.3-13A) - (III.3-13K) yield the matrix form of Eqs. (C.8) - (C.10). These matrix equations are as follows:

$$\mathbf{g} = - \mathbf{D} \delta \quad (\text{C.11})$$

where

$$\mathbf{g} = \begin{bmatrix} (G_1) \\ (G'_0) \\ (G'_1) \end{bmatrix}, \quad \delta = \begin{bmatrix} \delta^f_{C_1} \\ \delta^b_{C_1} \\ \delta E \end{bmatrix}$$

and

$$\mathbf{D} = \begin{bmatrix} \left(\frac{\partial G_1}{\partial^f_{C_1}} \right)_0 & \left(\frac{\partial G_1}{\partial^b_{C_1}} \right)_0 & \left(\frac{\partial G_1}{\partial E} \right)_0 \\ \left(\frac{\partial G'_0}{\partial^f_{C_1}} \right)_0 & \left(\frac{\partial G'_0}{\partial^b_{C_1}} \right)_0 & \left(\frac{\partial G'_0}{\partial E} \right)_0 \\ \left(\frac{\partial G'_1}{\partial^f_{C_1}} \right)_0 & \left(\frac{\partial G'_1}{\partial^b_{C_1}} \right)_0 & \left(\frac{\partial G'_1}{\partial E} \right)_0 \end{bmatrix} \quad (\text{C.12}).$$

Eqs. (C.11) and (C.12) show that in order to find the correction δ to the estimated values of the parameters it is necessary to know the values of G_1, G'_0, G'_1 and their partial derivatives with respect to the parameters $E, {}^f_{C_1}$ and ${}^b_{C_1}$. The quantities G_1, G'_0 and G'_1 are obtained by substituting in Eqs. (C.5) - (C.7) the value of γ and the values of the $F_s(r_c)$ and $F'_s(r_c)$. The partial derivatives of G_1, G'_0 and G'_1 with respect to these parameters are obtained by using $N = 1$ in Eqs. (III.3-17) - (III.3-19) and (III.3-23) - (III.3-25) where the quantities M and W , appearing in these equations, are obtained from Eqs. (III.3-27) and (III.3-28) by a procedure analogous to that employed to obtain the $F_s(r)$ from Eq. (II.2-3),

see Secs. III-3A and C.1. For the present example, $N = 1$, the finite difference equations representing Eqs. (III.3-27) and (III.3-28) read as

$$\begin{aligned} M_0(r+h) = & -2h^2 F_0(r) + [2h^2 (U_0(r) - E) + 2] M_0(r) \\ & - M_0(r-h) + \frac{2h^2}{\sqrt{3}} U_1(r) M_1(r) \end{aligned} \quad (C.13),$$

$$\begin{aligned} M_1(r+h) = & -2h^2 F_1(r) + \frac{2h^2}{\sqrt{3}} U_1(r) M_0(r) + \\ & [2h^2 (U_0(r) + \frac{2}{5} U_2(r) + \frac{1}{r^2} - E) + 2] M_1(r) \\ & - M_1(r-h) \end{aligned} \quad (C.14),$$

$$\begin{aligned} W_{01}(r+h) = & [2h^2 (U_0(r) - E) + 2] W_{01}(r) \\ & - W_{01}(r-h) + \frac{2h^2}{\sqrt{3}} U_1(r) W_{11}(r) \end{aligned} \quad (C.15)$$

and

$$\begin{aligned} W_{11}(r+h) = & \frac{2h^2}{\sqrt{3}} U_1(r) W_{01}(r) + [2h^2 (U_0(r) \\ & + \frac{2}{5} U_2(r) + \frac{1}{r^2} - E) + 2] W_{11}(r) \\ & - W_{11}(r-h) \end{aligned} \quad (C.16).$$

The forward and backward integrations of Eqs. (III.3-27) and (III.3-28) are performed by using Eqs. (C.13) - (C.16) and the boundary conditions of the W and M given by Eqs. (III.3-29) and (III.3-30). The derivatives of the M and W with respect to r are obtained by using the procedure used to find the $F'_s(r_c)$, see Sec. C.1. Thus all the quantities are found for solving Eq. (C.11) for δ which is

used to improve the values of the parameters E , $^f C_1$ and $^b C_1$, see Eq. (III.3-10). In the numerical calculations of this work the iterative process is terminated when δE , an element of the matrix δ , is reduced to the order of a preset small number, see Appendix D.

APPENDIX D

ILLUSTRATIVE NUMERICAL VALUES OF THE PARAMETERS AND RELATED QUANTITIES APPEARING IN THE NUMERICAL METHOD FOR SOLVING THE RADIAL EQUATIONS

This appendix contains examples of typical values of the quantities, $h, r_c, r_x, \gamma, \delta E, E, f_{C_1}, \dots, f_{C_N}, b_{C_1}, \dots, b_{C_N}$, involved in the numerical method for solving radial equations, see Sec. III.3 and Appendix C. The parameters $E, f_{C_1}, \dots, f_{C_N}, b_{C_1}, \dots, b_{C_N}$ are obtained by solving Eqs. (III.3-7) and (III.3-8). Since the energy E is the most important parameter in the present numerical calculation, the iterative process used to solve these equations is terminated, for convenience, when δE is reduced to a preset small number, see Appendix C and Sec. D.1 below.

The interaction energy[†] $E_{\text{int}} = E + \frac{Z_A Z_B}{R} + \frac{Z_A^2}{2n^2}$, see Eqs. (II.1-2) and (II.1-3), becomes small with respect to the electronic energy E or the total energy E_T as R becomes large. Therefore in order to obtain E_{int} accurately for large R the electronic energy E must be determined quite accurately. The accuracy in E , obtained by the

[†]For the state of interest in this work, the ground state of H_2^+ , $Z_A = Z_B = 1$ and $n = 1$.

numerical method, is easily improved by Richardson's h^2 -extrapolation technique^{74,75}, see Sec. D.2.

D.1 EXAMPLES OF NUMERICAL VALUES OF $h, r_c, r_\infty, \gamma, \delta E, E, f_{C_1}, \dots, f_{C_N}, b_{C_1}, \dots, b_{C_N}$

The number of iterations, required to obtain δE to the order of a preset small value, depends on the initial estimates of the parameters $E, f_{C_1}, \dots, f_{C_N}, b_{C_1}, \dots, b_{C_N}$. In this work, for any given grid size h , the preset value for δE is $\sim 10^{-9}$ and the initial estimates of the parameters used in this work yield $\delta E \sim 10^{-9}$ with less than 9 iterations. For given values of R, ρ_A and N , a suitable value of the grid size h is found by trial and error by observing the convergence of E as a function of h . To determine the accuracy in E and to use the Richardson's h^2 -extrapolation discussed in Sec. D.2, E is calculated for two grid sizes h_1 and h_2 such that $h_2 = \frac{h_1}{2}$. In some cases E is also calculated with a third grid size $h_3 = \frac{h_2}{2} = \frac{h_1}{4}$. The point r_∞ , see Sec. III.3A, is found by observing the change in E as a function of r_∞ . The values of r_∞ chosen in this work introduce in E an error that is smaller than the preset value of $\delta E = 10^{-9}$. The estimates of the parameters $E, f_{C_1}, \dots, f_{C_N}, b_{C_1}, \dots, b_{C_N}$ can be obtained by the procedure, discussed in Sec. III.4-2, for the estimates of the parameters of the analytical method. Numerical examples of these quantities are given below:

(a) Set $R = 2$, $\rho_A = 0$ and $N = 2$. Using the values
 $h_1 = 0.5000$ (-1), $r_C = 0.1825$ (1), $r_\infty = 0.1683$ (2),
 $(E)_0 = -0.1000$ (0), $(f_{C_1})_0^\dagger = -0.1000$ (1), $(f_{C_2})_0 = 0.1100$ (1),
 $(b_{C_1})_0 = 0.1200$ (1) and $(b_{C_2})_0 = 0.1010$ (0) we obtain the
 following results:

(i) $E(h_1) = -0.105459$ (1), $f_{C_1} = 0.1291$ (-1),
 $f_{C_2} = 0.2170$ (-3), $b_{C_1} = 0.1209$ (1), $b_{C_2} = 0.6778$ (0),
 $\gamma = 0.9116$ (-8),

(ii) $E(h_2 = \frac{h_1}{2}) = -0.105472$ (1), $f_{C_1} = 0.6365$ (-2),
 $f_{C_2} = 0.5357$ (-4), $b_{C_1} = 0.1209$ (1), $b_{C_2} = 0.6776$ (0),
 $\gamma = 0.9473$ (-8) and

(iii) $E(h_3 = \frac{h_1}{4}) = -0.105475$ (1), $f_{C_1} = 0.3162$ (-2),
 $f_{C_2} = 0.1331$ (-4), $b_{C_1} = 0.1209$ (1), $b_{C_2} = 0.6776$ (0),
 $\gamma = 0.9668$ (-8).

(b) Set $R = 2$, $\rho_A = 0$ and $N = 8$. Using the values
 $h_1 = 0.2500$ (-1), $r_C = 0.1675$ (1), $r_\infty = 0.1293$ (2),
 $(E)_0 = -0.109557$ (1), $(f_{C_1})_0 = 0.1000$ (-1), $(f_{C_2})_0 =$
 0.3000 (-3), $(f_{C_3})_0 = 0.7000$ (-5), $(f_{C_4})_0 = 0.2000$ (-6),
 $(f_{C_5})_0 = 0.6000$ (-8), $(f_{C_6})_0 = 0.3000$ (-9), $(f_{C_7})_0 =$
 0.1000 (-10), $(f_{C_8})_0 = 0.1000$ (-1), $(b_{C_1})_0 = 0.1000$ (1),
 $(b_{C_2})_0 = 0.9000$ (0), $(b_{C_3})_0 = 0.4000$ (0), $(b_{C_4})_0 = 0.1000$ (0),

The values of f_{C_0} and b_{C_0} are equal to unity, see
 Eqs. (III.3-4) and (III.3-6):

$(b_{C_5}) = 0.5000 \ (-1)$, $(b_{C_6}) = 0.1000 \ (-1)$, $(b_{C_7})_0 = 0.3000 \ (-2)$ and $(b_{C_8})_0 = 0.100 \ (-2)$ we obtain the following results:

(i) $E(h_1) = -0.109733 \ (1)$, $f_{C_1} = 0.7541 \ (-2)$,
 $f_{C_2} = 0.7132 \ (-4)$, $f_{C_3} = 0.8342 \ (-6)$, $f_{C_4} = 0.1195 \ (-7)$,
 $f_{C_5} = 0.2050 \ (-9)$, $f_{C_6} = 0.4121 \ (-11)$, $f_{C_7} = 0.9501 \ (-13)$,
 $f_{C_8} = 0.2460 \ (-14)$, $b_{C_1} = 0.1387 \ (1)$, $b_{C_2} = 0.9397 \ (0)$,
 $b_{C_3} = 0.4594 \ (0)$, $b_{C_4} = 0.1820 \ (0)$, $b_{C_5} = 0.6187 \ (-1)$
 $b_{C_6} = 0.1870 \ (-1)$, $b_{C_7} = 0.5130 \ (-1)$, $b_{C_8} = 0.1274 \ (-2)$
 $\gamma = 0.1536 \ (-5)$ and

(ii) $E(h_2 = \frac{h_1}{2}) = -0.109731 \ (1)$, $f_{C_1} = 0.3745 \ (-2)$,
 $f_{C_2} = 0.1771 \ (-4)$, $f_{C_3} = 0.1037 \ (-6)$, $f_{C_4} = 0.7432 \ (-9)$,
 $f_{C_5} = 0.6388 \ (-11)$, $f_{C_6} = 0.6435 \ (-13)$, $f_{C_7} = 0.7438 \ (-15)$,
 $f_{C_8} = 0.9664 \ (-17)$, $b_{C_1} = 0.1387 \ (1)$, $b_{C_2} = 0.9395 \ (0)$,
 $b_{C_3} = 0.4594 \ (0)$, $b_{C_4} = 0.1820 \ (0)$, $b_{C_5} = 0.6187 \ (-1)$,
 $b_{C_6} = 0.1870 \ (-1)$, $b_{C_7} = 0.5131 \ (-2)$, $b_{C_8} = 0.1275 \ (-2)$
and $\gamma = 0.1542 \ (-5)$.

The accuracy in E and E_{int} increases as the grid size is reduced. This can be seen by comparing the results in (a) and (b) with the corresponding values, obtained by using the analytical method, see Eqs. (II.1-2), (II.1-3) and Table IV.1-1, $E = -0.105476 \ (1)$ and $E = -0.109730 \ (1)$.

D.2 RICHARDSON'S h^2 -EXTRAPOLATION

In general, results obtained by numerical methods

improve when the grid size is reduced. Thus one can obtain, at least in principle, accurate results by reducing the grid size. However, the grid size cannot be reduced indefinitely without introducing practical difficulties. An alternative and often more convenient way to improve numerical results is to apply extrapolation techniques to results obtained with fairly large values of the grid size. In this work Richardson's h^2 -extrapolation^{74,75} is used to obtain better approximation for the energy.

For any given R , ρ_B and N , the energy eigenvalues, obtained by the numerical method discussed in Sec. III.3, depend on the grid size h ; $E = E(h)$. We assume that, for small h , an expansion of $E(h)$ exists^{74,75} in the form

$$E(h) = E + Ah^K + Bh^{K+1} + \dots \quad (D.1).$$

Here E is the true value of energy and K, A, B, \dots are unknown constants. If $E(h)$ is known for two different values of h , the constant A can be eliminated from Eq. (D.1). The relation obtained by eliminating A is called Richardson's h^K -extrapolation formula⁷⁴. Here we use[†]

[†] Since the global error in the numerical procedure used here is $O(h^2)$ it can be shown that $K = 2$, see Ref. [74]. An approximate value of K can be obtained by using the expression⁷⁴

$$2^K \approx \frac{E(h_2) - E(h_1)}{E(h_3) - E(h_2)}, \quad \text{where}$$

$$h_3 = \frac{h_2}{2} = \frac{h_1}{4}.$$

$K = 2$. It is clear that if $E(h)$ is known for more than two values of h , higher order coefficients can be eliminated from Eq. (D.1), see Eq. (D.3) later.

Let h_1 and h_2 be the two values of h such that $h_2 = \frac{h_1}{2}$. Using $h_1, h_2, E(h_1)$ and $E(h_2)$ in Eq. (D.1) and eliminating A we obtain, for $K = 2$, the relation

$$E \approx E(h_2) + \frac{1}{3}[E(h_2) - E(h_1)] + O(h_1^3) \quad (D.2).$$

The energy eigenvalues reported in this thesis, see Tables IV.1-1 - IV.1-3, are obtained by using this two-point extrapolation formula. If $E(h)$ is also known for h_3 where $h_3 = \frac{h_2}{2} = \frac{h_1}{4}$, we obtain, in addition to Eq. (D.2) another two-point formula which reads as

$$E \approx E(h_3) + \frac{1}{3}[E(h_3) - E(h_2)] + O(h_2^3) \quad (D.3).$$

Further by eliminating both A and B from Eq. (D.1) we obtain the three point formula,

$$E \approx E(h_3) + \frac{1}{84}[4E(h_1) - 48E(h_2) + 44E(h_3)] + O(h_1^4) \quad (D.4).$$

Equations (D.3) and (D.4) are used to check representative results obtained by using Eq. (D.2).

An example of the use of Eqs. (D.2) - (D.4) for improving the accuracy in the electronic and interaction energies, obtained by the numerical procedures of

Sec. III.3, is easy to construct. Set $R = 2$, $\rho_A = R/2$, and $N = 8$. Using the grid sizes $h_1 = 0.05$, $h_3 = \frac{h_2}{2} = \frac{h_1}{4}$, we obtain the approximate electronic and interaction energies,

$$E(h_1) = -0.110240633 (1), E_{\text{int}}(h_1) = -0.10240633 (0) \quad (\text{D.5}),$$

$$E(h_2) = -0.110154763 (1), E_{\text{int}}(h_2) = -0.10154763 (0) \quad (\text{D.6})$$

and

$$E(h_3) = -0.110133460 (1), E_{\text{int}}(h_3) = -0.10133460 (0) \quad (\text{D.7}).$$

Using these values of E in Eqs. (D.2) - (D.4) yield respectively

$$E \approx -0.110126139 (1), E_{\text{int}} \approx -0.10126139 (0) \quad (\text{D.8}),$$

$$E \approx -0.110126359 (1), E_{\text{int}} \approx -0.10126359 (0) \quad (\text{D.9})$$

and

$$E \approx -0.110126390 (1), E_{\text{int}} \approx -0.10126390 (0) \quad (\text{D.10}).$$

The analytical method of Sec. III.2 gives

$$E = -0.110126374 (1), E_{\text{int}} = -0.10126374 (0).$$

This example shows that although the individual $E_{\text{int}}(h_j)$, $j = 1, 2, 3$ are correct to only 2 or 3 figures, the extrapolated results are correct to 5 or 6 figures.

In the above example, the interaction energy is not very small compared to the electronic energy E . In order to have a better appreciation for the value of the extrapolation technique we take another example, corresponding to a large value of $R = 15$. With $R = 15$, $\rho_A = 0$, $N = 4$ and $h_1 = 0.008$ we obtain the following electronic and interaction energies:

$$E(h_1) = -0.566704169 (0), E_{\text{int}}(h_1) = -0.3750 (-4) \quad (\text{D.11}),$$

$$E(h_2) = -0.566710168 (0), E_{\text{int}}(h_2) = -0.4350 (-4) \quad (\text{D.12})$$

and

$$E(h_3) = -0.566711669 (0), E_{\text{int}}(h_3) = -0.4500 (-4) \quad (\text{D.13}).$$

Using these values of E in Eqs. (D.2) - (D.4) yield respectively

$$E \approx -0.566712167 (0), E_{\text{int}} \approx -0.4550 (-4) \quad (\text{D.14});$$

$$E \approx -0.566712169 (0), E_{\text{int}} \approx -0.4550 (-4) / \quad (\text{D.15})$$

and

$$E \approx -0.566712170 (0), E_{\text{int}} \approx -0.4550 (-4) \quad (\text{D.16}).$$

This example shows that although the individual $E(h_j)$, $j = 1, 2, 3$ agree with each other to 4 or 5 significant figures, the interaction energies agree with each other to only one significant figure, see Eqs. (D.11) - (D.13).

On the other hand the extrapolated interaction energies agree with each other to 4 significant figures. To obtain E_{int} accurate to 4 significant figures, without using the extrapolation technique, would require an inconveniently small grid size.

APPENDIX E

NORMALIZATION OF THE WAVE FUNCTIONS FOR THE GROUND STATE OF THE H_2^+ -MOLECULE

This appendix contains a discussion of the normalization of the approximate and the exact ground state wave functions of the H_2^+ molecule. The approximate wave functions are obtained by using the analytical method, discussed in Chapter III, for solving coupled radial differential equations and the exact wave function is obtained from Ref. [38].

The approximate wave function, $\Psi(r, \theta, \phi)$, is given by the general expression of Eq. (II.2-17). The wave function Ψ obtained by the analytical method of Chapter III is not normalized. Using Eqs. (II.2-17), (II.3-5) and (III.2-2), the normalized Ψ can be written for the ground state H_2^+ molecule as

$$\Psi(r, \theta, \phi) = B \sum_{s=0}^N \frac{f_s(r)}{r} y_s^0(\theta, \phi) \quad (E.1),$$

where the normalization constant B is yet to be determined;

$$B = \left\{ \sum_{s=0}^N \int_0^\infty F_s^2(r) dr \right\}^{-\frac{1}{2}} \quad (E.2).$$

For convenience the integral in Eq. (E.2) is written as

$$\int_0^{\infty} F_S^2(r) dr = \int_0^{\rho_B} F_S^2(r) dr + \int_{\rho_B}^{\infty} F_S^2(r) dr \quad (E.3).$$

The first integral on the right hand side of Eq. (E.3) belongs to Region I ($0 \leq r \leq \rho_B$) while the second integral belongs to Region II ($\rho_B \leq r \leq \infty$), see Eqs. (II.1-4) and (III.1-5). In Region I the $F_S(r)$ are given by, see Eqs. (III.2-10) and (III.2-12),

$$F_S(r) = r^{s+1} \sum_{j=0}^{\infty} a_j^{(s)} r^j \quad (E.4).$$

Using Eq. (E.4) it is easy to evaluate the normalization integral in Region I;

$$\int_0^{\rho_B} F_S^2(r) dr = \rho_B^{2s+3} \sum_{j=0}^{\infty} (a_j^{(s)} \rho_B^j) \sum_{\ell=0}^j \frac{a_{\ell}^{(s)} \rho_B^{\ell} (2 - \delta_{j\ell})}{(j + \ell + 2s + 3)} \quad (E.5).$$

In Region II the radial functions $F_S(r)$ are given by the stepwise and the asymptotic solution of the radial equations, see Sec. III.2B, and in Region II it is convenient to evaluate the normalization integral numerically. This integral can be evaluated using 96 point Gauss-Legendre quadrature[†], see for example Refs. [106,107]. Starting with a given set of numerical data for the $F_S(r)$ this technique yields the normalization constant accurate to at least

[†] For the use of Gauss-Legendre quadrature the limits of integration must be -1 and 1. If, however, a given integral has the arbitrary limits a and b then the substitution

$$x = \frac{b-a}{2}x + \frac{b+a}{2}$$

(continued)

6 significant figures for all R and ρ_B values used for calculating the wave functions in this work. The upper limit in the normalization integral in Region II is taken to be a sufficiently large value of r such that the $F_S(r)$ becomes negligible for practical purposes. For example in the case of $R = 2$ and $\rho_B = R$ the upper limit is taken to be $r = 15$. At this value of r the $F_S(r)$ are less than or of the order of 10^{-10} .

The Schrödinger wave equation for the H_2^+ molecule can be solved exactly in confocal elliptic coordinates³⁸⁻⁴⁰. In this coordinate system the exact ground state wave function of this molecule is given by

$$\Psi(\lambda, \mu) = \Lambda(\lambda)M(\mu) \quad (E.6),$$

where

$$\Lambda(\lambda) = (\lambda+1)^\sigma e^{-\frac{R\lambda\sqrt{-E'}}{2}} \sum_{t=0}^{\infty} g_t \left[\frac{\lambda-1}{\lambda+1}\right]^t \quad (E.7)$$

$$\sigma = \frac{2}{\sqrt{-E'}} - 1 \quad (E.8),$$

$E' =$ Electronic energy in Rydbergs,

$$M(\mu) = \sum_S f_S P_S(\mu) \quad (E.9)$$

yields

$$\begin{aligned} & \int_a^b y(x) dx \\ &= \frac{b-a}{2} \int_{-1}^1 y \left(\frac{b-a}{2}x + \frac{b+a}{2} \right) dx. \end{aligned}$$

and

$$1 \leq \lambda \leq \infty, \quad -1 \leq \mu \leq 1 \quad (\text{E.10}).$$

The quantities E' , g_t and f_s are given by Ref. [23]^o and the $P_s(\mu)$ are Legendre polynomials. In confocal elliptic coordinates the volume element, see for example Arfken¹⁰⁸ is

$$dv = \left(\frac{R}{2}\right)^3 [\lambda^2 - \mu^2] d\lambda d\mu d\phi \quad (\text{E.11})$$

where $0 \leq \phi \leq 2\pi$. Thus the normalization integral for the exact wave function is given by

$$\langle \Psi | \Psi \rangle = \frac{\pi R^3}{4} \int_1^\infty \int_{-1}^1 \lambda^2 (\lambda) M^2(\mu) [\lambda^2 - \mu^2] d\lambda d\mu \quad (\text{E.12}).$$

The integration in Eq. (E.12) is performed by using 96 point Gauss-Legendre quadrature. The upper limit in the λ -integration in Eq. (E.12) is taken[†] to be $\lambda = 14$.

The exact and the approximate proton and midpoint centred wave functions for the ground state H_2^+ molecule are compared in Figs. IV.2-1 - IV.2-6 for $R = 2, 4$ and 6. The plots in these figures are referred to the spherical polar coordinate system used in this work, see Fig. II.1-1. In this coordinate system the variables λ and μ are given by

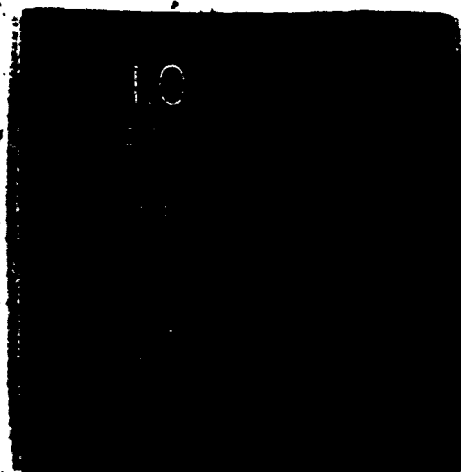
$$\left. \begin{aligned} \lambda &= \frac{r + |\underline{r} - \underline{R}|}{R} \\ \mu &= \frac{r - |\underline{r} - \underline{R}|}{R} \end{aligned} \right\} \text{for } \rho_B = R \quad (\text{E.13})$$

[†]Upper limits $\lambda = 10(5) 30$ yield the same value for the normalization integral.

3

OF/DE

3



and

$$\left. \begin{aligned} \lambda &= \frac{|\underline{r} + \frac{R}{2}| + |\underline{r} - \frac{R}{2}|}{R} \\ \mu &= \frac{|\underline{r} + \frac{R}{2}| - |\underline{r} - \frac{R}{2}|}{R} \end{aligned} \right\} \text{ for } \rho_B = R/2 \text{ (E.14).}$$

Some numerical values of normalized χ and ψ are given in Table E.1 as a function of R , ρ_B and the number of coupled differential equations used to approximate the exact Schrödinger equation for the molecule, see Eq. (II.2-18). For common values of R and r the values of the exact normalized wave function calculated in the present work agree to all the figures with those reported by Ref. [80].

TABLE E.1: Some numerical values of the normalized ψ and ψ at points along the z-axis for the ground state H_2^+ molecule for $R = 2$ and 6 with $\rho_B = R/2$ and R .

R, ρ_B	r	Number of Coupled Differential Equations Used					Exact ³⁸ ψ
		1	2	3	4	5	
$R = 2$ $\rho_B = R/2$	0	.3159	.3145	.3145	.3146	.3146	.3147
	.5	.2907	.3355	.3445	.3465	.3471	.3476
	1	.2223	.3232	.3697	.3935	.4074	.4579
	2	.0796	.1104	.1180	.1196	.1199	.1200
	4.9	.0019	.0021	.0021	.0021	.0021	.0021
$R = 2$ $\rho_B = R$	0	.5965	.5487	.5164	.4955	.4825	.4579
	.5	.3610	.3788	.3730	.3653	.3595	.3476
	1	.2171	.2682	.2928	.3044	.3097	.3147
	2	.0750	.1268	.1782	.2232	.2599	.4579
	4.9	.0021	.0040	.0057	.0070	.0077	.0085
$R = 6$ $\rho_B = R/2$	0	.0977	.0737	.0621	.0572	.0549	.0518
	1	.0919	.0877	.0803	.0764	.0745	.0718
	3	.0531	.1186	.1769	.2205	.2517	.3854
	5	.0151	.0317	.0411	.0448	.0461	.0465
	7	.0032	.0053	.0058	.0058	.0056	.0053
$R = 6$ $\rho_B = R$	0		.5606	.5593	.5584	.5578	.3854
	1		.2152	.2160	.2159	.2157	.1534
	3		.0345	.0375	.0391	.0402	.0517
	6		.0026	.0041	.0061	.0087	.3854
	8		.0004	.0007	.0012	.0018	.0465

APPENDIX F
CONVERGENCE OF THE SERIES FOR THE ELECTROSTATIC
POTENTIAL USED IN THE ONE CENTRE PARTIAL
WAVE METHOD

In order to solve the Schrödinger equation for the H_2^+ -like molecule using one centre methods both the wave function, Ψ , and the electrostatic potential, U , are expanded in an infinite series involving spherical harmonic functions, see Eqs. (II.2-1) and (II.2-5). In practice the infinite series for the wave function is approximated by a series with a finite number of terms, see Eq. (II.2-17). Because of the angular momentum coupling properties of the spherical harmonics, the exact Hamiltonian H given by Eq. (II.1-4) and the approximate Hamiltonian[†]

$$\hat{H} = -\frac{\nabla^2}{2} + \hat{U} \quad (F.1),$$

$$\hat{U} = \sum_{l=0}^{2N} U_l a_l Y_l^0(\theta, \phi) \quad (F.2).$$

yield the same system of coupled differential equations when the approximate wave function Ψ , see Eq. (II.2-17),

[†]It is important to realize that the truncation of the series for U does not truncate the series for Ψ although the converse is true.

is used in the partial wave method discussed in Chapters II and III, see Eq. (II.2-18). The solution of these coupled differential equations provide, for finite N , approximate energies and wave functions for the H_2^+ -like molecule. It is only in the limit $N \rightarrow \infty$ that one obtains $\tilde{H} \rightarrow H$, $\tilde{\Psi} \rightarrow \Psi$ and $E \rightarrow E$ (exact) for all R and ρ_A . The purpose of this appendix is to examine how well the approximate electrostatic potential \tilde{U} represents the exact electrostatic potential U for given values of N , R and ρ_A . This investigation is helpful, see Chapter IV and Sec. V.3, in understanding the convergence difficulties associated with the one centre partial wave results for the energy and the wave function, as a function of R , N and ρ_A .

We consider here only the H_2^+ molecule explicitly. For this molecule \tilde{U} and U have axial symmetry and they can be compared at any point (r, θ) . To simplify the discussion we compare these functions only at points along the z -axis, that is with $\theta = 0$, or π , for the two important cases where $\rho_A = 0$ and $\rho_A = R/2$. Using these choices for θ we obtain, see Sec. II.2,

$$d_l Y_l^0(0, \phi) = 1$$

and

$$d_l Y_l^0(\pi, \phi) = (-1)^l.$$

Thus Eq. (F.2) reads

$$\tilde{U} = \sum_{l=0}^{2N} U_l, \quad \theta = 0 \quad (F.3)$$

and

$$\tilde{U} = \sum_{\ell=0}^{2N} U_{\ell} \left(\frac{r}{R}\right)^{\ell}, \quad \theta = \pi \quad (\text{F.4}).$$

Case 1: Set $\rho_A = \rho_B = R/2$ and $z_A = z_B = 1$. From equations (II.2-3) and (II.2-4) we obtain

$$U_{\ell} = 0, \quad \ell \text{ odd}$$

and

$$U_{\ell} = -2 \frac{r_{<}^{\ell}}{r_{>}^{\ell+1}}, \quad \ell \text{ even},$$

where $r_{<}$ and $r_{>}$ are, respectively, the lesser and greater of r and $R/2$. Hence one obtains

$$\begin{aligned} \tilde{U} &= -\frac{2}{y} [1 + x^2 + x^4 + \dots + x^{2N}] \\ &= -\frac{2}{y} \left[\frac{1 - x^{2N+2}}{1 - x^2} \right] \\ &= -\frac{2}{y} \left[\frac{1 - e^{(2N+2) \ln x}}{1 - x^2} \right] \end{aligned} \quad (\text{F.5})$$

where

$$y = R/2, \quad x = \frac{2r}{R}, \quad 0 \leq r \leq R/2 \quad (\text{F.6})$$

or

$$y = r, \quad x = R/2r, \quad R/2 \leq r \leq \infty \quad (\text{F.7}).$$

The exact electrostatic potential is given by, see Eq. (II.1-4),

$$U = -2 \left[\frac{1}{R+2r} + \frac{1}{|R-2r|} \right] \quad (\text{F.8}).$$

The functions \tilde{U} and U are compared in Figs. F.1 - F.5 as a function of N for $\rho_A = R/2$ and $R = 2, 4, 6, 8$ and 20 .

These figures show that, for a given value of R , better

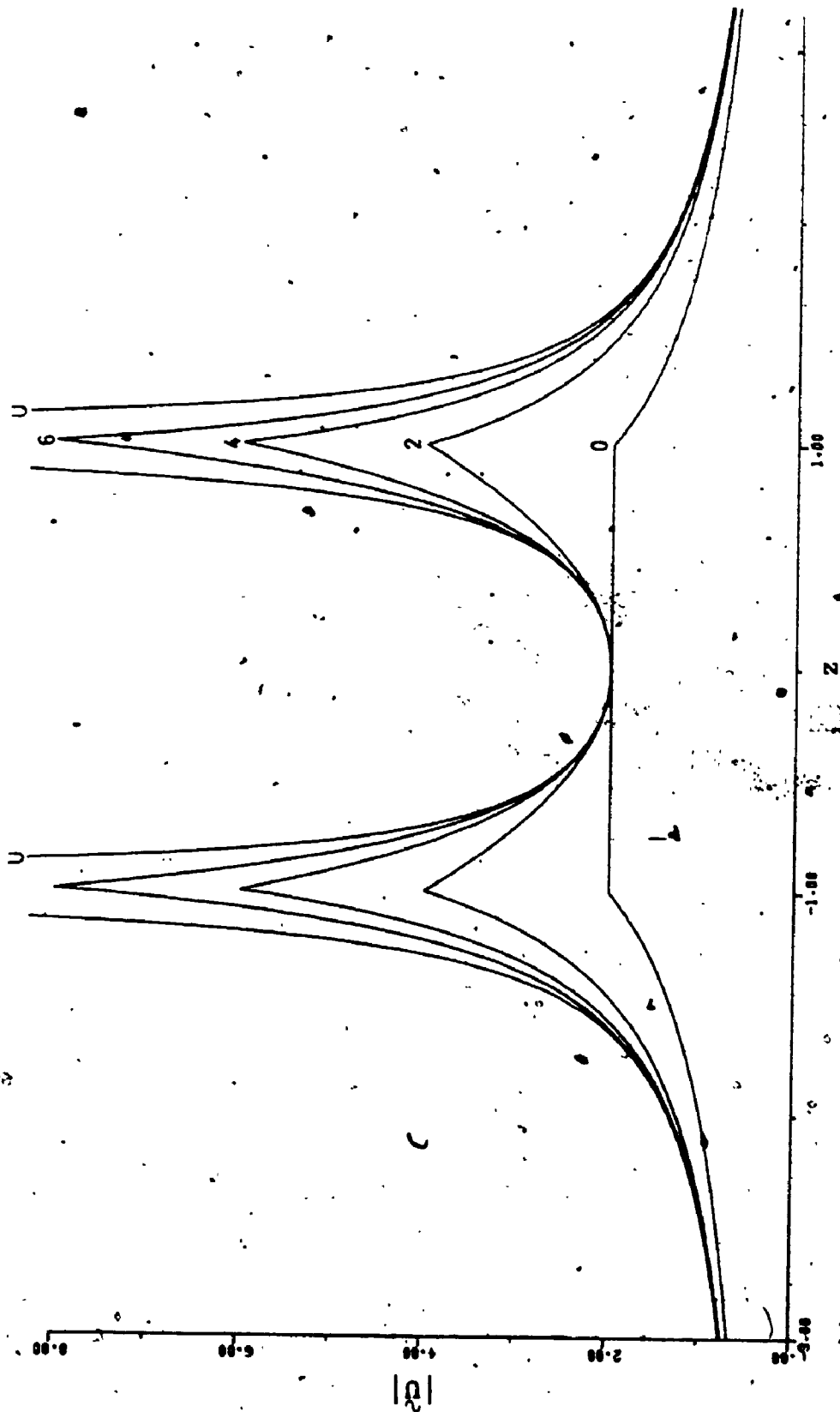


Figure F.1: The modulus of the electrostatic potential \tilde{U} , see Eqs. (F.3) - (F.7), at points along the z -axis for $R = 2$ and $\rho_A = \rho_B = R/2$. The graphs 0, 2, 4, and 6 correspond to $2N = 0, 2, 4$ and 6 respectively. The graph U represents the modulus of the exact potential \tilde{U} , see Eq. (F.8), at points along the z -axis.

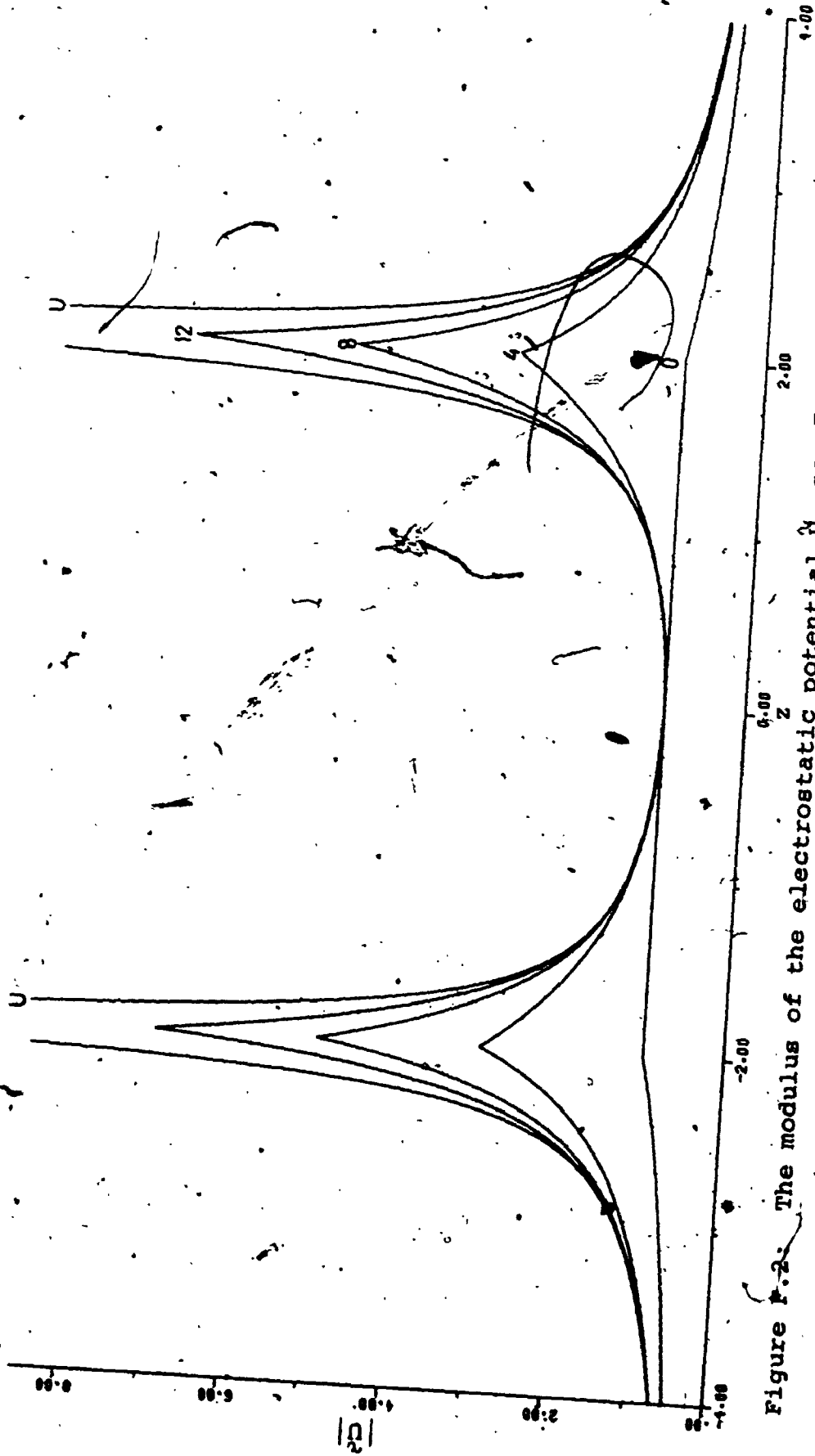


Figure F.2. The modulus of the electrostatic potential \tilde{U} , see Eqs. (F.3), - (F.7), at points along the z-axis, for $R = 4$ and $\rho_A = \rho_B = R/2$. The graphs 0, 4, 8 and 12 correspond to $2N = 0, 4, 8$ and 12 respectively. The graph U represents the modulus of the exact potential U , see Eq. (F.8), at points along the z-axis.

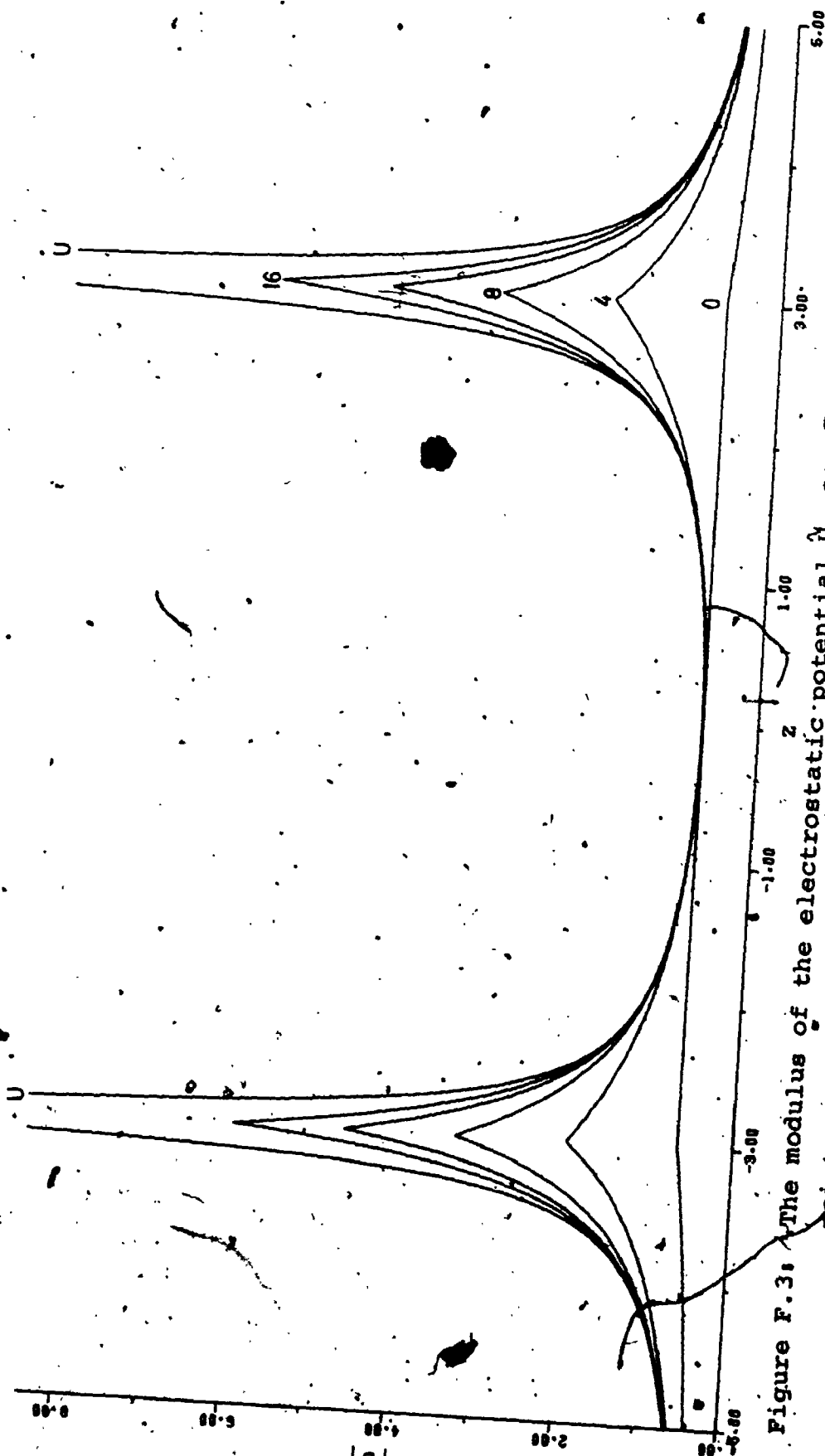


Figure F.3: The modulus of the electrostatic potential U , see Eqs. (F.3) - (F.7), at points along the z -axis for $R = 6$ and $\rho_A = \rho_B = R/2$. The graphs 0, 4, 8, ..., 16 correspond to $2N = 0, 4, 8, \dots, 16$ respectively. The graph U represents the modulus of the exact potential U , see Eq. (F.8), at points along the z -axis.

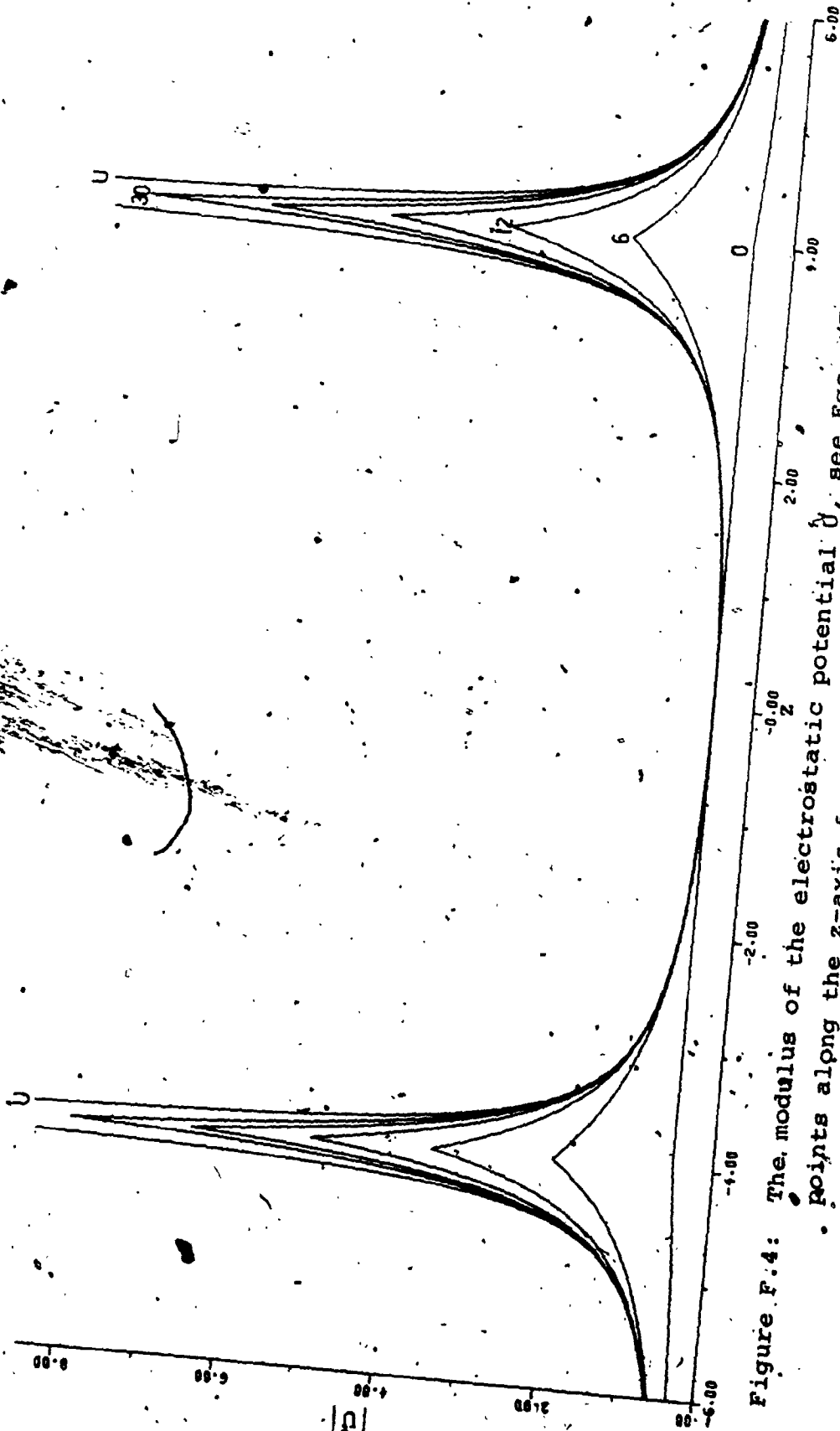


Figure F.4: The modulus of the electrostatic potential U , see Eqs. (F.3) - (F.7), at points along the z -axis for $R = 8$ and $\rho_A = \rho_B = R/2$. The graphs 0, 6, 12, ..., 30 correspond to $2N = 0, 6, 12, \dots, 30$ respectively. The graph U represents the modulus of the exact potential U , see Eq. (F.8), at points along the z -axis.

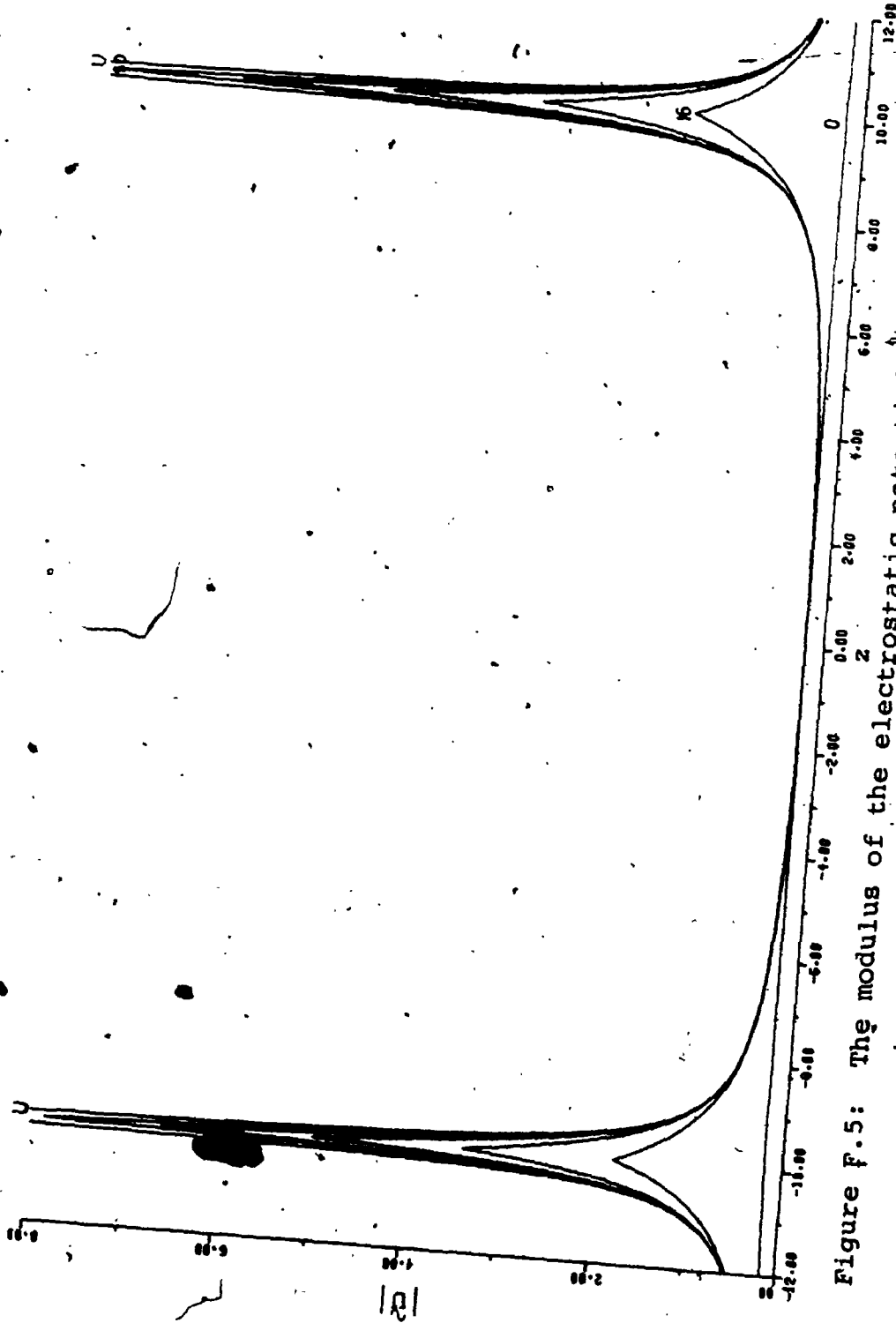


Figure F.5: The modulus of the electrostatic potential U , see Eqs. (F.3) - (F.7), at points along the z -axis for $R = 20$ and $\rho_A = \rho_B = R/2$. The graphs 0, 16, ..., 80 correspond to $2N = 0, 16, \dots, 80$ respectively. The graph U represents the modulus of the exact potential U , see Eq. (F.8), at points along the z -axis.

representations of U are obtained by using large values of N in \tilde{U} and that as N increases the changes in \tilde{U} occur mainly in the neighbourhood of the two nuclei. These figures also show that for a given N , \tilde{U} is a progressively poorer representation of U as R increases.

Since it is not possible to compare U and \tilde{U} graphically for all values of R , N and r we consider here these functions analytically for some special values of r . Consider values of the electronic radial coordinate r defined by

$$r = R/2 - \delta r, \quad 0 \leq \delta r < R/2 \quad (\text{F.9}).$$

For this choice of r , Eq. (F.5) yields

$$\tilde{U} = -\frac{4}{R} \left[\frac{1 - e^{-\mu(2N+2)}}{1 - x^2} \right] \quad (\text{F.10}),$$

where

$$\mu = |\ln x|$$

and

$$0 \leq |x| = \left| 1 - \frac{2\delta r}{R} \right| < 1 \quad (\text{F.11}).$$

If the condition given by

$$e^{-\mu(2N+2)} = e^{-(2N+2)|\ln(1 - \frac{2\delta r}{R})|} \ll 1 \quad (\text{F.12})$$

is satisfied then Eq. (F.10) gives

$$\tilde{U} \approx -\frac{1}{\delta r(1 - \frac{\delta r}{R})} \quad (\text{F.13}).$$

The exact potential obtained from Eq. (F.8) for this choice of r is given by

$$U = -\frac{1}{\delta r(1 - \frac{\delta r}{R})} \quad (\text{F.14}).$$

Comparison of Eqs. (F.13) and (F.14) shows that $\tilde{U} \rightarrow U$ when the condition given by Eq. (F.12) is satisfied. It is clear that if the distance between the electron and either of the nuclei is small compared to the separation between the nuclei, that is $\frac{\delta r}{R}$ is small, then one would require very large N in \tilde{U} to satisfy the relation given in Eq. (F.12). At a nuclear position where $\delta r = 0$, Eqs. (F.5) and (F.8) give respectively

$$\tilde{U} = - \frac{4(N+1)}{R} \quad (\text{F.15})$$

and

$$U = -\infty \quad (\text{F.16}).$$

Thus \tilde{U} can represent the Colomb singularities at the nuclear positions only when $N/R \rightarrow \infty$.

Case 2: Set $\rho_A = 0$, $\rho_B = R$ and $Z_A = Z_B = 1$. Using Eqs. (II.2-3) and (II.2-4) we obtain

$$U_\ell = -\frac{1}{r} \delta_{\ell 0} - \frac{r_\ell^\ell}{r_\ell^{\ell+1}} \quad (\text{F.17}),$$

where r_ℓ and r_ℓ are, respectively, the lesser and greater of r and R . Hence we obtain

$$\begin{aligned} \tilde{U} &= -\frac{1}{r} - \frac{1}{y} [1 + x + x^2 + \dots + x^{2N}] \\ &= -\frac{1}{r} - \frac{1}{y} \left[\frac{1 - x^{2N+1}}{1 - x} \right] \\ &= -\frac{1}{r} - \frac{1}{y} \left[\frac{1 - e^{(2N+1) \ln x}}{1 - x} \right], \quad \theta = 0 \end{aligned} \quad (\text{F.18})$$

and

$$\begin{aligned}
 \tilde{U} &= -\frac{1}{r} - \frac{1}{y} [1 - x + x^2 - \dots + x^{2N}] \\
 &= -\frac{1}{r} - \frac{1}{y} \left[\frac{1+x^{2N+1}}{1+x} \right] \\
 &= -\frac{1}{r} - \frac{1}{y} \left[\frac{1+e^{(2N+1)\ln x}}{1+x} \right], \quad \theta = \pi \quad (F.19),
 \end{aligned}$$

where

$$y = R, \quad x = \frac{r}{R}, \quad 0 \leq r \leq R$$

and

$$y = r, \quad x = R/r, \quad R \leq r \leq \infty \quad (F.20).$$

The exact electrostatic potential is given by, see Eq. (II.1-4),

$$U = -\frac{1}{r} - \frac{1}{|R-r|}, \quad \theta = 0 \quad (F.21)$$

and

$$U = -\frac{1}{r} - \frac{1}{R+r}, \quad \theta = \pi \quad (F.22)$$

The functions \tilde{U} and U are compared in Figs. F.6 - F.10 as a function of N for $\rho_A = 0$ and $R = 2, 4, 6, 8$ and 20. These figures show, for a given value of R , that better representation of U are obtained by using large values of N in \tilde{U} . When the expansion centre is located at the nucleus A, that is $\rho_A = 0$, \tilde{U} represents U quite well, even with small N , everywhere[†] except near the other nucleus B and

[†] It is important to realize that at the point $r = R$ and $\theta = \pi$ the approximate potential yields $\tilde{U} = -\frac{2}{R}$ for all N , see Eq. (F.19), while the exact potential gives $U = -\frac{3}{2R}$, see Eq. (F.22). Fig. F.6 provides an example of the convergence of \tilde{U} at and near the point $r = R$ and $\theta = \pi$ as

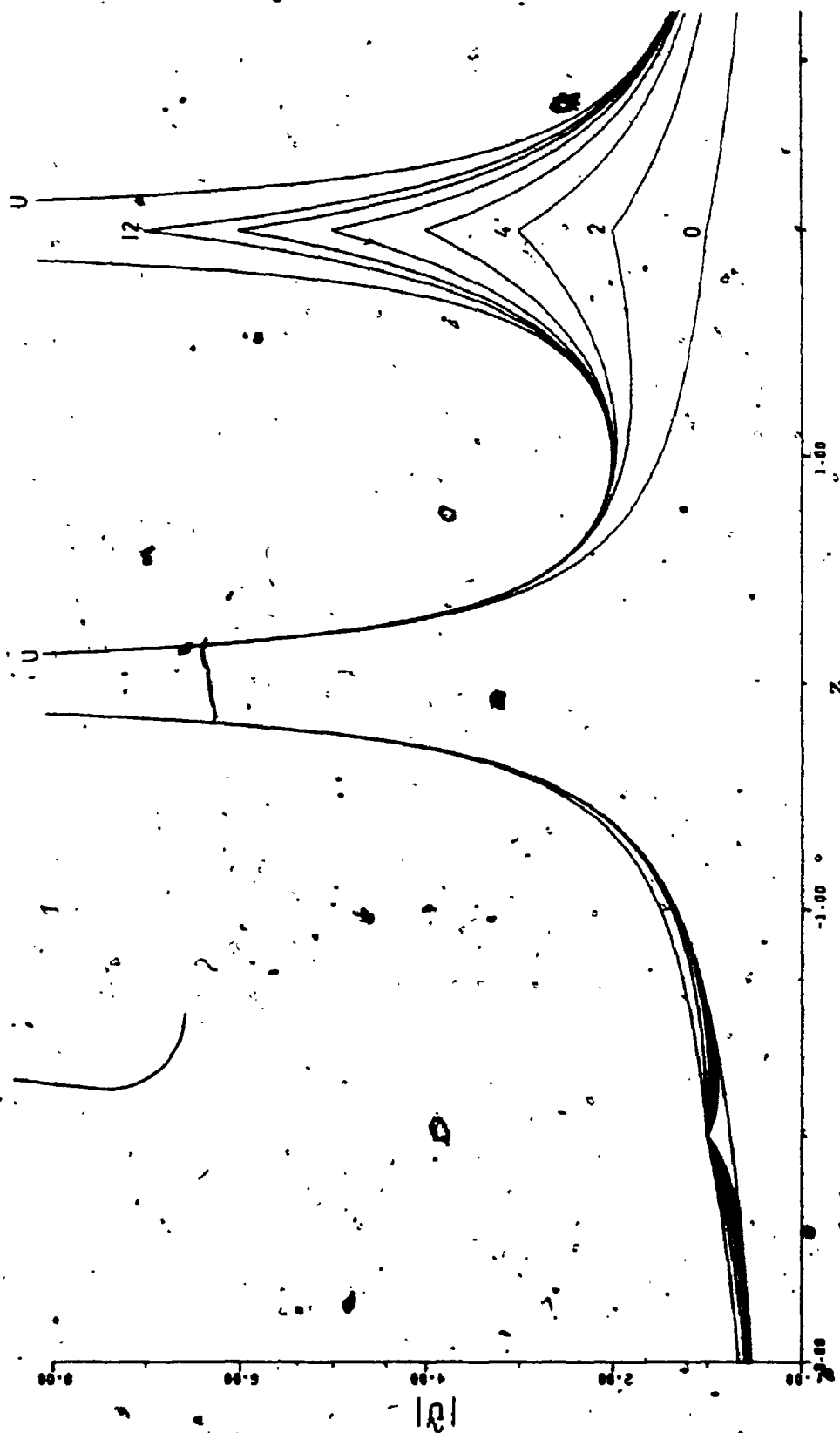


Figure F.6: The modulus of the electrostatic potential \tilde{U} , see Eqs. (F.17) - (F.20), at points along the z -axis for $R = 2$ and $\rho_A = 0$ ($\rho_B = R$). The graphs 0, 2, 4, ..., 12 correspond to $2N = 0, 2, 4, \dots, 12$ respectively. The graph U represents the modulus of the exact potential U , see Eqs. (F.21) and (F.22), at points along the z -axis.

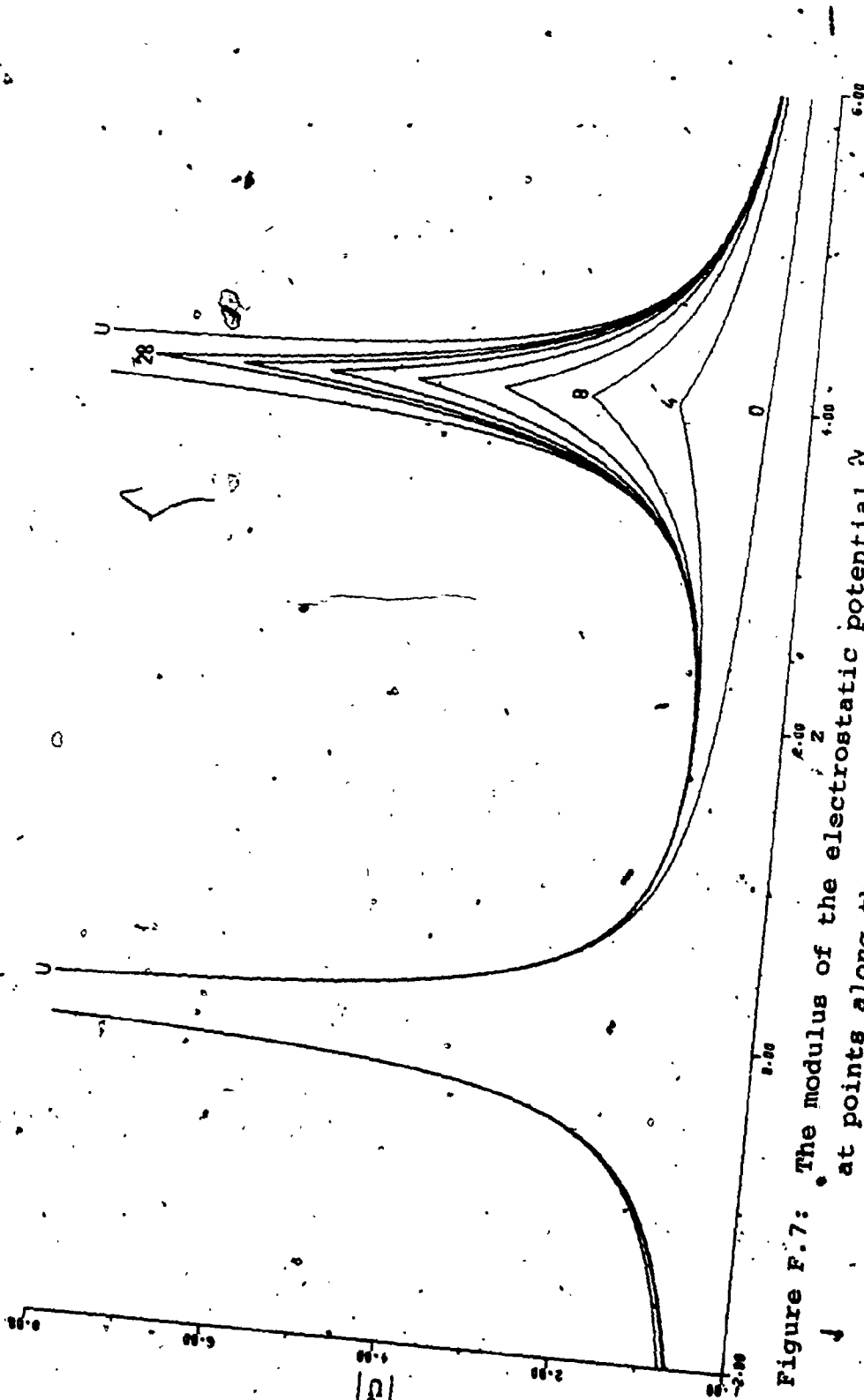


Figure F.7: The modulus of the electrostatic potential \tilde{U} , see Eqs. (F.17) - (F.20), at points along the z-axis for $R = 4$ and $\rho_A = 0$ ($\rho_B = R$). The graphs 0, 4, 8, ..., 28 correspond to $2N = 0, 4, 8, \dots, 28$ respectively. The graph U represents the modulus of the exact potential U, see Eqs. (F.21) and (F.22), at points along the z-axis.

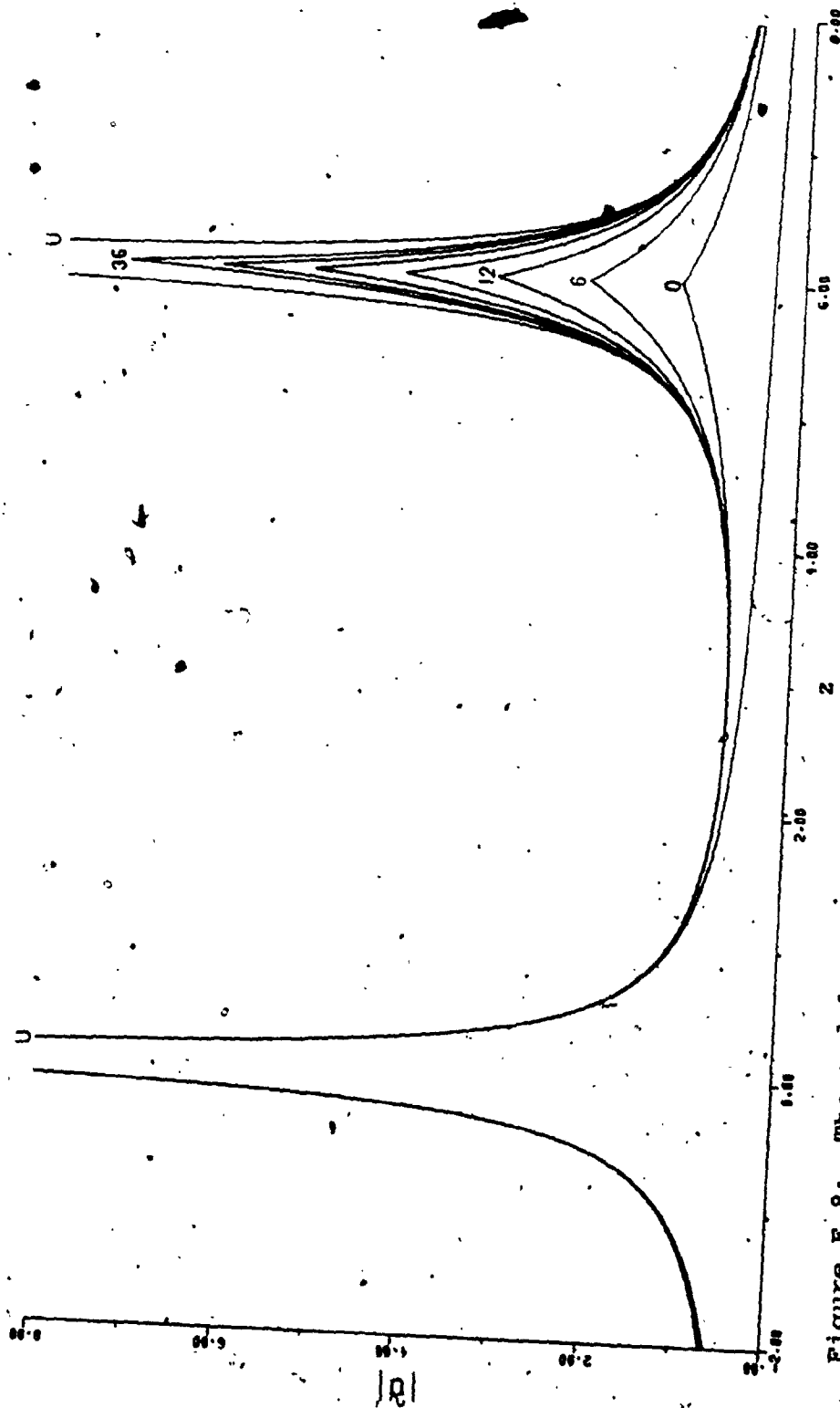


Figure F.8: The modulus of the electrostatic potential \tilde{U} , see Eqs. (F.17) - (F.20), at points along the z -axis for $K = 6$ and $\rho_A = 0$ ($\rho_B = R$). The graphs 0, 6, 12, ..., 36 correspond to $2N = 0, 6, 12, \dots, 36$ respectively. The graph U represents the modulus of the exact potential U , see Eqs. (F.21) and (F.22), at points along the z -axis.

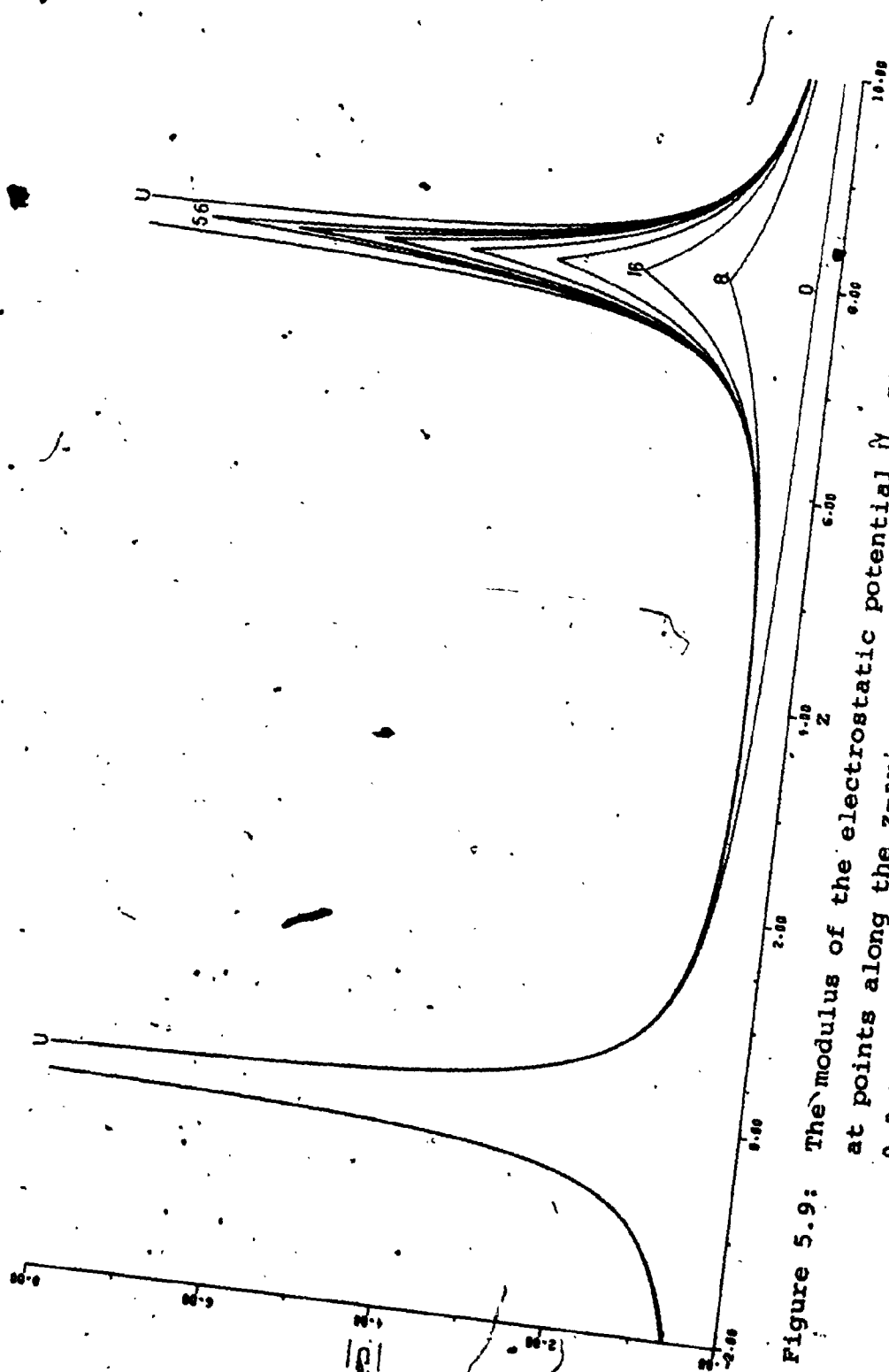


Figure 5.9: The modulus of the electrostatic potential U , see Eqs. (F.17) - (F.20) at points along the z -axis for $R = 8$ and $\rho_A = 0$ ($\rho_B = R$). The graphs U represents the modulus of the exact potential U , see Eqs. (F.21) and (F.22), at points along the z -axis.

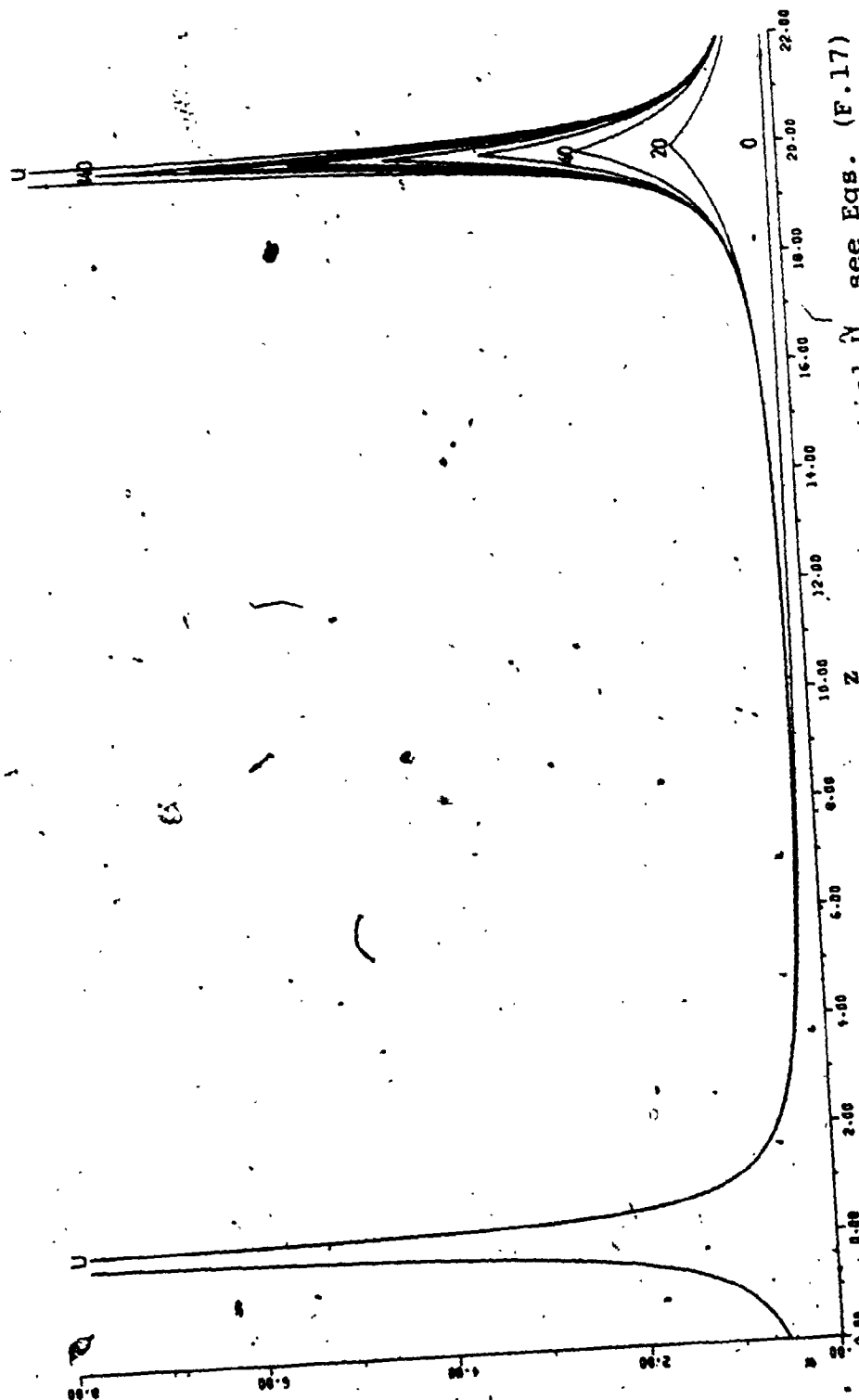


Figure 10: The modulus of the electrostatic potential \bar{U} , see Eqs. (F.17)

- (F.20), at points along the z-axis for $R = 20$ and $\rho_A = 0$ ($\rho_B = R$). The graphs 0, 20, 40, ..., 140 correspond to $2N = 0, 20, 40, \dots, 140$ respectively. The graph U represents the modulus of the exact potential U , see Eqs. (F.21) and (F.22), at points along the z-axis.

as N increases the changes in \tilde{U} occur mainly in the neighbourhood of the nucleus B. These figures also show that for a given N , \tilde{U} is a progressively poorer representation of U near the nucleus B as R increases.

Let us now compare \tilde{U} and U analytically for some special values of the electronic coordinates defined by

$$r = R - \delta r, \quad 0 \leq \delta r < R \quad (\text{F.23})$$

and

$$\theta = 0 \quad (\text{F.24})$$

For these choices of r and θ Eq. (F.18) yields

$$\tilde{U} = -\frac{1}{R-\delta r} - \frac{1}{R} \left[\frac{1-e^{-\mu(2N+1)}}{1-x} \right] \quad (\text{F.25})$$

where

$$\mu = |\ln x|$$

and

$$0 \leq |x| = \left| 1 - \frac{\delta r}{R} \right| < 1 \quad (\text{F.26})$$

If the condition given by

$$e^{-\mu(2N+1)} = e^{-(2N+1)|\ln(1 - \frac{\delta r}{R})|} \ll 1 \quad (\text{F.27}),$$

is satisfied then Eq. (F.25) gives

$$\tilde{U} \approx -\frac{1}{R-\delta r} - \frac{1}{\delta r} \quad (\text{F.28}).$$

a function of N with $R = 2$ and $\rho_A = 0$: The convergence difficulty of \tilde{U} at and near the point $r = R$ and $\theta = \pi$ for intermediate and large R will not significantly affect the rate of convergence of the proton centre results for the energy.

The exact potential obtained from Eq. (F.21) for this choice of r and θ is given by

$$U = -\frac{1}{R-\delta r} - \frac{1}{\delta r} \quad (F.29).$$

Comparison of Eqs. (F.28) and (F.29) show that $\tilde{U} \rightarrow U$ when the condition given by Eq. (F.27) is satisfied. It is clear that if the distance between the electron and the nucleus B is small compared to the separation between the nuclei, that is $\frac{\delta r}{R}$ is small, then one would require very large N in \tilde{U} to satisfy the relation given in Eq. (F.27). At the nucleus B where $\delta r = 0$, Eqs. (F.18) and (F.21) yield respectively

$$\tilde{U} = -\frac{2(N+1)}{R} \quad (F.30)$$

and

$$U = -\infty \quad (F.31).$$

Thus \tilde{U} can represent the coulomb singularity at the nucleus B only when $N/R \rightarrow \infty$. The coulomb singularity at the nucleus A is satisfied by U for all N .

General Discussion: The above remarks hold for the electrostatic potential without any reference to the physical problem. In the bound state problem the electron does not collapse into the nuclei, rather it stays, depending on the eigenstate of the molecule, at a certain average distance away from them³⁵. Thus \tilde{U} can be adequate for the physical problem (even if \tilde{U} does not satisfy the conditions, given by Eqs. (F.16) and (F.31), at the nuclear positions) if it adequately represents U in the

region where the probability of the presence of the electron is high. The average distances of the electron from the nuclei are larger for excited states than for the ground state of the molecule³⁵. Hence, by comparison with the excited states it is relatively more important in one centre ground state calculations that \bar{U} adequately represents U at points not too far from the nuclei.

The one centre partial wave solution of the Schrödinger equation for the ground state H_2^+ molecule, discussed in Chapter III, corresponds to the solution of this equation with the approximate Hamiltonian \bar{H} instead of the exact Hamiltonian H , see Eqs. (F.1) and (F.2). Hence some qualitative remarks can be made about this partial wave solution on the basis of the above investigations of the electrostatic potential. It is well known³⁸ that the exact ground state H_2^+ wave function has identical cusps at the two nuclear positions and that these cusps are attributed³⁵ to the two coulomb singularities occurring in U . Observing the convergence of \bar{U} as a function of N , ρ_A and R , especially near the nuclei, we can make the following qualitative remarks about the one centre partial wave solution of the Schrödinger equation for the ground state of this molecule.

1. Since $\bar{U} \rightarrow U$ as $N \rightarrow \infty$, both the proton centred and midpoint centred calculations will yield, for any given R , identical cusp characteristics in Ψ and the exact energy of the molecule for sufficiently large values of N ; see the trends in Ψ and E in Figs. IV.2-1 - IV.2-6 and

Tables IV.1-1 - IV.1-3 respectively.

2. As R increases one requires increasingly large values of N to obtain a good representation of the electrostatic potential U . Thus for large R it will not be feasible to obtain a good representation of Ψ by one centre calculations, see Sec. IV.2.

3. As $R \rightarrow \infty$ but N remains finite the proton centred calculations will yield hydrogenic wave functions centred on the nucleus A since in this case \bar{U} represents the hydrogenic potential centred on this nucleus. It is important to realize that although the proton centred calculations, for large R and small N , fail to yield identical cusp characteristics in Ψ , these calculations give accurate long range results for the energy, see Sec. V.3. On the other hand the midpoint centred calculations will yield the energy and the wave function of a free electron, see Chapter IV, since when $\rho_A = R/2$ and $R \rightarrow \infty$, $\bar{U} \rightarrow 0$ for finite values of N , see Eq. (F.15).

4. For any given R , as N increases, the contribution to \bar{U} , due to the increase in N , is mainly at the nuclear positions in both the proton centred and midpoint centred calculations. Hence for any given R , as N increases, the contribution to Ψ will be mainly at the nuclear positions, see Figs. IV.2-1 - IV.2-6.

5. Both the midpoint and proton centred calculations will yield accurate energy eigenvalues for small R with convenient values of N . For large R it will not be

feasible to obtain reasonable results by midpoint centred calculations. On the other hand from energy considerations, see point 3, for large R the suitable choice of the expansion centre is at one of the protons, see Sec. IV.1C.

Finally a comment can be made on the one centre partial wave solution of the Schrödinger equation for excited states of the H_2^+ molecule. For given R and ρ_A the rate of convergence of E_{int} to E_{int} (exact) and Ψ to Ψ , as a function of N , will be faster for the excited states than for the ground state of the molecule^{2,35,36,41,42}. This is because the average distance of the electron from the nuclei are larger for excited states than for the ground state of the molecule and it is relatively easier to adequately represent U_{int} points that are far away from the nuclei than at points close to the nuclei, see however the footnote on pages 188 and 194.

APPENDIX G

A DISCUSSION OF THE EVALUATION OF THE INTEGRALS AND CONSTANTS OF INTEGRATION APPEARING IN REFERENCE [7].

In Ref. [7], designated here as I, explicit calculations have been performed for the ground state H_2^+ energy through third order in the perturbation by using the screened hydrogen atom and the molecular puff as the unperturbed problems, see Sec. V.4B. In these perturbation schemes the Schrödinger equation for H_2^+ -like molecules has been solved through first order in the wave function in three separate regions, see Fig. II.1-1 and Eqs. (II.1-1) - (III.1-3), 1: $r \leq \rho_A, \rho_B$, 2: $\rho_A \leq r \leq \rho_B$ and 3: $r \geq \rho_A, \rho_B$. The solution of the equation for the entire range $0 \leq r \leq \infty$ is obtained by smoothly matching the solutions in these three regions at the common boundaries at $r = \rho_A$ and ρ_B . The details of the calculations for the energy through second order and the wave function through first order for the scheme based on the screened hydrogen atom is given in Ref. [6]. For the perturbation problem based on the molecular puff the first order wave function has been expanded in the form [7].

$$\psi^{(1)} = \sum_{\ell=1}^{\infty} F_{\ell}(r, \rho_A, R) P_{\ell}(\cos \theta),$$

where $P_\ell(\cos \theta)$ is a Legendre polynomial. In order to distinguish the solutions in the three separate regions, see above, the F_ℓ have been designated as JF_ℓ , $j = 1, 2, 3$. The purpose of this appendix is to discuss the procedures for evaluating the integrals and constants of integration appearing in I.

G.1 THE EVALUATION OF THE INTEGRALS

The integrals needed to be evaluated are given by Eqs. (I.22), (I.39), (I.62) and (I.63). The integrals in Eqs. (I.22) and (I.39) are of the form

$$\int_{\epsilon_0}^{\infty} G(r) dr = \int_{\epsilon_0}^{\rho_A} G(r) dr + \int_{\rho_A}^{\rho_B} G(r) dr + \int_{\rho_B}^{\infty} G(r) dr \quad (G.1),$$

where $\epsilon_0 = 0$ and ρ_A for Eqs. (I.22) and (I.39) respectively. It is obvious that the first integral on the right hand side of Eq. (G.1) vanishes when $\epsilon_0 = \rho_A$. The integrals from $r = 0$ to ρ_A and ρ_A to ρ_B are evaluated accurately by using 96-point Gauss-Legendre quadrature^{106,107} for each of these integrals. In order to perform the integration from $r = \rho_B$ to ∞ it has been found convenient to write the integral in the form

$$\int_{\rho_B}^{\infty} G(r) dr = \int_{\rho_B}^{\rho_B + \Delta} G(r) dr + \int_{\rho_B + \Delta}^{\rho_B + 2\Delta} G(r) dr + \dots \quad (G.2),$$

where Δ is a convenient number, see later. Each of the integrals on the right hand side of Eq. (G.2) is evaluated by using 96-point Gauss-Legendre quadrature. Since the wave function decreases exponentially at large r the series

in Eq. (G.2) converges very rapidly. It has been found that using 3 terms of this series with $\Delta = 6$ yields the energy and wave function accurate to at least 10 significant figures for all values of R reported in I.

Equations (I.62) and (I.63) involve double integrations, see Eqs. (I.52) - (I.61). These integrals can be written formally as

$$\int_0^\infty H(r) dr = \int_0^{\rho_A} H(r) dr + \int_{\rho_A}^{\rho_B} H(r) dr + \int_{\rho_B}^\infty H(r) dr \quad (G.3),$$

where $H(r)$ is given analytically in region 1, see Eqs. (I.3), (I.4), (I.30) - (I.32) and (I.47) - (I.51), and in regions 2 and 3 it is of the form

$$H(r) = \int_{\epsilon_1}^X M(s) ds \quad (G.4),$$

$$\epsilon_1 = \frac{2Z_A \rho_A}{K_0}, \quad X = \frac{2Z_A r}{K_0}; \quad \rho_A \leq r \leq \rho_B \quad (G.5)$$

and

$$\epsilon_1 = \frac{2Z \rho_B}{K}, \quad X = \frac{2Z r}{K}; \quad \rho_B \leq r \leq \infty \quad (G.6).$$

The quantities Z , Z_A , K and K_0 are defined by Eq. (I.34), see also Eq. (I.35). The procedure for evaluating the integrals over r in Eq. (G.3) is completely analogous to that used for evaluating the integrals in Eq. (G.1).

Before performing the inner integrals for finding $H(r)$ in regions 2 and 3, see Eqs. (G.4) - (G.6), we observe that the outer integration over r needs the determination of $H(r)$ at the Gauss-Legendre grid points r_1, r_2, r_3, \dots

such that $r_1 < r_2 < r_3 \dots$. Therefore in order to perform the outer integration over r the inner integrals are evaluated to obtain $H(r_1), H(r_2), H(r_3), \dots$. It is clear that

$$H(r_1) = \int_{\epsilon_1}^{X(r_1)} M(s) ds$$

$$H(r_2) = H(r_1) + \int_{X(r_1)}^{X(r_2)} M(s) ds$$

and in general

$$H(r_{n+1}) = H(r_n) + i_{n+1} \quad (G.7)$$

where

$$i_{n+1} = \int_{X(r_n)}^{X(r_{n+1})} M(s) ds, \quad n = 0, 1, 2, \dots \quad (G.8)$$

and

$$H(r_0) = 0, \quad X(r_0) = \epsilon_1.$$

For each n the i_{n+1} are evaluated by using 8-point Gauss-Legendre quadrature. It has been found that increasing the number of inner grid points makes a change in the overall integral $\int_{\rho_A}^{\infty} H(r) dr$ only in the 12th or higher significant figures.

G.2 EVALUATION OF THE CONSTANTS OF INTEGRATION

The constants of integration $\alpha_\ell, \beta_\ell, \gamma_\ell$ and ζ_ℓ appearing in Eqs. (I.47), (I.55) and (I.61), are determined by using the matching conditions for the first order wave

function, obtained in the three separate regions mentioned earlier in this appendix, at the boundaries $r = \rho_A$ and $r = \rho_B$. Because of the orthogonality properties of the Legendre polynomials, these matching conditions for $\psi^{(1)}$ imply, see Eqs. (I.47), (I.52) and (I.59)

$${}_1F_\ell(\rho_A, \rho_A, R) = {}_2F_\ell(\rho_A, \rho_A, R) \quad (G.9)$$

$${}_1F'_\ell(\rho_A, \rho_A, R) = {}_2F'_\ell(\rho_A, \rho_A, R) \quad (G.10),$$

$${}_2F_\ell(\rho_B, \rho_A, R) = {}_3F_\ell(\rho_B, \rho_A, R) \quad (G.11)$$

and

$${}_2F'_\ell(\rho_B, \rho_A, R) = {}_3F'_\ell(\rho_B, \rho_A, R) \quad (G.12).$$

In Eqs. (G.10) and (G.12) the prime denotes the first derivative with respect to r . Using the expressions of the F_ℓ and F'_ℓ , see Eqs. (I.47), (I.52), (I.55) - (I.59) and (I.61), we obtain

$$\beta_\ell = \alpha_\ell C_3 + C_4 \quad (G.13),$$

$$\gamma_\ell = \alpha_\ell C_5 + C_6 \quad (G.14),$$

$$\gamma_\ell = \zeta_\ell C_{10} + C_{11} - I_2(x_1, K_0, x_0) \quad (G.15)$$

and

$$\beta_\ell = \zeta_\ell C_{12} + C_{13} + J_2(x_1, K_0, x_0) \quad (G.16),$$

where K_0 and x_0 are defined in I and

$$x_1 = \frac{2Z_A \rho_B}{K_0},$$

$$\mu_1 = 1 + \ell - K_0, \mu_2 = 1 + \ell - K, \nu = 2\ell + 2,$$

$$C_0 = \frac{\Gamma(\mu_1)}{\Gamma(\nu)} x_0^{\ell+2} e^{-x_0/2},$$

$$C_1 = \frac{\rho_A \Omega'_\ell(\rho_A)}{x_0} + \left(\frac{1}{2} - \frac{\ell}{x_0}\right) \Omega_\ell(\rho_A),$$

$$C_2 = \frac{\rho_A Z'_\ell(\rho_A)}{x_0} + \left(\frac{1}{2} - \frac{\ell}{x_0}\right) Z_\ell(\rho_A),$$

$$C_3 = -C_0 [\Omega_\ell(\rho_A) \Psi'(\mu_1, \nu, x_0) - C_1 \Psi(\mu_1, \nu, x_0)],$$

$$C_4 = -C_0 [Z_\ell(\rho_A) \Psi'(\mu_1, \nu, x_0) - C_2 \Psi(\mu_1, \nu, x_0)],$$

$$C_5 = -C_0 [C_1 \Phi(\mu_1, \nu, x_0) - \Phi'(\mu_1, \nu, x_0) \Omega_\ell(\rho_A)],$$

$$C_6 = -C_0 [C_2 \Phi(\mu_1, \nu, x_0) - Z_\ell(\rho_A) \Phi'(\mu_1, \nu, x_0)],$$

$$C_7 = \frac{\Gamma(\mu_1)}{\Gamma(\nu)} x_1^\nu \left(\frac{y_0}{x_1}\right)^\ell e^{-\frac{1}{2}(x_1 + y_0)},$$

$$C_8 = \Phi'(\mu_1, \nu, x_1) - \frac{1}{2} \Phi(\mu_1, \nu, x_1) + \frac{y_0}{2x_1} \Phi(\mu_1, \nu, x_1),$$

$$C_9 = \Psi'(\mu_1, \nu, x_1) + \frac{1}{2} \Psi(\mu_1, \nu, x_1) - \frac{y_0}{2x_1} \Psi(\mu_1, \nu, x_1),$$

$$C_{10} = C_7 [C_8 \Psi(\mu_2, \nu, y_0) - \frac{y_0}{x_1} \Psi'(\mu_2, \nu, y_0) \Phi(\mu_1, \nu, x_1)],$$

$$C_{11} = C_7 J_3(\infty, K, y_0) [C_8 \Phi(\mu_2, \nu, y_0) - \frac{y_0}{x_1} \Phi'(\mu_2, \nu, y_0) \Phi(\mu_1, \nu, x_1)],$$

$$C_{12} = C_7 [C_9 \Psi(\mu_2, \nu, y_0) + \frac{y_0}{x_1} \Psi'(\mu_2, \nu, y_0) \Psi(\mu_1, \nu, x_1)],$$

and

$$C_{13} = C_7 J_3(\infty, K, y_0) [C_9 \Phi(\mu_2, \nu, y_0) + \frac{y_0}{x_1} \Phi'(\mu_2, \nu, y_0) \Psi(\mu_1, \nu, x_1)].$$

(G, 17).

All the quantities on the right hand side of Eqs. (G.17) are defined in I. It is now straightforward to calculate the constants of integration by using Eqs. (G.13) - (G.16) and we find

$$\zeta_\ell = \frac{C_5(C_4 - C_{13}) + C_3(C_{11} - C_6) - [J_2(x_1, K_0, x_0)C_5 + I_2(x_1, K_0, x_0)C_3]}{C_{12}C_5 - C_{10}C_3}$$

(G.18)

and

$$\alpha_\ell = \frac{C_{10}(C_{13} - C_4) + C_{12}(C_6 - C_{11}) + J_2(x_1, K_0, x_0)C_{10} + I_2(x_1, K_0, x_0)C_{12}}{C_3C_{10} - C_5C_{12}}$$

(G.19).

The constants β_ℓ and γ_ℓ are given in terms of α_ℓ , ζ_ℓ and the C 's, see Eqs. (G.13) - (G.16).

APPENDIX H
FLOATING ONE CENTRE
PERTURBATION CALCULATIONS
FOR H_2^+ -LIKE MOLECULES;
COPIES OF REFERENCES
[6] AND [7]

Copies of Refs. [6] and [7] may be found at the end
of this thesis.

APPENDIX I
OPTIMAL HELIUM AND CENTRE OF
NUCLEAR CHARGE CENTRED
PARTIAL WAVE CALCULATIONS FOR
THE $1s\sigma$, $2s\sigma$ and $2p\sigma$ STATES
OF HeH^{++}

While the optimal partial wave floating one centre methods discussed in general in Chapters II and III of this thesis are capable in principle of unifying the centre of nuclear charge one centre methods useful for small R with the long range intermolecular force methods appropriate for large R for all one electron diatomic molecules, in practice these methods are not feasible for intermediate values of R for the exchange dominated ground state of H_2^+ as discussed in Chapter IV and Sec. V-3. The purpose of this appendix is to illustrate the point that the optimal (floating) one centre partial wave method can yield accurate results for the interaction energy for many other molecules, in particular those whose interaction energy contains a substantial coulomb component for intermediate values of R, if the expansion centre is chosen appropriately as a function of R. In general the centre of nuclear charge is not the optimal choice for the expansion centre for most values of R.

In this appendix the $1s\sigma$, $2s\sigma$ and $2p\sigma$ state HeH^{++}

molecules are considered as models. It will be shown for these molecules that (1) the (floating) one centre optimal partial wave method smoothly unifies the non-expanded perturbation theory and the long range expanded R^{-1} theory approaches, which are useful for large R values, with the centre of nuclear charge centred approach suitable for small values of R , (2) the (floating) one centre partial wave technique furnishes a practical method for obtaining accurate and/or adequate results for the interaction energy for all values of R and (3) the (floating) optimal partial wave results for the interaction energy are much superior to the optimal centre of nuclear charge centred results obtained from the work of Rabinovich³ for these states; in general the results of Ref. [3] yield reasonable results for the interaction energy for only small values of R . For the states of HeH^{++} considered here the optimal (floating) partial wave results agree very well with the exact results for the interaction energy obtained by Bates and Carson¹⁰⁹ for common values of R and can be used to extend these results for other values of R in conjunction with the ability of the (floating) partial wave method to smoothly join the long range theory for large values of R . The effectiveness of this approach in obtaining accurate results for the interaction energy, as a function of the number of partial waves included in the calculation, depends of course on the value of R and is a strong function of the nature of the interaction, see Sec. (I.2).

I.1 CALCULATIONS AND RESULTS

The $1s\sigma$, $2s\sigma$ and $2p\sigma$ state HeH^{++} molecules, the systems of interest in this appendix, dissociate to form the products¹⁰⁹ (a) $\text{He}^+(1s) + \text{H}^+$, (b) $\text{He}^+(2s, 2p\sigma) + \text{H}^+$ and (c) $\text{He}^{++} + \text{H}(1s)$, respectively, when R becomes very large. A general discussion of the choice of the expansion centre, as a function of R , for one centre calculations of one electron diatomic molecules is given in Sec. II.3A, see also Secs. IV.1C and V.3C, and it is clear that for the one centre calculation of the above states of the HeH^{++} molecule the most suitable choice for the expansion centre for "large" R is at the He nucleus for the $1s\sigma$ and $2s\sigma$ states and at the proton for the $2p\sigma$ state while for "small" R the most suitable position for the expansion centre is at the centre of nuclear charge. It should be pointed out that the numerical values for which R is considered to be small or large depends markedly on the state of the molecule under consideration, for example see below and compare also with the results for the $1s\sigma_g$ state of H_2^+ given in Sec. IV.1. Using these choices[†] for the expansion

[†] Here the position of the expansion centre has not been energy optimized since the results obtained for the $1s\sigma_g$ state of H_2^+ in Sec. IV.1 indicate that for computational purposes a superposition of methods suitable for small and large R values is more economical than the optimized floating centre techniques; see also the specific results for the $1s\sigma$, $2s\sigma$ and $2p\sigma$ states of HeH^{++} given below.

centre in the one centre partial wave method discussed in Chapter III, interaction energies have been calculated for the $1s\sigma$, $2s\sigma$ and $2p\sigma$ states of the HeH^{++} molecule. The analytical method, see Sec. III.2, is used to perform the helium or proton centred calculations and since the analytical method has not been developed for arbitrary positions of the expansion centre, the numerical method, see Sec. III.3, is used to calculate the energies for the case in which the expansion centre is located at the centre of nuclear charge.

The results for the interaction energies for the $1s\sigma$ and $2s\sigma$ state HeH^{++} molecules, obtained by the analytical and the numerical methods are given, respectively, in Tables I.1 and I.2 as a function of R , the number of coupled differential equations, N , used in the calculation and the position of the expansion centre. The corresponding results for the $2p\sigma$ state of HeH^{++} with the centre of expansion at the proton and at the centre of nuclear charge are given in Tables I.3A and I.3B respectively. The centre of nuclear charge calculations given in all these tables for $N \leq 3$ and $R \leq 4$ are due to Rabinovich³ and have been checked for particular values of R . The exact results, which are available for $R \leq 5$, obtained from Bates and Carson¹⁰⁹ are also included in these tables for comparative purposes.

The number of coupled differential equations required to obtain reasonable results for the interaction energy depends on the choice of the expansion centre, the value

TABLE I.I: A comparison of the helium and centre of nuclear charge centred partial wave interaction energies with the exact values for the $1s\sigma$ state HeH^{++} molecule as a function of R and N . The exact and centre of the nuclear charge centred interaction energies are taken from Refs. [109] and [3] respectively. The helium centred interaction energies have also been calculated for $R = 1$ and 2 with $N = 4$ and are given by the values $0.9747(0)$ and $0.4893(0)$ respectively.

R	E_{int}						
	Helium centred			Centre of. nuclear charge			
	$N = 1$	$N = 2$	$N = 3$	Exact	$N = 1$	$N = 2$	$N = 3$
3	0.2500(0)	0.2495(0)	0.2494(0)	0.2494(0)	0.1271(1)	0.9953(0)	0.7535(0)
2	0.3333(0)	0.3316(0)	0.3313(0)	0.3312(0)	0.1164(1)	0.8978(0)	0.6707(0)
1	0.5008(0)	0.4925(0)	0.4903(0)	0.4878(0)	0.1055(1)	0.8372(0)	0.6523(0)
0.5	0.1048(1)	0.9986(0)	0.9818(0)	0.9667(0)	0.1209(1)	0.1105(1)	0.1002(0)
			0.2348(1)	0.2334(1)	0.2424(1)	0.2391(1)	0.2343(1)

TABLE I.2: A comparison of the helium and centre of nuclear charge centred partial wave interaction energies with the exact values for the 2s state HeH^{++} molecule as a function of R and N . The exact interaction energies are taken from Ref. [109] while the centre of nuclear charge interaction energies for $R \leq 4$ are obtained from Ref. [3].

R	E_{int}			
	Helium centred		Centre of nuclear charge	
	$N = 1$	$N = 2$	$N = 1$	$N = 3$
9	0.1111(0)	0.1275(0)	0.1273(0)	
8	0.1250(0)	0.1454(0)		
7	0.1429(0)	0.1689(0)		0.2170(0)
6	0.1669(0)	0.2012(0)		0.2347(0)
5	0.2013(0)	0.2477(0)	0.2470(0)	0.2469(0)
4	0.2563(0)	0.3203(0)	0.3192(0)	0.3190(0)
3	0.3620(0)	0.4474(0)	0.4455(0)	0.4450(0)
2	0.6248(0)	0.7178(0)	0.7146(0)	0.7129(0)
1	0.1563(1)	0.1600(1)	0.1595(1)	0.1592(1)
0.5			0.3490(1)	0.3488(1)
			0.3499(1)	0.3495(1)
				0.3489(1)

TABLE I. 3A. A comparison of the proton centred partial wave interaction energies for the $2p\sigma$ state HeH^{++} molecule with the exact 109 values as a function of R and N . In addition to the results given in the main table, the proton centred interaction energies have also been calculated with $N = 6$ and 8 for $R = 8$ and the values obtained are $-0.2522(-2)$ and $-0.2715(-2)$ respectively. This table also includes extrapolated partial wave results for E_{int} , see the text for a discussion of the extrapolation technique. For the centre of nuclear charge centred partial wave results for the $2p\sigma$ state of HeH^{++} see Table I.3B.

		$-E_{\text{int}}$					
		Partial wave calculations					
R		N = 3	N = 5	N = 7	N = 9	N = 11	Exact
8			0.2062(-2)	0.2646(-2)	0.2763(-2)		0.2873(-2)
7			0.3410(-2)	0.4633(-2)	0.5031(-2)	0.5279(-2)	0.5689(-2)
6			0.5218(-2)	0.8154(-2)	0.9348(-2)	0.1009(-1)	0.1111(-1)
5			0.6172(-2)	0.1296(-1)	0.1596(-1)	0.1775(-1)	0.2040(-1)
4	-0.6994(-1)		-0.5480(-3)	0.1360(-1)	0.1989(-1)	0.2340(-1)	0.2783(-1)
3	-0.1334(0)		-0.4185(-1)	-0.1573(-1)	-0.4422(-2)		0.4211(-2)
2	-0.3496(0)			-0.1006(0)			-0.1548(0)
1			-0.1194(1)				-0.1162(1)
0.5			-0.3305(1)				-0.3302(1)

TABLE I.3B: A comparison of the centre of nuclear charge centred partial wave interaction energies with the exact values¹⁰⁹ for the $2p\sigma$ state HeH^{++} molecule as a function of R and N . The results for $N = 3$ have been obtained from Ref. [3] which also gives results yielding the interaction energies 0.3306(1), 0.1203(1), 0.2757(0), 0.1269(0) and 0.1150(0) for $R = 0.5, 1, 2, 3$ and 4 respectively for $N = 2$. In addition to the data given in the main table, the centre of nuclear charge centred interaction energy for $R = 1$ with $N = 6$ has also been calculated and is given by 0.1165(1). This table also includes extrapolated partial wave results for E_{int} , see the text for a discussion of the extrapolation technique. For the helium centred partial wave results for the $2p\sigma$ state of HeH^{++} see Table I.3A.

R	Partial wave calculations					Exact
	N = 3	N = 5	N = 7	N = 9	N = 11	
4	0.9860(-1)					-0.3108(-1)
3	0.1076(0)	0.2866(-1)	0.5831(-2)	-0.2792(-2)	-0.6701(-2)	-0.1216(-1)
2	0.2562(0)	0.1814(0)	0.1651(0)	0.1598(0)		0.1548(0)
1	0.1196(1)	0.1167(1)	0.1164(1)			0.1162(1)
0.5	0.3305(1)					0.3302(1)

of R and the state of the molecule. The partial wave calculations reported here were initiated by making a few preliminary low order calculations for the $1s\sigma$, $2s\sigma$ and $2p\sigma$ state HeH^{++} molecules. These initial results indicated, particularly for the $2p\sigma$ state, that low order partial wave results would yield inadequate results for the interaction energy for certain values of R and choices of expansion centre. Consequently some low order partial wave calculations were not performed giving rise to most of the "missing" entries in Tables I.1 - I.3. It should be noted that the interaction energy obtained for the $2s\sigma$ state of HeH^{++} by using $N = 1$ in the helium centred calculation is lower than the exact values¹⁰⁹, see Table I.2. This however does not violate the Hylleraas-Undheim variational theorems^{3, 110} since, for $N = 1$, only one function is used in the calculation for the $2s\sigma$ state which is not the lowest state of its symmetry.

The results for the interaction energy for the $1s\sigma$ and $2s\sigma$ states of HeH^{++} , obtained with the most suitable choice of the expansion centre for a given value of R , converge quite rapidly as a function of N . However for $3 \lesssim R \lesssim 6$ the rate of convergence of the calculated partial wave results for the $2p\sigma$ state is relatively slow. Hence in order to obtain better approximations to the interaction energy using the calculated partial wave values for this state use is made of an extrapolation technique¹¹¹ which is often employed in approximating the limit of slowly convergent sequences. In

this extrapolation technique if S_{n-1} , S_n and S_{n+1} are a sequence of three successive approximations then the extrapolated value S is given by¹¹¹

$$S \sim \frac{S_{n-1} S_{n+1} - S_n^2}{S_{n-1} + S_{n+1} - 2S_n} \quad (I.1)$$

The results for the extrapolated values of the interaction energy for the $2p\sigma$ state are included in Tables I.3A and I.3B. For any given R these extrapolated results are obtained by using the energy values corresponding to the last three N values given in Tables I.3A and I.3B. In order to illustrate the usefulness of the extrapolation technique we consider, as an example, the results obtained with $N = 5, 7$ and 9 for $R = 5$ in the proton centred calculations, see Table I.3A. By using the extrapolation technique for these N values we obtain the result $E_{int} = -0.1834(-1)$ which is lower than the value $-0.1775(-1)$ obtained with $N = 11$ but not lower than the exact value $-0.2255(-1)$ of Bates and Carson¹⁰⁹. It is important to notice that the extrapolated results are not lower than the exact values even if the last member in the sequence of approximations used in the extrapolation technique

is very close to the exact value. For example[†] at $R = 1$ and $R = 2$ the centre of nuclear charge centred results obtained with $N = 5, 6$ and 7 and $5, 7$ and 9 , respectively, yield extrapolated results which are very close to but above the exact values obtained by Bates and Carson¹⁰⁹, see Table I.3B. In general it appears that the extrapolated results based on S_{n-1} , S_n and S_{n+1} are comparable to or better than those that would be obtained from the approximation S_{n+2} for the partial wave results of this work.

Since one of the purposes of this appendix is to compare the exact partial wave results of this work with previous perturbation theory results for the interaction energies of the $1s\sigma$, $2s\sigma$ and $2p\sigma$ states of HeH^{++} , the partial wave and the exact interaction energies for the $1s\sigma$ and $2p\sigma$ state molecules of Tables I.1 and I.3 have been augmented by the relevant perturbation results in Tables I.4 and I.5 respectively. The perturbation theory calculations for the $2s\sigma$ state have not been performed previously and will be

[†] Another nice example of the usefulness of the extrapolation technique is given by the results for $R = 1$ for the $1s\sigma$ state HeH^{++} molecule. The helium centred results for the interaction energy for this R value with $N = 2, 3$ and 4 yield the extrapolated result $0.9695(0)$ which provides a better approximation for the exact interaction energy than the explicit $N = 4$ result, see Table I.1.

TABLE I.4: A comparison, for the lso state HeH^{++} molecule, of the partial wave interaction energies with the exact values¹⁰⁵ and with the non-expanded perturbation theory and expanded long range R^{-1} perturbation theory results as a function of R . The non-expanded perturbation theory results through second order, $E_{\text{int}}^{\text{Coul}}(2)$, are taken from Ref. [112] while the long range R^{-1} results through n th order $E_{R^{-1}}(n)$, for $n = 2, 3$ and 5 , are taken from Ref. [59]. The partial wave results given in this table are the lowest partial wave values for the interaction energies given in Table I.1 for given R values.

R	Nonexpanded perturbation theory through second order	E_{int}				Exact
		Long range R^{-1} theory through			partial wave calculations	
		second order	third order	fifth order		
4	0.2494(0)	0.2494(0)	0.2494(0)	0.2494(0)	0.2494(0)	0.2494(0)
3	0.3314(0)	0.3314(0)	0.3312(0)	0.3312(0)	0.3313(0)	0.3312(0)
2	0.4911(0)	0.4889(0)	0.4881(0)	0.4880(0)	0.4893(0)	0.4878(0)
1	0.9847(0)	0.8006(0)	0.6968(0)	0.6697(0)	0.9747(0)	0.9667(0)

TABLE I.5: A comparison, for the $2p\sigma$ state HeH^{++} molecule, of the partial wave interaction energies with the exact values¹⁰⁹ and with the non-expanded perturbation theory and expanded long range R^{-1} theory results as a function of R . The non-expanded perturbation theory results through second order are taken from Ref. [112] while the expanded long range R^{-1} results through second, third and fifth order are essentially taken from Ref. [59]. The non-expanded perturbation theory results for the third-order energy are obtained by using $\text{H}_2^+(1s\sigma_g)$ third order energies^{14b}, see the discussion in the main text. The partial wave results are the lowest extrapolated partial wave values for the interaction energies for this state of HeH^{++} given in Tables I.3A and I.3B for given R values.

-E_{int}

R	Nonexpanded perturbation theory through			Long range R^{-1} theory through			Partial wave calculations	Exact
	second order	third order	fourth order	second order	third order	fifth order		
8	0.2331(-2)	0.2619(-2)		0.2329(-2)	0.2595(-2)	0.2622(-2)	0.2873(-2)	
7	0.4055(-2)	0.4855(-2)		0.4056(-2)	0.4792(-2)	0.4870(-2)	0.5689(-2)	
6	0.7702(-2)	0.1020(-1)		0.7779(-2)	0.1024(-1)	0.1050(-1)	0.1131(-1)	
5	0.1626(-1)	0.2470(-1)		0.1721(-1)	0.2803(-1)	0.2917(-1)	0.2040(-1)	0.2255(-1)
4	0.3826(-1)	0.6714(-1)		0.4448(-1)	0.5748(-1)	0.6426(-1)	0.2783(-1)	0.3108(-1)
3	0.9613(-1)	0.1247(0)		0.1723(0)	0.2697(0)	0.3374(0)	0.9943(-2)	0.1216(-1)
2	0.2261(0)	0.4120(0)		0.5625(0)	0.5625(0)	0.5625(0)	-0.1583(0)	-0.1548(0)
1	0.2559(0)	0.3038(0)		0.9000(1)	0.9000(1)	0.9000(1)	-0.1163(1)	-0.1162(1)

partially discussed later in this appendix. The perturbation theory results given in Tables I.4 and I.5 have been obtained by decomposing the Hamiltonian H as, see also Sec. V.1B,

$$H = H_0 + V_e \quad (I.2),$$

where

$$H_0 = -\frac{\nabla^2}{2} - \frac{Z_A}{r_A} \quad (I.3),$$

and

$$V_e = \frac{Z_A Z_B}{R} - \frac{Z_B}{r_B} \quad (I.4).$$

The symbols occurring in Eqs. (I.3) and (I.4) have been defined previously in Chapter II, and here the coordinate origin is chosen at the nucleus A. Choosing the unperturbed wave function and energy, respectively, as

$$\psi(0) = \left(\frac{Z_A^3}{\pi}\right)^{1/2} e^{-Z_A r_A} \quad (I.5)$$

and

$$E(0) = -\frac{Z_A^2}{2n^2} \quad (I.6)$$

the results corresponding to the $1s\sigma$ state are obtained by using^{59,112} $Z_A = 2$ and $Z_B = 1$ while the results for the $2p\sigma$ state are obtained by setting^{59,112} $Z_A = 1$ and $Z_B = 2$. The

perturbation theory results for the interaction energy obtained by this treatment through n -th order in V_e has the form

$$E_{\text{int}}^{\text{coul}}(n) = E_{\text{coul}}^{(1)} + E_{\text{coul}}^{(2)} + \dots + E_{\text{coul}}^{(n)} \quad (\text{I.7})$$

where $E_{\text{coul}}^{(n)}$ is the n -th order perturbation energy corresponding to Eqs. (I.2) - (I.6). Since the wave function in this perturbation treatment corresponds to the electron being localized about the nucleus A, Eq. (I.7) can be taken to be an approximation to the coulomb interaction energy for the $1s\sigma$ and $2p\sigma$ states of HeH^{++} . These perturbation theory results include charge overlap effects between the species forming the HeH^{++} molecule. Results for $E_{\text{int}}^{\text{coul}}(n)$ through second order in V_e for the $1s\sigma$ state have been obtained by Dalgarno and Lynn¹¹², see also Refs. [6,33], and are given in Table I.4. The corresponding results through third order for the $2p\sigma$ state are given in Table I.5. Here the results for $E_{\text{coul}}^{(1)}$ and $E_{\text{coul}}^{(2)}$ are obtained from Dalgarno and Lynn¹¹² while those for $E_{\text{coul}}^{(3)}$ can be obtained by scaling the third order coulomb energy for the $1s\sigma$ H_2^+ molecule given by Singh, Kreek and Meath^{14(b)}, see also Chapter V; the scaling relation is given by

$$E_{\text{HeH}^{++}}^{(3)} = Z_B^3 E_{\text{H}_2^+}^{(3)} \quad (\text{I.8})$$

The interaction energies represented by Eq. (I.7) are often called non-expanded^{13,14,18,20,21} interaction energies since

the interaction perturbation V_e , see Eq. (I.4), has not been expanded in its R^{-1} multipolar expansion in the derivation of these results.

If we now neglect charge overlap effects^{10,13,14,18,20} between the nuclei of the HeH^{++} molecule, that is take $r_A < R$, the perturbation V_e occurring in Eq. (I.4) can be expanded in the multipole R^{-1} long range expansion⁹⁻¹¹. Substitution of this expansion for V_e into Eqs. (I.2) - (I.7) yields the usual R^{-1} expanded interaction energies for the $1s\sigma$ and $2p\sigma$ states. The R^{-1} expanded interaction energies, through n -th order in V_e , will be designated by

$$E_{R^{-1}}^{(n)} = E_{R^{-1}}^{(1)} + E_{R^{-1}}^{(2)} + \dots + E_{R^{-1}}^{(n)} \quad (\text{I.9})$$

where $E_{R^{-1}}^{(n)}$ is the long range R^{-1} theory equivalent of $E_{\text{coul}}^{(n)}$. Explicit formulae for the various terms in Eq. (I.9) have been given by Dalgarno and Stewart⁵⁹ for the $1s\sigma$ and $2p\sigma$ states of HeH^{++} through $n = 5$ and $O(R^{-11})$. For example, in atomic units

$$E_{R^{-1}}^{(1)} = Z_B (Z_A - 1)/R \quad (\text{I.10})$$

and

$$E_{R^{-1}}^{(2)} = -\frac{Z_B^2}{2Z_A^3} \left(\frac{9}{2R^4} + \frac{15}{Z_A^2 R^6} + \frac{525}{4Z_A^4 R^8} + \frac{8505}{4Z_A^6 R^{10}} + O(R^{-12}) \right) \quad (\text{I.11})$$

The long range results for the $1s\sigma$ state are obtained from these expressions by setting $Z_A = 2$ and $Z_B = 1$ and here

$E_{R^{-1}}^{(1)}$ corresponds to the R^{-1} charge-charge interaction between the two positively charged species H^+ and $He^+(1s)$ and $E_{R^{-1}}^{(2)}$ is made up of terms arising from the induction of multipole moments in $He^+(1s)$ by the proton. The results for the $2p\sigma$ state are obtained by setting $Z_A = .1$ and $Z_B = 2$ and here $E_{R^{-1}}^{(1)} = 0$ and the second order energy is again made up of a series of expanded induction energies beginning with the R^{-4} charge induced dipole energy. Numerical results for $E_{R^{-1}}(n)$, through $n = 2, 3$ and 5 have been taken from Dalgarno and Stewart⁵⁹, or have been obtained using their R^{-1} results, for the $1s$ and $2p\sigma$ states of HeH^{++} and are given in Tables I.4 and I.5 respectively. It is important to note that these R^{-1} expansions are asymptotic^{12,14,16-18} in the variable R^{-1} and the results given in Ref. [59] and Tables I.4 and I.5 have been obtained^{17,59} by truncating the series as a function of R , in each order of perturbation, at the term before the smallest term and adding $\frac{1}{2}$ of the smallest term to the sum of the truncated series. The perturbation R^{-1} energy series, see Eq. (I.9) is truncated at the smallest term in this energy series⁵⁹ For sufficiently small R the smallest term in the R^{-1} interaction energy series for the $2p\sigma$ state of HeH^{++} is the R^{-4} charge induced dipole interaction energy and for these values of R the complete R^{-4} term is used to obtain the R^{-1} representation of the interaction energy given in Table I.5.

I.2 DISCUSSION

Here the optimal helium and centre of nuclear charge centred partial wave, the exact, and the various perturbation theory results for the interaction energies for the $1s\sigma$, $2s\sigma$ and $2p\sigma$ state HeH^{++} molecules will be used as models to illustrate the importance of the (floating) one centre partial wave method with respect to evaluating accurate results for molecular interaction energies.

$\text{HeH}^{++}(1s\sigma)$: A comparison of the helium and centre of nuclear charge centred partial wave results for the interaction energy for the $1s\sigma$ state, see Table I.1, shows that except for very small $R \lesssim 0.5$, the centre of nuclear charge is not the most appropriate choice for the expansion centre for the partial wave method. The centre of nuclear charge results for the interaction energy obtained from Ref. [3] are very poor representations of the exact values except for small $R \lesssim 1$ and become progressively worse as R increases. On the other hand the helium centred partial wave results for the interaction energy are in very good agreement with the exact results of Bates and Carson¹⁰⁹ for all values of R quoted in Table I.1. It is important to realize, see Ref. [6], that since the $\text{HeH}^{++}(1s\sigma)$ state dissociates to yield a tightly bound $\text{He}^+(1s)$ ion and a proton the long range interaction energy is dominated by the charge-charge term given by R^{-1} . The results of Table I.1 show that the exact interaction energy at $R = 4$ is given by R^{-1} for all practical purposes

and this fact can be used to extend the exact results for E_{int} of Table I.4 to all values of $R > 4$.

The comparison of the best optimal partial wave results with the non-expanded and R^{-1} expanded perturbation theory interaction energies for the $1s\sigma$ state given in Table I.4 shows that while the non-expanded perturbation theory results give an adequate representation of E_{int} for all R they are not as accurate as the partial wave results for small $R = 1$ and 2. Thus since the low order partial wave calculations are no more difficult to carry out than the exact solution of the non-expanded perturbation theory problem through second order, see Ref. [6], this furnishes a nice example of the practical usefulness of the partial wave method. Table I.4 also shows that while the R^{-1} expanded perturbation theory energies give very good representations of E_{int} for "large" $R \geq 2$, they do misbehave for small $R < 2$. This is a consequence of the asymptotic^{12,14,16-18} nature of the R^{-1} results for the second and higher order expanded interaction energies, which are negative in sign, and it can be seen from the data for $R = 1$ in Table I.4 that retaining higher order perturbation results in the R^{-1} calculations yields poorer results for the interaction energy even though these terms should be retained in the R^{-1} representation of the interaction energy on the basis of the usual truncation method^{17,59} used for such asymptotic series, see the discussion at the end of Sec. I.1. The R^{-1} expanded results, which are relatively easy to obtain computationally, are very useful in obtaining adequate representations of E_{int} for most values

of R for the $1s\sigma$ state of HeH^{++} . This is often not the case and arises for this state of the HeH^{++} molecule because of the dominance of the interaction energy by the R^{-1} charge-charge term for most values of R; compare for example with the $2p\sigma$ state HeH^{++} molecule below and see also Refs. [6,13,14,18,20].

$\text{HeH}^{++}(2s\sigma)$: A comparison of the helium and centre of nuclear charge centred results for the $2s\sigma$ state HeH^{++} , see Table I.2, leads to conclusions similar to those arrived at in the discussion of the results for the $1s\sigma$ state of HeH^{++} . In the case of $2s\sigma$ state HeH^{++} , however, the misbehaviour of the centre of nuclear charge centred results does not become very serious until R becomes fairly large $R \gtrsim 4$. This can be understood from the long range properties of this molecule. The $\text{HeH}^{++}(2s\sigma)$ molecule dissociates to form a bound $\text{He}^+(2s,2p)$ ion and a proton. Since the electron in the $\text{He}^+(2s,2p)$ ion is more loosely bound than in the $\text{He}^+(1s)$ ion charge overlap effects are more pronounced in the $2s\sigma$ state than in the $1s\sigma$ state for a given value of R and therefore the charge distribution is more evenly shared between the He and H nuclei for given values of R in the $2s\sigma$ state than in the $1s\sigma$ state. However it is clear from Table I.2 that as R becomes progressively larger the centre of nuclear charge centred results become progressively worse. On the other hand the low order helium centred partial wave results are in excellent agreement with the exact results of Bates and Carson¹⁰⁹ for all common values of $R \leq 5$ and for $R > 5$

the helium centred results obtained from just 2 coupled differential equations can be taken as accurate values of the interaction energy and therefore used to extend the results of Bates and Carson¹⁰⁹ to these values of R .

The long range R^{-1} results for the $\text{HeH}^{++}(2s\sigma)$ molecule have not been discussed previously. However since this molecule dissociates to form a $\text{He}^+(2s,2p)$ ion the proper zeroth order wave function for a perturbation calculation of the interaction energy for large values of R must be constructed from a $(2s,2p)$ resonance^{11,15} hybrid, $\psi^{(0)} \sim (2s+2p\sigma)$, where here $2s$ and $2p\sigma$ represent $2s$ and $2p\sigma$ He^+ orbitals. This treatment is analogous to that used in the discussion of the interaction between $\text{H}(2s,2p)$ and a proton, see Refs. [11,15,113]. It is easy to show that the first order R^{-1} expanded interaction energy for the $2s\sigma$ state of HeH^{++} is given by

$$E_{R^{-1}}(1) = \frac{1}{R} + \frac{3}{2R^2} - \frac{6}{4R^3} + O\left(\frac{1}{R^4}\right) \quad (\text{I.12})$$

where the terms $\frac{1}{R}$, $\frac{3}{2R^2}$ and $\frac{6}{4R^3}$ are, respectively, due to charge-charge, charge-resonance dipole and charge-resonance quadrupole interactions between the positively charged proton and the positively charged $\text{He}^+(2s,2p)$ ion. The second order energy begins^{15,113} with an R^{-4} term which will be discussed briefly in what follows. Evaluating $E_{R^{-1}}(1)$ given by Eq. (I.12) for $R = 2(1)9$ yields for the interaction energy the values 0.6875(0), 0.4444(0), 0.3203(0), 0.2480(0), 0.2014(0), 0.1691(0), 0.1455(0) and 0.1276(0), respectively, in excellent agreement with the corresponding optimal partial

wave helium centred results given in Table I.2. Thus

Eq. (I.12) can be used to extend the accurate helium centred partial wave results of Table I.2 to all values of $R > 9$. It is important to emphasize that although

Eq. (I.12) yields results in good agreement with the optimal helium centred partial wave results for small R considerably less than $R = 9$, the validity of the R^{-1} expansion of E_{int} for these values of R is in serious question. For example, using the $H(2s,2p)-H^+$ long range results of Ref. [113a], it can be shown that the lead charge-induced dipole second order long range energy is of the order of $(\frac{-84}{16}) R^{-4} \sim -5 R^{-4}$ and for example when $R = 2(1)4$ this lead term has the values $-0.31, -0.06$ or -0.02 respectively. All the other R^{-1} long range second and higher order energies are also negative and together with the lead R^{-4} results will, when added to the results obtained from Eq. (I.12), yield results for "small" R that will be considerably lower than the correct values even though these second and higher order R^{-1} results should be retained in the R^{-1} representation of E_{int} on the basis of the usual truncation scheme^{17,59} for summing asymptotic series; see the corresponding discussions for the $\text{HeH}^{++}(1s\sigma)$ results given above.

It is interesting to note that as in the case of $\text{HeH}^{++}(1s\sigma)$ molecule there is a strong charge-charge interaction energy, varying as R^{-1} , contributing to the interaction energy of the $\text{HeH}^{++}(2s\sigma)$ molecule. However for the $2s\sigma$ state of HeH^{++} this charge-charge term is not the dominant term in the expression

for the interaction energy for many of the R values given in Table I.2 because of the R^{-2} energy arising in Eq. (I.12) due to the resonance hybrid effects discussed above, compare Eq. (I.10) for $Z_A = 2$ and $Z_B = 1$ with Eq. (I.12). For example at $R = 4$, the R^{-1} term for the $1s\sigma$ and $2s\sigma$ states of HeH^{++} contribute 100% and 78%, respectively, of the exact interaction energy. As in the case of the $\text{HeH}^{++}(1s\sigma)$ molecule the R^{-1} expanded results for the interaction energy will be very useful in obtaining adequate representations of E_{int} for $\text{HeH}^{++}(2s\sigma)$ for many values of R . For both of these molecules this situation arises because of the strong first order energies occurring in the R^{-1} expansion of E_{int} and is due in part to the fact that R^{-1} expanded first order interaction energies, which are due to the interaction of "permanent" multipole moments, are usually not affected by charge overlap effects to the same extent as second and higher order R^{-1} energies are, see the above discussions relating to the charge-charge energy and Refs. [113(a), 114, 115]. Since the full R^{-1} treatment for the interaction energy for the $\text{HeH}^{++}(2s\sigma)$ molecule is not available a complete assesment of the asymptotic nature of these results, which depend on charge overlap effects, can not be given here as in the discussion of the $1s\sigma$ state of HeH^{++} .

$\text{HeH}^{++}(2p\sigma)$: A comparison of the optimal proton centred partial wave interaction energies, see Table I.3A, with the optimal centre of nuclear charge results, see Table I.3B, for this state of HeH^{++} shows that the most suitable choice of the

expansion centre for $R \lesssim 3$ is at the centre of nuclear charge while for $R > 3$ it is at the proton. The very low order centre of nuclear charge results obtained from Ref. [3], $R \leq 4$ and $N \leq 3$ in Table I.3B, are very poor representations of the exact interaction energies of Bates and Carson¹⁰⁹ for $R > 1$ and indicate a repulsive state instead of a bound state for the $\text{HeH}^{++}(2p\sigma)$ molecule. Extending these centre of nuclear charge results to higher partial wave order yields adequate results for E_{int} for $R \lesssim 3$ if N is chosen to be sufficiently large as a function of R . For example at $R = 3$, the interaction energies corresponding to $N = 3, 9$ and 11 are, respectively, -88% , 23% and 55% of the exact result while the extrapolated partial wave result, which probably corresponds to $N \sim 14$, is 82% of the exact value. The convergence of the centre of nuclear charge centred calculations improves as R decreases, for example for $R = 2$, the values of E_{int} corresponding to $N = 3, 5$ and 9 are, respectively, about 166% , 122% and 103% of the exact value while the extrapolated partial wave result, which probably corresponds to $N \sim 11$ is about 102% of the exact value. The optimal proton centred partial wave calculations, see Table I.3A, yield adequate representations for E_{int} for $R \geq 4$ if N is taken sufficiently large and as R increases fewer partial wave terms are needed to obtain accurate results for the interaction energy. For example for $N = 5, 7, 9$ and 11 , the proton centred results provide about -2% , 44% , 64% and 75% , respectively, of the exact value of Bates and Carson¹⁰⁹ when $R = 4$ while at $R = 5$ using these N values yields about 27% , 57% , 71% and

79% of the exact result for E_{int} . The extrapolated partial wave results, which correspond to $N \sim 13$, for $R = 4$ and 5 yield about 90% and 91%, respectively, of the exact interaction energies. Hence it would appear that the extrapolated proton centred partial wave results for $R = 6, 7$ and 8 should correspond to about 92%, 94% and 96% of the exact values of E_{int} and therefore these proton centred partial wave results can be used in conjunction with the long range perturbation theory results, see what follows for details, to augment the precise results for E_{int} of Bates and Carson¹⁰⁹ to values of $R > 5$ in a reasonably reliable way.

The comparison of the best (extrapolated) optimal partial wave results with the non-expanded and the R^{-1} expanded perturbation interaction energies for the $2p\sigma$ state given in Table I.5 shows that the perturbation theory results are not a very reliable representation of E_{int} for most of the values of R considered in this table. This is very clear for $R \leq 5$ where all the perturbation theory results are either considerably below the exact results of Bates and Carson¹⁰⁹ or in the case of the non-expanded and the expanded perturbation results through second order at $R = 5$ considerably above the exact values; the partial wave results are always above and agree reasonably well with E_{int} (exact). The perturbation theory results are all higher than the optimal partial wave results for $R > 6$ and it is not until $R > 8$ that the R^{-1} results

accurately represent[†] the partial wave results, to within ~ 6% say. It is however clear that the long range R^{-1} results will, for most practical purposes, match with the partial wave results for $R \gtrsim 9$ and consequently the combination of the partial wave and perturbation theory approaches provides an economical way to extend the results of Bates and Carson¹⁰⁹ and therefore to treat the system of interest for all R . It is clear that the difficulty of the fixed centre of nuclear charge optimal partial wave calculations with respect to obtaining reasonable values for E_{int} for all but small values of R and the difficulty of the long range perturbation calculations with respect to obtaining reasonable values for E_{int} for all but large values of R can be eliminated in a reasonably practical way by the (floating) one centre partial wave approach by superimposing optimal helium and centre of nuclear charge partial wave results.

A comparison of the results for the $1s\sigma$, $2s\sigma$ and $2p\sigma$ states of HeH^{++} shows that it is relatively harder to treat

[†]The close agreement between the R^{-1} expanded result through third or fifth order and the partial wave result at $R = 6$, see Table I.5, is fortuitious since at this value of R the R^{-1} expanded results switch from being above the exact results to being lower than the exact values.

the $2p\sigma$ state of HeH^{++} than the $1s\sigma$ and $2s\sigma$ states of HeH^{++} by the optimal one centre partial wave method. This is not hard to understand using notions from the theory of intermolecular forces. The interaction energy for the $1s\sigma$ and $2s\sigma$ states are essentially dominated for most R values by first order coulomb interaction energies, and their charge overlap and electron exchange corrections for smaller R values, and these are relatively easy to evaluate by using low order partial wave calculations. On the other hand the first order energy vanishes for the $2p\sigma$ state of HeH^{++} for large R and for all except small R the dominant contribution to E_{int} comes from second and higher order induction energies and their charge overlap and exchange correction terms. The partial wave calculations of these high order energies require substantially more partial wave components to be included in the one centre calculations than in the case of the strong first order energies characterizing the $1s\sigma$ and $2s\sigma$ states.

It is interesting to compare the optimal partial wave one centre calculations of the $2p\sigma$ state of HeH^{++} with the corresponding calculations of the $1s\sigma_g$ state of H_2^+ . From an intermolecular force point of view $\text{HeH}^{++}(2p\sigma)$ is the heteronuclear analogue of $\text{H}_2^+(1s\sigma_g)$ since in both cases the long range forces are due to the induction of multipole moments in $\text{H}(1s)$ by a positive charge, He^{++} in the case of $\text{HeH}^{++}(2p\sigma)$ and H^+ in the case of $\text{H}_2^+(1s\sigma_g)$. The induction energies in HeH^{++} are of course much stronger than for H_2^+ because of the factor of two difference in the charge inducing

the permanent moments in $H(1s)$ and hence $HeH^{++}(2p\sigma)$ is a coulomb dominated molecule relative to $H_2^+(1s\sigma_g)$. Thus while (floating) partial wave one centre results corresponding to about 14 (usually much less than 14) partial wave terms in the wave function are capable of yielding at least 90% of the interaction energy of $HeH^{++}(2p\sigma)$ for all values of R , the same type of calculations fail to represent E_{int} well for the $H_2^+(1s\sigma_g)$ molecule for many important intermediate values of R , see Chapters IV and V for details. The reason for the difficulty in the case of $H_2^+(1s\sigma_g)$ relative to $HeH^{++}(2p\sigma)$ is due to the symmetry dilemma between the $1s\sigma_g$ and the $2p\sigma_u$ states of the homonuclear molecule for the proton centred partial wave calculations, see Chapter V; the heteronuclear molecule has no such symmetry difficulty. This suggests that except for centre of nuclear charge centred partial wave calculations carried out to very low order^{2(b)}, which are usually useful only for very small R values, heteronuclear molecules will in general be easier to treat using partial wave theory methods than homonuclear molecules. It should also be pointed out that while the proton centred partial wave results for E_{int} are clearly superior and more reliable than the long range R^{-1} values for the interaction energy for $HeH^{++}(2p\sigma)$, this is not so easy to demonstrate, with respect to obtaining accurate results for the total interaction energy, for $H_2^+(1s\sigma_g)$ since for this molecule strong negative electron exchange energies tend to mask the convergence problems associated with the negative R^{-1} long range results for E_{int} , the charge overlap corrections to these R^{-1} results are positive.

I.3 GENERAL COMMENTS

Based on the optimal one centre partial wave calculations for the $1s\sigma_g$ state of H_2^+ and the $1s\sigma$, $2s\sigma$ and $2p\sigma$ states of HeH^{++} the following "general" remarks can be made about the utility of the one centre methods discussed in this work with respect to evaluating the interaction energy as a function of R for one electron diatomic molecules:

- (1) The floating one centre partial wave method can, in principle and in practice, unify previous techniques that were generally suitable only for large and small values of R .
 - (2) The centre of nuclear charge is not the most suitable choice for the expansion centre for most values of R .
 - (3) The (floating) one centre technique can provide a practical method for obtaining adequate and/or accurate results for the interaction energy for all values of R . The effectiveness of the approach depends on the value of R and is a function of the nature of the state of the molecule under consideration. In general the method can be very effective for evaluating interaction energies for coulomb dominated systems.
-
- Often heteronuclear H_2^+ -like molecules will be easier to treat by floating partial wave methods than homonuclear H_2^+ -like molecules.
- (4) The floating one centre method yields results for E_{int} that are in general much more reliable than those obtained by either non-expanded or R^{-1} expanded

perturbation theory methods. The partial wave results yield a controlled upper bound for E_{int} .

- (5) The combination of the optimal floating partial wave method with the long range R^{-1} approach for evaluating interaction energies can yield an approach for obtaining good values of the interaction energy, in a relatively economical manner, for most values of R .
- (6) The non-expanded perturbation theory approach for evaluating interaction energies is very tedious to carry out past second (or possibly third) order in the energy. The partial wave method avoids the ordering of the energy in powers of V_e and contains contributions from all orders of the perturbation V_e consistent with the partial wave wave-function employed in the calculation. Thus the partial wave approach is much more useful than the non-expanded perturbation method for intermediate and for relatively small values of R where the higher order terms in V_e can become very important.

As has been discussed earlier, see Chapters I and VI, the one centre partial wave method is not useful in obtaining reasonable interaction energies for multielectron diatomic molecules for intermediate and large values of R . The extension of this approach to a two-floating centre partial wave method has been discussed briefly in Chapter VI, see also Ref. [8]. The use of variational procedures to solve the two floating centre partial wave differential equations may provide a useful method for evaluating reliable interaction

energies in a unified way for all values of R , particularly for coulomb dominated heteronuclear and homonuclear multi-electron diatomic molecules. The experience gained in the study of the optimal floating one centre partial wave treatment of one electron diatomic molecules should be helpful as a guide in carrying out the analogous multielectron calculations. Hopefully the semi-analytical results for the optimum partial wave orbitals given in Chapter III will be useful in selecting efficient basis functions for the two centre partial wave variational calculations, see Chapter VI.

REFERENCES

- 1(a) D.M. Bishop, Advances in Quantum Chemistry, Vol. 3, P.O. Löwdin, Ed. (Academic Press, New York, 1967).
- (b) E.F. Hayes and R.G. Parr, Supplement of the Prog. of Theoret. Phys., 40, 78 (1967).
- 2(a) K.M. Howell and H. Shull, J. Chem. Phys., 30, 627 (1959).
- (b) A. Temkin, J. Chem. Phys., 39, 161 (1963).
- (c) Z. Dvoracek and Z. Horak, J. Chem. Phys., 43, 874 (1965).
3. H. Rabinovich, J. Chem. Phys., 43, 3144 (1965).
4. A.K. Bhatia and A. Temkin, J. Chem. Phys., 44, 3656 (1966).
- 5(a) W.C. Mackrödt, J. Chem. Phys., 54, 2952 (1971).
- (b) P. Hauk, H. Kim, R.G. Parr and H.F. Hameka, J. Chem. Phys., 47, 2677 (1967) (For more numerical data see Document No. 9506, ADI Auxiliary Publications Project, Photoduplication Service, Library of Congress, Washington, D.C.).
- (c) I.N. Levine, J. Chem. Phys., 41, 2044 (1964).
6. M.K. Ali and W.J. Meath, Int. J. Quant. Chem., 6, 949 (1972).

7. M.K. Ali and W.J. Meath, Int. J. Quant. Chem., 7, 119 (1974).
8. Y.H. Pan, Ph.D. Thesis, The University of Western Ontario, 1973.
9. H. Margenau, Rev. Mod. Phys., 11, 1 (1939).
10. H. Margenau and N. Kestner, Theory of Intermolecular Forces (Pergamon Press, Oxford, 1969).
11. J.O. Hirschfelder and W.J. Meath, Adv. Chem. Phys., 12, 3 (1967).
- 12(a) L.C. Cusachs, Phys. Rev., 125, 561 (1962).
(b) L.C. Cusachs, J. Chem. Phys., 38, 2038 (1963).
13. J.N. Murrell and G. Shaw, J. Chem. Phys., 49, 4731 (1968).
- 14(a) H. Kreek and W.J. Meath, J. Chem. Phys., 50, 2289 (1969).
(b) T.R. Singh, H. Kreek and W.J. Meath, J. Chem. Phys., 52, 5565 (1970).
15. J.O. Hirschfelder, C.F. Curtiss and R.B. Bird, Molecular Theory of Gases and Liquids (Wiley, New York, 1964).
16. F.C. Brooks, Phys. Rev., 86, 92 (1952).
17. A. Dalgarno and J.T. Lewis, Proc. Phys. Soc., A69, 57 (1956).

- 18(a) H. Kreek, Y.H. Pan and W.J. Meath, *Molec. Phys.*, 19, 513 (1970).
- (b) Y.H. Pan and W.J. Meath, *Molec. Phys.*, 20, 873 (1971).
19. R.J. Buehler and J.O. Hirschfelder, *Phys. Rev.*, 83, 628 (1951); 85, 149 (1952).
20. W. Kolos, Technical Report No. 356, Quantum Chemistry Project, University of Florida, (1974).
21. J.S. Dahler and J.O. Hirschfelder, *J. Chem. Phys.*, 25, 986 (1956).
- 22(a) C.A. Coulson, *Valence* (Oxford Univ. Press, 1961).
- (b) H. Eyring, J. Walter and G.E. Kimball, *Quantum Chemistry* (Wiley, New York, 1963).
- 23(a) R.S. Mulliken, *J. Phys. Chem.*, 56, 295 (1952).
- (b) F.O. Ellison, *J. Chem. Phys.*, 34, 2100 (1961).
- (c) S. Fraga and R.S. Mulliken, *Rev. Mod. Phys.*, 32, 254 (1960).
- 24(a) J.N. Murrell, M. Randic and D.R. Williams, *Proc. Roy. Soc. (London)*, A284, 566 (1965).
- ~~(b) J.N. Murrell and G. Shaw, *J. Chem. Phys.*, 46, 1768 (1967).~~
- 25(a) J.I. Musher and L. Salem, *J. Chem. Phys.*, 44, 2943 (1966).
- (b) A. van der Avoird, *J. Chem. Phys.*, 47, 3649 (1967).
- (c) J.I. Musher and A.T. Amos, *Phys. Rev.*, 164, 31 (1967).
- (d) L. Jensen, *Phys. Rev.*, 162, 63 (1967).

26. D.M. Chipman and J.O. Hirschfelder, J. Chem. Phys., 59, 2838 (1973) and references therein.
27. B. Linder and J.O. Hirschfelder, J. Chem. Phys., 28, 197 (1958).
- 28(a) P.O. Löwdin, Revs. Mod. Phys., 34, 80 (1962).
- (b) G. Herring in "Magnetism", G.T. Rado and H. Suhl, Eds. (Academic Press, New York, 1966), Vol. 2B, Chapt. 1.
- 29(a) I. Tamásy-Lentei and A. Bába, Acta Phys. Acad. Scient. Hung., 16, 13 (1963).
- (b) I. Tamásy-Lentei, Acta Phys. Acad. Scient. Hung., 29, 67 (1970).
- (c) I. Tamásy-Lentei, Acta Phys. Chem. Debr., 11, 5 (1965).
30. D.M. Bishop and J.R. Hoyland, Molec. Phys., 7, 161 (1963).
31. D.M. Bishop, J.R. Hoyland and R.G. Parr, Molec. Phys., 6, 467 (1963).
32. L.L. Combs and L.K. Runnels, J. Chem. Phys., 49, 4216 (1968).
-
33. Z.J. Horák and J. Sisková, J. Chem. Phys., 59, 4884 (1973).
34. J. Katriel, Int. J. Quant. Chem., 6, 541 (1972).
35. M. Cohen and C.A. Coulson, Proc. Camb. Phil. Soc., 57, 96 (1961).

36. M. Cohen, Proc. Camb. Phil. Soc., 58, 130 (1961).
37. P. Hauk and R.G. Parr, J. Chem. Phys., 43, 548 (1965).
38. D.R. Bates, K. Ledsham and A.L. Stewart, Phil. Trans. Roy. Soc., A246, 215 (1954).
39. H. Wind, J. Chem. Phys., 42, 2371 (1965).
40. J.M. Peek, J. Chem. Phys., 43, 3004 (1965).
41. J.R. Hoyland, J. Chem. Phys., 44, 2533 (1966).
42. E.F. Hays and R.G. Parr, J. Chem. Phys., 46, 3577 (1967).
43. F.A. Matsen, J. Chem. Phys., 21, 928 (1953).
44. M. Born and J.R. Oppenheimer, Ann. Phys., (Germany), 84, 457 (1927).
45. M. Born and K. Huang, Dynamical Theory of Crystal Lattices, pp. 166 and 402 (Oxford Univ. Press, 1954).
46. M.E. Rose, Elementary Theory of Angular Momentum, Chapt. 4 (John Wiley, New York, 1957).
47. E.U. Condon and G.H. Shortley, The Theory of Atomic Spectra (Cambridge, 1967).
48. L. Fox, Boundary Problems in Differential Equations, R.E. Langer, Ed. (University of Wisconsin, Madison, 1960).

49. J.V. Moloney, M.K. Ali and W.J. Meath, Phys. Lett., 49A, 207 (1974).
50. J.V. Moloney and W.J. Meath, Molec. Phys., in press and to be submitted for publication.
- 51(a) K. Shimoda and T. Shimizu, Nonlinear Spectroscopy of Molecules, Progress in Quantum Electronics (Pergamon Press, 1972).
- (b) F. Biraben, B. Cagnac and G. Grynberg, Phys. Rev. Lett., 32, 643 (1974).
52. W. Byers-Brown and J.D. Power, Proc. Roy. Soc., A317, 545 (1970).
53. H.A. Bethe and E.E. Salpeter, Quantum Mechanics of One and Two Electron Atoms (Academic Press, New York, 1957).
54. J.O. Hirschfelder, Ed., Intermolecular Forces, Vol. 12, Advances in Chemical Physics (Wiley, New York, 1967).
55. J.O. Hirschfelder, W.B. Brown and S.T. Epstein, Advances in Quantum Chemistry, Vol. 1, P.O. Löwdin, Ed. (Academic Press, New York, 1964).
56. J.D. Jackson, Classical Electrodynamics, Chapt. 3 (John Wiley, New York, 1962).
57. A. Dalgarno and N. Lynn, Proc. Phys. Soc., A69, 821 (1956).

58. H. Kreek, Ph.D. Thesis, The University of Western Ontario, 1971.
59. A. Dalgarno and A.L. Stewart, Proc. Roy. Soc. (London), A238, 276 (1956).
60. A. Messiah, Quantum Mechanics, Vol. 1 (Wiley, New York, 1966).
61. P.A.M. Dirac, The Principles of Quantum Mechanics, (Oxford, Univ. Press, 1958).
62. E. Merzbacher, Quantum Mechanics, Chapt. 10 (Wiley, New York, 1967).
63. Z. Rubinstein, A Course in Ordinary and Partial Differential Equations, Chapt. 8 (Academic Press, New York, 1969).
64. E.L. Ince, Ordinary Differential Equations (Longmans, Green and Co. Ltd., 1927).
65. F.G. Tricomi, Differential Equations, Chapt. 5 (Blackie, London, 1961).
66. E.T. Whittaker and G.N. Watson, A Course of Modern Analysis, Chapt. 5 (Camb. Univ. Press, 1969).
67. P.M. Morse and H. Feshbach, Methods of Theoretical Physics, Chapt. 4 and 5 (McGraw-Hill, New York, 1953).
68. L. Fox, The Numerical Solution of Two-Point Boundary

- Problems in Ordinary Differential Equations (Oxford Univ. Press, 1957).
69. D.R. Hartree, The Calculation of Atomic Structures, Chapt. 4 (John Wiley, New York, 1957).
70. F.B. Hildebrand, Introduction to Numerical Analysis, Chapt. 10 (McGraw-Hill, New York, 1956).
71. L. Collatz, Functional Analysis and Numerical Mathematics (Academic Press, New York, 1966).
72. H. Jeffreys, Asymptotic Approximations, Chapt. 7 (Oxford Press, 1962).
73. H. Jeffreys and B.S. Jeffreys, Methods of Mathematical Physics, Chapt. 17 (Camb. Univ. Press, 1966).
74. Modern Computing, Chapt. 13 (H.M. Stationary Office, London, 1961).
75. L.F. Richardson and J.A. Gaunt, Phil. Trans., A226, 299 (1926).
- 76(a) W.A. Bingel, J. Chem. Phys., 30, 1250 (1959).
- (b) W.B. Brown and E. Steiner, J. Chem. Phys., 44, 3934 (1966).
- 77(a) A. Messiah, Quantum Mechanics, Vol. 2 (Wiley, New York, 1966).
- (b) L. Pauling and E.B. Wilson, Introduction to Quantum Mechanics (McGraw-Hill, New York, 1935).
78. A. Dalgarno, in "Quantum Theory" D.R. Bates, Ed., Vol. 1; Chapt. 5 (Academic Press, New York, 1961).

79. P. Hauk, R.G.² Parr and H.F. Hameka, J. Chem. Phys., 39, 2085 (1963).
80. W.D. Lyon, R.L. Matcha, W.A. Sanders, W.J. Meath and J.O. Hirschfelder, J. Chem. Phys., 43, 1095 (1965);
Erratum, J. Chem. Phys., 51, 3151 (1969).
81. L. Pauling, Chem. Revs., 5, 173 (1928).
- 82(a) G. Jaffé, Z. Phys., 87, 335 (1934).
(b) E.A. Hylleraas, Z. Phys., 71, 739 (1931).
83. A. Dalgarno and G. Poots, Proc. Phys. Soc., A67, 343 (1954).
84. R.W. McCarroll and M.R.C. McDowell, Proc. Phys. Soc., A68, 810 (1955).
85. M. Geller and O.G. Ludwig, J. Chem. Phys., 36, 1442 (1962).
86. P.C. Trivedi, J. Phys. B, 4, 420 (1971).
87. T.J. Houser, P.G. Lykos and E.L. Mehler, J. Chem. Phys., 38, 583 (1963).
88. H.W. Joy and G.S. Handler, J. Chem. Phys., 42, 3047 (1965).
89. S. Hagstrom and H. Shull, J. Chem. Phys., 30, 1314 (1959).

90. H.W. Joy and G.S. Handler, J. Chem. Phys., 43, S252 (1965).
91. W. Kolos and L. Wolniewicz, J. Chem. Phys., 41, 3663 (1964); 43, 2429 (1965).
92. H.W. Joy and R.G. Parr, J. Chem. Phys., 28, 448 (1958).
93. D.M. Bishop, Molec. Phys., 6, 305 (1963).
94. R. Ahlrichs, W. Kutzelnigg and W.A. Bingel, Theoret. Chim. Acta, 5, 305 (1966).
95. E.F. Hayes, J. Chem. Phys., 46, 4004 (1967).
96. T.R. Singh, J.F. Bukta and W.J. Meath, Int. J. Quant. Chem., 6, 201 (1972).
97. T.R. Singh and W.J. Meath, J. Chem. Phys., 54, 1137 (1971).
98. A. Riera and W.J. Meath, Int. J. Quant. Chem., 6, 501 (1972).
99. T.S. Nee, R.G. Parr and S.Y. Chang, J. Chem. Phys., 59, 4911 (1973).
-
- 100(a) D.M. Chipman, J.D. Bowman and J.O. Hirschfelder, J. Chem. Phys., 59, 2830 (1973).
- (b) H.N.W. Lekkerkerker and W.G. Laidlaw, J. Chem. Phys., 52, 2953 (1970).
101. D.G. Pettifor, J. Chem. Phys., 59, 4320 (1973).

102. A. Temkin and A.K. Bhatia, J. Chem. Phys., 42, 644 (1965).
- 103(a) E.R. Davidson, J. Chem. Phys., 33, 1577 (1960); 35, 1189 (1961).
- (b) W. Kolos and L. Wolniewicz, J. Chem. Phys., 50, 3228 (1969).
- 104(a) J.R. Hoyland, J. Chem. Phys., 45, 3928 (1966).
- (b) Y. Kato, E.F. Hayes and A.B.F. Duncan, J. Chem. Phys., 41, 986 (1964).
105. W.E. Milne, Numerical Calculus (Princeton Univ. Press, New Jersey, 1949).
106. Z. Kopal, Numerical Analysis, Chapt. 7 (Chapman and Hall, Ltd., London, 1955).
107. P.J. Davis and I. Polonsky, Natl. Bur. Std. (U.S.), Appl. Math. Ser. 55, Chapt. 25 (1964).
108. G. Arfken, Mathematical Methods for Physicists, Chapt. 2 (Academic Press, New York, 1968).
109. D.R. Bates and T.R. Carson, Proc. Roy. Soc., A234, 207 (1956).
-
- 110(a) E. Hylleraas and B. Undheim, Z. Physik, 65, 759 (1930).
- (b) J.K.L. MacDonald, Phys. Rev., 43, 830 (1933).
- (c) Reference 77(b), pp. 186-189.

- 111(a) D. Shanks, J. Math. Phys., 34, 1 (1955).
(b) Reference 74, pp. 123.
112. A. Dalgarno and N. Lynn, Proc. Phys. Soc., A70, 223
(1957).
- 113(a) P.D. Robinson, Proc. Phys. Soc., A71, 828 (1958).
(b) C.A. Coulson and C.M. Gillam, Proc. Roy. Soc. Edinb.,
A62, 362 (1947).
114. ~~A. Riera and W.J. Meath, Molec. Phys., 24, 1407 (1972).~~
115. Kin-Chue Ng, A.R. Allnatt and W.J. Meath, to be
published.

- (2) "Floating One-Centre Perturbation Treatments for H_2^+ -like Molecules Based on Screened Hydrogen Atom or Molecular Puff Unperturbed Problems", M.K. Ali, and W.J. Meath, Int. J. Quantum Chem., 8, 119 (1974).
- (3) "A Floating One-Centre Perturbation Treatment for H_2^+ -like Molecules", M.K. Ali and W.J. Meath, Int. J. Quantum Chem., 6, 949 (1972).
- (4) "The Emission Spectrum of Diatomic Bismuth", S.P. Reddy and M.K. Ali, J. Mol. Spectroscopy, 35, 285 (1970).
- (5) "Mineralogy of Clay Deposits Near Bagh (33° 45' 30"; 70° 11' 40"), Rawalpindi Division", M.A. Qaiser, M.K. Ali and A.H. Khan, Pakistan J. Sci. Ind. Res., 12, 483 (1969).
- (6) "Study of Indigenous Minerals by DTA", M.A. Qaiser, M.K. Ali and A.H. Khan, Pakistan J. Sci. Ind. Res., 11, 23 (1968).
- (7) "Mineralogy of Some Asbestos from North West Pakistan", M.A. Qaiser, M.K. Ali and A.H. Khan, Pakistan J. Sci. Ind. Res., 10, 116 (1967).